SYNTHETIC STUDIES RELATED TO REDUCTIVELY ACTIVATED ANTITUMOUR ANTIBIOTICS

by

S. Mithani

A thesis

presented to the University of Waterloo

in fulfilment of the

thesis requirement for the degree of

Doctor of Philosophy

in

Chemistry

Waterloo, Ontario, Canada, 1996

© S. Mithani 1996

National Library of Canada
Bibliothèque nationale du Canada

Acquisitions and Bibliographic Services
Acquisitions et services bibliographiques

395 Wellington Street
Ottawa ON K1A 0N4
Canada

395, rue Wellington
Ottawa ON K1A 0N4
Canada

Your file Votre référence

Our file Notre référence

The author has granted a non-exclusive licence allowing the National Library of Canada to reproduce, loan, distribute or sell copies of his/her thesis by any means and in any form or format, making this thesis available to interested persons.

L'auteur a accordé une licence non exclusive permettant à la Bibliothèque nationale du Canada de reproduire, prêter, distribuer ou vendre des copies de sa thèse de quelque manière et sous quelque forme que ce soit pour mettre des exemplaires de cette thèse à la disposition des personnes intéressées.

The author retains ownership of the copyright in his/her thesis. Neither the thesis nor substantial extracts from it may be printed or otherwise reproduced with the author's permission.

L'auteur conserve la propriété du droit d'auteur qui protège sa thèse. Ni la thèse ni des extraits substantiels de celle-ci ne doivent être imprimés ou autrement reproduits sans son autorisation.

0-612-21413-3

Canada

The University of Waterloo requires the signatures of all persons using or photocopying this thesis. Please sign below, and give address and date.

Synthetic Studies related to Bioreductively Activated Antitumour Antibiotics

ABSTRACT

Exploration of synthetic approaches to two classes of antitumour antibiotics, believed to function through DNA alkylation after bioreductive activation analogous to that established for mitomycin C, is described. Transformation of mitomycin-related pyrrolo[1,2-a]indoles into the bicyclic hydroxylamine hemiketal ring system found in antitumour antibiotic FR-900482 via a bromination-methanolysis sequence followed by oxidative ring expansion with N-benzenesulfonyl oxaziridines (Davis' reagent) is presented. Attempts at improving the two-step transformation using Davis' reagent to effect both steps are observed to yield anomalous addition products. Mechanistic studies suggest that this addition reaction proceeds via a zwitterionic intermediate. The possibility that such an intermediate is also involved in oxygen atom transfer reactions of Davis' reagent is discussed.

A synthetic route to prekinamycin, a biosynthetic precursor to the kinamycins which were proposed to incorporate an N-cyanobenzo[b]carbazole ring system, is described. A preparation of what was expected to be O-acetyl-O-methyl prekinamycin (**190**), in an unambiguous manner, in 21% overall yield from *o*-anisidine is presented. Careful comparison of the spectroscopic characteristics of **190** with those of the kinamycins is shown to prove that the kinamycins are derivatives of diazofluorene and not of N-cyanocarbazole as previously believed. The significance of this structural revision in the context of the biosynthesis and possible mode of action of the kinamycins is discussed.

Finally, a synthetic route to the carbon skeleton present in the revised structure of prekinamycin, but lacking the substituents present in the D-ring of the natural product, is presented as well as a route to an aromatic acid (**283**) which is a logical precursor to prekinamycin via this synthetic strategy.

ACKNOWLEDGEMENTS

I would like to thank Dr. Gary Dmitrienko for his time and guidance throughout the course of my research and in the preparation of this thesis. My thanks are also extended to fellow graduate students for their encouragement and advice.

I would also like to thank Dr. N. J. Taylor for the X-ray difraction studies and Dr. S. Mooibroek for her help with NMR experiments.

Table of Contents

LIST OF FIGURES ..... **VIII**

LIST OF SCHEMES ..... **XIII**

LIST OF ABBREVIATIONS ..... **XXII**

CHAPTER 1: INTRODUCTION **1**

1.1 THE MITOMYCINS 2

1.1.1 Isolation, Structure and Stereochemistry *3*

1.1.2 Mode of Action *6*

1.1.3 Synthetic Approaches to the Mitomycins *14*

1.2 FR-900482 18

1.2.1 Isolation, Structure and Stereochemistry *18*

1.2.2 Mode of Action *20*

1.2.3 Synthetic Studies *23*

1.3 THE KINAMYCINS 27

1.3.1 Isolation and Structure *27*

1.3.2 Biosynthesis of Kinamycins *33*

1.3.3 Mode of Action *45*

CHAPTER 2: SYNTHETIC STUDIES TOWARD FR-900482 ..... **48**

2.1 OXIDATIVE RING EXPANSION 48

2.2 REACTION OF DAVIS' REAGENT WITH 114 58

2.2.1 Proton NMR Experiments *61*

2.2.2 Mechanism for the formation of the adduct 138a *70*

CHAPTER 3: SYNTHETIC STUDIES TOWARD PREKINAMYCIN **87**

CHAPTER 4: SPECTROSCOPIC COMPARISON OF 190 WITH THE DIACETATE DERIVATIVE OF PREKINAMYCIN.....122

4.1 ^{15}N AND ^{13}C NMR EXPERIMENTS 126

4.2 STRUCTURE ASSIGNMENT OF THE KINAMYCINS 129

4.3 INDEPENDENT STRUCTURAL REVISION OF THE KINAMYCINS BY GOULD AND CO-WORKERS.....136

4.4 OTHER SYNTHETIC APPROACHES TO THE STRUCTURE ORIGINALLY ASSIGNED TO THE KINAMYCINS 139

4.5 A RE-EXAMINATION OF THE ECHAVARREN SYNTHESIS OF PREKINAMYCIN.....141

4.6 SIGNIFICANCE OF THE STRUCTURAL REVISION OF THE KINAMYCINS TO CURRENTLY ACCEPTED BIOGENETIC MECHANISMS.....149

4.7 SIGNIFICANCE OF THE STRUCTURAL REVISIONS OF THE KINAMYCINS IN RELATION TO THE PROPOSED MECHANISM OF BIOLOGICAL ACTIVITY 152

CHAPTER 5: SYNTHETIC STUDIES TOWARD THE REVISED STRUCTURE OF PREKINAMYCIN 157

5.1 SUMMARY OF RESULTS IN THE AREA OF THE KINAMYCINS.....191

CHAPTER 6: EXPERIMENTAL 193

6.1 GENERAL PROCEDURES.....193

6.2 EXPERIMENTAL PROCEDURES.....195

APPENDIX A 239

APPENDIX B 250

REFERENCES.....287

List of Figures

FIGURE 1: THE STRUCTURES OF THE MITOMYCINS, FR-900482 AND THE KINAMYCINS 2

FIGURE 2: MITOSANE AND MITOSENE SUBSTRUCTURES 3

FIGURE 3: THE STRUCTURES OF THE MORE COMMON MITOMYCINS. 4

FIGURE 4: THE STRUCTURES OF ISOMITOMYCIN A AND ALBOMITOMYCIN A 5

FIGURE 5: THE EQUILIBRIUM BETWEEN ISOMITOMYCIN A, ALBOMITOMYCIN A AND MITOMYCIN A. 5

FIGURE 6: TWO POSSIBLE MODES OF BIOREDUCTIVE ACTIVATION OF MITOMYCIN C 7

FIGURE 7: ISOLATED MITOMYCIN-DNA ADDUCTS 8

FIGURE 8: THREE POSSIBLE WAYS IN WHICH MITOMYCIN C COULD POTENTIALLY CROSS-LINK DNA 8

FIGURE 9: SYNTHETIC STRATEGIES TO THE MITOMYCIN SKELETON. 14

FIGURE 10: STRUCTURES OF FR-900482, FK-973, FR-66979 AND MITOMYCIN C 19

FIGURE 11: DNA ADDUCTS ISOLATED FROM THE REDUCTION OF FR-900482 AND MITOMYCIN C 23

FIGURE 12: KEY STEPS IN FUKUYAMA'S TOTAL SYNTHESIS OF FR-900482. 23

FIGURE 13: THE KEY STEPS IN DANISHEFSKY'S TOTAL SYNTHESIS OF FR-900482 26

FIGURE 14: STRUCTURES OF THE MORE COMMON KINAMYCINS 28

FIGURE 15: SPECTROSCOPIC PROPERTIES OF THE KINAMYCINS 30

FIGURE 16: KINAMYCINS ISOLATED FROM *SACCHAROTHRIX*. 30

FIGURE 17: A NEW KINAMYCIN ISOLATED FROM AN UNIDENTIFIED ACTINOMYCETE DESIGNATED AS A83016A 31

FIGURE 18: KINAMYCINS ISOLATED FROM *STREPTOMYCES CHATTANOOGENSIS*. 31

FIGURE 19: ^{1}H NMR SPECTRUM SIGNALS FOR PREKINAMYCIN, THE DIACETYL DERIVATIVE, KETO-ANHYDROKINAMYCIN AND KINAMYCIN E. 33

FIGURE 20: BIOSYNTHESIS OF KINAMYCIN FROM TWO UNSYMMETRICAL POLYKETIDE CHAINS 34

FIGURE 21: INCORPORATION OF LABELLED ACETATE INTO THE KINAMYCINS 35

FIGURE 22: INCORPORATION OF DOUBLY LABELLED ACETATE INTO THE KINAMYCINS 35

FIGURE 23: INCORPORATION OF $^{18}O_2$ INTO THE KINAMYCINS 36

FIGURE 24: PROBABLE MECHANISM FOR D-RING FUNCTIONALIZATION OF THE KINAMYCINS 36

FIGURE 25: THE KINAMYCINS ARE DERIVED FROM ACETATE VIA A SINGLE POLYKETIDE CHAIN 37

FIGURE 27: PROBABLE ORIGIN OF CYANAMIDE CARBON 38

FIGURE 28: STRUCTURES OF DEHYDRORABELOMYCIN AND PD 116470 39

FIGURE 29: 93 AND 95 ARE DERIVED FROM TWO DIFFERENT POLYKETIDE CHAINS 40

FIGURE 30: THE STRUCTURE OF PHENANTHROVIRIDINE AGLYCONE 41

FIGURE 31: REVISED BIOSYNTHETIC PATHWAY. 42

FIGURE 32: PROPOSED BIOSYNTHETIC TRANSFORMATION OF PHENANTHROVIRIDINE AGLYCONE TO THE KINAMYCINS. 43

FIGURE 33: STRUCTURES OF KINAFLUORENONE AND ITS TRIACETYL DERIVATIVE 107 44

FIGURE 34: MECHANISM BY WHICH PREKINAMYCIN MIGHT BE FORMED FROM DEHYDRORABELOMYCIN. 44

FIGURE 35: OVERALL BIOSYNTHETIC SCHEME. 45

FIGURE 36: THE STRUCTURES OF THE KINAMYCINS AND MITOMYCIN C 46

FIGURE 37: POSSIBLE RESONANCE INTERACTIONS FOR THE KINAMYCINS 46

FIGURE 39: PROTON NMR SPECTRUM OF THE MAJOR PRODUCT ISOLATED FROM THE REACTION OF 114 WITH DAVIS' REAGENT. 60

FIGURE 40: SELECTIVE TOCSY WITH IRRADIATION AT 6.39 PPM 62

FIGURE 41: SELECTIVE TOCSY WITH IRRADIATION AT 6.53 PPM 63

FIGURE 42: SUMMARY OF TOCSY EXPERIMENTS IN THE AROMATIC REGION 63

FIGURE 43: THE UNUSUAL DOUBLET OF A QUARTET AT 6.78 PPM IS COMPOSED OF TWO APPARENT TRIPLETS. 64

FIGURE 44: DIFFERENCE NOE EXPERIMENT WITH IRRADIATION AT 6.39 PPM 65

FIGURE 45: DIFFERENCE NOE EXPERIMENT WITH IRRADIATION AT 6.53 PPM 66

FIGURE 46: SUMMARY OF TOCSY EXPERIMENTS IN THE ALIPHATIC REGION 67

FIGURE 47: PART STRUCTURES CONTAINED IN 138 AS DETERMINED BY NMR EXPERIMENTS 67

FIGURE 48: STRUCTURES COMPATIBLE WITH 138 68

FIGURE 49: STRUCTURE OF 138 THAT IS COMPATIBLE WITH NMR STUDIES 69

FIGURE 50: OBSERVED NOE ENHANCEMENTS UPON IRRADIATION OF THE SIGNALS AT 1.42 AND 1.50 PPM 70

FIGURE 51: ORTEP PLOT OF 141A 72

FIGURE 52: ORTEP PLOT OF 143B 73

FIGURE 53: SUMMARY OF DISTINGUISHING CH SIGNALS IN THE PROTON NMR SPECTRA OF THE ADDUCTS 76

FIGURE 54: OXAZIRIDINE MODEL USED IN AB INITIO CALCULATIONS 85

FIGURE 55: STRUCTURES OF THE KINAMYCINS AND PREKINAMYCIN 87

FIGURE 56: PREKINAMYCIN IS A KEY INTERMEDIATE IN THE BIOSYNTHESIS OF THE KINAMYCIN ANTIBIOTICS. 87

FIGURE 57: COEFFICIENTS OF THE HOM AND LUMO OF 155 AND 160 90

FIGURE 58: STRUCTURE OF 165 93

FIGURE 59: STEREO REPRESENTATION OF 155 PRIOR TO MOPAC GEOMETRY OPTIMIZATION 99

FIGURE 60: STEREO REPRESENTATION OF 165 BEFORE MOPAC GEOMETRY OPTIMIZATION 100

FIGURE 61: GEOMETRY OPTIMIZED STEREO STRUCTURE OF DIENE 155 WITH THE HOMO COEFFICIENTS FOR THE RELEVANT CARBONS. 101

FIGURE 62: GEOMETRY OPTIMIZED STEREO STRUCTURE OF QUINONE 184 WITH THE LUMO COEFFICIENTS FOR THE RELEVANT CARBONS. 101

FIGURE 63: STRUCTURES OF 177 AND 175 112

FIGURE 64: PROTON NMR SIGNALS AND ASSIGNMENTS FOR 190 AND PREKINAMYCIN DIACETATE. 123

FIGURE 65: STRUCTURES OF THE TWO DIASTEREOMERIC FORMS OF 178 125

FIGURE 66: ORTEP PLOTS OF THE TWO DIASTEREOMERIC FORMS OF 178 125

FIGURE 67: STRUCTURE OF MODELS 160 AND 192 127

FIGURE 68: ^{1}H / ^{13}C LONG-RANGE HMQC EXPERIMENTS ESTABLISHED CONNECTIVITIES AND ASSIGNMENTS FOR 160. 127

FIGURE 69: ORTEP PLOT OF N-CYANO-2,3-DIMETHYLINDOLE. 128

FIGURE 70: DIRECT AND INDIRECT OBSERVATION OF ^{15}N NMR SIGNALS RELATIVE TO AMMONIA OF MODEL COMPOUNDS. 129

FIGURE 71: THE STRUCTURE OF KINAMYCIN C *P*-BROMOBENZOATE. 130

FIGURE 72: THE X-RAY DATA FAILED TO UNAMBIGUOUSLY ASSIGN A THREE ATOM FRAGMENT IN THE KINAMYCINS 131

FIGURE 73: THE STRUCTURES OF MODEL DIAZO COMPOUNDS 132

FIGURE 74: THE STRUCTURE OF LAGUNAMYCIN 133

FIGURE 75: THE THREE POSSIBILITIES FOR THE UNRESOLVED THREE ATOM FRAGMENT IN THE KINAMYCINS 135

FIGURE 76: REVISED STRUCTURES OF THE KINAMYCINS 136

FIGURE 77: ORTEP PLOT OF A-METHYL BUTYRATE DERIVATIVE OF KINAMYCIN D 137

FIGURE 78: STRUCTURES OF RECENTLY ISOLATED KINAMYCINS 137

FIGURE 79: THE STRUCTURES OF JADOMYCIN AND THE STEALTHINS 150

FIGURE 80: THE STRUCTURES OF SYNTHETICALLY PRODUCED DERIVATIVE OF PREKINAMYCIN AND REVISED STRUCTURE OF PREKINAMYCIN 157

FIGURE 81: ^{13}C NMR DATA PUBLISHED FOR 254 AS WELL AS ^{13}C DATA FOR BROMINATION PRODUCTS OBTAINED IN THIS STUDY 167

FIGURE 82: PROTON NMR SPECTRUM OF TRIACETATE 275 181

FIGURE 83: PROTON NMR SPECTRUM AT 250K OF TRIACETATE 275 182

List of Schemes

SCHEME 1: RESONANCE INTERACTION OF THE NITROGEN IN MITOMYCIN C 9

SCHEME 2: ONE ELECTRON REDUCTION OF MITOMYCIN C..... 10

SCHEME 3: A TWO ELECTRON REDUCTION OF MITOMYCIN C TO THE HYDROQUINONE IS NOT SUFFICIENT TO TRIGGER LOSS OF METHANOL. 10

SCHEME 4: A ONE ELECTRON REDUCTION OF MITOMYCIN C TO THE SEMIQUINONE RESULTS IN THE LOSS OF METHANOL. 11

SCHEME 5: MECHANISM FOR THE ALKYLATION OF DNA BY MITOMYCIN C SEMIQUINONE 12

SCHEME 6: POSSIBLE PATHWAYS LEADING TO MONO AND BIS ALKYLATED DNA. 13

SCHEME 7: THE KEY STEPS IN KISHI'S SYNTHESIS OF THE MITOMYCIN C. 15

SCHEME 8: KEY STEPS IN FUKUYAMA'S TOTAL SYNTHESIS OF MITOMYCIN A AND MITOMYCIN C..... 17

SCHEME 9: INTERCONVERSION OF THE TWO DIASTEREOMERIC FORMS OF FR-900482 VIA KETO INTERMEDIARY 20

SCHEME 10: FUKUYAMA'S PROPOSAL FOR BIOREDUCTIVE ACTIVATION OF FR-900482..... 21

SCHEME 11: DANISHEFSKY'S PROPOSAL FOR BIOACTIVATION OF FR-900482. 21

SCHEME 12: KEY STEPS IN FUKUYAMA'S TOTAL SYNTHESIS OF FR-900482. 25

SCHEME 13: DANISHEFSKY'S TOTAL SYNTHESIS OF FR-900482 27

SCHEME 14: PROPOSED MECHANISM FOR THE BISALKYLATION OF DNA BY THE KINAMYCINS 47

SCHEME 15: POSSIBLE BIOSYNTHETIC PATHWAYS TO FR-900482 FROM A MITOMYCIN-LIKE INTERMEDIATE. 49

SCHEME 16: BROMINATION METHANOLYSIS OF INDOLES. 50

SCHEME 17: BROMINATION METHANOLYSIS OF PYRROLO[1,2-A]INDOLE 114 51

SCHEME 18: PROBABLE MECHANISM FOR THE BROMINATION METHANOLYSIS REACTION 51

SCHEME 19: OXIDATION OF 115 WITH HYDROGEN PEROXIDE AND MCPBA 52

SCHEME 20: REACTION OF DAVIS' REAGENT WITH OLEFINS AND AMINES 53

SCHEME 21: OXIDATIVE RING EXPANSION OF THE ALCOHOL 115 WITH DAVIS' REAGENT 54

SCHEME 22: TWO POSSIBLE MECHANISMS FOR OXIDATIVE RING EXPANSION OF THE ALCOHOL 115 BY DAVIS' REAGENT 55

SCHEME 23: REACTION OF THE INDOLINE 129 WITH DAVIS' REAGENT 55

SCHEME 24: SYNTHETIC STUDIES TOWARD FR-900482 BY WANG AND JIMENEZ 57

SCHEME 25: TWO STEP PROCESS FOR THE GENERATION OF THE RING EXPANDED PRODUCT 121 FROM THE PYRROLO[1,2-A]INDOLE 114 58

SCHEME 26: DESIRED ONE STEP OXIDATIVE TRANSFORMATION OF 114 TO 121C 58

SCHEME 27: POTENTIAL ONE POT SYNTHESIS OF 137 FROM 114 USING DAVIS' REAGENT AS THE OXIDANT 59

SCHEME 28: POSSIBLE STRUCTURES OF 138 61

SCHEME 29: PROBABLE MECHANISM FOR THE FORMATION OF THE ADDUCT VIA A ZWITTERIONIC INTERMEDIATE. 71

SCHEME 30: OXYGEN ATOM TRANSFER MECHANISM FOR THE EPOXIDATION OF OLEFINS BY DAVIS' REAGENT 71

SCHEME 31: REACTION OF 2,3-DIMETHYLINDOLE WITH DAVIS' REAGENT 72

SCHEME 32: REACION OF CYCLOPENTANOINDOLE WITH DAVIS' REAGENT 73

SCHEME 33: AN ALTERNATIVE MECHANISM TO THAT DEPICTED IN SCHEME 29 74

SCHEME 34: SYNTHESIS OF THE NITRO ANALOG OF DAVIS' REAGENT 75

SCHEME 35: SYNTHESIS OF NITRO ADDUCTS 147, 148 AND 149 FROM THE INDOLES 114, 140 AND 142, RESPECTIVELY 75

SCHEME 36: PRODUCT DISTRIBUTION EXPECTED IN CROSS-OVER EXPERIMENT. 77

SCHEME 37: REACTION OF DAVIS' REAGENT WITH THE NITRO IMINE 146 78

SCHEME 38: CROSS-OVER EXPERIMENTS WITH THE PYRROLO[1,2-A]INDOLE 114. 79

SCHEME 39: CROSS-OVER EXPERIMENTS WITH 2,3-DIMETHYLINDOLE 140. 80

SCHEME 40: CROSS-OVER EXPERIMENTS WITH CYCLOPENTANOINDOLE 142 81

SCHEME 41: POSSIBLE TIGHT ASSOCIATION OF EPOXIDE 135 WITH IMINE 144 82

SCHEME 42: SYNTHESIS OF THE HYDROXY INDOLENINE 152 BY THE METHOD OF DAVE. 83

SCHEME 43: REACTION OF THE HYDROXYINDOLENINE 152 WITH THE IMINE 144 83

SCHEME 44: HYDROLYSIS OF THE IMINE 144. 83

SCHEME 45: REACTION OF THE PYRROLO[1,2-A]INDOLE 114 WITH DAVIS' REAGENT IN THE PRESENCE OF A LARGE EXCESS OF WATER 84

SCHEME 46: OXIDATION OF N-ACYLINDOLE 153 WITH DIMETHYLDIOXIRANE. 86

SCHEME 47: OXIDATION OF PYRROLO[1,2-A]INDOLE 114 WITH DIMETHYLDIOXIRANE. 86

SCHEME 48: INTRODUCTION OF A SUBSTITUTED AROMATIC RING INTO A QUINONE SYSTEM THROUGH A DIELS-ALDER REACTION 88

SCHEME 49: REACTION OF 155 WITH JUGLONE (159). 89

SCHEME 50: DIELS-ALDER REACTION OF 155 WITH QUINONE 160 PROGRESSES WITH COMPLETE REGIOSELECTIVITY 90

SCHEME 51: STRATEGY FOR THE AROMATIZATION OF THE A-RING OF 161 91

SCHEME 52: TREATMENT OF 161 WITH SODIUM HYDRIDE FOLLOWED BY OXIDATION WITH SILVER OXIDE 92

SCHEME 53: RETROSYNTHETIC ANALYSIS OF THE SYNTHETIC STRATEGY TOWARD PREKINAMYCIN 93

SCHEME 54: FISCHER INDOLE SYNTHESIS OF A POSSIBLE PRECURSOR TO PREKINAMYCIN 94

SCHEME 55: STRATEGY FOR THE CONSTRUCTION OF THE D-RING FROM AN ACYCLIC B,C RING PRECURSOR VIA AN INDOLE-2,3-QUINODIMETHANE 94

SCHEME 56: RETROSYNTHETIC ANALYSIS OF THE STRATEGY FOR THE CONSTRUCTION OF A BCD RING SYNTHON OF PREKINAMYCIN 95

SCHEME 57: REACTION OF O-ANISIDINE WITH 167 YIELDED THE ANILINE 168 95

SCHEME 58: THE CARBAZOLE 169 WAS GENERATED FROM THE ANILINE 168 96

SCHEME 59: A MORE EFFICIENT ROUTE TOWARD THE CARBAZOLE 169 96

SCHEME 60: PREPARATION OF PHENYL CYANATE 97

SCHEME 61: CYANATION OF THE CARBAZOLE 169 WITH PHENYL CYANATE AND TRIETHYLAMINE IN THF 98

SCHEME 62: CYANATION OF THE CARBAZOLE 169 WITH PHENYL CYANATE AND TRIETHYLAMINE IN DMSO 98

SCHEME 63: OXIDATION OF 174 WITH CERIC AMMONIUM NITRATE 98

SCHEME 64: STRATEGY FOR THE INTRODUCTION OF THE A-RING INTO BCD RING SYNTHON OF PREKINAMYCIN 99

SCHEME 65: CONSIDERING PRIMARY ORBITAL INTERACTIONS ONLY IN THE FMO ANALYSIS. 102

SCHEME 66: CONSIDERING SECONDARY ORBITAL INTERACTIONS ONLY IN FMO ANALYSIS 103

SCHEME 67: DIELS-ALDER REACTION OF THE DIENE 155 WITH THE QUINONE 165 103

SCHEME 68: STRATEGY FOR THE AROMATIZATION OF THE A-RING OF 175 104

SCHEME 69: BIS-ENOLIZATION OF THE DIKETONE 175 WITH ACID 105

SCHEME 70: STRATEGY FOR THE AROMATIZATION OF THE A-RING OF THE HYDROQUINONE 178 106
SCHEME 71: ATTEMPTED OXIDATION OF THE HYDROQUINONE 178 WITH OXYGEN IN DMSO 106
SCHEME 72: REACTION OF DIKETONE 175 WITH SELENIUM DIOXIDE 107
SCHEME 73: ATTEMPTED COPPER CATALYZED OXIDATION OF HYDROQUINONE 175 108
SCHEME 74: OXIDATION OF HYDROQUINONE 175 WITH DDQ IN METHANOL 108
SCHEME 75: TRANFORMATION OF THE DIKETONE 175 TO THE QUINONE 176 IN 93% YIELD 109
SCHEME 76: AROMATIZATION OF THE A-RING BY A RETRO-DIELS-ALDER REACTION 110
SCHEME 77: AROMATIZATION OF THE D-RING OF A DERIVATIVE OF PREKINAMYCIN 110
SCHEME 78: REACTION 177 WITH DDQ IN DIOXANE 111
SCHEME 79: PROPOSED STRATEGY FOR D-RING AROMATIZATION. 111
SCHEME 80: ATTEMPTED BROMINATION OF THE D-RING OF 177 WITH NBS 112
SCHEME 81: ATTEMPTED BROMINATION OF 177 WITH COPPER BROMIDE 112
SCHEME 82: BROMINATION OF 174 WITH COPPER BROMIDE 113
SCHEME 83: ATTEMPTED BROMINATION / DEHYDROBROMINATION OF 177 113
SCHEME 84: ATTEMPTED AROMATIZATION OF THE D-RING OF 177 WITH DDQ UNDER ALKALINE CONDITIONS 114
SCHEME 85: STRATEGY FOR THE AROMATIZATION OF THE C-RING OF 174 WITH DDQ UNDER ACIDIC CONDITIONS 115
SCHEME 86: ATTEMPTED AROMATIZATION OF THE C-RING OF 174 WITH DDQ UNDER ACIDIC CONDITIONS 115
SCHEME 87: STRATEGY FOR THE AROMATIZATION OF THE C-RING OF 174 VIA AN ENOL ETHER 116

SCHEME 88: REACTION OF 174 WITH TRIEMETHYLSILYL CHLORIDE AND TRIETHYLAMINE IN ACETONITRILE 117

SCHEME 89: STRATEGY FOR THE AROMATIZATION OF THE C-RING OF 174 UNDER STRONGLY ALKALINE CONDITIONS 117

SCHEME 90: REACTION OF 174 WITH LDA 118

SCHEME 91: FORMATION OF AN ENOL ACETATE FROM A KETONE WITH ISOPROPENYL ACETATE 118

SCHEME 92: REACTION OF 174 WITH ISOPROPENYL ACETATE AND A CATALYTIC AMOUNT OF SULFURIC ACID 119

SCHEME 93: AROMATIZATION OF THE C-RING OF 174 WITH DDQ, ISOPROPENYL ACETATE AND A CATALYTIC AMOUNT OF SULFURIC ACID 119

SCHEME 94: AROMATIZATION OF THE D-RING OF 177 WITH DDQ, ISOPROPENYL ACETATE AND A CATALYTIC AMOUNT OF SULFURIC ACID 120

SCHEME 95: REACTION OF 191 WITH PHENYL CYANATE AND TRIETHYLAMINE 121

SCHEME 96: HYDROLYSIS OF CYANAMIDES AND ISOCYANAMIDES WITH AQUEOUS BASE 131

SCHEME 97: MECHANISM FOR THE FORMATION AND HYDROLYSIS OF AN AZINE 133

SCHEME 98: O'SULLIVAN'S SYNTHETIC STUDY TOWARD PREKINAMYCIN 139

SCHEME 99: THE KEY TO THE ECHAVARREN SYNTHESIS. 141

SCHEME 100: THE SALIENT FEATURES OF ECHAVARREN'S SYNTHETIC STUDIES 143

SCHEME 101: DEPROTECTION AND CYANATION OF KEY INTERMEDIATES IN ECHAVARREN'S SYNTHETIC STUDIES 144

SCHEME 102: PROPOSED STRUCTURES IN ECHAVARREN'S SYNTHETIC STUDY 146

SCHEME 103: PROPOSED STRUCTURES IN ECHAVARREN'S CYANATION REACTIONS 148

SCHEME 104: THE ACCEPTED BIOSYNTHETIC PATHWAY TO THE KINAMYCINS. 150

SCHEME 105: PROPOSED BIOGENETIC HYPOTHESIS 151

SCHEME 106: KINOBSCURINONE IS AN INTERMEDIATE IN THE BIOSYNTHESIS OF KINAMYCIN C 152

SCHEME 107: PROPOSED MECHANISM FOR THE ALKYLATION OF DNA BY THE KINAMYCINS 153

SCHEME 108: PROPOSED MECHANISM FOR THE ALKYLATION OF DNA BY THE REVISED STRUCTURE OF THE KINAMYCINS 154

SCHEME 109: AN ALTERNATIVE PATHWAY FOR THE ALKYLATION OF DNA BY THE REVISED STRUCTURE 155

SCHEME 110: ALKYLATION OF DNA BY THE REVISED STRUCTURE OF THE KINAMYCINS 156

SCHEME 111: ONE POSSIBLE STRATEGY TO THE REVISED STRUCTURE OF PREKINAMYCIN. 158

SCHEME 112: BIOGENETIC INSPIRED STRATEGY FOR THE SYNTHESIS OF NATURAL PRODUCTS RELATED TO THE KINAMYCINS 159

SCHEME 113: ONE POSSIBLE STRATEGY TOWARD 231. 161

SCHEME 114: AN ALTERNATIVE STRATEGY TOWARD 231 162

SCHEME 115: REACTION OF A SUBSTITUTED NAPHTHOQUINONE WITH CYANIDE 163

SCHEME 116: SYNTHESIS OF BROMO-NAPHTHOQUINONE 247 163

SCHEME 117: REACTION OF BROMO-NAPHTHOQUINONE 247 WITH 167 AND 249 UNDER ALKALINE CONDITIONS 164

SCHEME 118: SYNTHESIS OF 250 IN FIVE STEPS FROM 1,5-DIMETHOXY-NAPHTHALENE. 165

SCHEME 119: SYNTHESIS OF CHLORO-NAPHTHOQUINONE 252 165

SCHEME 120: SYNTHESIS OF BROMO-NAPHTHOQUINONE 254 165

SCHEME 121: SYNTHESIS OF TRICHLORO COMPOUND 255 168

SCHEME 122: SYNTHESIS OF THE TRIBROMO COMPOUND 256 168

SCHEME 123: THE MECHANISM PROPOSED FOR THE FORMATION OF 254. 169

SCHEME 124: REACTION OF 254 WITH 167 UTILIZING DIISOPROPYLETHYLAMINE AS THE BASE AT -78°C. 170

SCHEME 125: PROBABLE MECHANISM FOR THE FORMATION OF 258 AND 259 171

SCHEME 126: RESONANCE STABILIZATION OF THE ANION OF BROMO-JUGLONE 172

SCHEME 127: AN ALTERNATIVE STRATEGY TO SCHEME 111. 173

SCHEME 128: ATTACHMENT OF AN ISOPRENYL GROUP TO A BENZOQUINONE SYSTEM THROUGH THE OXIDATIVE DECARBOXYLATION OF THE ACID 264 174

SCHEME 129: ATTACHMENT OF AN ISOPRENYL GROUP TO A NAPHTHOQUINONE 174

SCHEME 130: SYNTHESIS OF TETRANGULOL 175

SCHEME 131: SYNTHETIC STRATEGY TOWARD THE DIACETATE OF THE REVISED STRUCTURE OF PREKINAMYCIN 175

SCHEME 132: DECARBOXYLATIVE COUPLING OF SOME READILY AVAILABLE ACIDS TO THE BROMO-JUGLONE DERIVATIVE 254 176

SCHEME 133: ATTEMPTED INTRAMOLECULAR HECK-LIKE COUPLING OF 270C 177

SCHEME 134: ATTEMPTED INTRAMOLECULAR METAL PROMOTED COUPLING OF 270D AND 270E 177

SCHEME 136: SYNTHETIC STRATEGY TOWARD 272 178

SCHEME 137: DITHIONITE REDUCTION OF 270E 179

SCHEME 138: REDUCTION OF 270E WITH AQUEOUS TRIETHYL PHOSPHITE 179

SCHEME 139: ACETYLATION OF 273 AND 274 WITH ACETIC ANHYDRIDE AND A CATALYTIC AMOUNT SULFURIC ACID 180

SCHEME 140: ONE POT REDUCTION AND ACETYLATION OF 270E 182

SCHEME 141: ATTEMPTED INTRAMOLECULAR METAL PROMOTED COUPLING OF 275 183

SCHEME 142: INTRAMOLECULAR ZINC PROMOTED COUPLING OF 275 183

SCHEME 143: THE ACID 279 WAS GENERATED FROM 167 IN 3 STEPS. 184

SCHEME 144: SYNTHESIS OF THE ACID 279 FROM 167 184

SCHEME 145: ATTEMPTED AROMATIZATION OF THE ESTER 278 185

SCHEME 147: AROMATIZATION OF AN ENONE WITH ISOPROPENYL ACETATE 186

SCHEME 148: ATTEMPTED AROMATIZATION OF THE ENONE 278 WITH ISOPROPENYL ACETATE 187

SCHEME 149: SYNTHESIS OF THE AROMATIC ACID 283 188

SCHEME 150: AN ALTERNATIVE SYNTHESIS OF THE AROMATIC ACID 283 188

SCHEME 151: POSSIBLE SYNTHETIC ROUTE TO THE REVISED STRUCTURE OF PREKINAMYCIN BASED ON METHODOLOGY DEVELOPED IN THIS SECTION 189

SCHEME 152: HECK-TYPE COUPLING REACTION TO GIVE 284 PROGRESSES WITH THE OPPOSITE REGIOCHEMISTRY 190

SCHEME 153: STRATEGY TOWARD THE BROMO-SUBSTITUTED ACID 288 190

SCHEME 154: PROPOSED STRATEGY TOWARD A TETRACYCLIC SYSTEM 190

List of Abbreviations

Ac.....acetyl

Ar.....aryl

Bn.....benzyl

BOC.....*tert*-butoxycarbonyl

br.....broad

calcd.....calculated

CAN.....ceric ammonium nitrate

CI.....chemical ionization (in mass spectrometry)

d .....doublet

DBU.....1,8-diazabicyclo[5.4.0]undec-7-ene

DDQ.....2,3-dichloro-5,6-dicyano-1,4-benzoquinone

DIBALH.....diisobutylaluminum hydride

DMAP.....4-(dimethylamino)pyridine

DMD .....dimethyldioxirane

DMF.....dimethylformamide

DMSO .....dimethyl sulfoxide

DNA.....deoxyribonucleic acid

DPA .....diisopropylethylamine

EI.....electron impact

EtOAc .....ethyl acetate

g .....gram(s)

Hex .....hexane

HOMO .....highest occupied molecular orbital

HPLC.....high-performance liquid chromatography

LDA.....lithium diisopropylamide

LUMO.....lowest unoccupied molecular orbital

m/z .....mass to charge ratio (in mass spectrometry)

*m*CPBA .....*meta*-chloroperoxybenzoic acid

Me.....Methyl

MHz .....megahertz

mol.....mole(s)

mp.....melting point

MS .....mass spectrometry

NBS.....*N*-bromosuccinimide

NMR.....nuclear magnetic resonance

NOE.....Nuclear Overhauser Effect

p-TSA.....*para*-toluenesulfonic acid

Ph.....phenyl

ppm.....parts per million

q .....quartet

t.....triplet

THF.....tetrahydrofuran

TLC.....thin layer chromatography

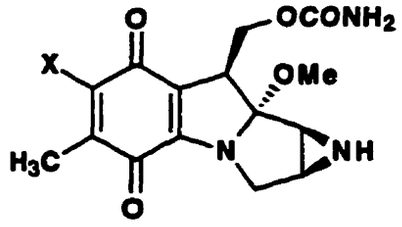
TMSCl.....trimethylsilyl chloride

Chapter 1: Introduction

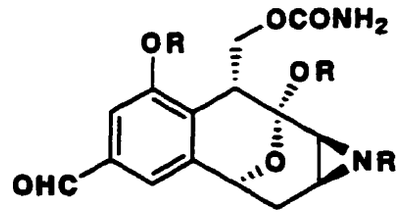
The search for naturally occurring compounds with therapeutically effective anticancer activity has been underway for some time. Although useful anticancer agents have been isolated from plant sources, the screening of novel strains of soil bacteria for bioactive substances has become one of the most productive avenues of research in this area.

One of the notable successes in this area was the isolation of the mitomycins[1] (1) from *Streptomyces* cultures some decades ago. The mitomycins (e.g. mitomycin C, X=NH_2, Figure 1) have not only proven to be useful chemotherapeutic agents, especially against solid tumours due to their hypoxic environments[2-6], but have also helped to define a novel strategy towards selective antitumour activity based on bioreductive activation which had not been previously imagined.[3] Two decades ago, the structurally novel kinamycins (3) were isolated[7-9] from *Streptomyces murayamaensis* and proposed to function as antitumour antibiotics via a bioreductive activation mechanism[10] related to that established for the mitomycins. Much more recently, antitumour antibiotic FR-900482 (2) has been isolated[11,12] from *Streptomyces sandaensis* and has been shown, as its triacetyl derivative (FK-973), to possess antitumour activity which is superior to that of mitomycin C with some tumour cell lines and to function via a bioreductive activation mechanism which results in DNA alkylation analogous to that observed with mitomycin C.[13,14]

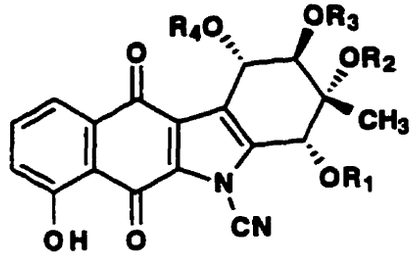
Outlined below is an overview of the current state of knowledge related to each of these antitumour agents followed in Chapter 2-6 by a disclosure of the results of chemical studies in the development of methods for the synthesis of the kinamycins and FR-900482 as well as bioactive analogues.



1 mitomycin



2a R = H FR900482
R = Ac FK-973



3 kinamycin

Figure 1

1.1 The Mitomycins

As indicated above, the mitomycins are a class of structurally unique potent antitumour antibiotics.[15] One member in particular, mitomycin C, shows strong activity against a variety of tumours. As a result of the favourable activity against neoplasms, considerable effort was directed toward determining its mode of action.[16] It is believed that the favourable therapeutic index is owed to selective bioactivation within a tumour cell followed by either mono or bisalkylation of DNA eventually resulting in the death of the cancerous cell.[10,17] Furthermore, the mitomycins have also garnered considerable attention from synthetic chemists[18-22], in the belief that analogues generated synthetically might show enhanced activity toward tumour cells or decreased toxicity toward healthy cells. Construction of the unique carbon-nitrogen skeleton of the mitomycins has proved, however, to be synthetically difficult.

As a result, there has been a large number of published approaches[18-22] but only two successful, albeit lengthy, total syntheses[23-25] of the mitomycins.

1.1.1 Isolation, Structure and Stereochemistry

The mitomycins are a class of potent antitumour antibiotics which share a distinctive carbon-nitrogen skeleton commonly referred to as a mitosane nucleus (**4**) (Figure 2). The mitosane nucleus is comprised of the following moieties: aminobenzoquinone, aziridine, pyrrolo[1,2-a]indole system as well as a carbamate moiety at C-10. The unsaturated form is generally referred to as a mitosene (**5**).

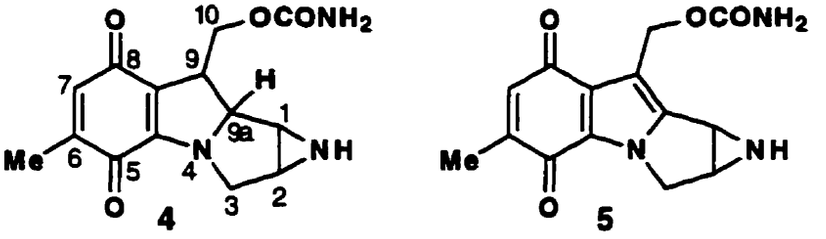


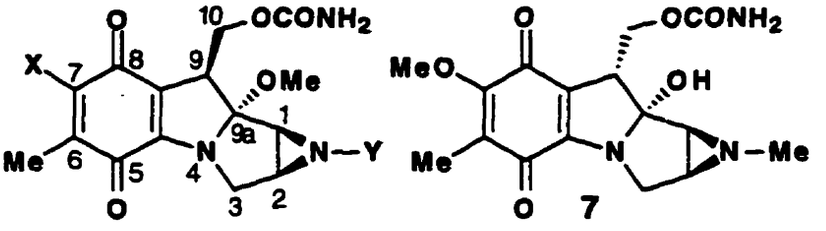
Figure 2

The observation by Hata *et al.*[1] that the fermentation broth of certain strains of soil bacteria of the genus *Streptomyces* showed a remarkably high activity against a diverse group of organisms, including specific cancers, led to the isolation of mitomycin A (**6**) and B (**7**). Shortly thereafter, mitomycin C (**8**)[26], porfiromycin (**9**)[27] and mitiromycin[28] were discovered by others. Presently, there are fifteen known mitomycins.

In general, it is found that mitomycin A (**6**) is produced in greatest abundance, although minor alterations in the fermentation conditions can result in mitomycin C

(**8**) in greatest yield.[26,29] This suggests a close biosynthetic relationship between mitomycin A and mitomycin C.

The elucidation of this unusual carbon-nitrogen skeleton posed a considerable challenge. The structure was eventually defined by a combination of chemical and spectroscopic studies by Webb *et al.*[30] Tulinsky[31] and later Hornemann and Heins[32] confirmed the assigned structure by single crystal X-ray diffraction studies. The more common mitomycins as well as the stereochemical relationships between them are shown in Figure 3.[32]



		X	Y
6	mitomycin A	OMe	H
8	mitomycin C	NH_2	H
9	porfiromycin	NH_2	Me

Figure 3: The structures of the more common mitomycins.

Mitomycin A (**6**), mitomycin C (**8**) and porfiromycin (**9**) have the carbamoyloxymethyl group trans to the substituent at C-9a and cis to the aziridine ring. Mitomycin B (**7**) on the other hand, has the carbamoyloxymethyl group cis to the C-9a substituent and trans to the aziridine ring (Figure 2).[32]

Isomitomycin A (**10**) and albomitomycin A (**11**), two structurally novel mitomycins, have been discovered more recently (Figure 4).[33,34] At first glance, both isomitomycin A (**10**) and albomitomycin A (**11**) lack some of the features of the

mitosane nucleus. They do, however, contain the aminobenzoquinone and carbamate functionalities. Both isomitomycin A (**10**) and albomitomycin A (**11**) exist in equilibrium with mitomycin A (**6**). The equilibrium in solvents with differing polarities strongly favours mitomycin A (**6**) (Figure 5). In acetonitrile the equilibrium composition is 85% mitomycin A (**6**), 4% albomitomycin A (**11**) and 11% isomitomycin A (**10**), while in THF the composition is 95% mitomycin A (**4**), 3% albomitomycin A (**11**) and trace amounts of isomitomycin A (**10**) (Figure 5).[33,34]

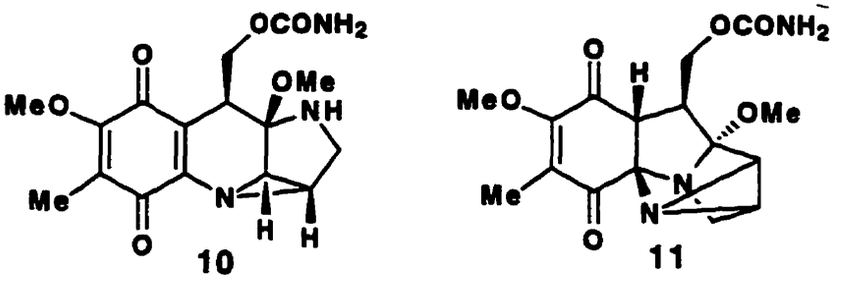


Figure 4

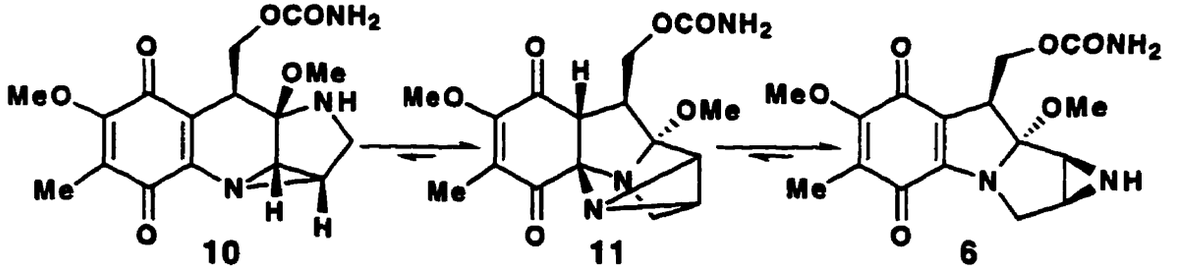


Figure 5: **The equilibrium between isomitomycin A, albomitomycin A and mitomycin A.**

Fukuyama and Yang[25] capitalized on this equilibrium in one of only two total syntheses of the mitomycins which will be discussed later in more detail.

1.1.2 Mode of Action

The mode of action of the mitomycins will be discussed in terms of mitomycin C, which is currently being utilized clinically and is the most studied member of its class.[29]

Although, mitomycin C is currently being utilized clinically in the treatment of specific tumours (e.g. Sarcoma 180), its relatively high toxicity has precluded its use as an antibiotic. Regardless of the general toxicity, mitomycin C still shows a favourable therapeutic index and has thus been the focus of attention by both biochemists and organic chemists. Biochemists have been interested in the mode of action as well as the biosynthesis of mitomycin C, whereas synthetic chemists have been interested in the synthesis of the unusual carbon-nitrogen skeleton.

Mitomycin C requires bioactivation within a cell before damaging the DNA which eventually results in cell death. This activation involves a bioreduction which then triggers a cascade of events in the presence of DNA resulting in monofunctional or bifunctional alkylation of the nucleic acid.[35] Initially, it was believed that activation was in the form of a two electron reduction to the hydroquinone (Figure 6, path a); but more recently evidence suggests that a one electron reduction to the semiquinone is adequate (Figure 6, path b).[15,36-40]

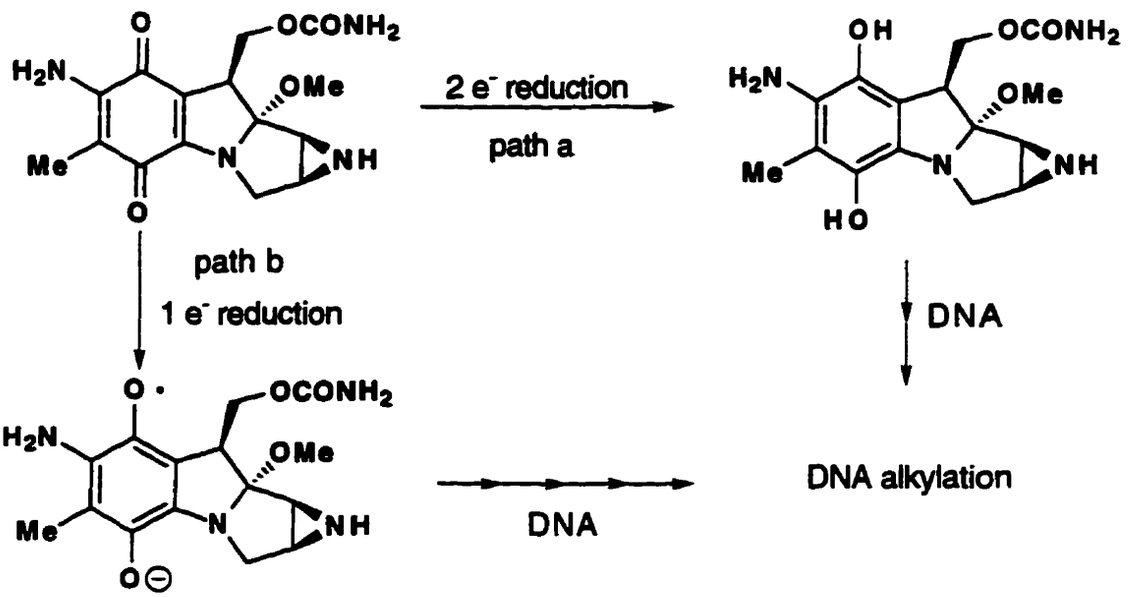


Figure 6: Two possible modes of bioreductive activation of mitomycin C.

It has also been found that acidic conditions favour more rapid activation. The mode of activation of mitomycin C (**8**) as well as the enhanced rate of activation in acidic environments is intriguing in light of evidence indicating that many solid tumours have reductive and acidic environments. The poor vascularization of some solid tumours causes hypoxia which leads to the observed reductive and acidic environments.

Once activated, mitomycin C (**8**) alkylates guanine residues on DNA either monofunctionally or bifunctionally. Tomasz *et al.* [41]reduced mitomycin C with sodium dithionite in the presence of DNA which was then digested and the components isolated. Adducts isolated were in the quinone oxidation state with mitosenes mostly alkylated monofunctionally at C-1 (**12** and **13**) with a minor amount having alkylation at both C-1 and C-10 (**14**) (Figure 7).[42]

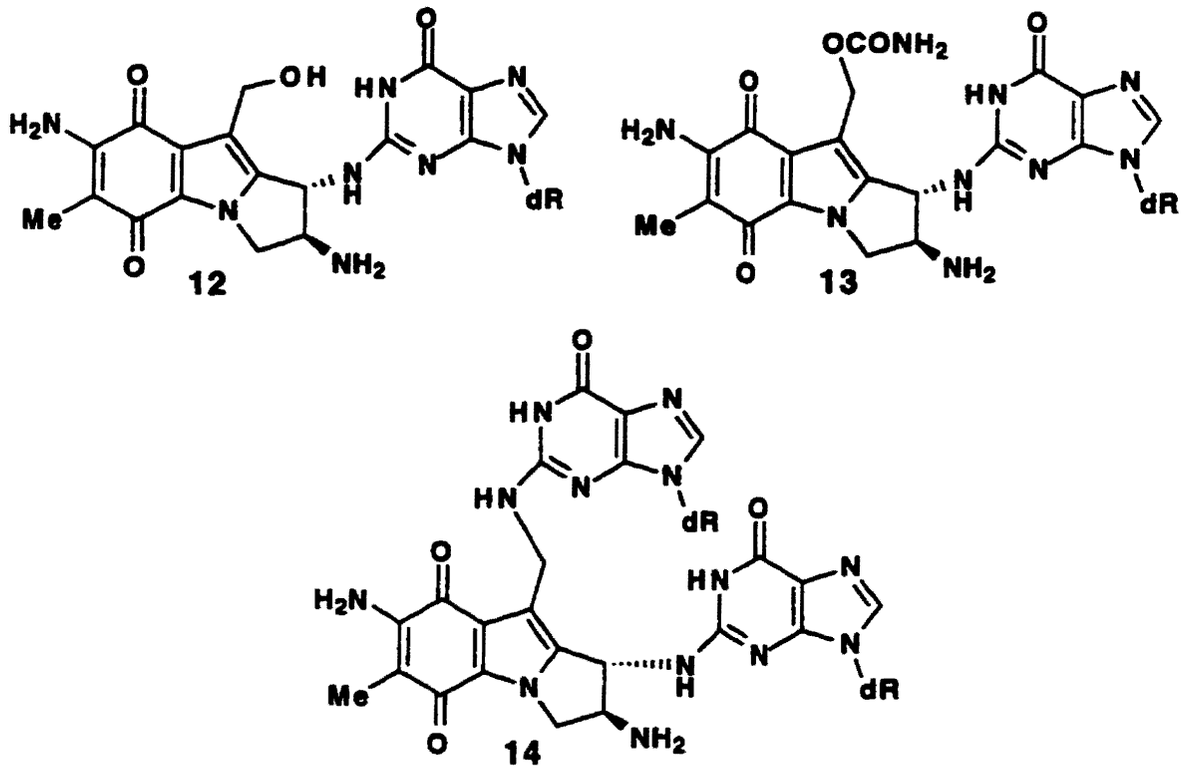
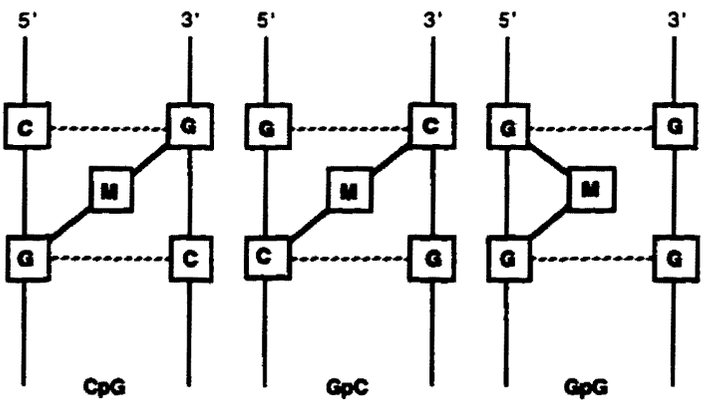


Figure 7

The ratio of monoalkylation (**12** and **13**) to bisalkylation (**14**) was 10-20:1 and it was likely that the cross-linking was responsible for the effectiveness of mitomycin C as an antitumour compound.[42] Cross-linking of DNA is potentially possible in three ways: CpG, GpC and GpG (Figure 8)

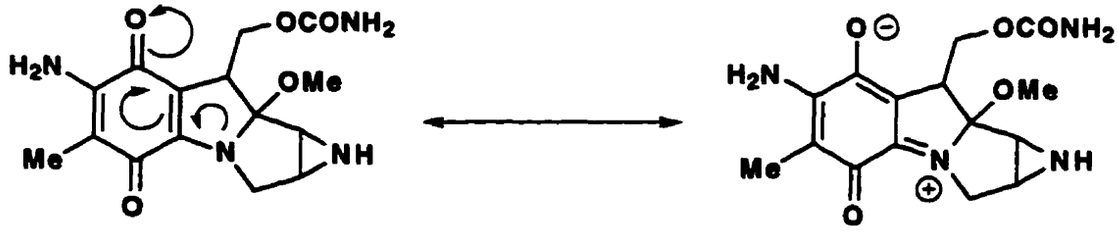


C = cytosine; G = guanine; M = mitomycin

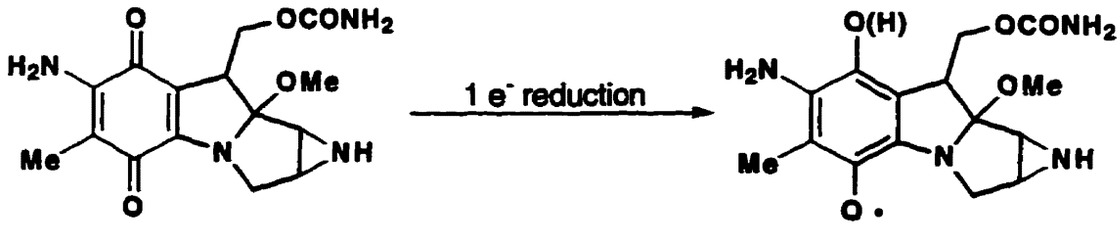
Figure 8: **Three possible ways in which mitomycin C could potentially cross-link DNA.**

Experiments aimed at determining sequence specificity showed that cross-linking of DNA by mitomycin C was indeed sequence specific and that the site of cross-linking was exclusively CpG.[42,43] Furthermore, extensive molecular modeling experiments[16,36] indicated that it was likely that once mitomycin C was reduced within the cell, it was directed into the appropriate position for cross-linking by secondary interactions with the polynucleotide. It was also found that monovalent complexes in the major groove were energetically destabilizing relative to their minor groove counterparts.[36] Cross-linking in the major groove resulted in a two base pair disruption; whereas cross-linking in the minor groove left the base pairs intact. It appears that monoalkylation is not sequence specific and only in those monalkylation sites that have a guanine on the opposite strand in the correct geometric location, as with CpG sequences, will mitomycin C form cross-links.[36] Moreover, when several CpG units are present in a row, the cross-linking is enhanced relative to that for an isolated CpG unit.[16] The origin of this enhancement is not well understood.[41-43]

Prior to reduction, the lone pair of the nitrogen of the pyrrolo[1,2-a]indole functionality is in resonance with the quinone (Scheme 1). Upon reduction of mitomycin C the importance of this type of resonance is greatly diminished (Scheme 2).

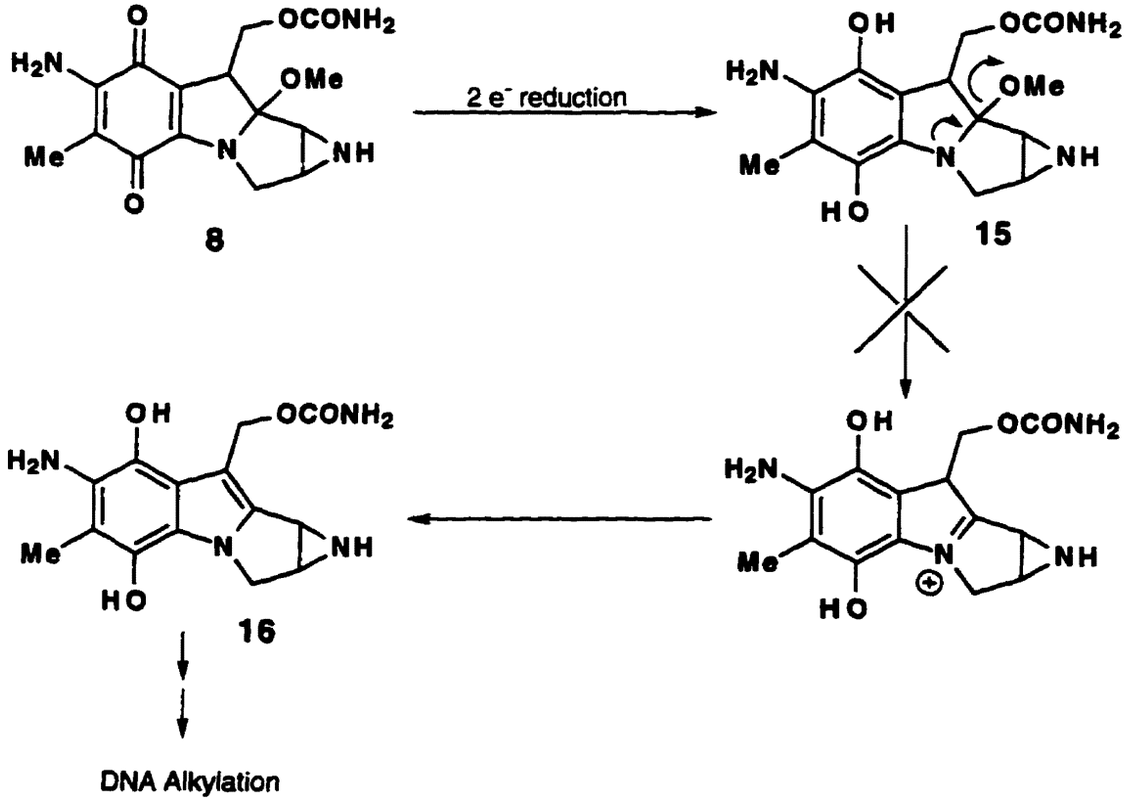


Scheme 1



Scheme 2

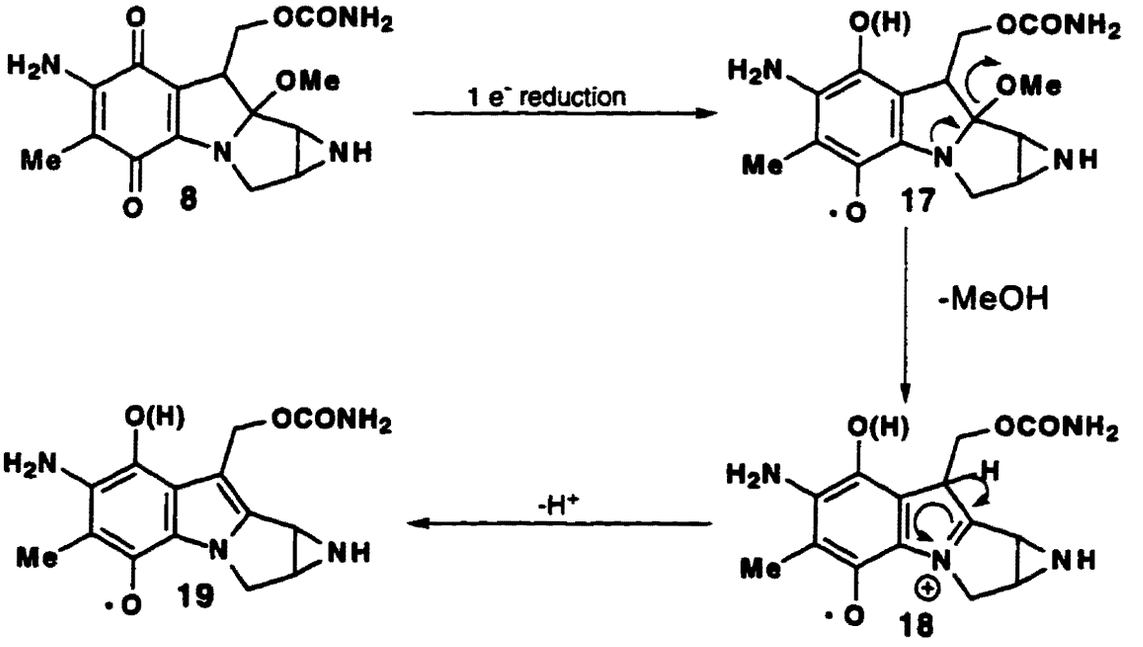
Although a two electron reduction model for the activation of mitomycin C has been proposed[15], recent evidence has suggested that the active form is the semiquinone, which may or may not be protonated.[36] It was believed that reduction to the hydroquinone (**15**) triggered a release of methanol followed by loss of a proton to the aromatic (aziridinomitosene) system (**16**) which then underwent a cascade of events leading to the alkylation of DNA (Scheme 3).



Scheme 3: **A two electron reduction of mitomycin C to the hydroquinone is not sufficient to trigger loss of methanol.**

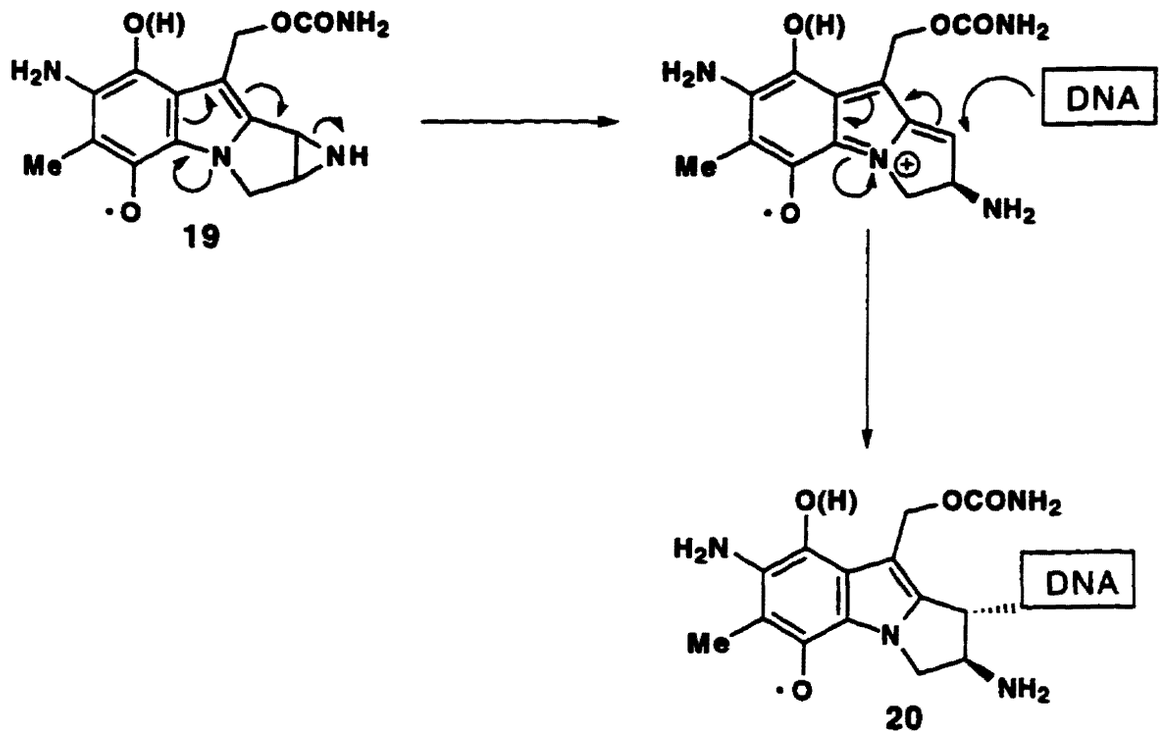
Danishefsky and Egbertson[38] found that, with an excess of reducing agent and rigorous exclusion of oxygen, the hydroquinone was stable and showed little tendency to lose methanol. However, the hydroquinone **15** in the presence of oxygen or the quinone **8** in the presence of ascorbic acid readily lost methanol.[38] Also, the quinone **8** in the presence of a catalytic amount of dithionite and in the presence of a nucleophile resulted in 80% of combined yield of alkylated products, suggesting that the process was autocatalytic.[36] This correlates well with an active species in the semiquinone oxidation state and observed products in the quinone oxidation state.

The cascade of events leading to DNA alkylation for the one electron reductive activation model will now be described. Upon reduction to the semiquinone **17**, there is participation of the lone pair of the nitrogen in the concomitant loss of methanol to form the iminium ion **18**, which is followed by conversion to the aziridinomitosene **19** (Scheme 4).[36,38]



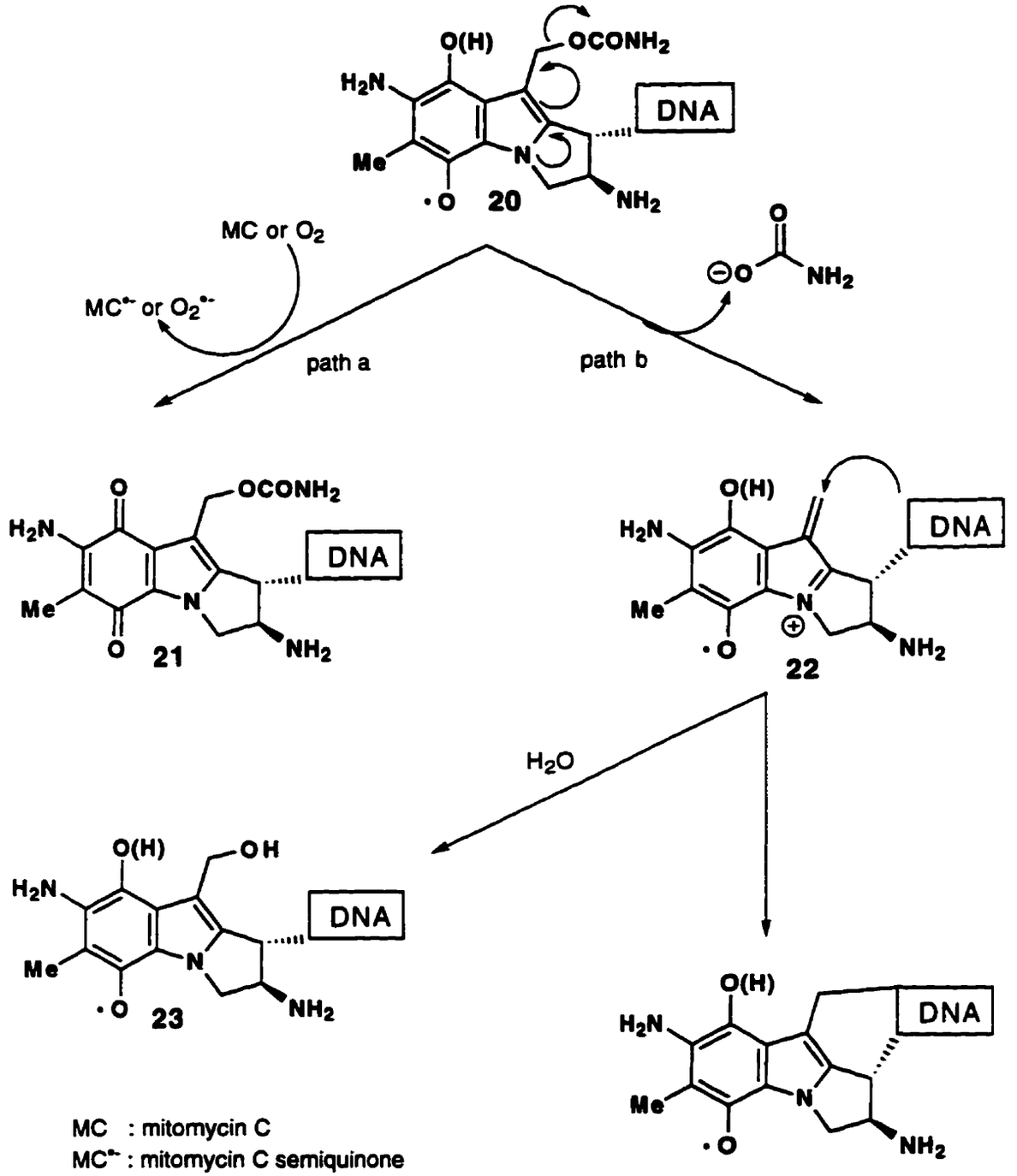
Scheme 4: **A one electron reduction to the semiquinone results in the loss of methanol.**

The aziridinomitosene **19** can then undergo ring opening at the aziridine which is then primed for alkylation by DNA. Nucleophilic attack by DNA at C-1 results in monofunctional alkylation to give **20** (Scheme 5).



Scheme 5

The monoalkylated product may then react by either of two pathways: in path a (Scheme 6), an electron transfer to either oxygen or an unactivated mitomycin C (**8**) to give the stable mono adduct in the quinone oxidation state **21** (Scheme 6). In path b, loss of carbamate results in **22** which is activated toward nucleophilic attack. The iminium ion **22** may then cross-link DNA if a guanine residue is in a favourable position, or alternatively the activated form may be attacked by water to give **23** (Scheme 6). The reaction of the semiquinone with oxygen (path a) may explain the observed oxidative scission of DNA observed in aerated cells when treated with mitomycin C.



Scheme 6: Possible pathways leading to mono and bis alkylated DNA.

Scheme 6 would suggest that only a catalytic amount of electron reducing equivalents is necessary to induce a stoichiometric activation in a chain reaction to alkylate the mitomycins. This scheme would also seem to indicate that product distribution is subject to reaction conditions; thus, the extent of monoalkylation

versus bisalkylation may be controlled. Also, this autocatalytic mechanism would favour products in the quinone oxidation state which is what is observed.[37] It was also found that the overall binding of mitomycin C to DNA in the presence of oxygen decreased by 20% as compared with the anaerobic counter experiment.[43] Furthermore, reduction of mitomycins with 0.3 equivalents of sodium dithionite in the presence of a nucleophile gave 80% alkylated products.[36] Therefore, the extent of alkylation substantially exceeds the availability of reducing agent.[36]

1.1.3 Synthetic Approaches to the Mitomycins

Although a considerable number of approaches to the unique carbon-nitrogen skeleton of the mitomycins has been published[22,44], only two total syntheses have appeared in the literature. The synthetic strategies explored to date can be broken down into four basic approaches. Routes I, II and III involve the construction of a two ring system followed by development of rings A, B or C to complete the synthesis (Figure 9). Route IV, however, utilized by Kishi in his total synthesis of mitomycin A and C, involves formation of a bicyclic system followed by a transannular cyclization to complete the synthesis.

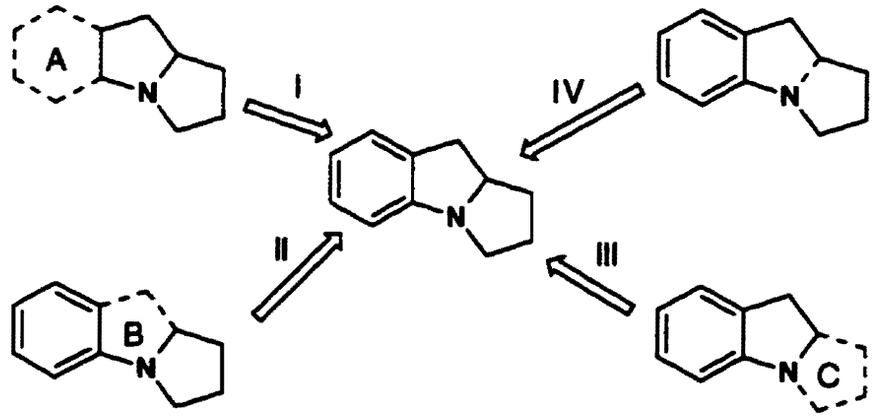
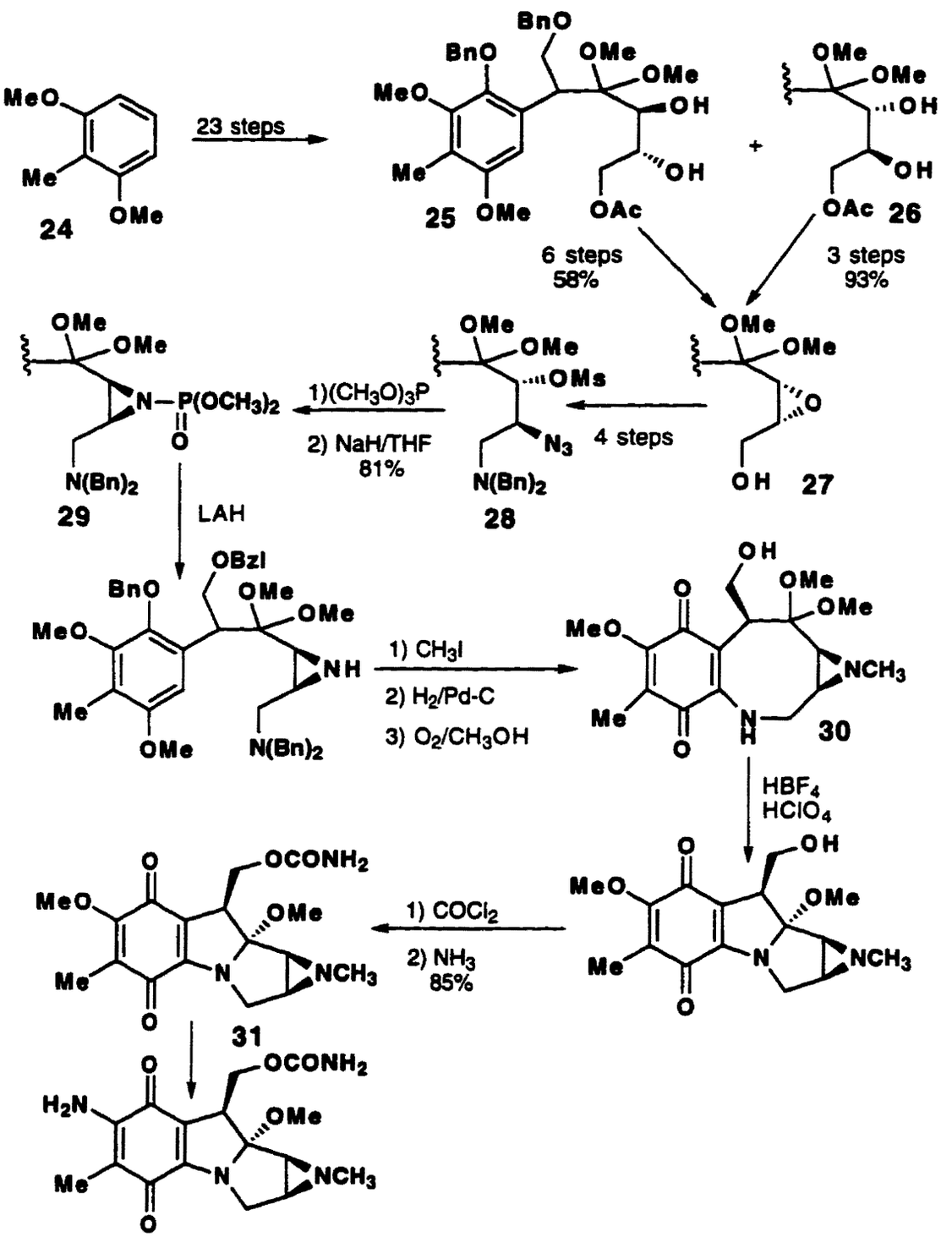


Figure 9: **Synthetic strategies to the mitomycin skeleton.**

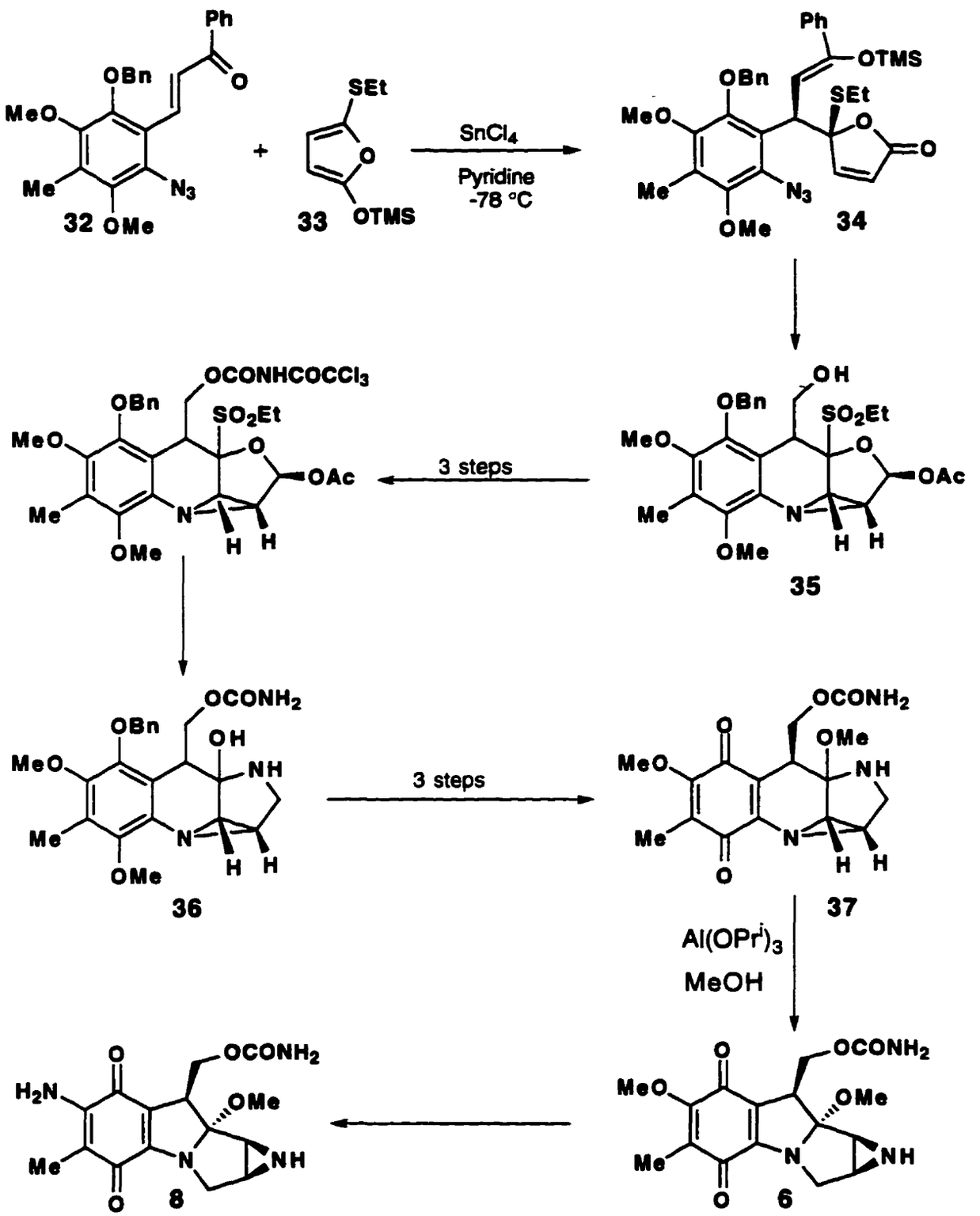
Kishi's synthesis[23,24] was the first successful total synthesis of the mitomycins and the key steps are outlined in Scheme 7.



Scheme 7: The key steps in Kishi's synthesis of the mitomycin C.

The starting material for this lengthy synthesis was the commercially available dimethoxytoluene (**24**) which was converted to a diastereomeric mixture of diols **25** and **26**, in racemic form, in twenty three steps. The diastereomers were separated and were converted to the epoxide **27** in separate sequences. This epoxide was then converted to the azide **28** in four steps and then cyclized to the substituted aziridine **29**. The substituent on the aziridine ring was then removed with lithium aluminum hydride. Reductive removal of the benzyl protecting groups followed by oxidation afforded the bicyclic product **30**. Lewis acid catalyzed cyclization followed by functionalization of C(10) gave N-methylmitomycin A (**31**). Although the synthesis is flexible enough to provide the mitomycin A, the large number of steps coupled with the low overall efficiency makes the strategy impractical for either the commercial production of the known mitomycins or for the synthesis of analogues. The unique approach utilizing a transannular cyclization to complete the synthesis of the mitomycin nucleus makes the strategy interesting.

The more recent total synthesis by Fukuyama[25], capitalizes on the known equilibrium between isomitomycin A (**10**) and mitomycin A (**6**) (Figure 5). The key steps in the synthesis are outlined in Scheme 8.



Scheme 8: **The key steps in Fukuyama's total synthesis of mitomycin A and mitomycin C.**

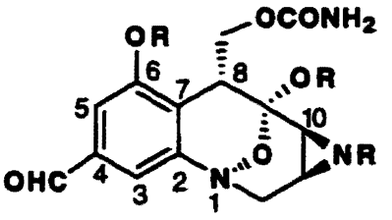
Fukuyama also began his synthesis with the commercially available dimethoxytoluene (**24**) and arrived at the chalcone **32** in thirteen steps. The chalcone **32** was reacted with 2-trimethylsiloxy-5-ethylthiofuran (**33**) in the presence of stannic chloride at -78 °C to give the TMS enol ether **34**. In four steps the labile enol ether was converted to the alcohol, the sulfide to the sulfone, the lactone to the acetate, and the azido-olefin to the aziridine to give **35**. A further four steps yielded the hemi-aminal **36** which was then converted to the quinone **37** in three more steps. The quinone **37** in methanol underwent rearrangement to mitomycin A (**6**), which was then converted to mitomycin C (**8**) under ammonolysis conditions. The synthesis of mitomycin A was accomplished in 30 steps with an overall yield of 6% from dimethoxytoluene. Athough this synthesis is more efficient than Kishi's synthesis from the same starting material, it still involves a large number of steps making the synthesis of analogues impractical by this route.

1.2 FR-900482

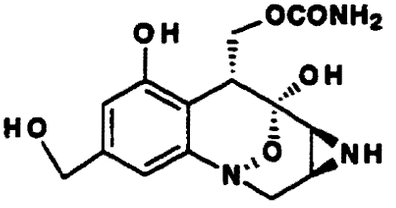
1.2.1 Isolation, Structure and Stereochemistry

FR-900482 (**2**) and its reduction product, FR-66979 (**38**) have recently been discovered in the fermentation broth of *Streptomyces sandaensis* No. 6897 at Fujisawa Pharmaceutical Co. in Japan.[11,12] (Figure 10). This structurally novel compound shows weak antimicrobial activity against both gram-positive and gram-negative organisms as well potent antitumour activity against a variety of tumours (e.g. mammary carcinoma FM3A, leukemia p388 and melanoma B16).[11,12] The triacetyl derivative, FK-973 (**39**) shows much stronger antitumour activity than mitomycin C with less toxicity.[45] Structurally related to the mitomycins, FR-900482 contains an aziridine, a carbamoyloxymethyl group but differs from the mitomycins by

lacking the quinoid portion. It also contains a unique bicyclic hydroxylamine hemiketal moiety.

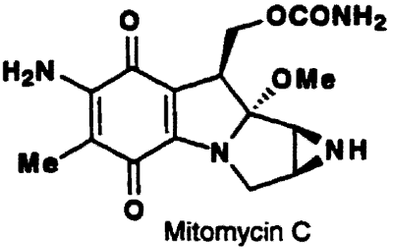


2a) FR-900482 (R = H)
39) FK-973 (R = Ac)



FR-66979

38

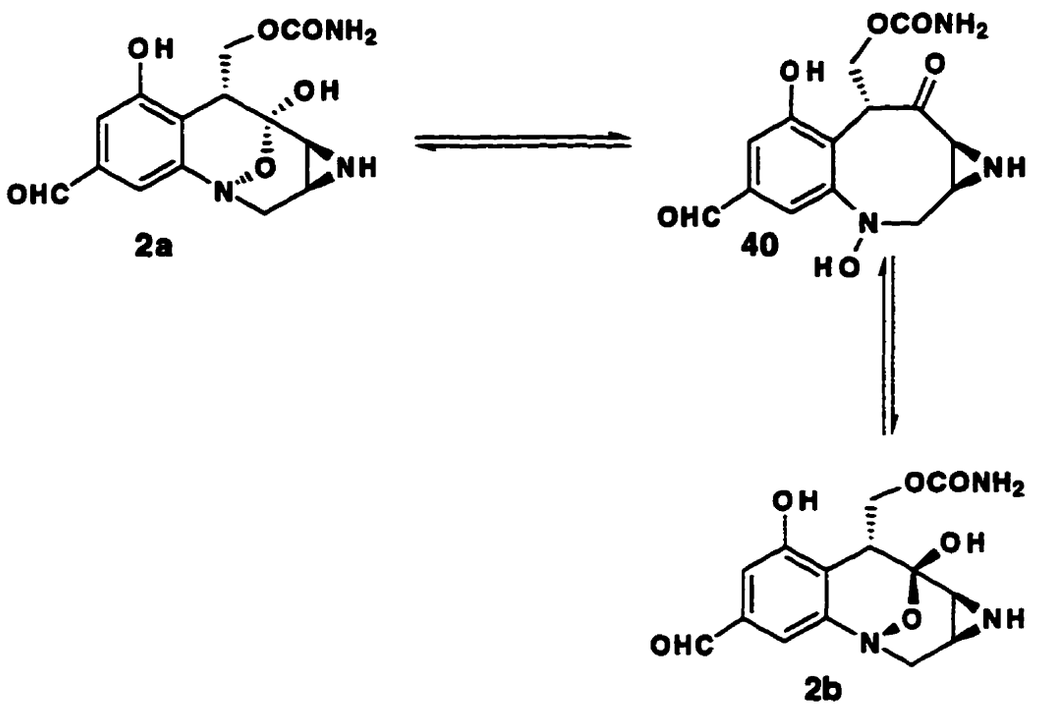


Mitomycin C

8

Figure 10

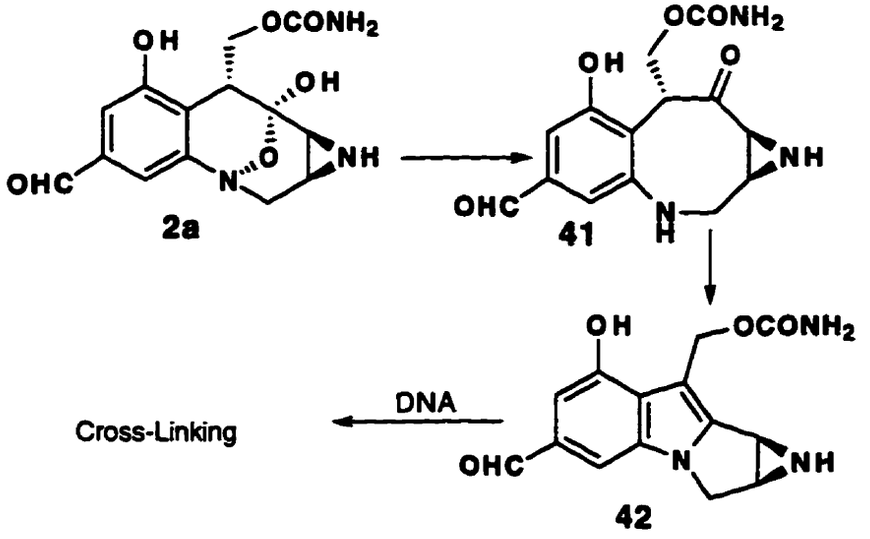
FR-900482 (**2**) exists as a mixture of diastereomers (**2a** and **2b**) which probably interconvert via a keto intermediary **40** (Scheme 9). Structure **2b** is favoured in this equilibrium because of intramolecular hydrogen bonding between the aziridine NH and the bridging oxygen.



Scheme 9

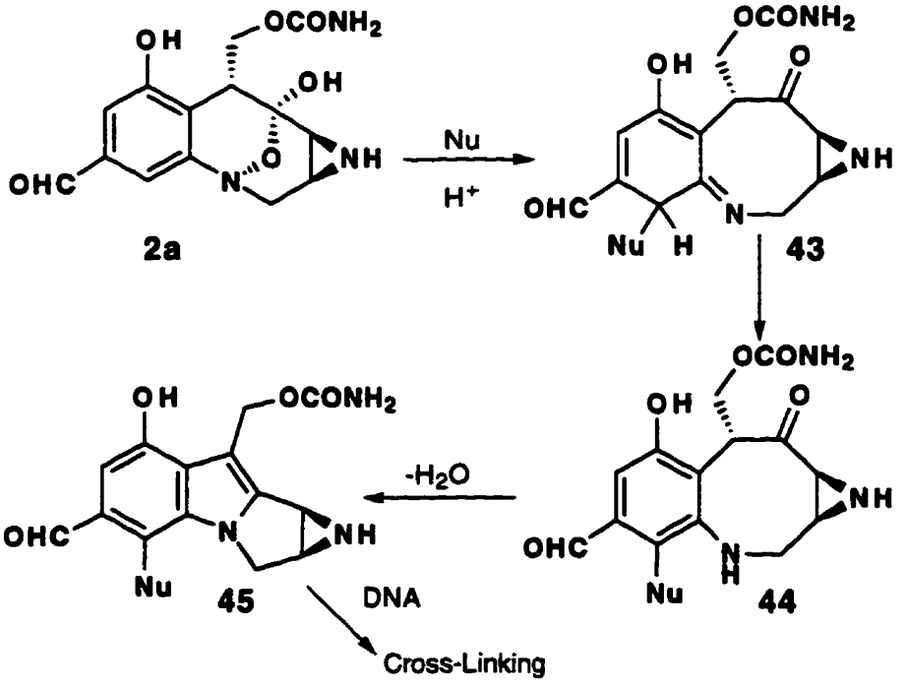
1.2.2 Mode of Action

Both FR-900482 (**2**) and its reduction product, FR-66979 (**38**) have been shown to form DNA cross-links upon activation within cells.[14,46] The nature and requisite activation in forming these cross links is similar to what is observed with mitomycin C. It has been suggested that FR-900482 may undergo a reductive activation to a mitosene-like intermediate which then goes on to alkylate DNA[14] (Scheme 10). Fukuyama[47] has proposed that FR-900482 may undergo a two electron reduction resulting in cleavage of the N-O bond of the hemiacetal to afford **41**. This aniline **41** could then undergo cyclization followed by dehydration to give a mitosene-like structure **42** (Scheme 10).[47] This mitosene-like structure could participate in a cascade of events analogous to those proposed for mitomycin C (Schemes 4 and 5), resulting in the alkylation of DNA (Scheme 10).



Scheme 10: Fukuyama's proposal for bioreductive activation of FR-900482.

McClure and Danishefsky[21] have also proposed a mitosene-like intermediate which is suggested to alkylate DNA (Scheme 11). The form of activation, however, is suggested to be a nucleophilic attack on the aromatic system leading to a ring opened compound **44**. The aniline **44** then cyclizes followed by dehydration leading to the mitosene-like intermediate **45**.[21]



Scheme 11: Danishefsky's proposal for bioactivation of FR-900482.[21]

Experiments carried out by Williams and Rajski[14] in which FR-900482 was reacted with duplex DNA in the presence of mercaptan additives showed cross-linking. In the absence of mercaptans, however, cross linking was not observed. It was found that a molar equivalent of mercaptan was required for efficient cross linking. FR-66979 under the same conditions showed more efficient cross linking than FR-900482. Interestingly, FR-66979 showed good cross-linking in the absence of mercaptans, suggesting that FR-66979 may function without requiring reductive bioactivation.[14]

Woo *et al.* [13] also observed greatly enhanced cross-linking in reducing environments for both FR-900482 and FR-66979. In contrast to Williams and Rajski[14,45], Woo has found that cross-linking was not observed in the absence of a reducing agent for FR-66979; suggesting that reductive activation is necessary for cross-linking.[13] It was also observed, as with the mitomycins, that there was a high degree of sequence specificity in cross-linking of DNA by both FR-900482 and FR-66979. As with the mitomycins DNA cross-linking occurred at CpG sites (Figure 8) and also showed the same specificity for flanking sequences 5'-d(ACGT) >> 5'-d(TCGA) ≈ 5'-d(CCGG) as found for mitomycin C.[13] Furthermore, Woo *et al.*[13] have isolated and characterized DNA-FR-900482 and DNA-FR-66979 adducts which have been tentatively assigned as **46a** and **46b** (Figure 11). These are structurally similar to adducts such as **47** isolated from the reaction of DNA with mitomycin C. This suggests that the mitosene-like intermediate postulated as the bioreactive species is likely involved in DNA alkylation, although the mechanistic details need to be worked out further. The observation of these adduct also appears to favour the mechanism of activation proposed by Fukuyama[47] rather than that proposed by Danishefsky.[21]

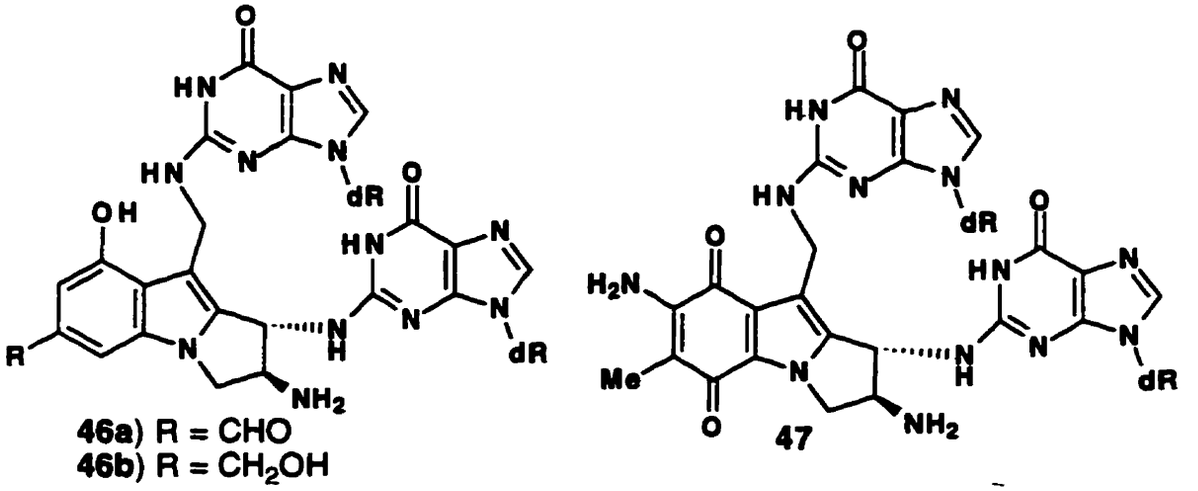


Figure 11: **DNA adducts isolated from the reduction of FR-900482 and mitomycin C in the presence of DNA**

1.2.3 Synthetic Studies

There are many[20,21,47-50] novel and interesting synthetic approaches to FR-900482 in the literature but only two total syntheses.[51,52] The first total synthesis was reported in 1992 by Fukuyama *et al.*[51] The key to this synthesis was a unique transannular cyclization which provided the core of the FR-900482 system (Figure 12).

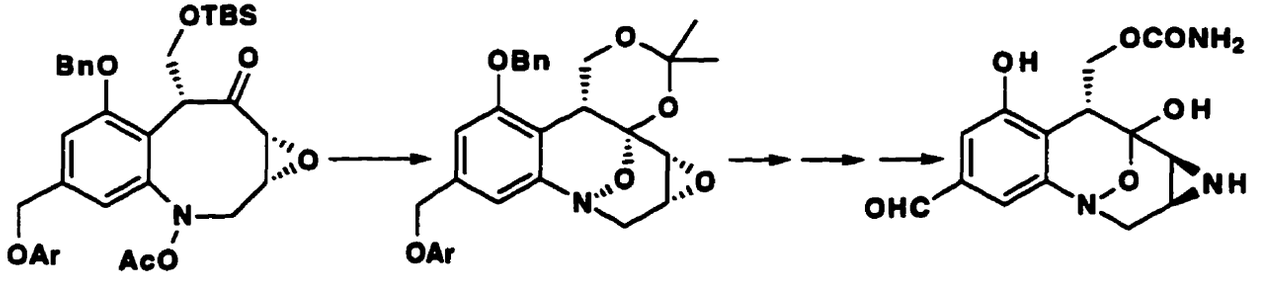
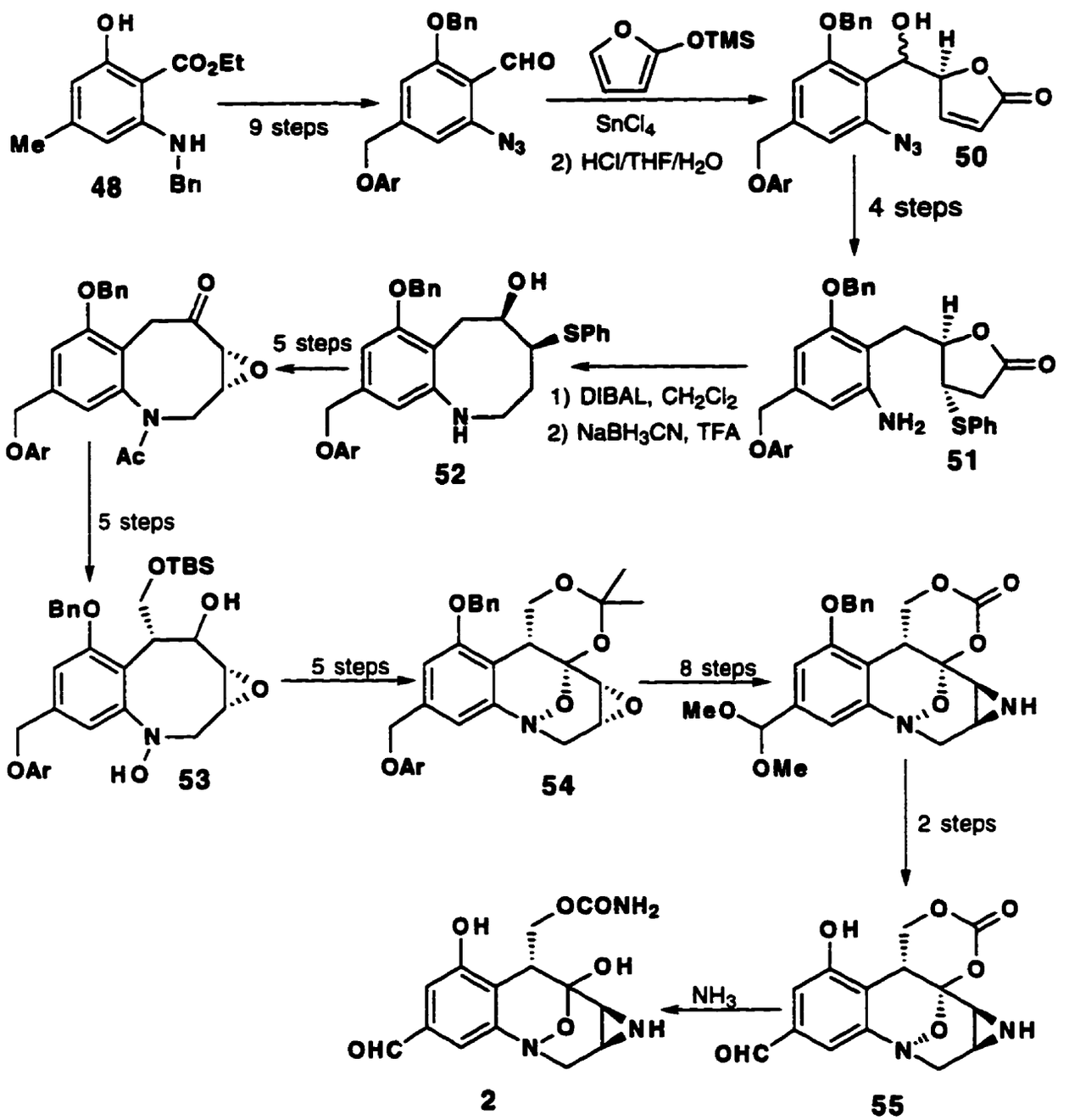


Figure 12: **Key steps in Fukuyama's total synthesis of FR-900482.**

The readily available N-benzylamine **48** was utilized as the starting material (Scheme 12). In nine steps the ester was converted to the aldehyde, the benzylamine to the azide, the phenol to the benzyl ether and the methyl group to an aryl benzyl ether. Condensation with 2-trimethylsilyloxy-furan (**49**) gave the alcohol **50**. In four steps the alcohol was removed, the azide was reduced to the amine and the olefin was masked as the thioether to give **51**. The cyclization to the eight membered ring compound **52** was achieved by sequential reduction of **51** by DIBALH and by sodium cyanoborohydride. In five steps, the alcohol was oxidized to the ketone, the masked olefin was liberated and epoxidized and the amine was protected as the acetonide. In five more steps, Fukuyama obtained **53**. Oxidation of the free alcohol, deprotection of the silyl ether and acetonide formation afforded **54**, containing the desired ring system of FR-900482. In a further ten steps the protecting groups were removed, the epoxide was converted to the aziridine and the aldehyde unmasked to give **55**. This was then treated with ammonia in methylene chloride to give the desired ring system of FR-900482 (**2**).



Scheme 12: **Key steps in Fukuyama's total synthesis of FR-900482.**

The second more recent strategy by Schkeryantz and Danishefsky[52] utilizes a key Heck cyclization to arrive at the central core of the FR-900482 system (Figure 13).

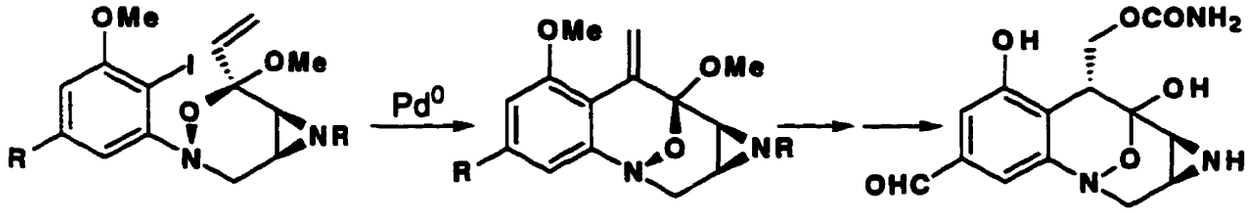
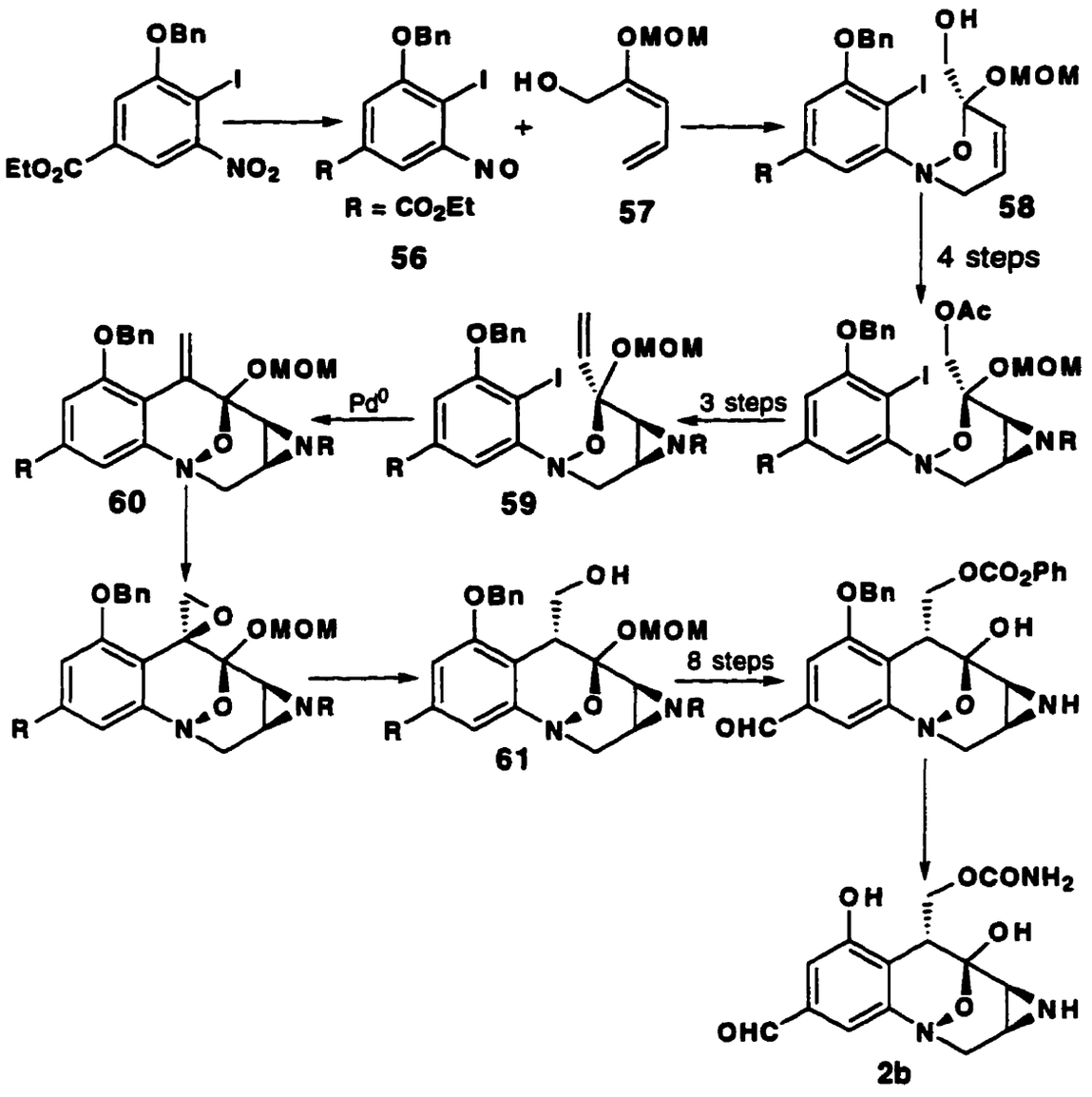


Figure 13: The key steps in Danishefsky's total synthesis of FR-900482

A hetero Diels-Alder reaction of the heavily functionalized nitroso compound **56** with the diene **57** provided the adduct **58** (Scheme 13). The free hydroxyl was then converted to the olefin to give **59** which then underwent a Heck cyclization[53,54] to gave **60**, containing the core of FR-900482 (**2**). The olefin was then epoxidized and subsequently ring opened and reduced with samarium iodide to give **61** which contains the appropriate handles to introduce the desired functionalities. In a further ten steps, the desired system **2b** was generated.



Scheme 13: Danishefsky's total synthesis of FR-900482

1.3 The Kinamycins

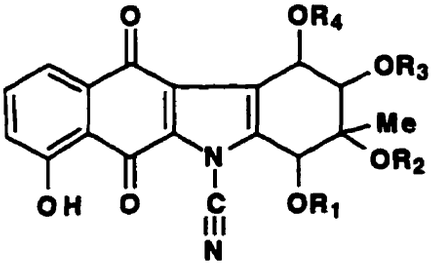
1.3.1 Isolation and Structure

The kinamycin antibiotics were first isolated from the culture broth of *Streptomyces murayamaensis*.[7,9] They are strongly active against gram positive organisms and show much weaker activity against gram negative bacteria.[7,9] Erlich ascites carcinoma as well as sarcoma 180 are weakly affected by the kinamycin

antibiotics.[9] Four structurally similar components were isolated and were denoted as kinamycins A, B, C and D, of which C and D are the major components (Figure 14).[9] These compounds were found to be soluble in methanol, chloroform, ethyl acetate, benzene; only slightly soluble in diethyl ether; and insoluble in petroleum ether, hexane and water.[9] Although stable in neutral or acidic solutions, the kinamycins were found to be quite unstable in alkaline solutions.[9]

Spectroscopic studies assigned only a partial structure to the kinamycin antibiotics.[8,55] The fragments of the kinamycin skeleton which remained unassigned were determined by a single crystal X-ray diffraction study of kinamycin C p-bromobenzoate derivative.[55]

The proposed structure contains a 1,4-naphthoquinone, a pyrrole, a highly oxygenated cyclohexene ring and an unprecedented cyano group on the pyrrole ring nitrogen (Figure 14).[8,55]

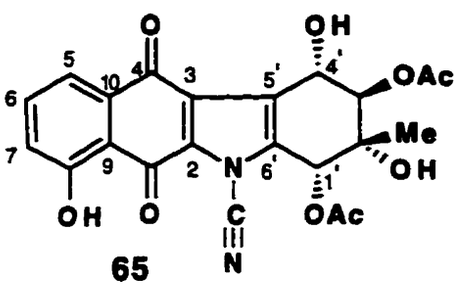


	Kinamycin	R_1	R_2	R_3	R_4
62	A	Ac	Ac	Ac	Ac
63	B	H	Ac	H	H
64	C	Ac	H	Ac	Ac
65	D	Ac	H	Ac	H

Figure 14

The ^{13}C NMR spectrum of kinamycin D (**65**) was partially assigned by Ajisaka *et al.*[56] Oddly, the carbon spectrum lacked a signal assignable to the cyanamide.[56]

The absence of the cyanamide signal was attributed to either an unusually long relaxation time or an incidental overlap with other signals at approximately 120 ppm.[56] The carbon spectrum was reassigned in 1985 by Sato *et al.*[57], utilizing long range COSY experiments with kinamycin D (**65**). These 2D NMR range experiments also failed to identify a carbon signal assignable to the cyanamide of the kinamycins. The assigned proton and carbon NMR signals appear in Figure 15.[57]



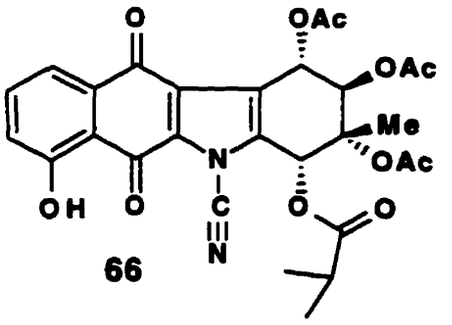
65

Proton Position	^{1}H-Chemical Shifts (ppm) (J_{HH} in Hz)
OH at C-8	12.13
H-5	7.68, t, J=8
H-6	7.58, d, J=8
H-7	7.22, d, J =8
H-3'	5.59, d, J=8
H-1'	5.48, s
OH at C-4'	5.43, s
H-4'	4.78, d, J=8
OH at C-2'	3.10, bs
CH3COO-	2.26, s
CH3COO-	2.19, s
CH3-	1.22, s

Carbon Position	^{13}C- Chemical Shift (ppm)	Carbon Position	^{13}C-Chemical Shift (ppm)
1	183.6	7'	124.3
4	180.8	5	120.3
$CH_3\underline{C}OO$-	172.3	9	115.6
$CH_3\underline{C}OO$-	171.2	3'	75.7
8	162.4	2'	73.7
6	136.3	1'	71.3
10	133.8	4'	67.3
2	132.8	$\underline{C}H_3COO$-	21.2
5'	132.1	$\underline{C}H_3COO$-	20.9
3'	129	$\underline{C}H3$	18.3
6'	127.8		

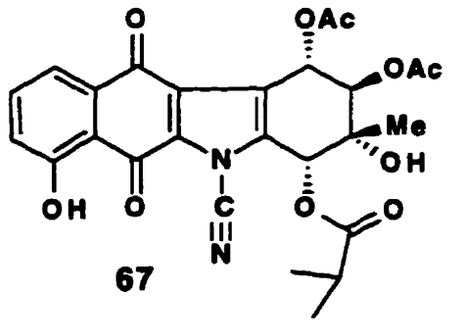
Figure 15: Spectroscopic properties of the kinamycin D[57]

Nine new kinamycin antibiotics have been discovered recently from *Saccharothrix* (**66** and **67**)[58] (Figure 16), from an unidentified actinomycete designated as A83016A (**68**)[58] (Figure 17), and from *Streptomyces chattanoogensis* (**69** to **74**)[59,60] (Figure 18).



66

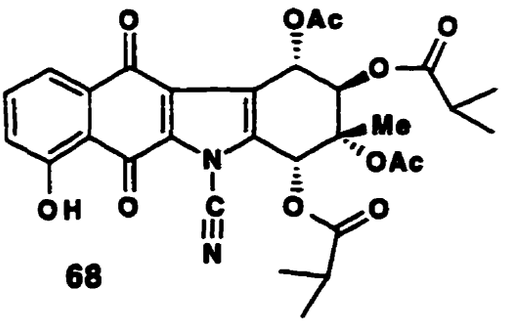
3-O-isobutyrylkinamycin C



67

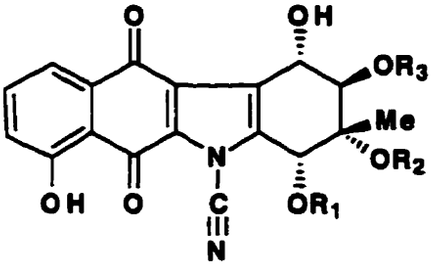
4-deacetyl-4-O-isobutyrylkinamycin C

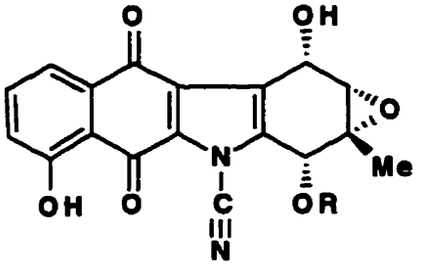
Figure 16: Kinamycins isolated from *Saccharothrix*.



68

Figure 17: **A new kinamycin isolated from an unidentified actinomycete designated as A83016A.**

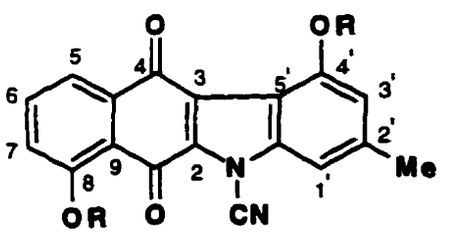


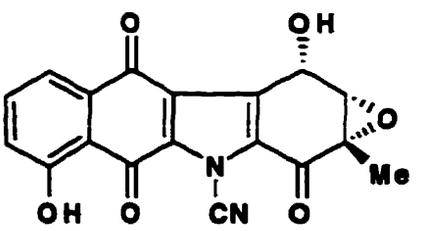


	FL-120	R1	R2	R3		FL-120	R
69	A	Ac	$COCH(CH_3)_2$	Ac	73	B	COCH(CH3)2
70	C	$COCH(CH_3)_2$	H	Ac	74	B'	Ac
71	C'	$COCH_2CH_3$	H	Ac			
72	D'	$COCH(CH_3)_2$	H	H			

Figure 18: **Kinamycins isolated from *Streptomyces chattanoogensis*.**

Furthermore, Seaton and Gould[61] have isolated two new kinamycins denoted as kinamycin E (**75**) and F (**76**), as well as prekinamycin (**77**) and keto-anhydrokinamycin (**78**), believed to be intermediates in the biosynthesis of the kinamycincs (Figure 19). The assignment of the signals in the ^1H NMR spectrum for prekinamycin, the diacetate derivative, keto-anhydrokinamycin and kinamycin E is also shown in Figure 19.

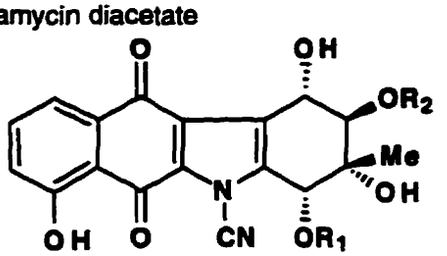




78

keto-anhydrokinamycin

77 R = H, prekinamycin
79 R = Ac, prekinamycin diacetate



75 R_1 =Ac, R_2 = H, kinamycin E
76 R_1 = R_2 = H, kinamycin F

Position	prekinamycin	prekinamycin diacetate
8 (OR)	12.32 (1H, s)	2.48 (3H, s)
7	7.04 (1H, dd, J=0.9, 7.2 Hz)	7.14 (1H, dd, J=1.1, 7.4 Hz)
6	7.17 (1H, dd, J=0.9, 7.2 Hz)	7.34 (1H, dd, J=7.4, 7.0 Hz)
5	7.24 (1H, dd, J=0.9, 7.0 Hz)	7.52 (1H, dd, J=1.1, 7.2 Hz)
4′ (OR)	11.60 (1H, s)	2.49 (3H, s)
3′	6.60 (1H, d, J=9.1 Hz)	6.95 (1H, br, s)
3′ (OR)		
2′ (OR)		
2′ (CH_3)	2.39 (3H, s)	2.46 (3H, s)
1′	6.69 (1H, d, J=9.1 Hz)	6.84 (1H, d, J=1.2 Hz)

Position	keto-anhydro kinamycin	kinamycin E
8 (OR)	12.06 (1H, s)	12.17 (1H, s)
7	7.27 (1H, d)	7.22 (1H, dd, J=1.1, 7.7 Hz)
6	7.63 (1H, t, J=7.7 Hz)	9.58 (1H, t, J=7.8 Hz)
5	7.76 (1H, d, J=7.6 Hz)	7.71 (1H, dd, J=1.3, 7.9 Hz)
4'	5.34 (1H, dd, J=1.7, 2.9 Hz)	4.61 (1H, dd, 1.3, 7.9 Hz)
4' (OR)	5.94 (1H, d, J=1.6 Hz)	5.71 (1H, d, J=1.3 Hz)
3'	3.89 (1H, d, J=2.7 Hz)	4.24 (1H, d, J=7.9 Hz)
3' (OR)		3.0 (1H, br)
2' (OR)		2.8 (1H, br)
2' (CH_3)	1.64 (3H, s)	1.48 (3H, s)
1'		5.53 (1H, s)
1' (OR)		2.62 (3H, s)

Figure 19: ^{1}H NMR spectrum signals for prekinamycin, the diacetyl derivative, keto-anhydrokinamycin and kinamycin E.[61]

1.3.2 Biosynthesis of Kinamycins

Early feeding experiments with ^{13}C labeled acetate showed that the kinamycin skeleton was entirely derived from acetate possibly via condensation of two non-symmetrical intermediates[62], likely a naphthoquinone **80** and a 3-amino-5-hydroxytoluene (**81**) (Figure 20).[63]

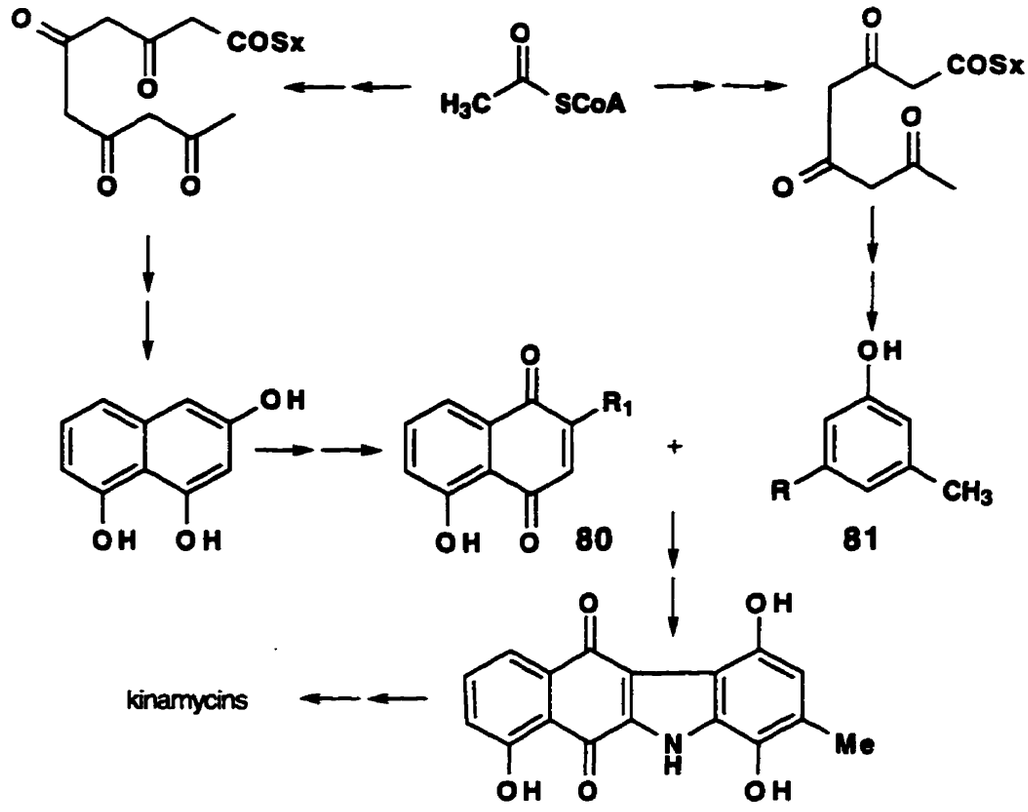


Figure 20: Biosynthesis of kinamycin from two unsymmetrical polyketide chains.

This model of kinamycin biosynthesis (Figure 20), based on the experiments described below, was later revised to one involving a single polyketide chain (Figure 25). Incorporation experiments in which doubly labeled acetate, [1,2-$^{13}C_2$]-acetate (**82**), was added to the medium showed ^{13}C-^{13}C coupling between the carbons (heavy lines, **83**) indicated in Figure 21.[63] The incorporation of labeled acetate into the kinamycin skeleton is consistent with two polyketide chains, one leading to a naphthoquinone and the other leading to a hydroxytoluene (Figure 20).[63] Furthermore, in experiments where sodium [1-^{13}C,2,2,2-$^{2}H_3$]acetate (**84**) was incorporated, the indicated sites in **85** (Figure 21) were enriched.[63] The ester functionalities (a and b) each showed one deuterium isotope shifted peak in the ^{13}C spectrum while C-2' showed two additional peaks.[63]

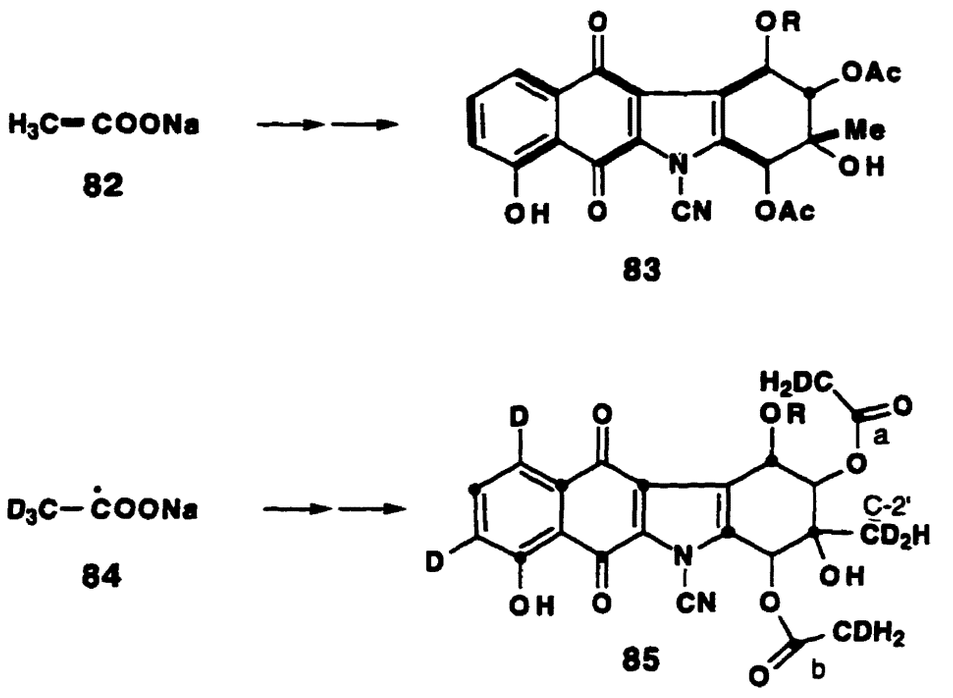
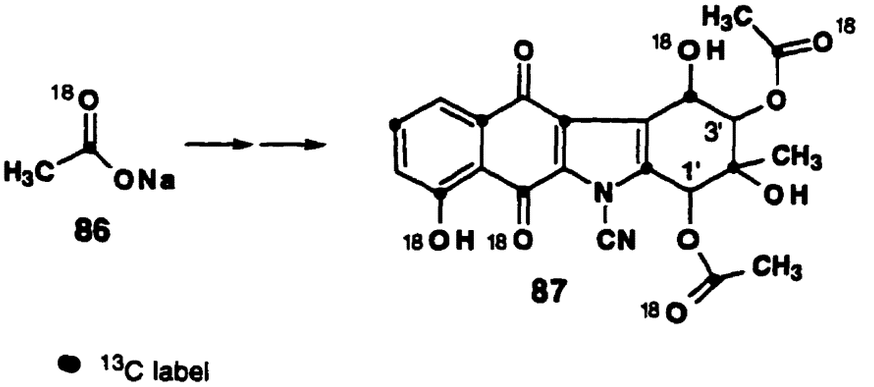


Figure 21

Attention was then turned to the origin of the oxygens. Feeding experiments with ^{18}O labeled acetate, [1-^{13}C,1,1-$^{18}O_2$]acetate (**86**), showed five ^{18}O isotope shifted peaks in the ^{13}C NMR spectrum: C-1, C-8, C-4', and the ester carbonyls (Figure 22, **87**).[63] The labels of the esters were assigned to the doubly bonded oxygens from the magnitude of the ^{18}O isotope induced shifts in the ^{13}C NMR.[63]



● ^{13}C label

Figure 22

Fermentation in the presence of $^{18}O_2$ showed three isotope shifted resonances in the ^{13}C NMR spectrum, corresponding to C-4', C-1' and C-2' (Figure

23, **88**).[63] The remaining unaccounted oxygen, C-3' oxygen, must be derived from water (Figure 23).[63]

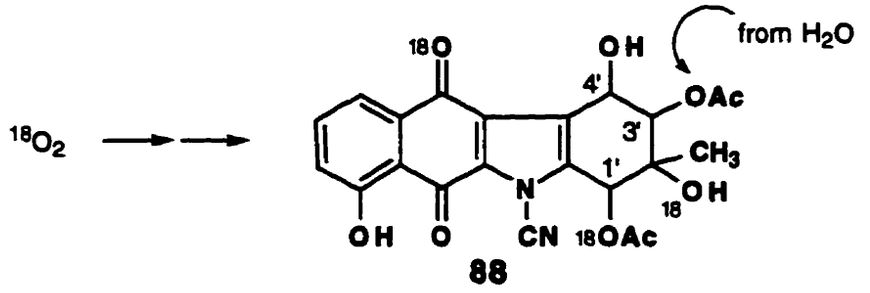


Figure 23

The determination of the origin of the carbon skeleton and the origin of the D-ring oxygens prompted Sato and Gould[63] to propose a likely biosynthetic scheme for the elaboration of the D-ring (Figure 24). An aromatized precursor, prekinamycin, is hydroxylated and epoxidized to afford **89**. This diene is tautomerized to the enone which is then reduced to the alcohol **91**. Attack by water opens the epoxide **91** and affords **92**, which contains the desired oxygen substitutions on the D-ring.

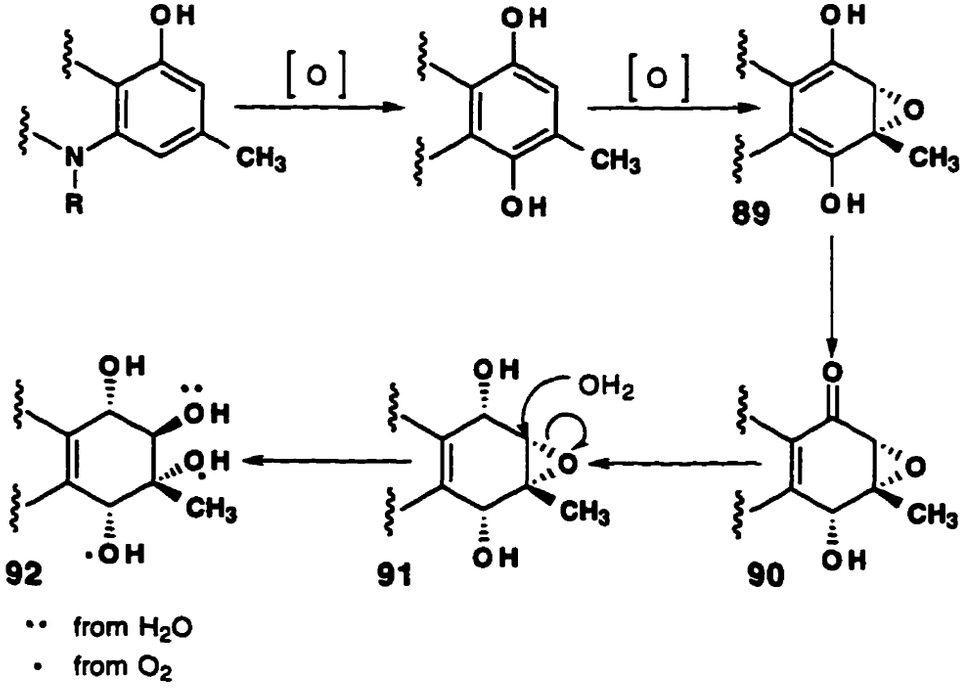


Figure 24

At this point, the origin of the cyano moiety was still unclear. The isolation of dehydrorabelomycin (**93**), a known compound derived from the acid catalyzed dehydration of rabelomycin[61], from the culture broth of *Streptomyces* led to the speculation that the kinamycins are derived from a single polyketide chain and that dehydrorabelomycin (**93**) is an intermediate (Figure 25).[64] Biosynthesis of the kinamycins via dehydrorabelomycin (**93**) would necessitate a fracture of the ring system with an excision of a two carbon fragment, a novel polyketide metabolism (Figure 25).[63,64]

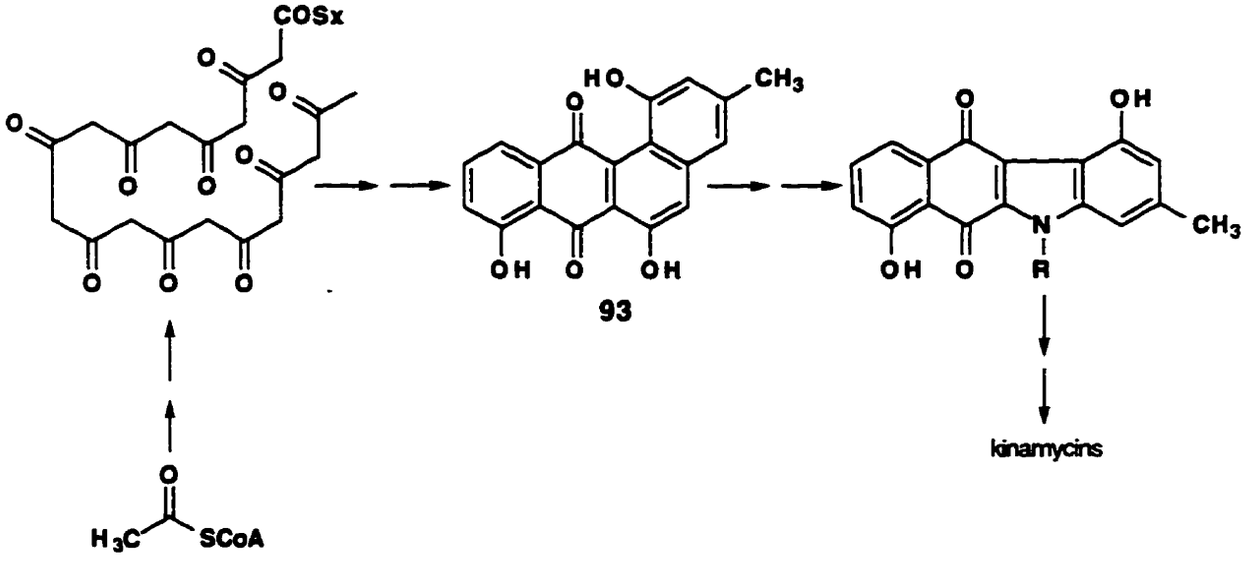
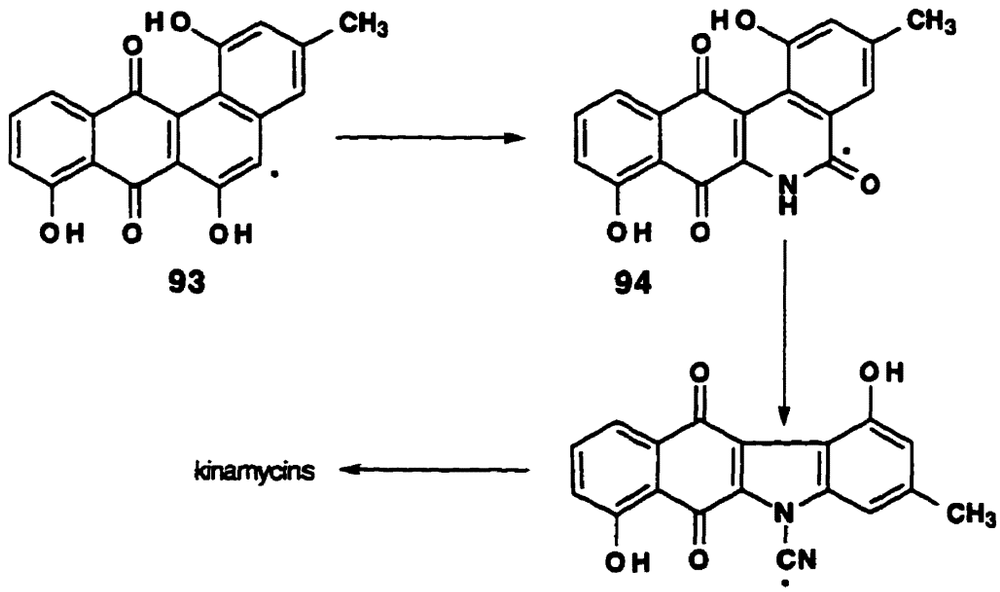


Figure 25: **The kinamycins are derived from acetate via a single polyketide chain.**

The apparent absence of the cyanamide resonance from the ^{13}C spectrum of the kinamycins hampered the determination of the origin of this unusual structural feature. The ^{15}N NMR spectrum obtained from kinamycin D (**76**) when $(^{15}NH_4)_2SO_4$ was utilized as the sole nitrogen source shows two doublets (J_{CN} = 3.4 Hz) at 344.5 and 241.6 ppm, relative to $H^{15}NO_3$ at 362.0 ppm.[65] The ^{13}C NMR spectrum contained ^{15}N coupled doublets corresponding to C-5' (131.7 ppm, J_{CN}=2.9 Hz), C-6' (128.0 ppm, J_{CN}=2.2 Hz), C-2 (132.2 ppm, J_{CN}=2.3 Hz) and C-3 (128.4 ppm, J_{CN}=2.8 Hz).[65] The authors were surprised to find a doublet of doublets at 78.5

ppm (J_{CN}=21.2, 5.4 Hz) in the doubly ^{15}N labelled natural product.[65] Upon examination of the ^{13}C spectra obtained previously, Seaton and Gould[65] noted a small singlet largely obscured by $CDCl_3$ signals at 78.5 ppm which was initially believed to be an impurity. It was noted that the resonance at 78.5 ppm was unusual for a cyano group which is more commonly observed at approximately 100 to 110 ppm.[65]

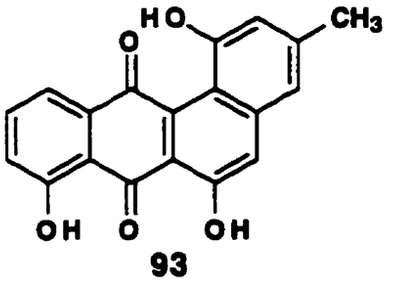
Returning to feeding experiments with labeled acetate, Seaton and Gould[65] observed relatively uniform enrichment in the carbon skeleton of the kinamycins, including the cyanamide. Consequently, a biosynthetic scheme in which the cyanamide carbon is derived from C-5 of **94** was proposed (Figure 26).[65] This scheme would require oxidation of **93**, nitrogen insertion as well as a ring contraction/rearrangement (Figure 26).[65]



• marks carbon through biosynthetic pathway

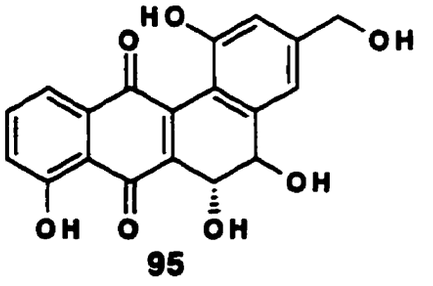
Figure 26

Recent isolation of PD 116470 (**95**), structurally related to dehydrorabelomycin (**93**), created speculation that it may also be involved in the biosynthesis of the kinamycins (Figure 27).[66,67]



93

dehydrorabelomycin



95

PD 116470

Figure 27

Labeling experiments clearly show, however, that **93** and **95** are derived from different pre-aromatic intermediates (Figure 28).[67] Dehydrorabelomycin (**93**) and PD 116470 (**95**) are derived from two slightly different polyketides, **96** and **97** respectively (Figure 28). Cyclization leads to slightly different prearomatic systems, **98** and **99**. These are further processed into two different aromatic systems, **93** and **100**, neither of which can serve as a precursor to the other.

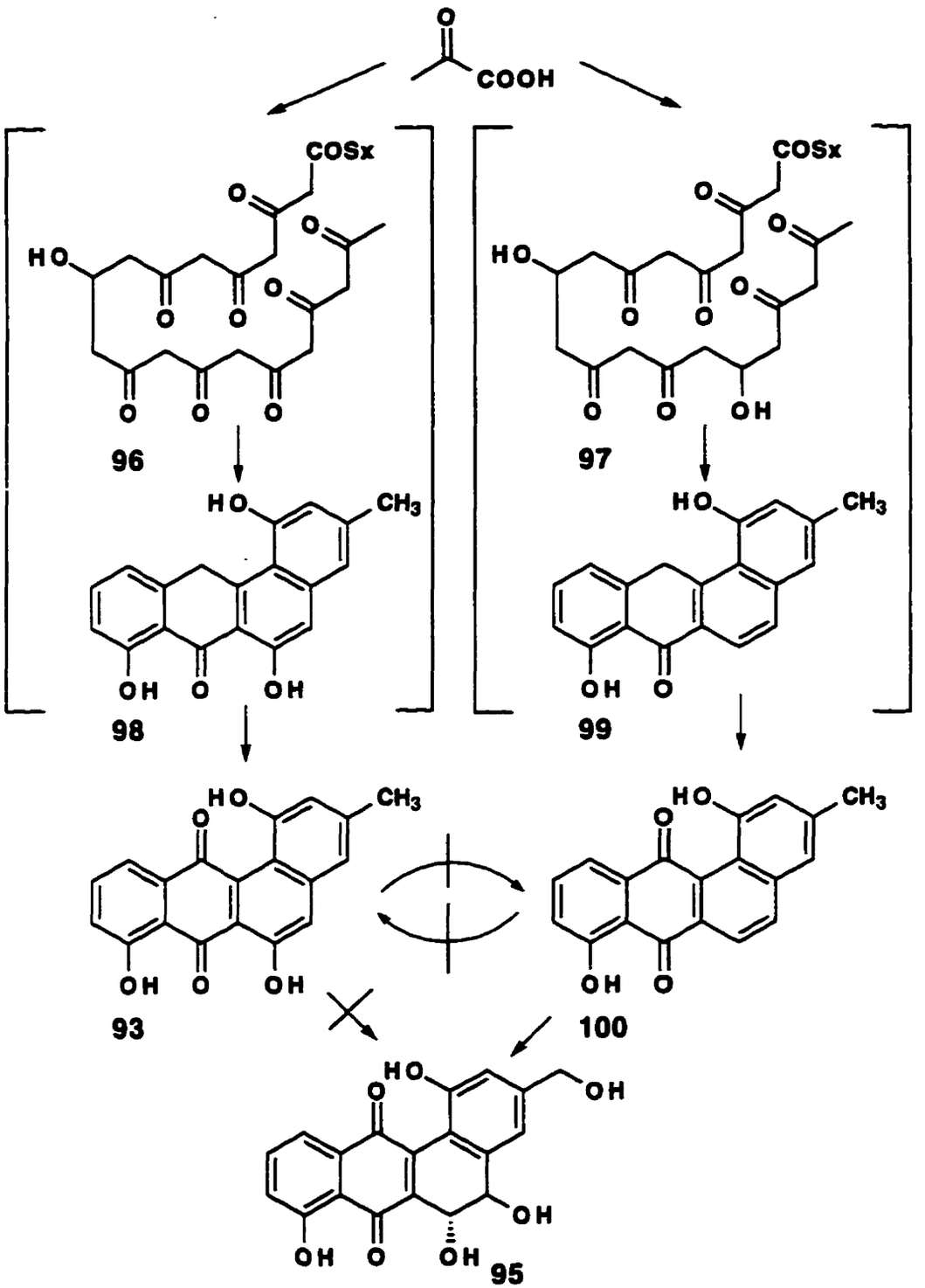
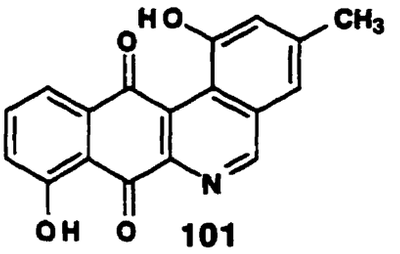


Figure 28

Recently, phenanthroviridine aglycone (**101**) was isolated from *S. viridiochromagenes DSU3972* (Figure 29)[68] and was considered to be an intermediate in the biosynthesis of the kinamycins (Figure 30).[68] In this scheme, dehydrorabelomycin (**93**) undergoes oxidative scission to give **102**. Decarboxylation, nitrogen insertion and cyclization affords phenanthroviridine aglycone (**101**) which then undergoes oxidation, ring contraction/rearrangement to the prekinamycin system. Prekinamycin (**77**) is then processed further to the kinamycin skeleton. More recently, phenanthroviridine aglycone (**101**) has been discovered in extracts from a mutant strain, *S. murayamaensis MC2*, consistent with the proposed biosynthetic pathway (Figure 30).[69]



phenanthroviridine aglycone

Figure 29

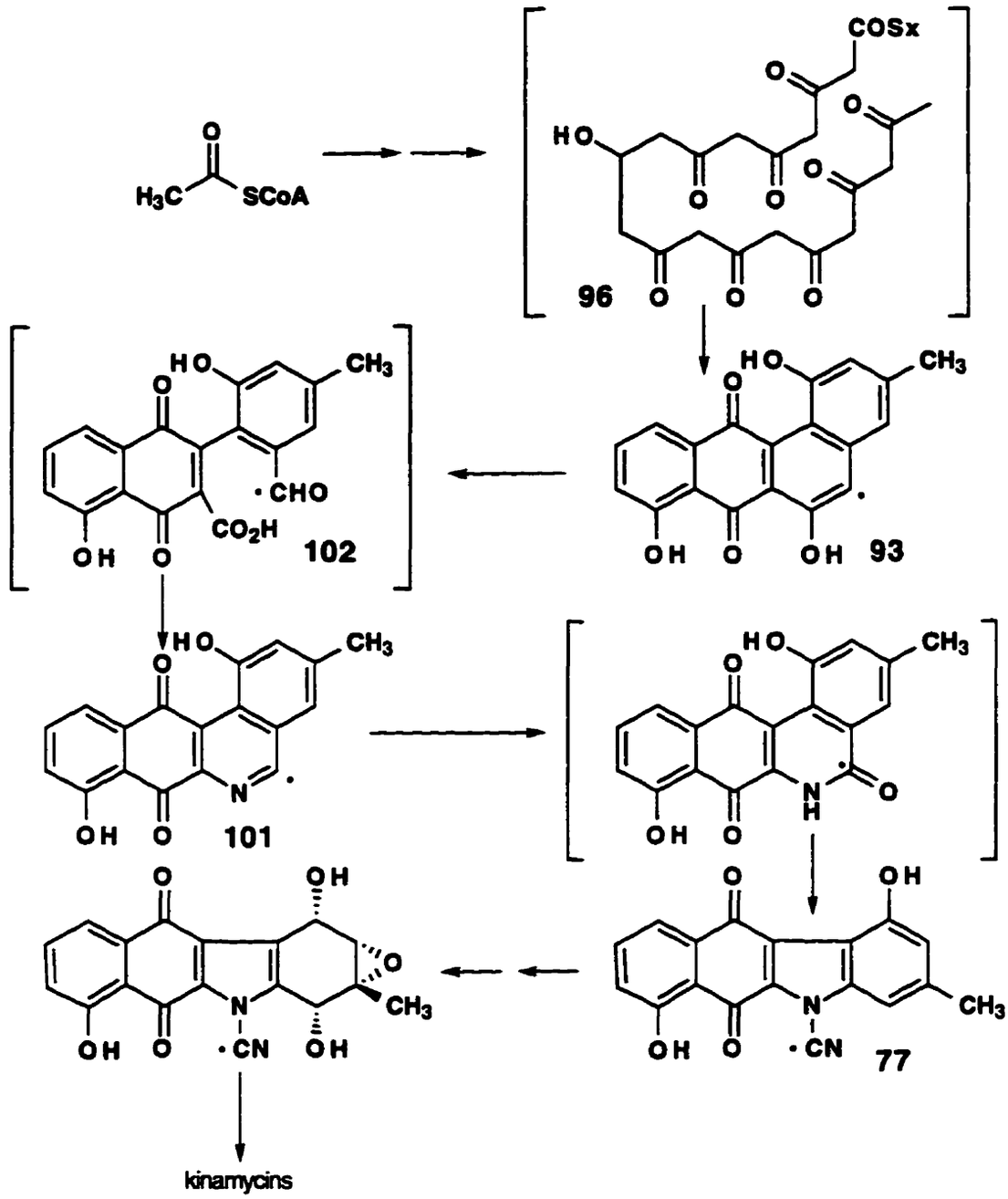


Figure 30: Revised biosynthetic pathway.

Gore *et al.*[68] also proposed a possible mechanism for the transformation of phenanthroviridine aglycone (**101**) to that of the prekinamycin (**77**) ring system (Figure 31). The proposed scheme involves nucleophilic attack of ammonia on phenanthroviridine aglycone (**101**) to give the amine **103**. The amine **103** is

oxidized to the quinone **104** which then undergoes ring contraction affording **105**, which is simply prekinamycin in the hydroquinone oxidation state.

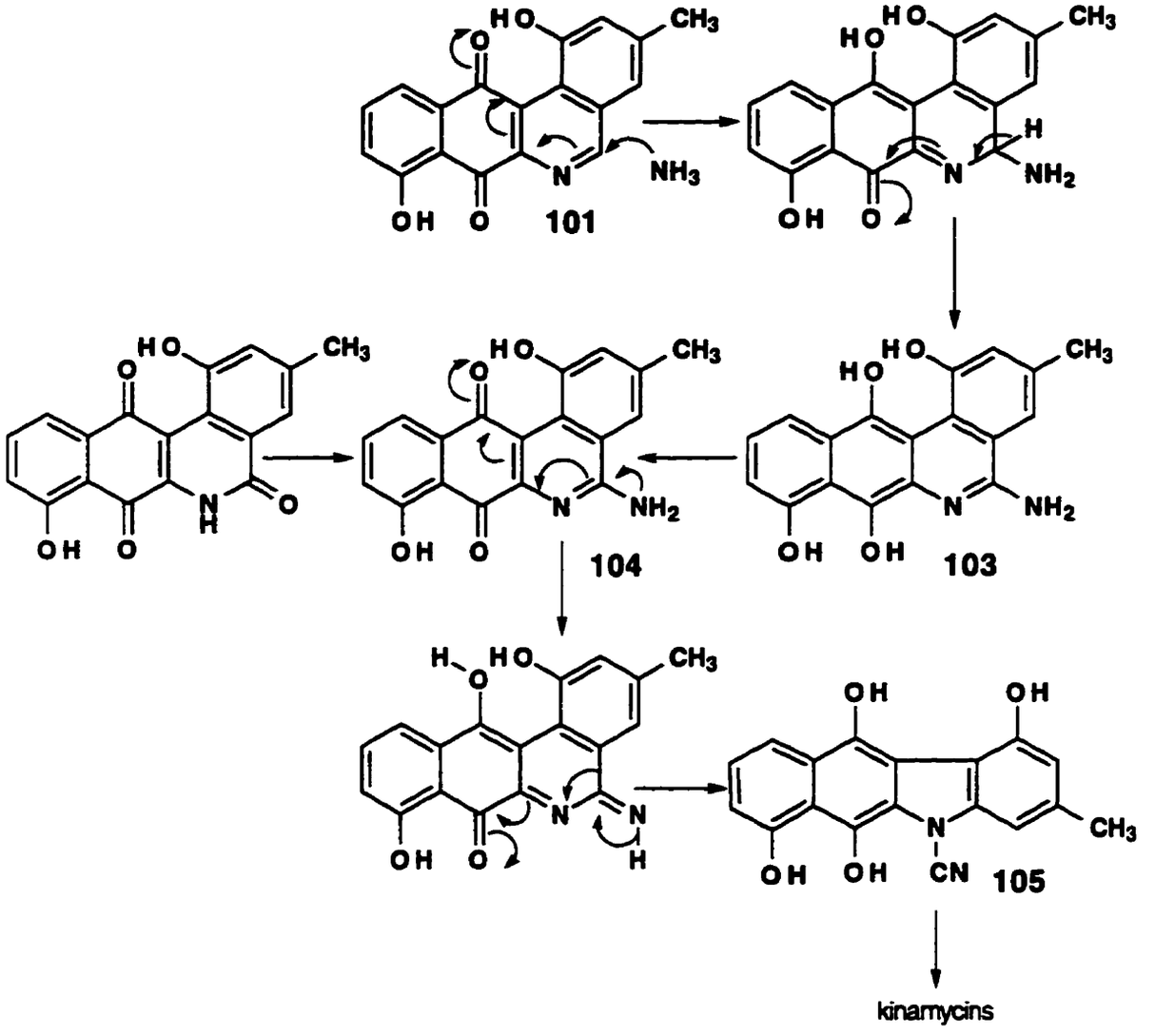
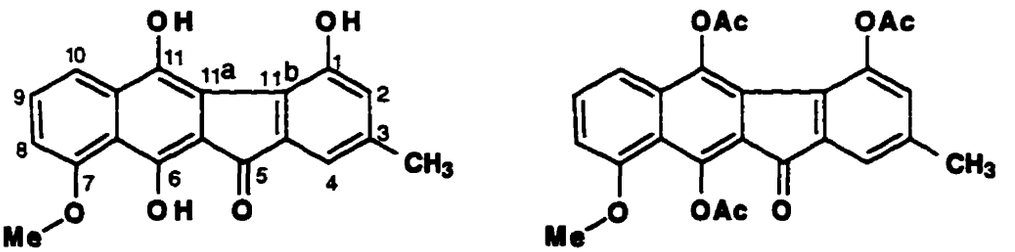


Figure 31: **Proposed biosynthetic transformation of phenanthroviridine aglycone to the kinamycins.**

Kinafluorenone (**106**) has been isolated from a mutant strain of *S. murayamaensis* blocked in the biosynthesis of the kinamycin antibiotics and was believed to be a shunt metabolite.[70] The structure of **106** has been established unambiguously via a single crystal X-ray diffraction study of the triacetyl derivative **107**.[70]



106 107

Figure 32

A mechanism by which kinafluorenone (**106**) might be formed from dehydrorabelomycin (**93**) is shown in Figure 33.[70] It was argued that, unable to form the kinamycins in the mutant strain, **108** undergoes cyclization to form the five membered system **109**, which decarboxylates and is oxidized to afford **106**.

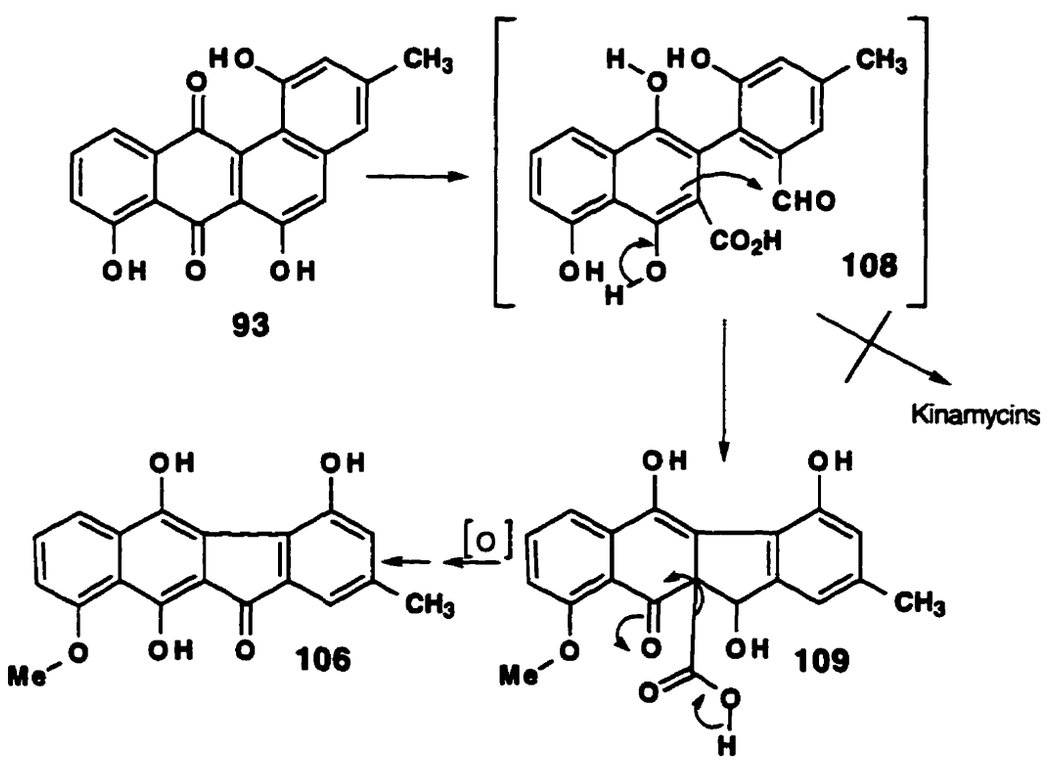


Figure 33: Mechanism by which prekinamycin might be formed from dehydrorabelomycin.

A summary of the overall proposed biosynthetic scheme is depicted in Figure 34.[70]

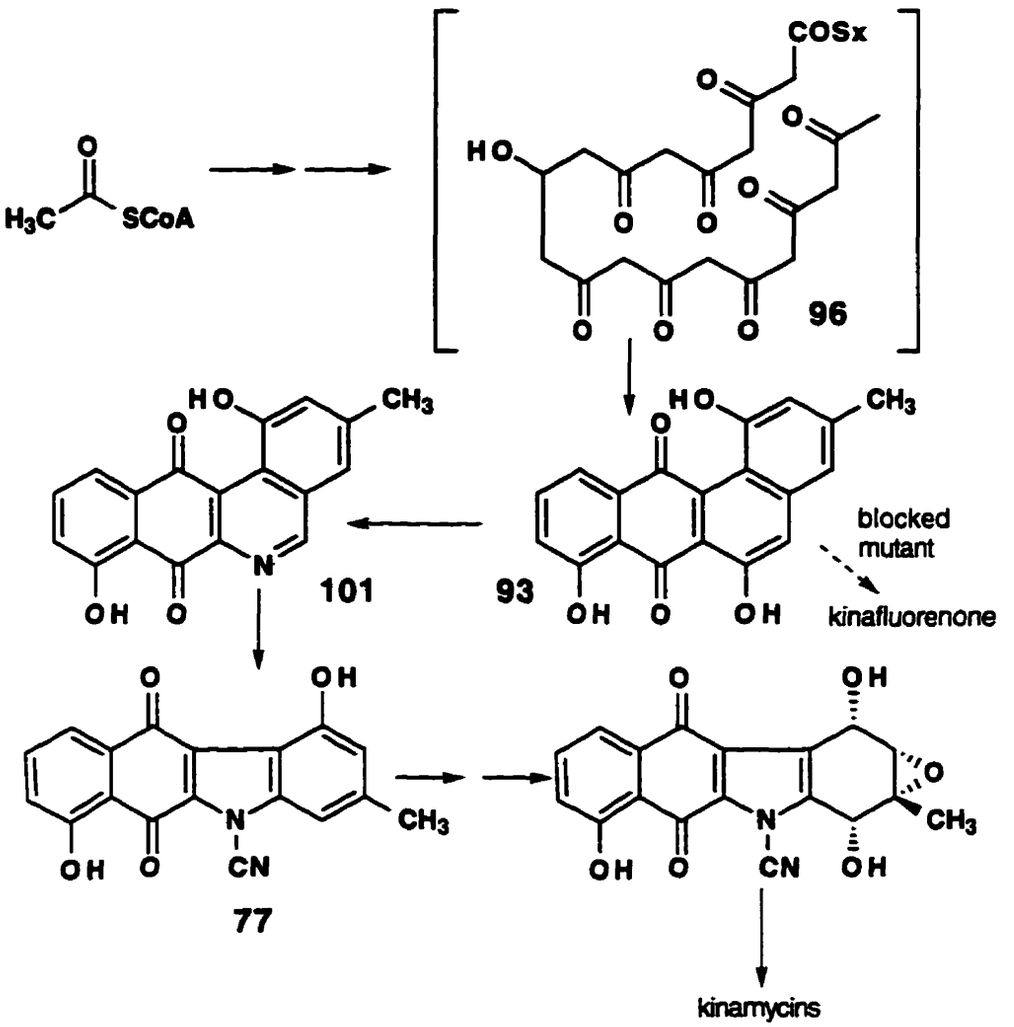
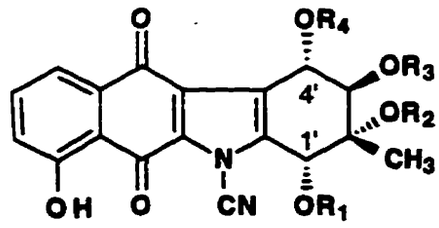


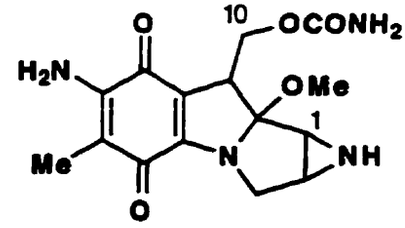
Figure 34: Overall biosynthetic scheme.

1.3.3 Mode of Action

To date no studies of the mechanism of the antibiotic or antitumour activity of the kinamycins have been reported. There is, however, an obvious structural relationship between the kinamycins and the mitomycins: the kinamycins also contain an indoloquinone with potential leaving groups at C1' and C4' of ring D analogous to C-1 and C-10 of the mitomycins (Figure 35). Thus it was proposed by Moore[10] some years ago that, like the mitomycins, the kinamycins might undergo a bioreductive activation and then might participate in DNA alkylation.



kinamycins



mitomycin C

Figure 35

Prior to reduction of the quinone portion to the hydroquinone, the lone pair of the nitrogen is in resonance with the cyanide moiety and with the quinone (Figure 36).

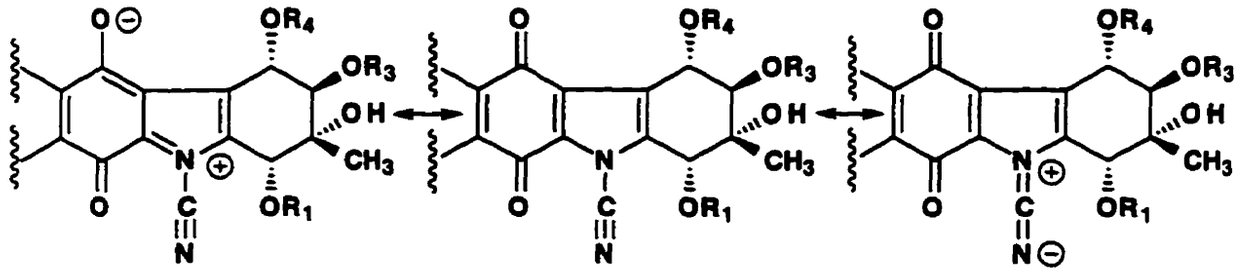
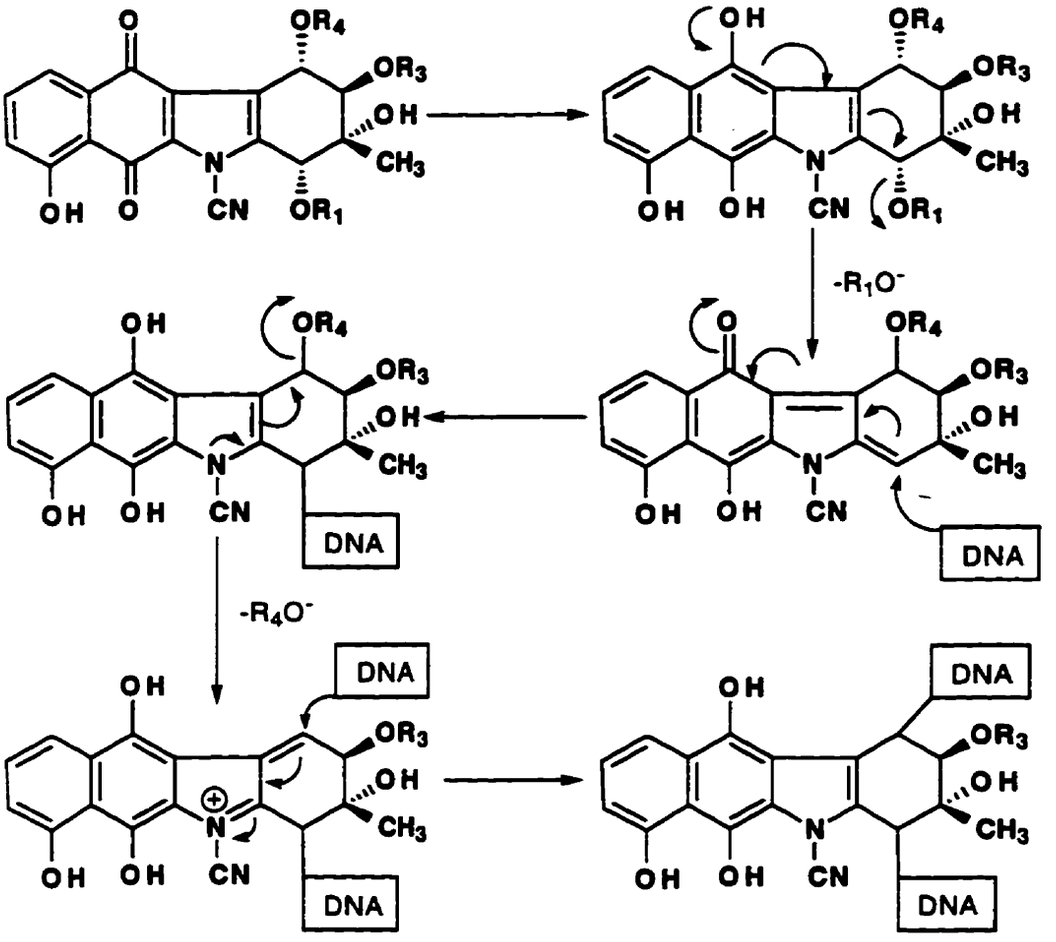


Figure 36

Once reduced, the kinamycins can undergo a cascade of events leading to a bisalkylating agent, similar to the mitomycins (Scheme 14). Upon reduction to the hydroquinone, a sequence of events might lead to the elimination of two of the D-ring oxygen substituents; thereby, creating two reactive sites. DNA might then attack these sites resulting in monoalkylation or bisalkylation.



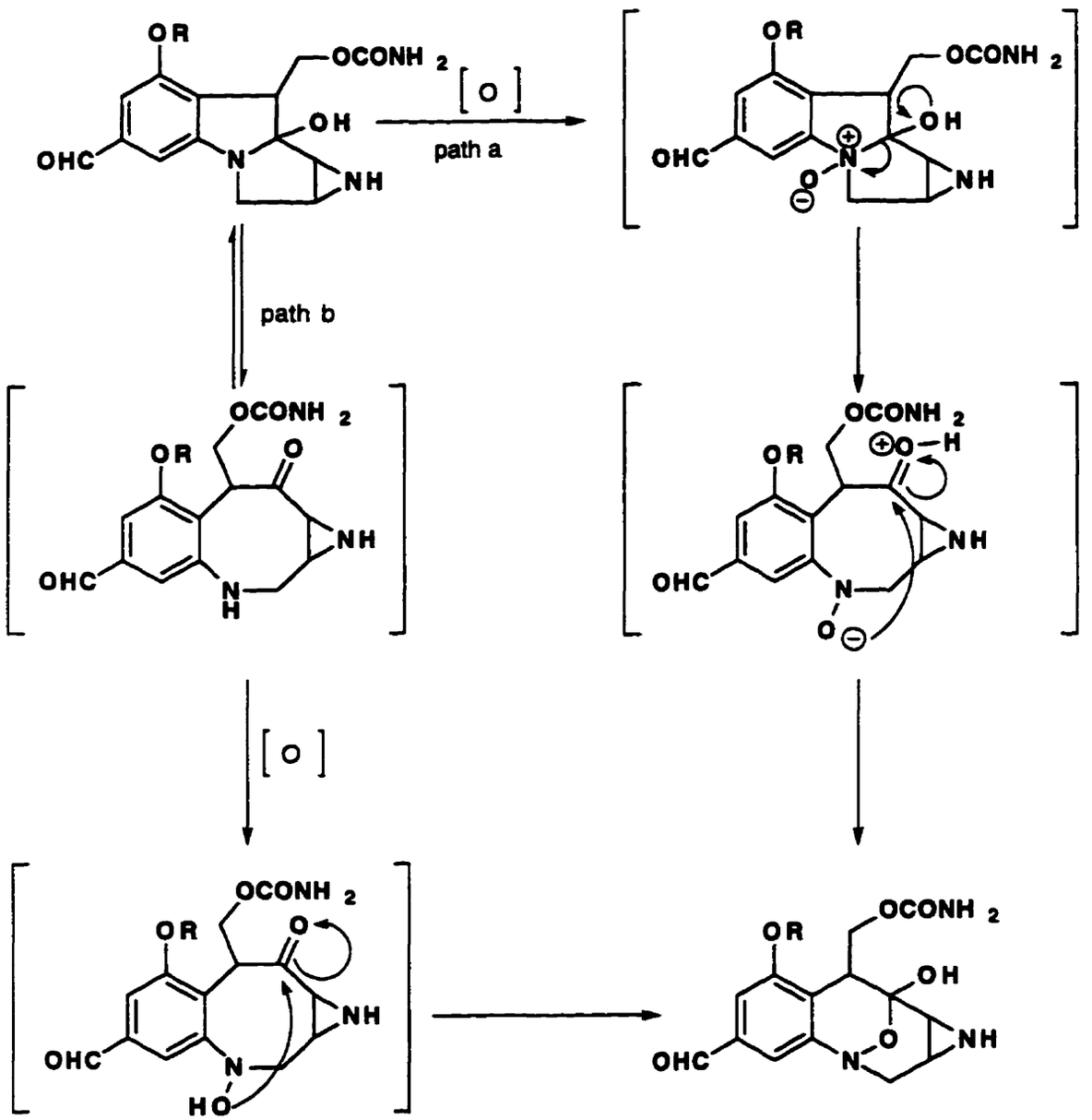
Scheme 14

Chapter 2: Synthetic Studies Toward FR-900482

2.1 Oxidative Ring Expansion

The structural similarity of FR-900482 to the mitomycins suggests a similar biosynthetic pathway. In support of this, it has been found that 3-amino-5-hydroxybenzoic acid and D-glucosamine, known to be precursors of the mitomycins, are also incorporated into FR-900482.[71] Hence, it seems likely that FR-900482 and the mitomycins are derived from a similar intermediate.

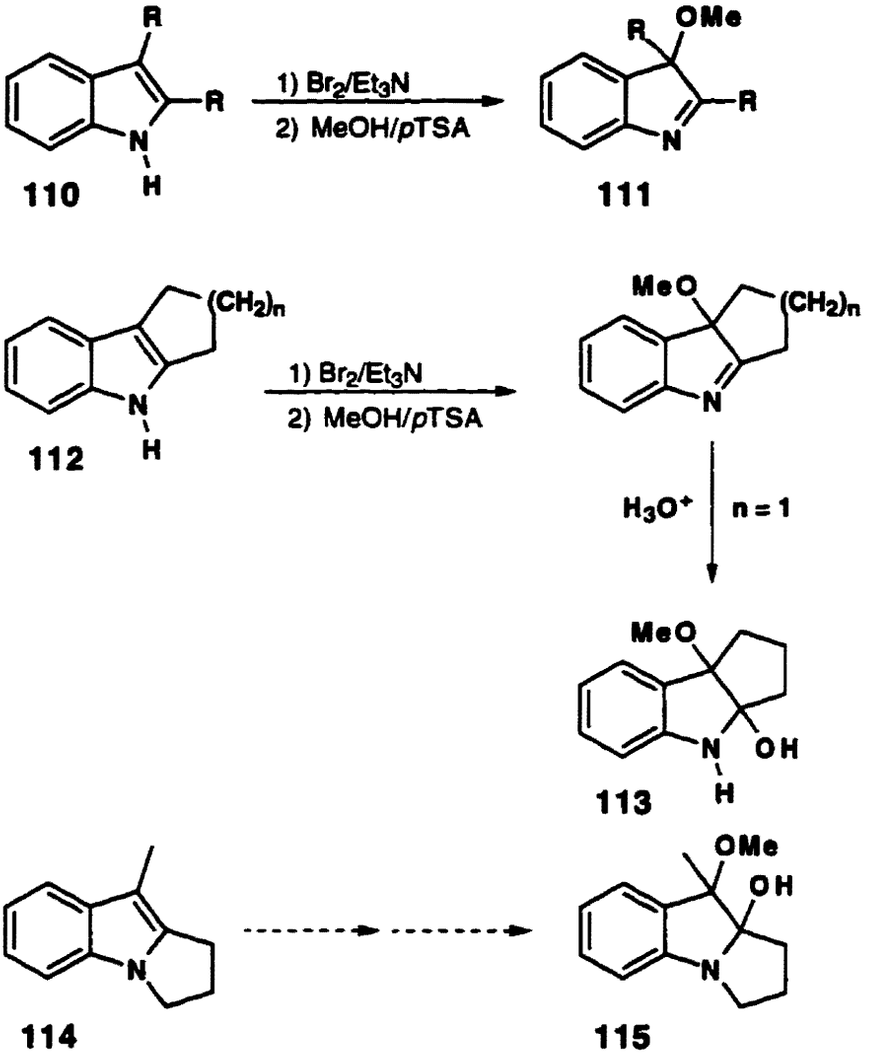
Research in this laboratory[72] has been aimed at developing methodology for the transformation of mitomycin-like systems into FR-900482-like structures. The strategy chosen for the transformation of mitomycin-like skeletons to that of FR-900482-like skeletons is believed to be biomimetic: an appropriately substituted mitomycin-like skeleton might be oxidized to the N-oxide which might then undergo a ring opening and recyclize incorporating the oxygen to afford the FR-900482 system (Scheme 15, path a). Alternatively, it was reasoned that ring opening might occur prior to the oxidation step to give a hydroxylamine which might then cyclize incorporating the oxygen (Scheme 15, path b).



Scheme 15: Possible biosynthetic pathways to FR-900482 from a mitomycin-like intermediate.

Previous studies in this laboratory have shown that 2,3-disubstituted indoles, **110**, when treated with bromine in the presence of triethylamine followed by acid catalyzed methanolysis yielded 3-methoxyindolenines (**111**) (Scheme 16). Furthermore, this reaction was found to be general to cycloalkanoindoles **112** in which n > 1 (Scheme 16). However with n = 1, the stable hydrate **113** was isolated as the major product (Scheme 16). It is believed that in such ring fused systems,

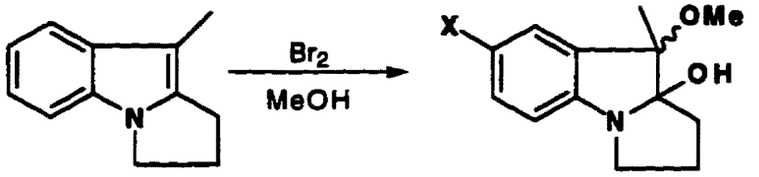
there is less ring strain when C-2 is sp^3 hybridized than when it is sp^2 hydridized. Since pyrrolo[1,2-a]indole **114** is expected to exhibit similar ring strain, it was felt that reaction under the same conditions might yield **115** which would serve as a suitable model for oxidative ring expansion studies.



Scheme 16: Bromination methanolysis of indoles.

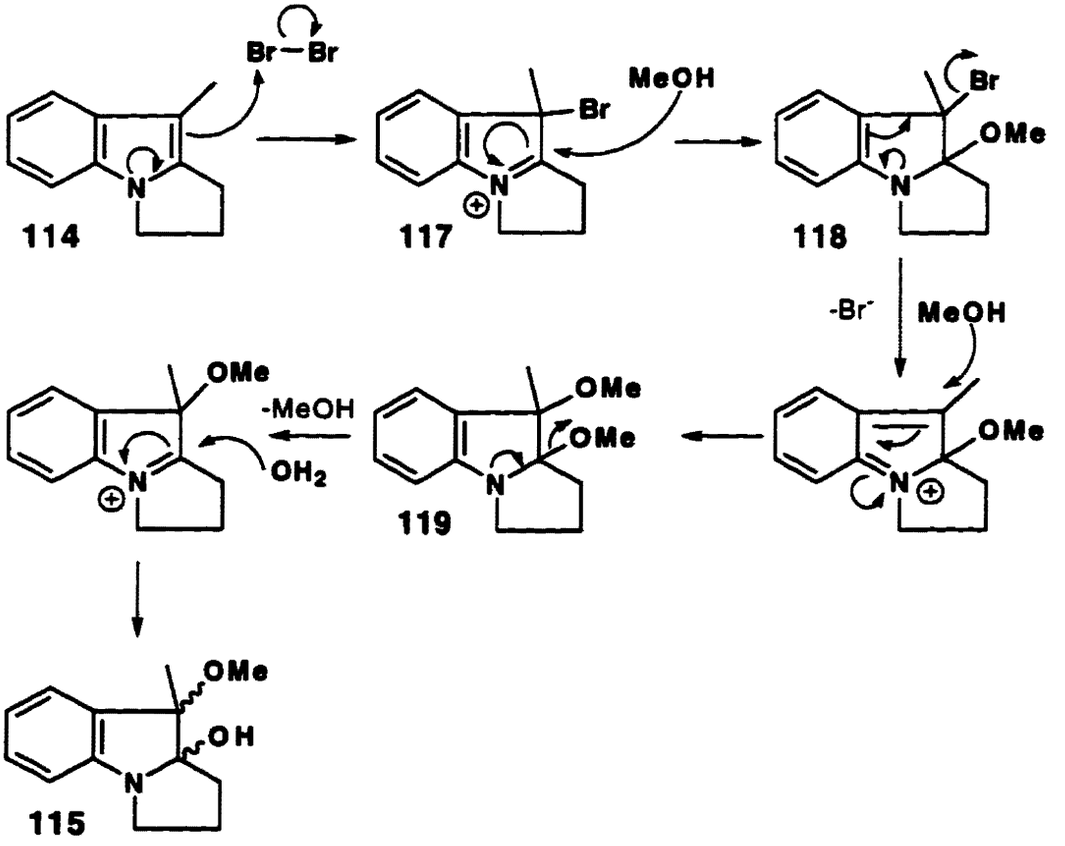
It was found that when the pyrrolo[1,2-a]indole **114**[73] was treated with bromine in methanol followed by a basic aqueous workup, the major product was the alcohol **115**, which was largely contaminated with some of the bromo analogue **116** (Scheme 17). It was found that the bromo contaminant **116** could be reduced to 1-

2% by a very slow addition of dilute solutions of bromine in methanol. The mechanism for this reaction is believed to involve nucleophilic attack on bromine to give **117** (Scheme 18). Nucleophilic attack of methanol on **117** affords the ether **118**. S_N1-like solvolysis of the benzylic bromide gives the diether **119**. Loss of methanol followed by nucleophilic attack by water during the aqueous workup provides the observed product.



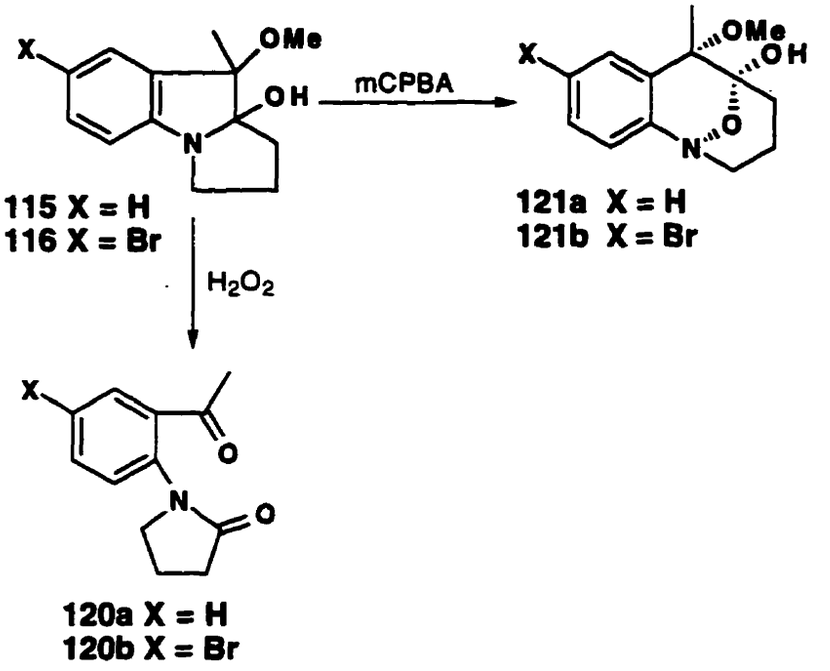
114 **115 X = H** **116 X = Br**

Scheme 17



Scheme 18: Probable mechanism for the bromination methanolysis reaction.

Initial attempts at oxidation of the pyrrolo[1,2-a]indole **115** with hydrogen peroxide gave only the ring cleavage product **120** (Scheme 19). However, early experiments in which a mixture of the alcohol and the bromo analog was treated with *m*CPBA, provided the desired bicyclic hydroxylamine hemiketal ring system **121a** in low yield (~40%) contaminated with the bromo analog **121b** (Scheme 19).

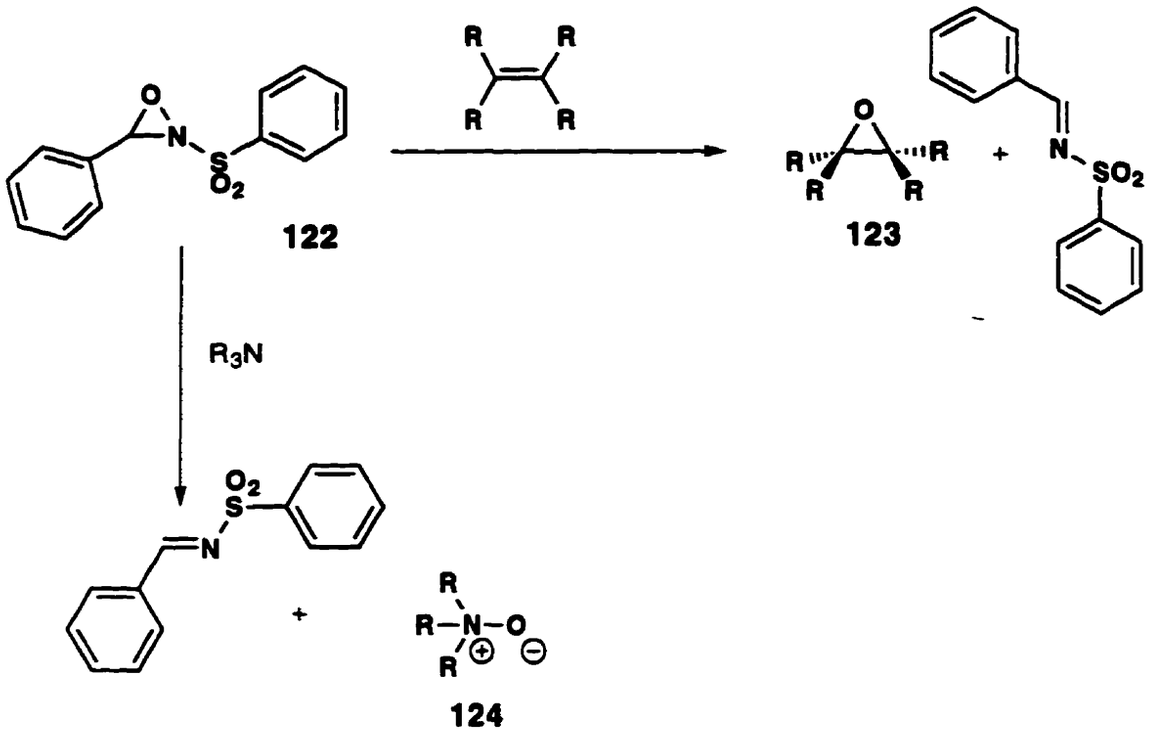


Scheme 19

The ring expanded product **121a** and the bromo analogue **121b** were separated by HPLC. The recrystallization of **121b** yielded crystals suitable for a single crystal X-ray diffraction study which established the structure as shown (Scheme 19) unambiguously.

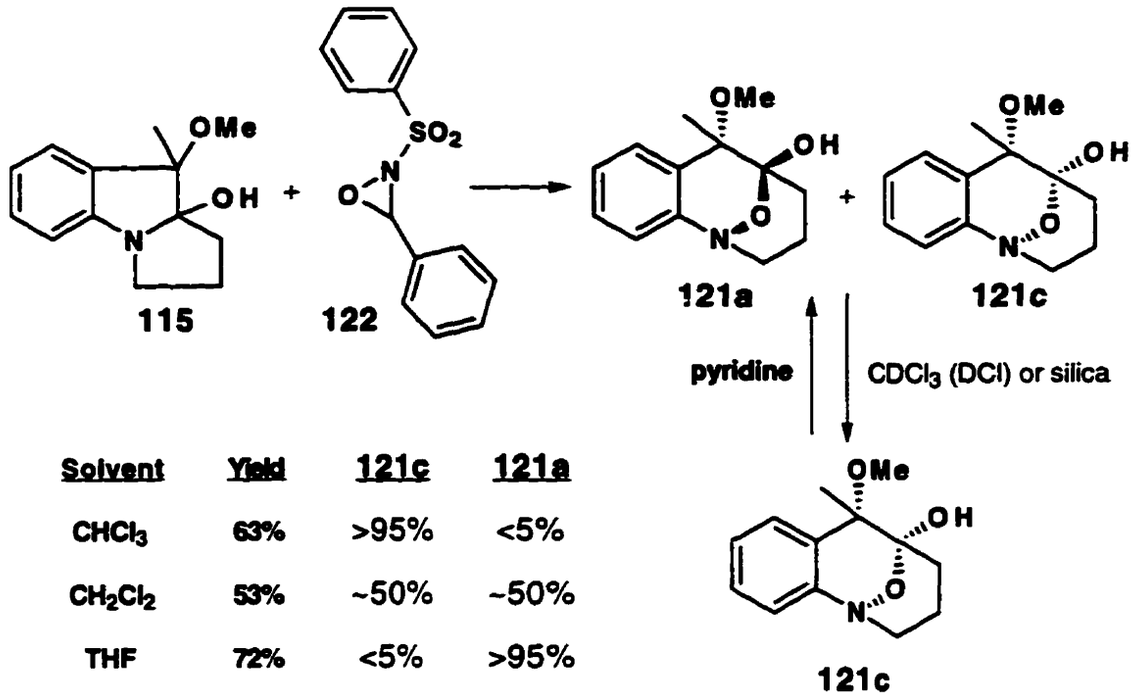
Although the desired bicyclic hydroxylamine hemiketal ring system **121** was obtained, the overall yield was low (~30%). It was felt that a milder oxidant capable of oxygen atom transfer might cleanly provide the desired system. It is well known N-sulfonyloxaziridines (Davis' reagent) **122** [74] react with olefins and tertiary amines,

via an oxygen atom transfer mechanism, to afford epoxides **123** and N-oxides **124**, respectively (Scheme 20).[75-80]



Scheme 20

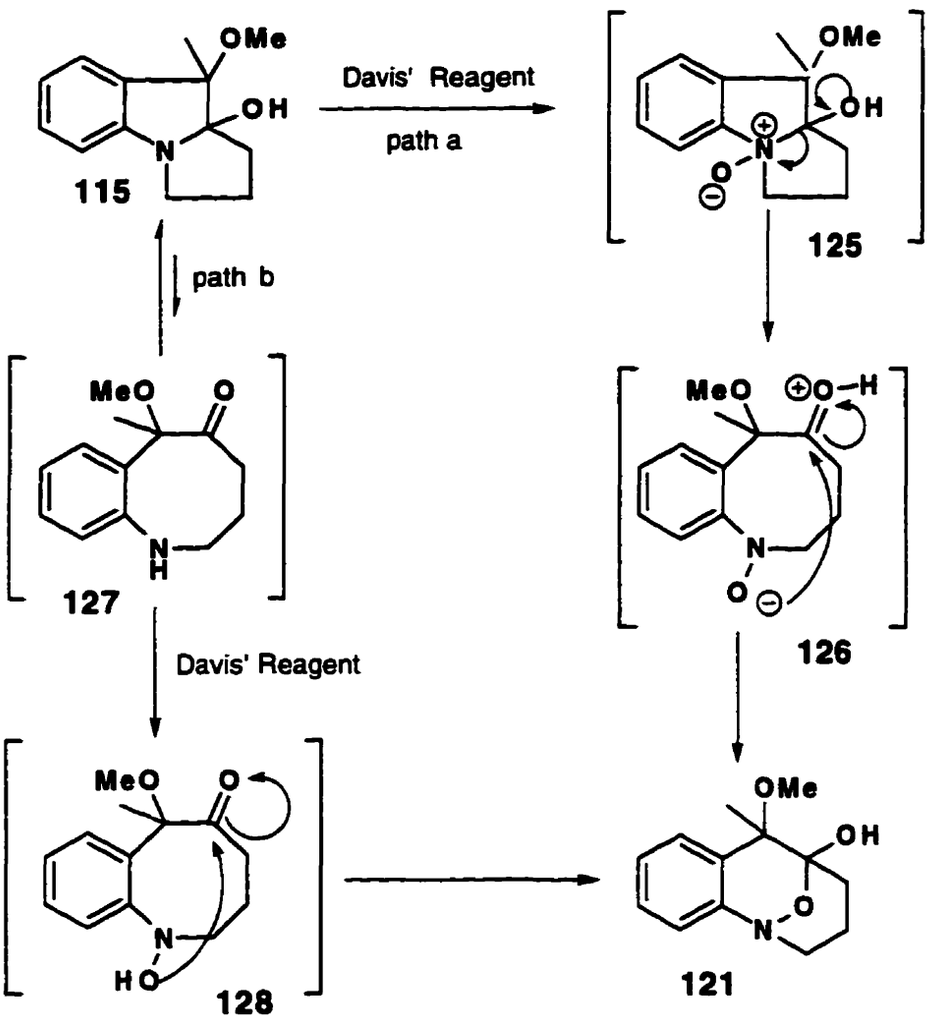
In this laboratory[72,81] it was found that reaction of Davis' reagent **122** with the alcohol **115** afforded the desired ring expansion product **121** as a mixture of diastereomers in good yield (70%) (Scheme 21). It was found that if the reaction was run in chloroform, only a single diastereomer **121c** was obtained (Scheme 21). On the other hand, if the reaction was carried out in THF, only diastereomer **121a** was obtained. In addition, if the reaction was run in methylene chloride, a roughly one to one mixture of **121a** and **121c** was produced. Exposure of the mixture of diastereomers **121a** and **121c** to trace amounts of DCl in $CDCl_3$ or to silica gel gave only one diastereomer **121c** (Scheme 21). Interestingly, heating of diastereomer **121c** in pyridine yields a mixture of **121a** and **121c**.



Solvent	Yield	121c	121a
$CHCl_3$	63%	>95%	<5%
CH_2Cl_2	53%	~50%	~50%
THF	72%	<5%	>95%

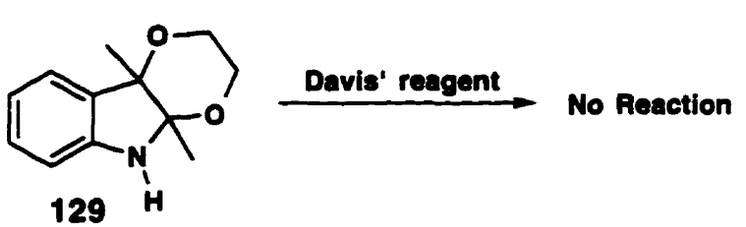
Scheme 21

Ring expansion may occur by either of two possible pathways: in path a, the alcohol **115** is oxidized by Davis' reagent to the N-oxide **125** which undergoes ring opening to form the ketone (Scheme 22). Ring closure incorporating the oxygen affords **121**, containing the bicyclic hydroxylamine hemiketal ring system. In path b, the alcohol **115** is in equilibrium with the ring opened form **127** (Scheme 22). N-oxidation of the ring opened form **127** to the N-hydroxy compound **128** followed by cyclization affords the desired system **121**. Presently, it is unclear which of the two paths is in operation in the ring expansion reaction.



Scheme 22: Two possible mechanisms for oxidative ring expansion of the alcohol 115 by Davis' reagent

Interestingly, the indoline **129** could not be oxidized with Davis' reagent to the corresponding N-hydroxy compound (Scheme 23)

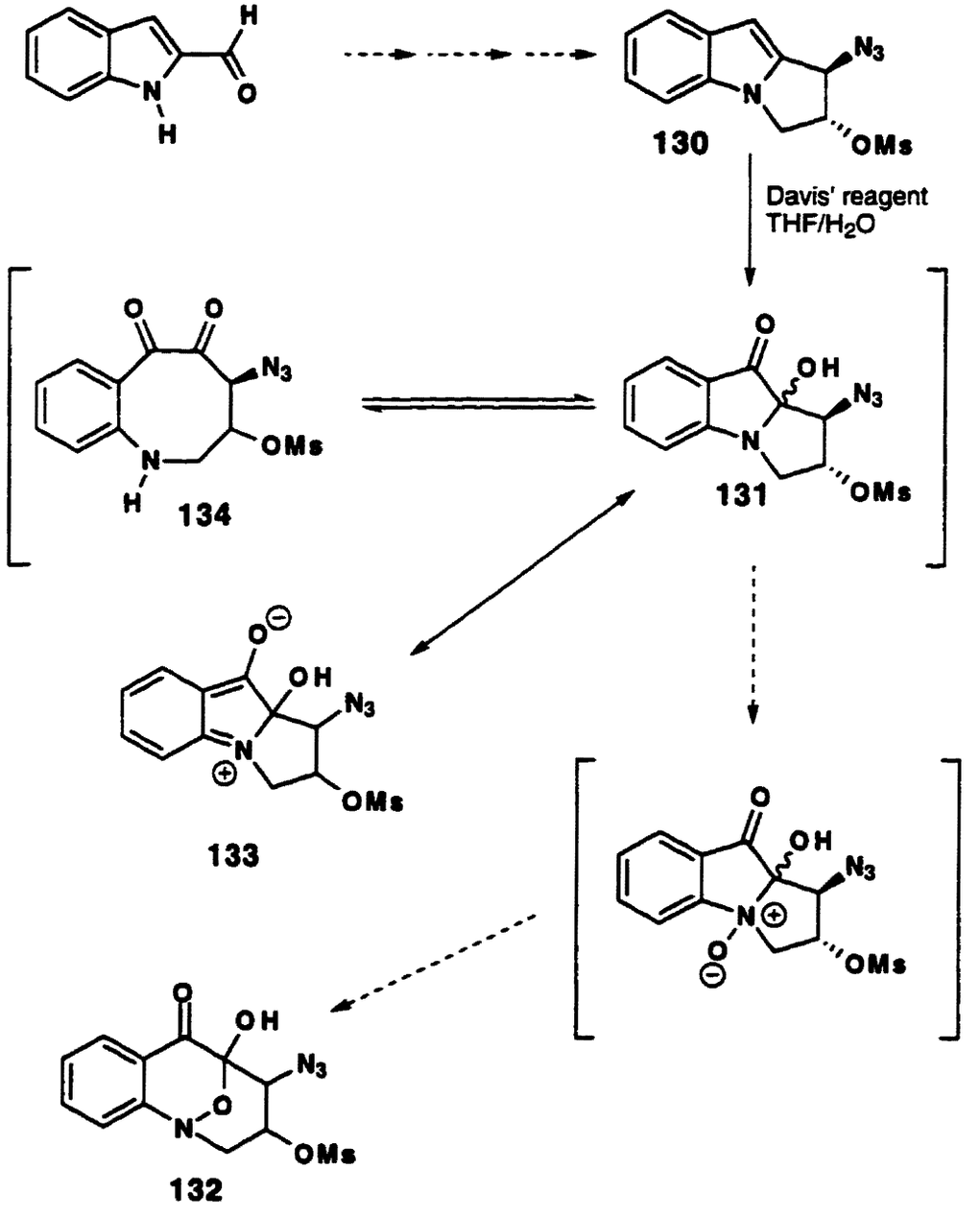


Scheme 23

Recently, Wang and Jimenez[82] have generated the indole **130** in synthetic studies towards FR-900482 (**2**) (Scheme 24). Their approach to **2** was based on an extension of our earlier studies[72,81] on oxidative ring expansion of pyrrolo[1,2-a]indoles. They reasoned that Davis' reagent might be used for oxidation of the indole **130** to the hydroxy ketone **131** as well as for oxidative ring expansion of **131** to **132**. In practice, oxidation of **130** with Davis' reagent in aqueous THF was found to yield **131** which could not be oxidized further to **132**. It was reasoned that the failure of **131** to undergo oxidative ring expansion was a consequence of resonance delocalization of the nitrogen lone pair in **131** into the keto group as shown in Scheme 24 (**131** <--> **133**) which would decrease the nucleophilicity of the nitrogen atom in **131**, decreasing the tendency for formation of the corresponding N-oxide.

Recent observations in this laboratory suggest an alternative explanation for the low reactivity of **131** with Davis' reagent. As indicated earlier (Scheme 23), the indoline in **129** is also inert to Davis' reagent even though it lacks a resonance stabilizing keto group. We have reasoned that the failure of **129** to react with an N-phenylsulfonyl oxaziridine arises from steric effects caused by the quaternary center adjacent to the nitrogen atom. A similar steric argument would predict that **131** (Scheme 24) and **115** (Scheme 22) would not react with Davis' reagent to form an N-oxide and eventually the oxidatively ring products (**132** and **121** respectively). A fundamental difference between **129** and **115** is that whereas **115** is expected to exist in equilibrium with the ring opened keto form **127** (Scheme 22), **129** cannot form a similar ring opened tautomer. Thus, it is reasoned that the oxidative ring expansion of **115** actually involves an oxidative conversion of the ketoaniline **127** to the hydroxylamine **128** which undergoes cyclization to give **121** (Scheme 22, path b).

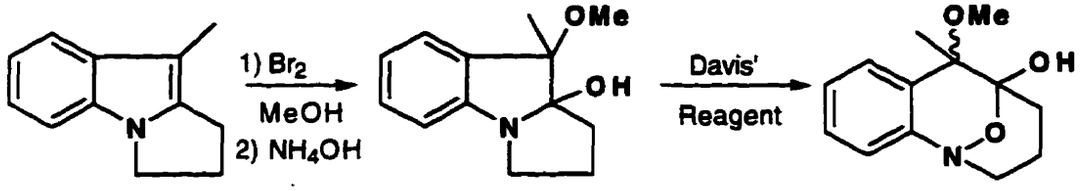
This argument would require that oxidative ring expansion of **131** would proceed via the ring-opened keto form **134** (Scheme 24). The formation of **134** from **131** would, however, be expected to be substantially less favourable than the formation of **127** from **115** (Scheme 22) since **134** experiences the unfavourable interactions of the parallel dipoles of 1,2-diketone system whereas **127** does not.



Scheme 24

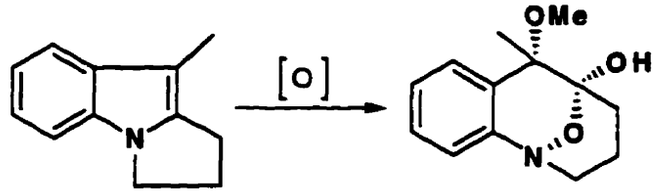
2.2 Reaction of Davis' Reagent with 114

In any event, it was clear, when the present study was initiated, that the desired bicyclic hydroxylamine hemiketal ring system **121** could be generated from the pyrrolo[1,2-a]indole **114** in two steps in moderate yield (Scheme 25). Attention was then directed toward developing a more efficient one step process for the oxidative ring expansion of the pyrrolo[1,2-a]indole ring system, **114** (Scheme 26).



114 **115** **121**

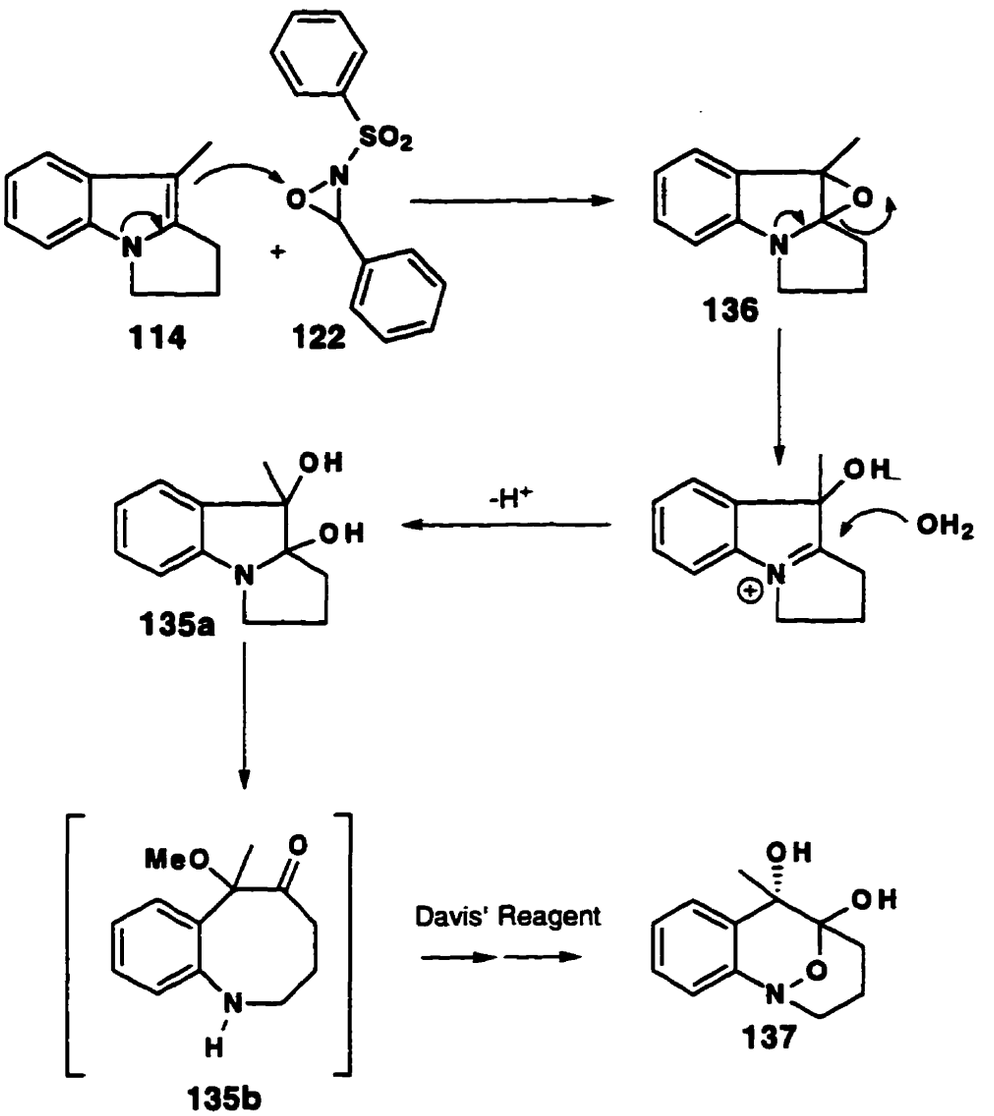
Scheme 25



114 **121c**

Scheme 26

In light of the observations of Wang and Jimenez[82] with **130**, it was felt that Davis' reagent might be used to effect the oxidation of the pyrrolo[1,2-a]indole **114** in the presence of water to generate the diol **135a** via the epoxide **136** *in situ* and that **135a** would undergo the oxidative ring expansion via the ring opened form **135b** to give **137** by analogy with our previous report of the conversion of **115** to **121** (Scheme 27).



Scheme 27: **Potential one pot synthesis of 137 from 114 using Davis' reagent as the oxidant.**

In practice, however, it was observed that the product obtained upon reaction of the pyrrolo[1,2-a]indole **114** with the oxaziridine **122** in the presence of water was clearly not the ring expanded product **137** (Scheme 28). Analysis of the major product by ^{1}H NMR revealed a large number of aromatic signals with a doubling of certain signals suggestive of a mixture of diastereomers (see NMR spectrum, Figure 37, see also Appendix A, pp. 240-242). The mass spectrum contained a molecule ion with a mass of 432 rather than the expected molecule ion with a mass of 221.

Based on the ^1H NMR spectrum and the mass spectrum the structure was tentatively assigned as a mixture of addition products incorporating all of the atoms of **114** as well as all of the atoms of **122** (Scheme 28).

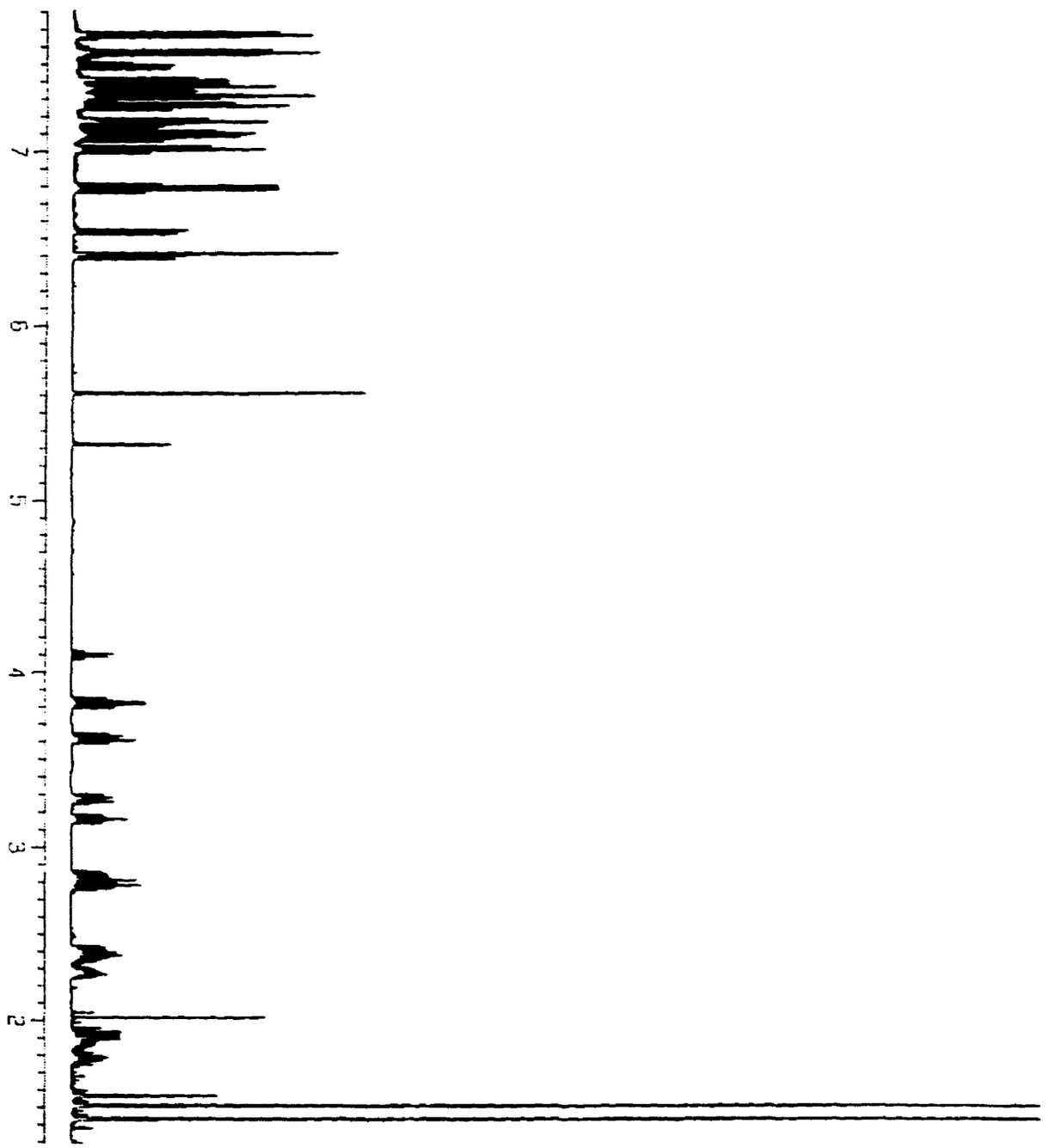
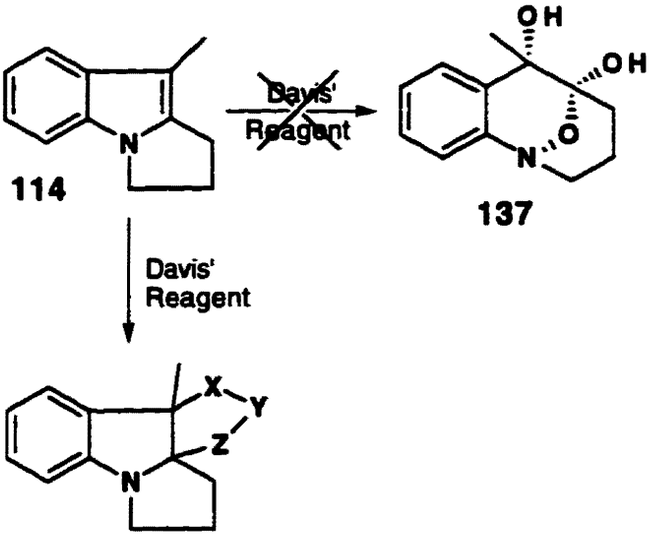


Figure 37: **Proton NMR spectrum of the major product isolated from the reaction of 114 with Davis' reagent (122).**



138	X	Y	Z
a	O	CHPh	NSO_2Ph
b	NSO_2Ph	CHPh	O
c	CHPh	NSO_2Ph	O
d	O	NSO_2Ph	CHPh
e	CHPh	O	NSO_2Ph
f	NSO_2Ph	O	CHPh

Scheme 28

2.2.1 Proton NMR Experiments

Although it was suspected from the outset that the products obtained were diastereomers of **138a**, the alternative formulations **138b-f** could not be excluded *a priori*. Since chromatographic separation of the components proved difficult, structural analysis by ^1H NMR was pursued with the mixture of components. In this case it proved possible to separate the complex overlapping ^1H NMR signals from

the two components into distinct signals for each of the individual hydrogen atoms of the two diastereomers using selective TOCSY experiments.[83-85]

In a selective TOCSY experiment a signal enhancement is observed to move through spin systems over time by the use of a train of pulses of varying mixing times to distribute magnetization from one nucleus to the next in the spin system.[85] A selective TOCSY involving irradiation at the doublet at 6.39 ppm (Appendix A, page 245), C(7)-H, of component A resulted in an early appearance of a triplet at 7.07 ppm, due to C(6)-H, as well as a later appearance in a triplet at 6.79 ppm, corresponding to C(5)-H (Figure 38). That the signal at 6.39 ppm corresponded to C(7)-H rather than C(4)-H was suggested by the high field shift characteristic of a π-electron rich center adjacent to an aniline type nitrogen. It should be noted that the numbering system shown was chosen to be consistent with that which was arbitrarily selected for assignment of co-ordinates of the X-ray crystallographic structures for compounds **141** and **143** discussed on pages 72 and 73.

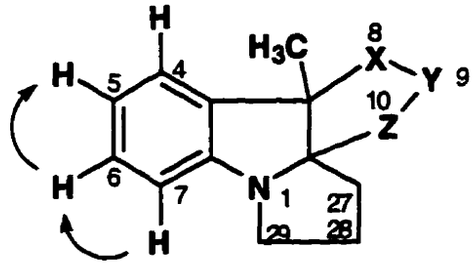
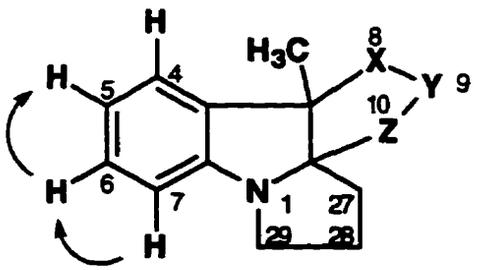


Figure 38: Selective TOCSY with irradiation at 6.39 ppm.

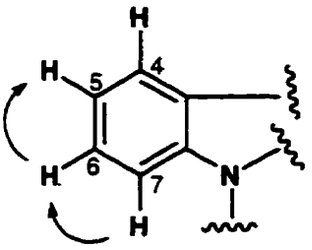
In a parallel experiment, a selective TOCSY experiment involving irradiation of the doublet at 6.53 ppm (Appendix A, page 246), assigned to C(7)-H of component B showed an early rise in intensity of a triplet at 7.13 ppm, C(6)-H, as well as a later rise in a triplet at 6.77 ppm, corresponding to C(5)-H (Figure 39).

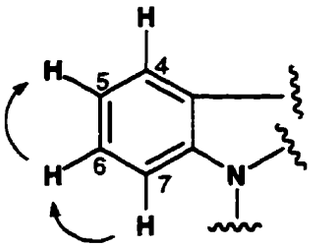


δ 6.53

Figure 39: A selective TOCSY with irradiation at 6.53 ppm.

A summary of the TOCSY experiments for the aromatic hydrogens for the two components is shown below (Figure 40).





	Component A		Component B	
Irradiation site :	6.39 (td) ppm	C(7)-H	6.53 (td) ppm	C(7)-H
Order of Appearance of Signals:	7.07 (td) ppm	C(6)-H	7.13 (td) ppm	C(6)-H
	6.79 (td) ppm	C(5)-H	6.77 (td) ppm	C(5)-H

Figure 40

These two selective TOCSY experiments aided in the clarification of an unusual signal at 6.78 ppm, which at first glance appeared to be a "a quartet of doublets". The selective TOCSY experiments clearly showed that this signal was composed of two apparent triplets, C(6)-H, from the components A and B (Figure 41). The remaining signals for the C(4)-H's of the two components were identified as a doublet at 7.14 ppm for component B and a doublet at 7.10 ppm for component A by difference NOE experiments which are described below. Thus the aromatic

hydrogens for components A and B could be assigned to specific signals in the ^1H NMR spectrum of the mixture each corresponding to an ABCD spin system.

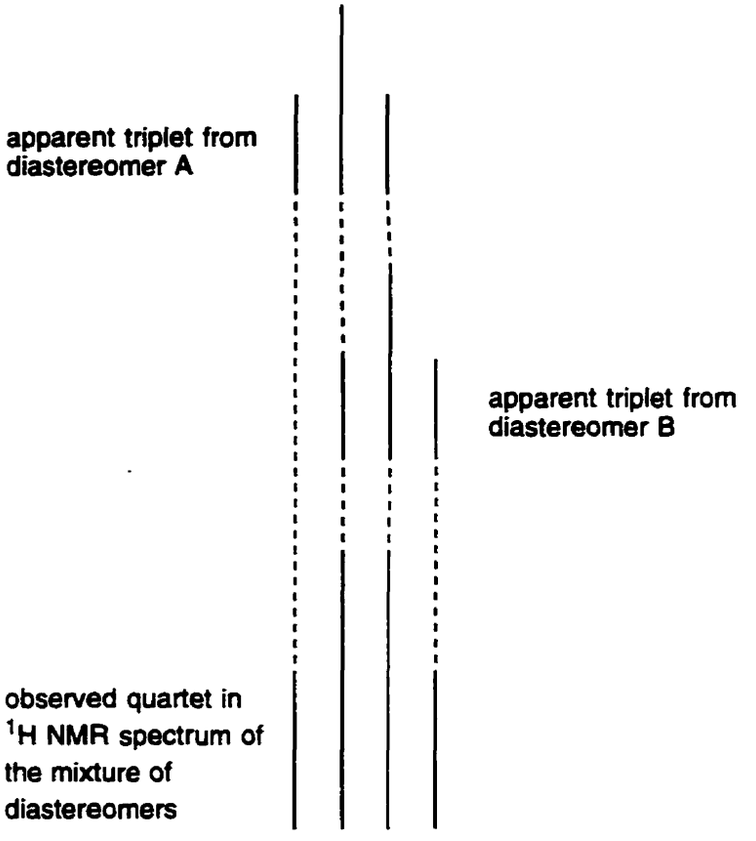
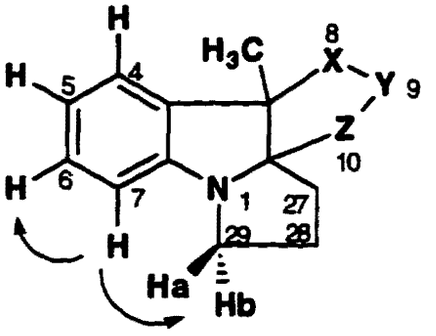


Figure 41: The unusual doublet of a quartet at 6.78 ppm is composed of two apparent triplets from the two diastereomers.

Attention was then turned to analysis of the aliphatic hydrogens. On the basis of chemical shift, the signal at 3.81 ppm was tentatively assigned to one of the hydrogens at C(29). A selective TOCSY experiment with irradiation at 3.81 ppm (Appendix A, page 244) clearly shows the initial rise of a multiplet at 3.15 ppm, suggesting that the multiplets at 3.81 and at 3.15 are the two hydrogens on C(29). Later, there is a rise in intensity of multiplets at 1.78 and 2.28 ppm corresponding to the hydrogens on C(28) followed by a rise in intensity of multiplets at 2.82 and 2.40 ppm, corresponding to the hydrogens on C(27). This experiment established the existence of a continuous chain of three methylene groups in one of the components.

That this particular trimethylene bridge was that from the so-called component A was established by a difference NOE experiment (Appendix A, page 249) involving irradiation of the doublet at 6.39 ppm previously tentatively assigned C(7)-H of component A which resulted in an enhancement in the signal at 3.15 ppm (Figure 42). This NOE experiment also clearly confirmed the validity of the tentative assignments of the signals at 6.39 ppm and 3.15 ppm as C(7)-H and C(29)-H which were based initially upon chemical shift reasoning.



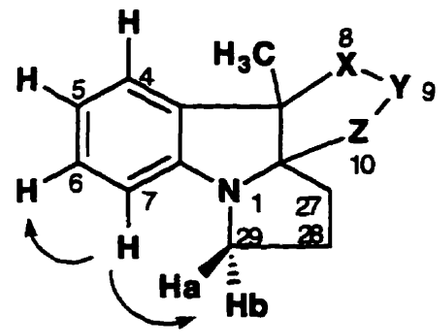
A

Figure 42

In a parallel experiment, in which a selective TOCSY experiment was initiated by irradiation at 3.61 ppm (Appendix A, page 243), a multiplet at 3.28 ppm arising from C(29)-H appeared initially. Over time, two multiplets at 1.88 ppm and 2.36 ppm appeared and were assigned to the C(28) hydrogens. Finally the appearance of multiplets at 1.94 ppm and 2.78 ppm, corresponding to the hydrogens on C(27) of component B was observed.

This TOCSY experiment established the presence of a continuous chain of three methylene groups in the structure of the second component of the mixture. The spatial relationship of the chain to the aromatic hydrogens was established by a difference NOE experiment.

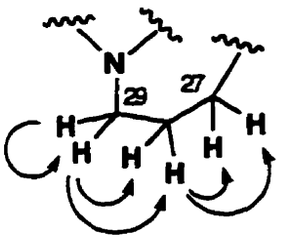
Irradiation of the doublet at 6.53 ppm (Appendix A ,page 249), assigned to C(7)-H of component B, resulted in a NOE enhancement in an apparent triplet at 7.13 ppm, corresponding to C(6)-H, as well as a weak enhancement of a multiplet at 3.28 ppm, corresponding to one hydrogen of C(29)-H. This observation confirmed the validity of the assignments of the C(7)-H and C(29)-H signals which were based initially on chemical shift arguments.

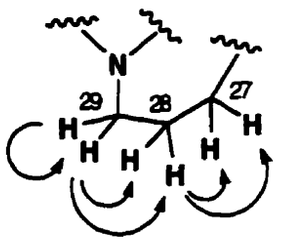


B

Figure 43

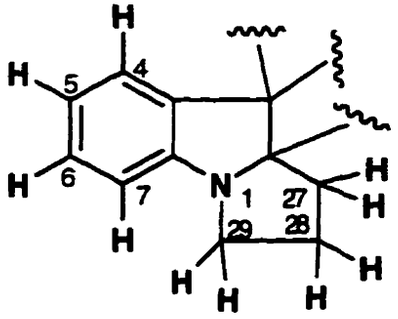
A summary of the TOCSY experiments for the aliphatic hydrogens appears below (Figure 44).

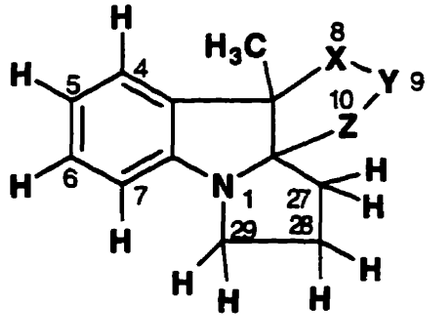




	Component A		Component B	
Irradiation site :	3.81 (m) ppm	C(29)-H	3.61 (m) ppm	C(29)-H
Order of Appearance of Signals:	3.15 (m) ppm	C(29)-H	3.28 (m) ppm	C(29)-H
	1.78 (m) ppm	C(28)-H	1.88 (m) ppm	C(28)-H
	2.28 (m) ppm	C(28)-H	2.36 (m) ppm	C(28)-H
	2.82 (m) ppm	C(27)-H	1.94 (m) ppm	C(27)-H
	2.40 (m) ppm	C(27)-H	2.78 (m) ppm	C(27)-H

Figure 44



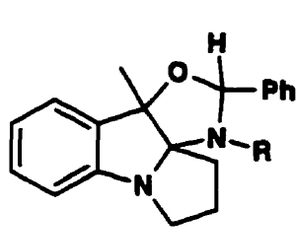


Z **Z'**

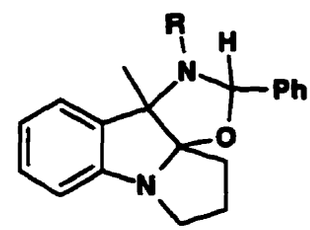
Figure 45

Thus, these NMR experiments strongly supported the existence of the part structure Z in each component of the mixture (Figure 45). Justification of the expansion of the part structure Z to Z' was found in the results of difference NOE experiments involving irradiation of the signals from the CH_3 singlet from the two

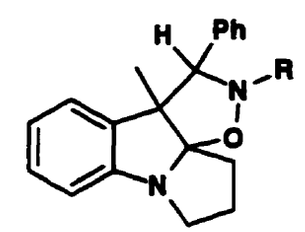
components (at 1.42 and 1.50 ppm, Appendix A, page 247) which resulted in intensity enhancements in signals at 7.14 ppm (C(4)-H of component B) and 7.10 ppm (C(4)-H of component A). The NMR data described thus far could be considered, in qualitative terms, as being compatible with any of the six regioisomers represented by **138a-f** (Figure 46).



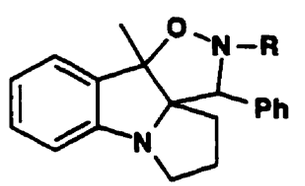
138a



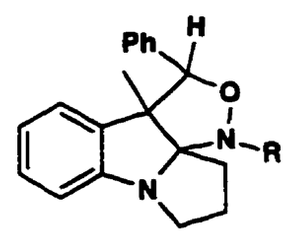
138b



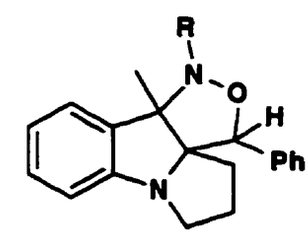
138c



138d



138e



138f

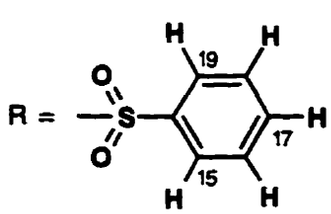


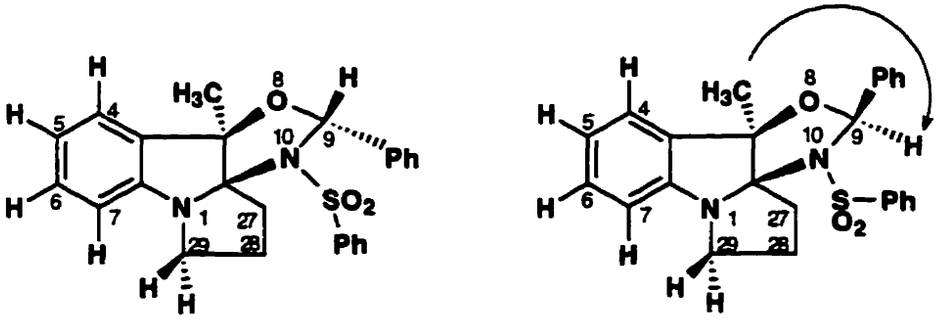
Figure 46

The observation of an NOE enhancement in the doublet at 7.56 ppm arising from the benzene sulfonyl group upon irradiation of the singlet at 5.60 ppm (Appendix A, page 248) corresponding to the benzylic hydrogen of component A, established a close proximity between the benzylic hydrogen and the benzene

sulfonyl group which is expected for structures **138a**, **b**, **c** or **d** but not for structures **138e** or **f**. Similarly, irradiation of the singlet at 6.40 ppm (Appendix A, page 248) corresponding to the benzylic hydrogen of component B results in an NOE enhancement of an apparent doublet at 7.67 ppm assignable to the C15,9-H's of the benzenesulfonyl group.

A distinction between the remaining possible structures **138a-d** becomes possible by analysis of the observation that irradiation of the aromatic doublet at 6.39 ppm (Appendix A, page 249) (assigned to C(7)-H of component A) results in an NOE enhancement in the apparent doublet at 7.56 ppm (assigned to the C(15,19)-H's of the benzene sulfonyl group of component A). Of the four structures, **138a-d**, the spatial proximity necessary to allow for such an NOE effect is found only in **138a**. As a result, it was concluded that the components A and B were diastereomers of the structure **138a**.

If it is reasoned that ring strain effects would strongly disfavour compounds with a trans 5/5 ring fusion, the structural possibilities are limited to **138a1** and **138a2** (Figure 47).



138a1 **138a2**

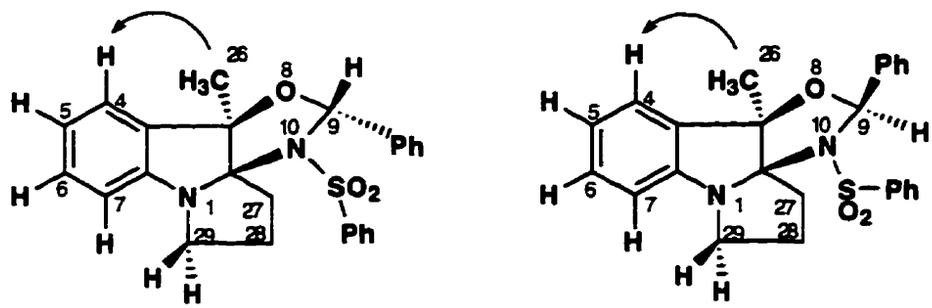
Figure 47: Observed NOE enhancements upon irradiation of the signals at 1.42 and 1.50 ppm of components A and B.

That component B was represented by structure **138a2** was deduced from the observation that irradiation of the methyl singlet at 1.42 ppm (Appendix A, page

247) resulted in an NOE enhancement in the benzylic hydrogen singlet at 6.40 ppm. Consistent with assignment of structure **138a1** to component A was the absence of an NOE enhancement for the benzylic hydrogen singlet at 5.60 ppm upon irradiation of the methyl group signal at 1.50 ppm (Appendix A, page 247).

In addition, the C(4)-H signal of component B (**138a2**) was assigned to a doublet at 7.14 ppm based on the observation of a NOE enhancement upon irradiation of the methyl singlet (C(26)) at 1.42 ppm (Appendix A, page 249). In a parallel experiment, the C(4)-H doublet of component A (**138a1**) was assigned to a doublet at 7.10 ppm based on the observation of an NOE enhancement upon irradiation of the methyl singlet (C(26)) at 1.50 ppm (Appendix A, page 247) (Figure 48).

The spectra of the TOCSY and NOE experiments appear in Appendix A.



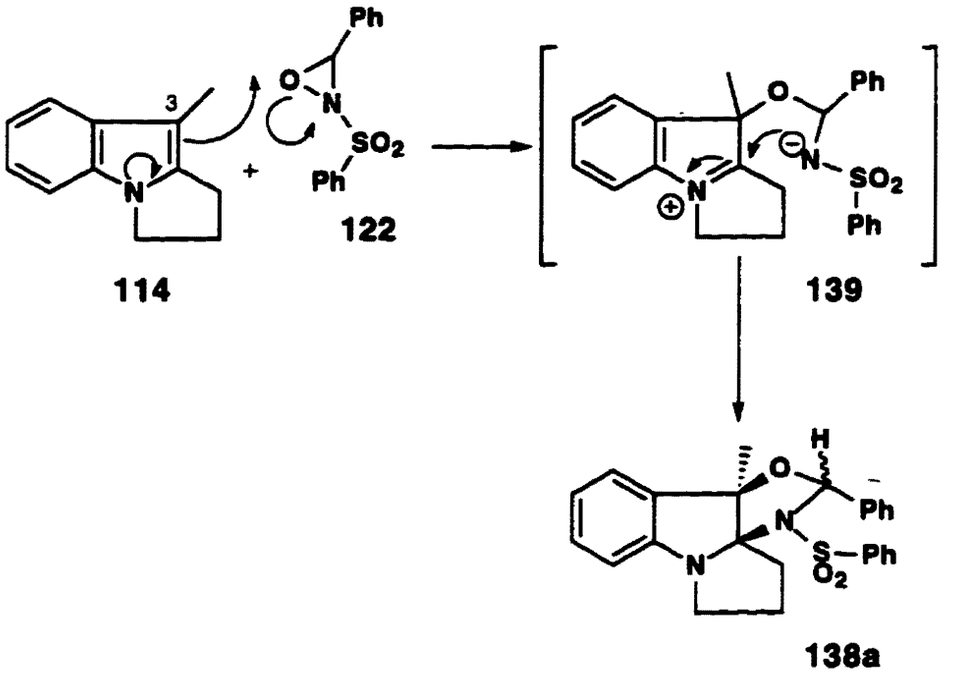
138a1 **138a2**

(component A) **(component B)**

Figure 48: **Observed NOE enhancement at 7.14 ppm and 7.10 ppm upon irradiation of singlets at 1.42 ppm and 1.50 ppm, respectively.**

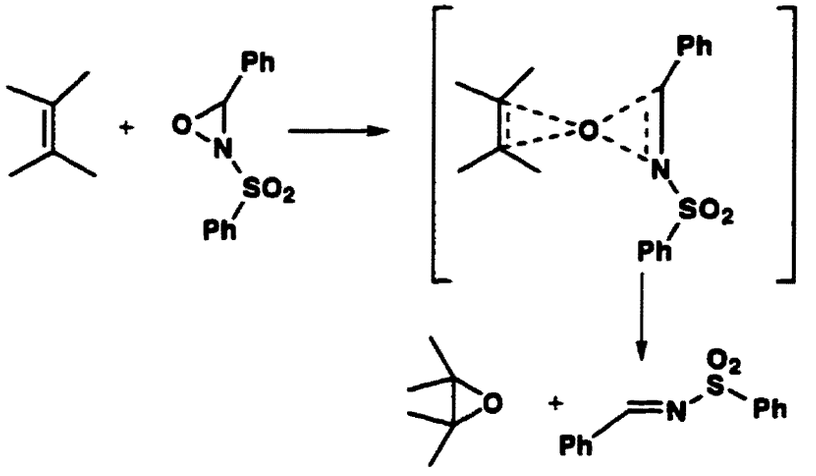
2.2.2 Mechanism for the formation of the adduct 138a

A possible mechanism for the formation of the adduct involves nucleophilic attack of the C(3) of the pyrrolo[1,2-a]indole **114** on the oxygen of Davis' reagent, affording a zwitterionic intermediate **139** (Scheme 29). This intermediate might then cyclize to the observed adduct **138**.



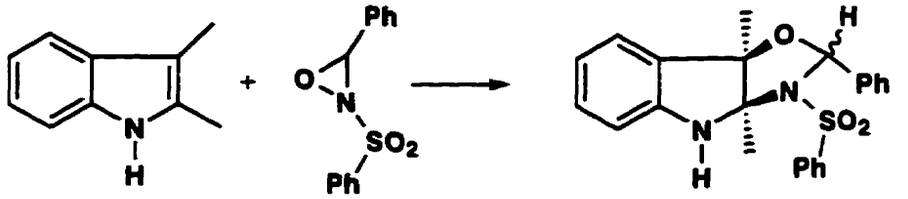
Scheme 29: Possible mechanism for the formation of the adduct via a zwitterionic intermediate.

We were, however, concerned by the fact that this proposed mechanism represented a substantial deviation from the mechanisms of reaction of Davis' reagent with nucleophiles. It is widely believed that Davis' reagent reacts with olefins, enamines and enolates via a concerted S_N2-like oxygen atom transfer mechanism (Scheme 30).[86] This view has been supported by extensive *ab initio* calculations.[87-89]



Scheme 30

In order to ascertain whether the anomalous reaction of **114** with **122** was a consequence of unusual reactivity of the pyrrolo[1,2-a]indole ring system or a general property of 2,3-dialkylindoles, reaction of **122** with 2,3-dialkylindole **140** was examined. To explore this possibility, the less strained 2,3-dimethyl indole **140** was reacted with Davis' reagent. The major product isolated from the reaction mixture had a mass of 406 and the ^{1}H NMR spectrum suggested a mixture of diastereomers of the addition product **141** analogous to **138** (Scheme 31).



140 **122** **141**

Scheme 31

The diastereomers of **141** were separated chromatographically and a crystal of one of the diastereomers, **141a**, of sufficient quality was grown to allow a single crystal X-ray diffraction study (Figure 49). The co-ordinates and bond angles for the X-ray structure appear in Appendix B, page 252.

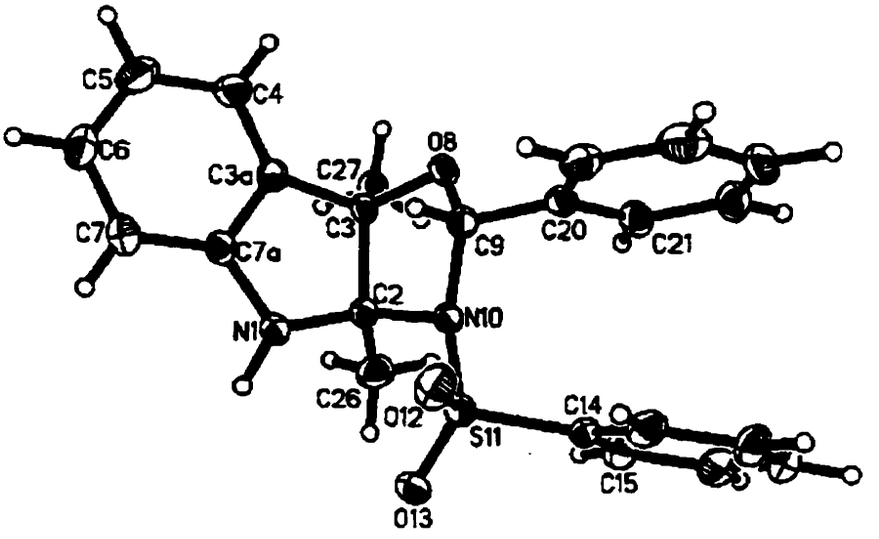
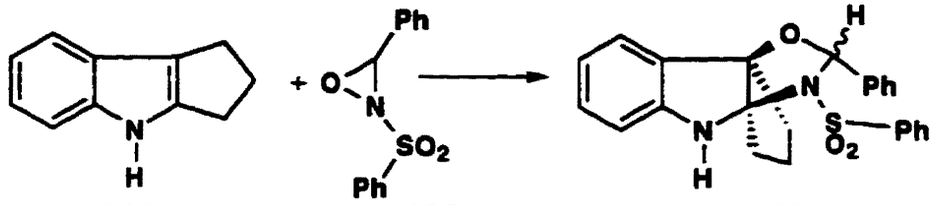


Figure 49

Furthermore, reaction of cyclopentanoindole **142** with **122** also yielded an adduct, in this case with a mass of 418. Again the major product appeared to be the addition product **143** as a mixture of diastereomers (Scheme 32). The diastereomers were separated by fractional crystallization and a suitable crystal of one of the diastereomers, **143b**, was grown for a single crystal X-ray diffraction study (Figure 50). The X-ray data appears in Appendix B, page 260.



142 **122** **143**

Scheme 32

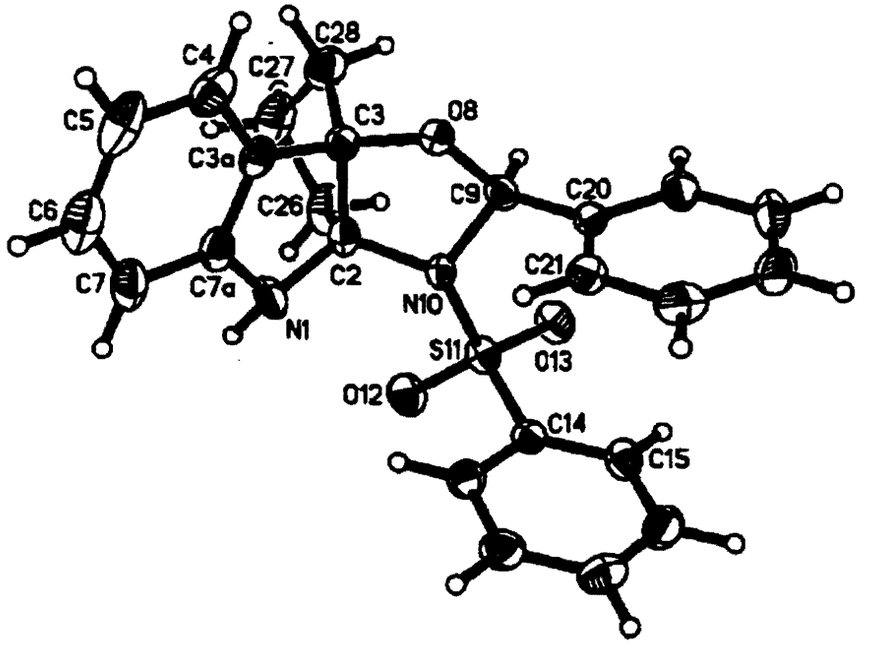
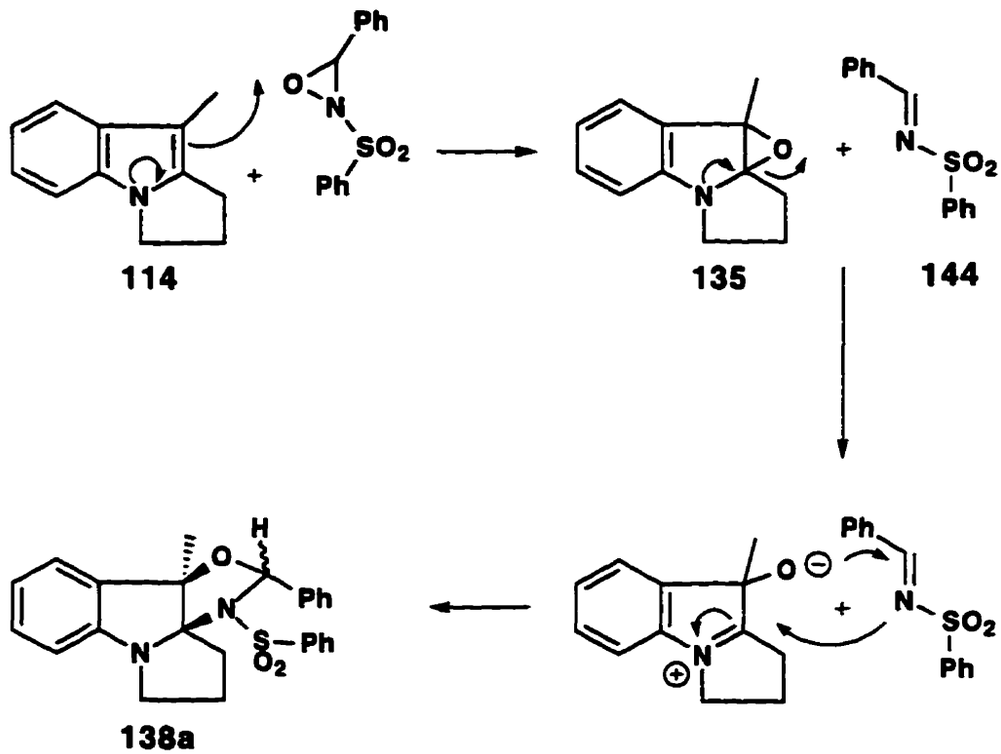


Figure 50

Interestingly, the stereochemistry of **141a** corresponds with that of **138a1** whereas that of **143b** corresponds with that assigned to **138a2**. Given the widespread acceptance of the direct-oxygen atom transfer mechanism, the

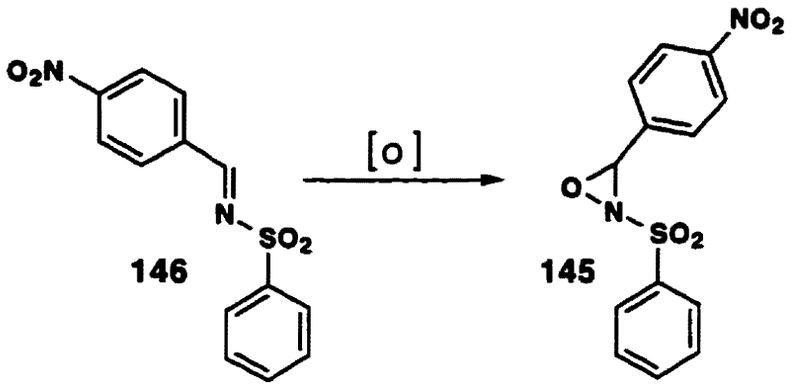
possibility exists that the observed products might be produced by a route which is not in conflict with the currently accepted mechanism. It was reasoned that it might be possible that **114** was reacting with Davis' reagent via the oxygen atom transfer mechanism to give the epoxide **135** initially (Scheme 33). Ring opening of the epoxide **135** followed by reaction with the elimination product **144** in a second step, might yield the observed adduct **138a**.



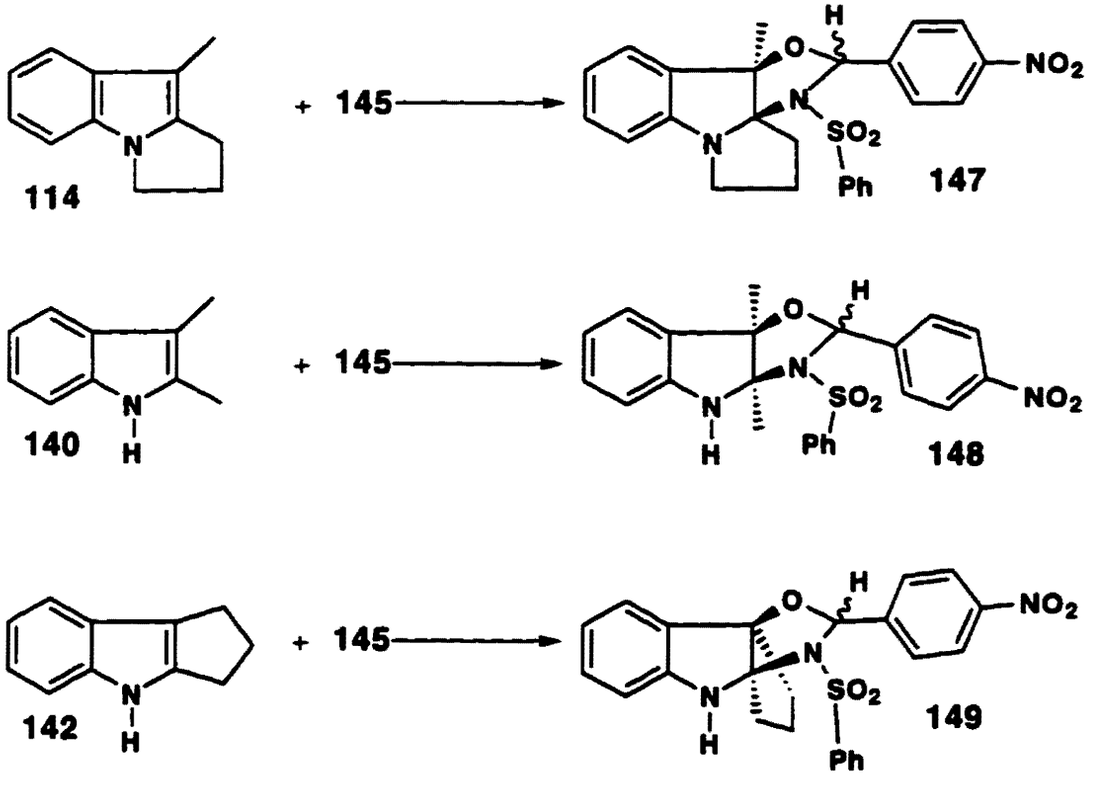
Scheme 33

It was necessary to consider means of distinguishing between the two possible mechanisms (i.e. Scheme 29 verses Scheme 33). In order to obtain information by which the two mechanisms might be distinguished, the possibility of performing cross-over experiments was considered. For this purpose, the nitro analog of Davis reagent **145** was made from the nitro substituted imine **146** (Scheme 34). This was then reacted with the indoles: pyrrolo[1,2-a]indole (**114**), 2,3-dimethyl indole (**140**) and cyclopentanoindole (**142**) (Scheme 35). The

products **147**, **148** and **149** were isolated and characterized . It was found that the products **147**, **148** and **149** could easily be distinguished from the analogous adducts **138**, **141** and **143** respectively by the chemical shifts of the C(9)-H signals in the ^{1}H NMR spectra. A summary of the distinguishing signals in the ^{1}H NMR spectra appears in Figure 51.



Scheme 34



Scheme 35

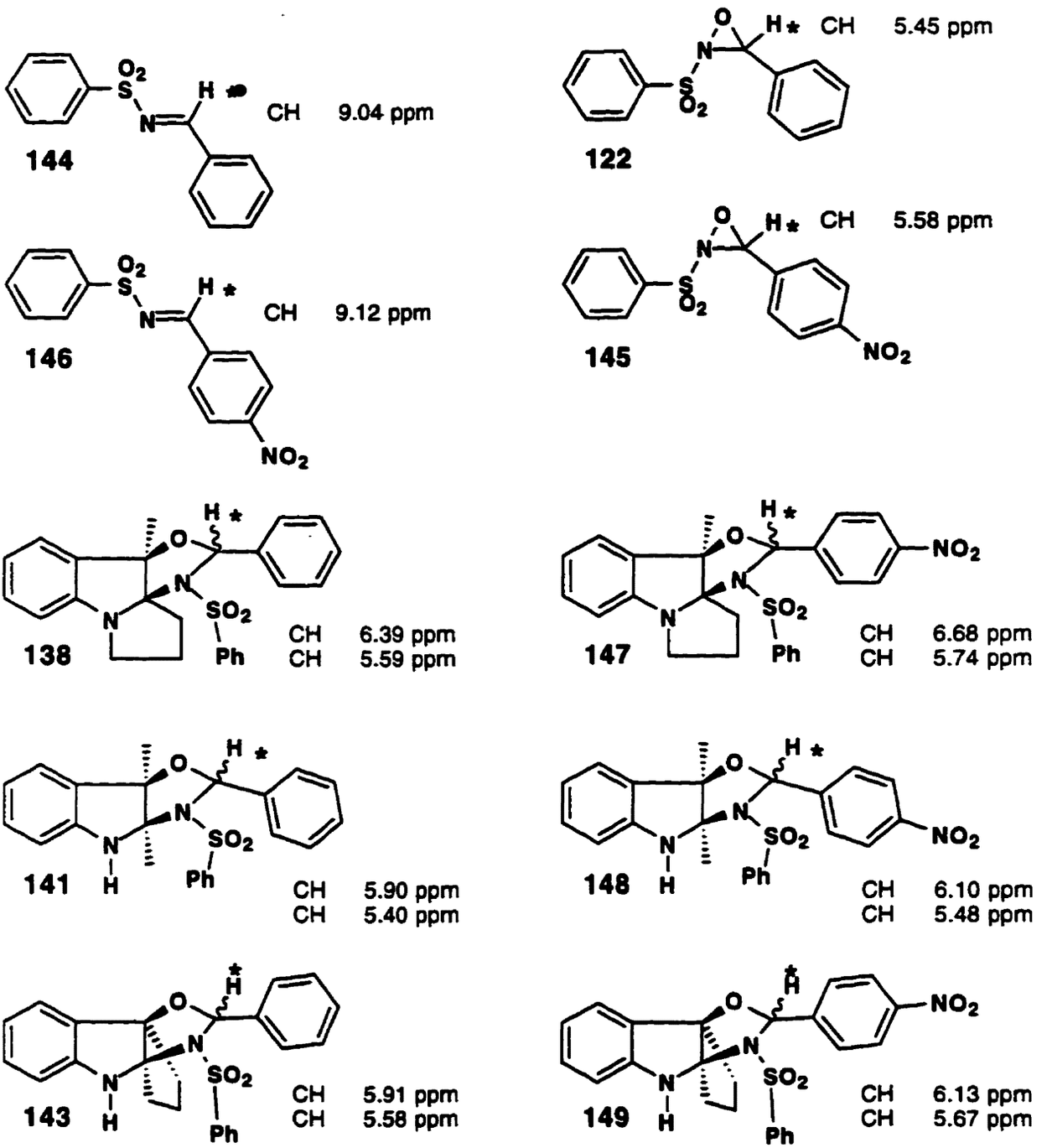
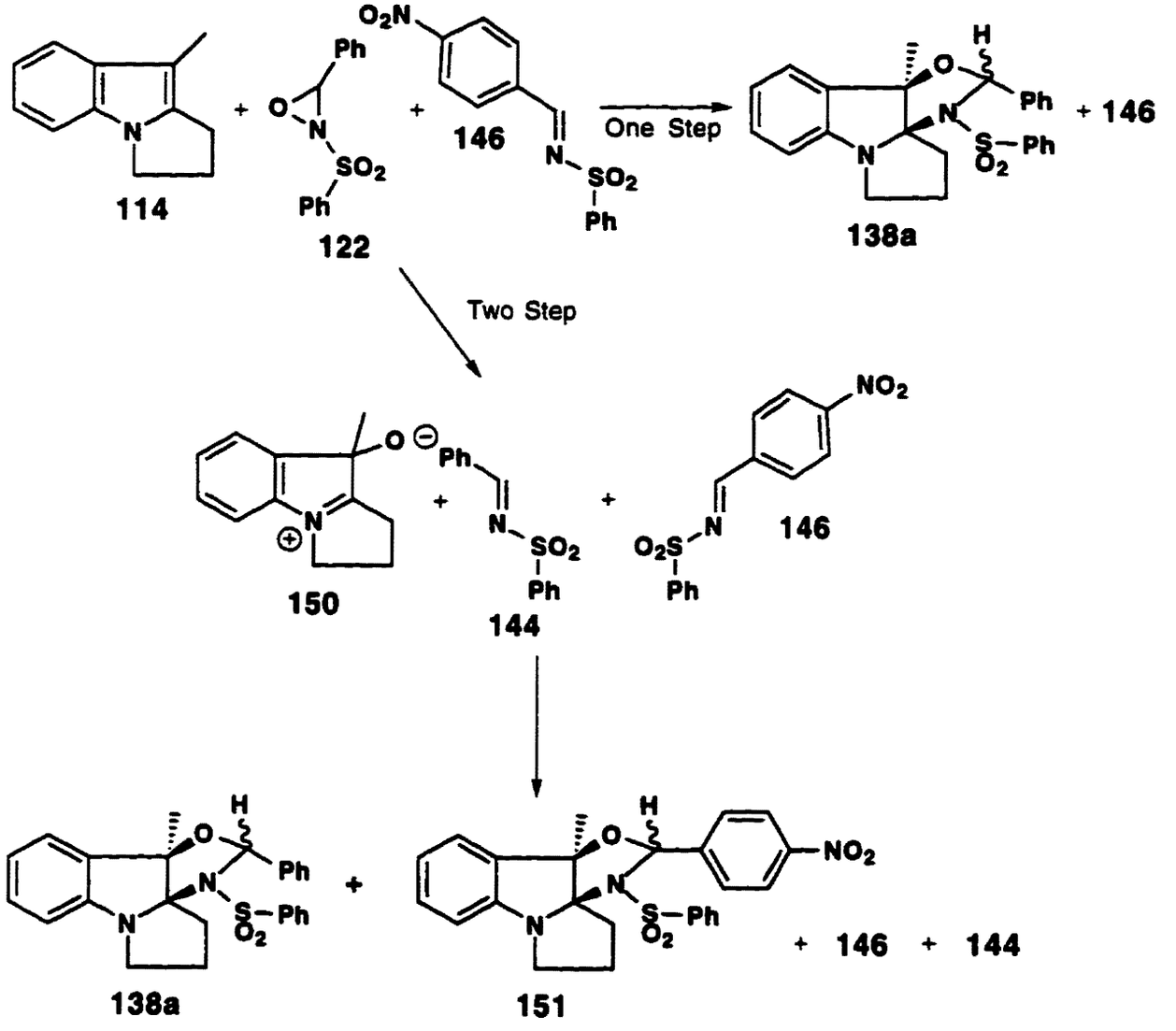


Figure 51: Summary of distinguishing CH signals in the proton NMR spectra of the adducts.

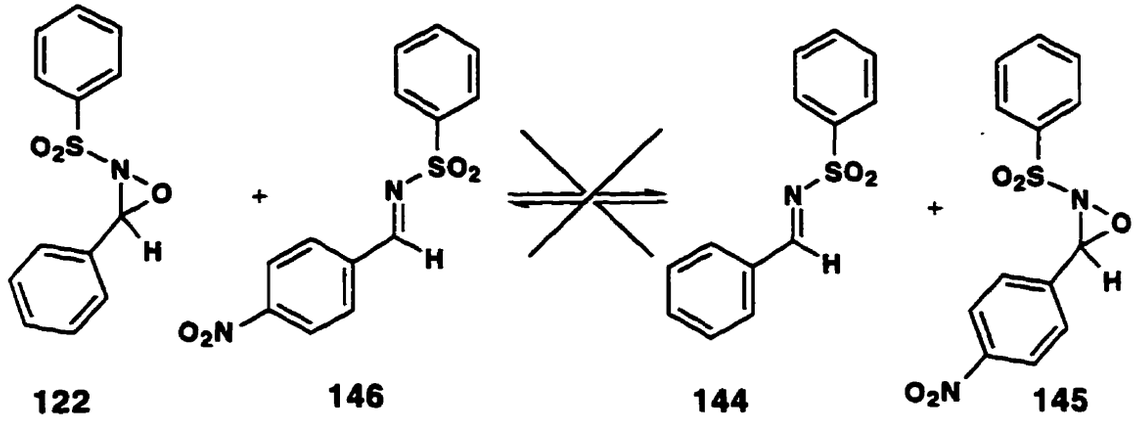
It was felt that the distinguishing features in the proton NMR spectra of the adducts might be utilized in cross-over experiments to distinguish between the two mechanisms. Cross-over experiments are often used to distinguish between one and two step mechanisms. Consider the reaction of a one to one to one mixture of

indole **114**, Davis' reagent **122** and the nitro substituted imine **146**. If the one step mechanism (Scheme 29) was in operation then analysis of the product distribution should show the adduct **138a** and unreacted nitro-imine **146** (Scheme 36). On the other hand, if the reaction progresses through two discrete steps (Scheme 33), then the zwitterionic intermediate **150** could react with the imine **144** or with the nitro imine **146** to yield a mixture of adducts **138a** and **151** (Scheme 36). The presence of a mixture of **138a** and **151** or the presence of **138a** as the only adduct can easily be determined by the examination of the ^{1}H NMR spectrum of the products.



Scheme 36: Product distribution expected in cross-over experiment.

However, prior to carrying out the cross-over experiments it was necessary to eliminate the possibility of oxygen atom transfer between the oxaziridine **122** and the imine **146** (Scheme 37). In practice, no oxygen atom transfer was observed by TLC or by ^{1}H NMR analysis, under the conditions of the cross-over experiments (Scheme 37).

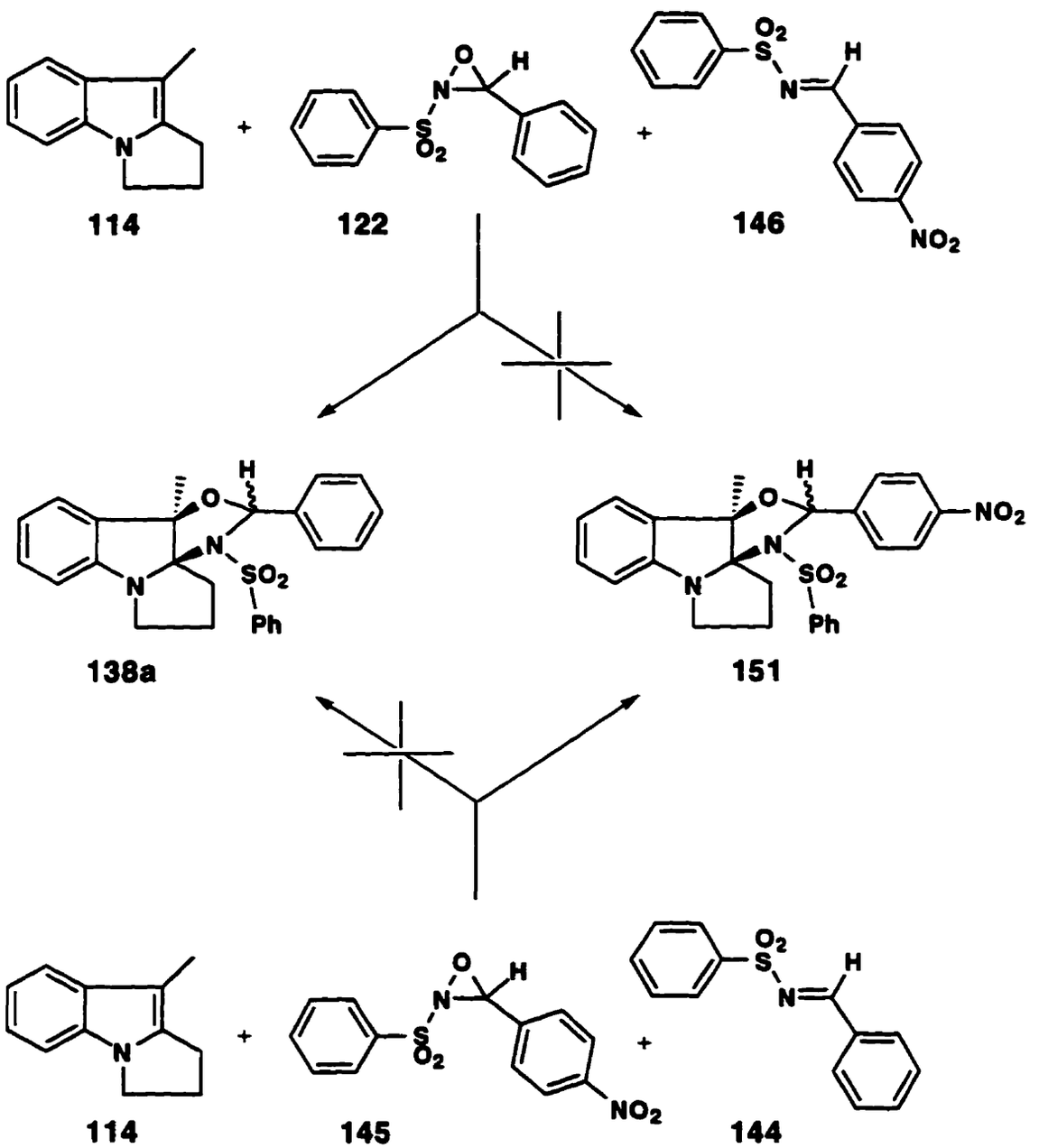


122 **146** **144** **145**

Scheme 37

A cross-over experiment in which the pyrrolo[1,2-a]indole **114** was reacted with the oxaziridine **122** in the presence of one equivalent of the imine **146** was carried out (Scheme 38). If the adduct was formed via the zwitterionic pathway described earlier (Scheme 29) then only **138** should be formed. However, if oxygen atom transfer mechanism was in operation prior to adduct formation then the reaction mixture should contain some of the nitro-analog **151** (cross-product), formed via the mechanism described in Scheme 33. In fact, none of the cross-product **151** was observed by ^{1}H NMR (Scheme 38). In a complementary experiment, the pyrrolo[1,2-a]indole (**114**) was reacted with the nitro substituted oxaziridine **145** in the presence of one equivalent of the unsubstituted imine **144** (Scheme 38). Again, the cross-product, in this case, **138a** was not observed in the reaction mixture. The observed product distribution in both experiments is consistent with the ionic mechanism

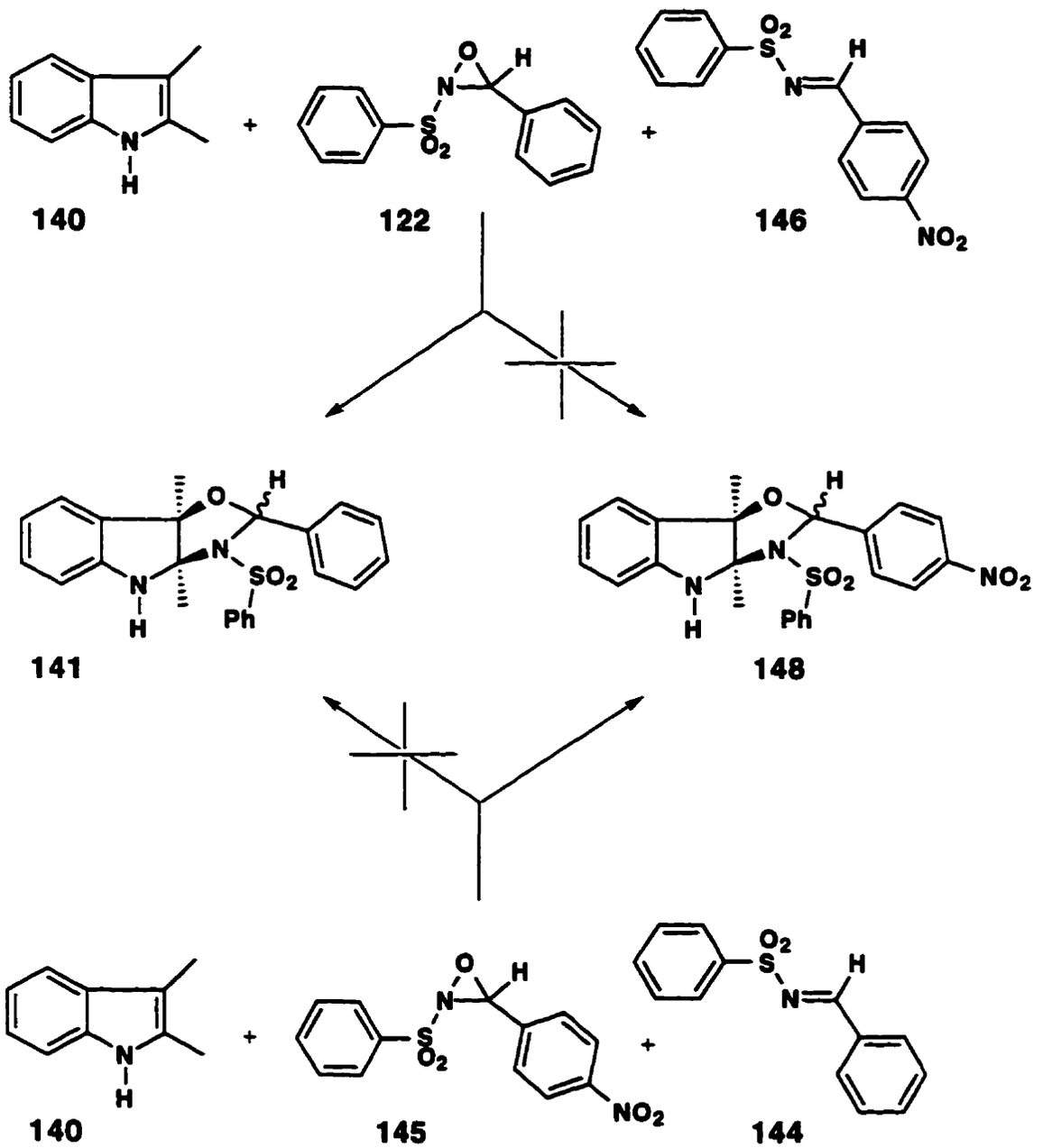
(Scheme 29) and not the currently accepted S_N2-like oxygen atom transfer mechanism.



Scheme 38: Cross-over experiments with the pyrrolo[1,2-a]indole 114.

In addition, cross-over experiments with 2,3-dimethylindole **140** were also carried out (Scheme 39). In the reaction of **140** with the oxaziridine **122** in the presence of the nitro substituted imine **146**, the cross-over product **148** was not

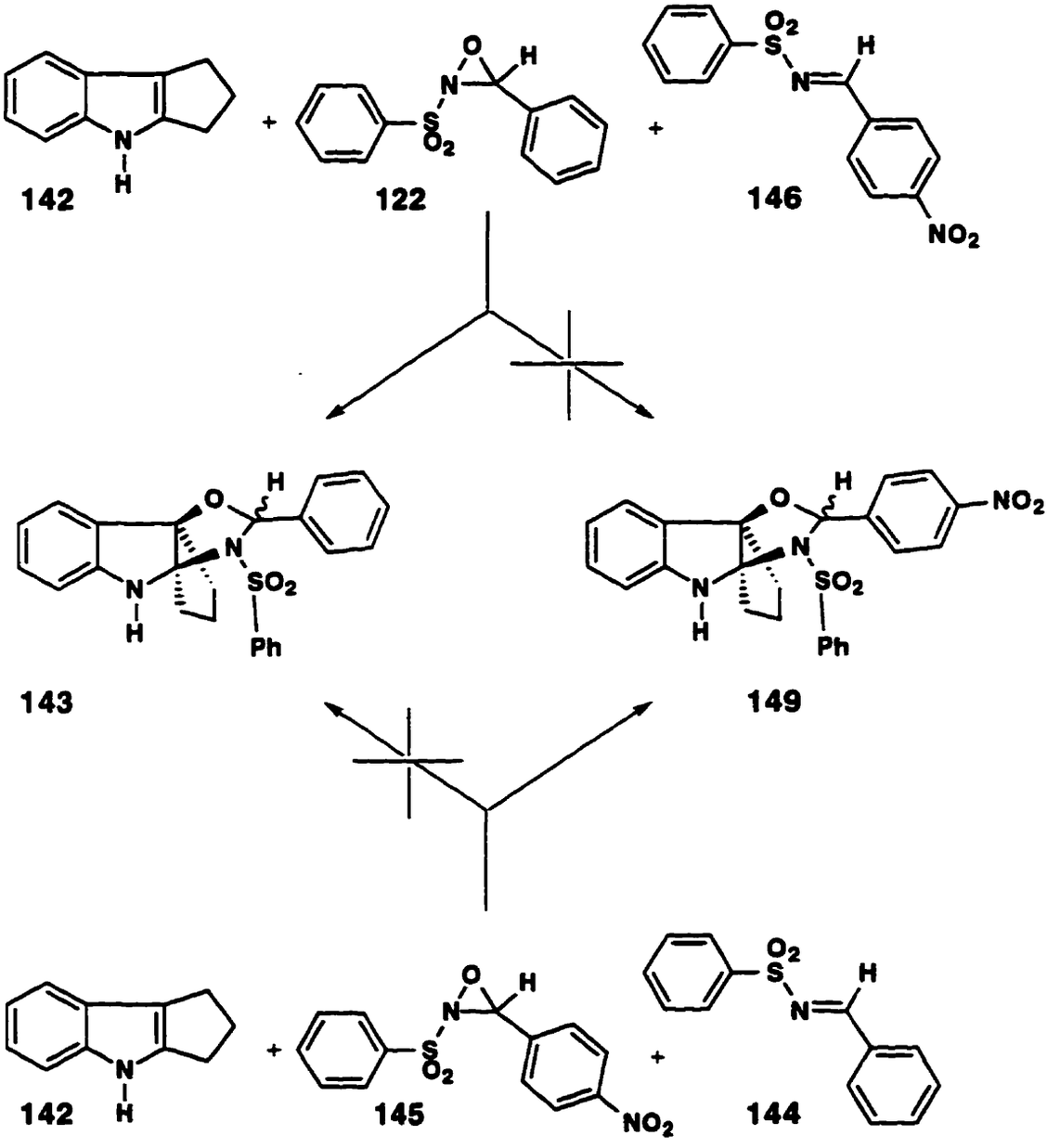
observed by ^{1}H NMR. This was also true of the complementary experiment in which 2,3-dimethylindole (**140**) was reacted with the nitro substituted oxaziridine **148** in the presence of the unsubstituted imine **144** (Scheme 39).



Scheme 39: Cross-over experiments with 2,3-dimethylindole 140.

Furthermore cross-over experiments involved cyclopentanoindole **142** with the oxaziridine **122** in the presence of the imine **146** (Scheme 40). Again, none of

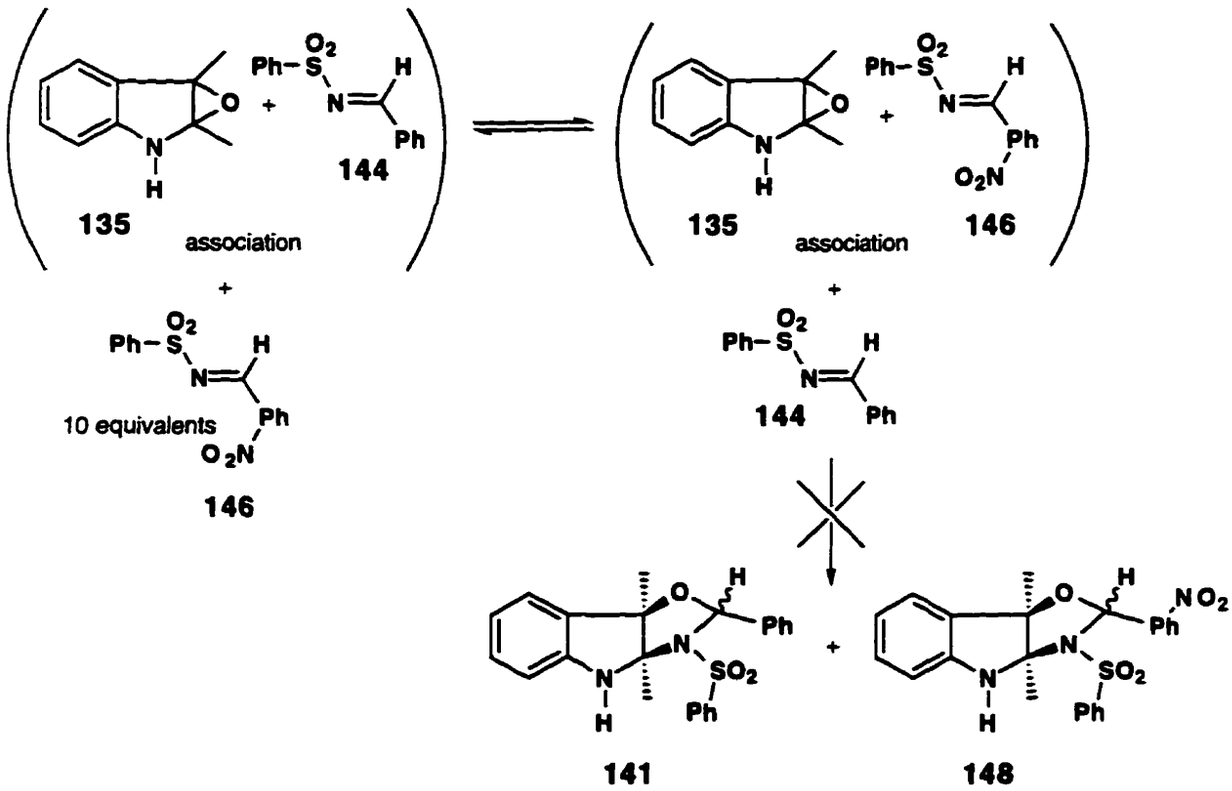
the cross-over product **149** was observed in the reaction mixture by ^{1}H NMR and similarly, none of the cross-product **143** was observed upon reaction of **142** in the presence of **144**.



Scheme 40: Cross-over experiments with cyclopentanoindole 142.

The cross-over experiments support the ionic mechanism rather than the currently accepted S_N2-like oxygen atom transfer mechanism. Another possibility

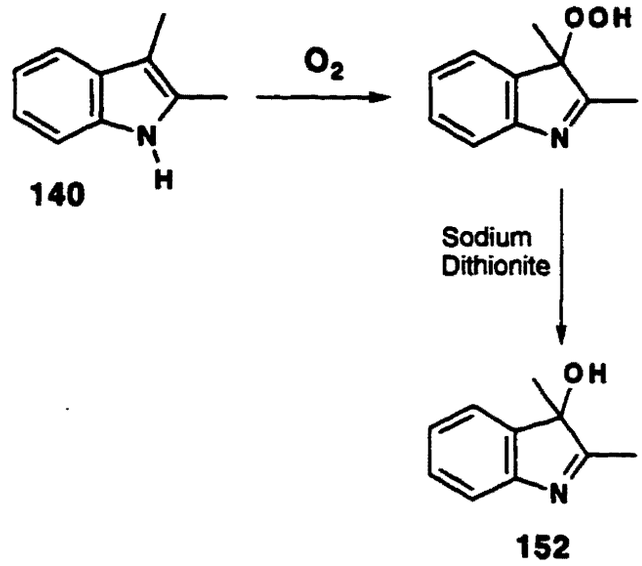
that was considered was that the reaction was progressing through the oxygen atom transfer mechanism to form the epoxide **135** but that there was a strong association of the epoxide **135** with the formed imine **144** (Scheme 41). This would suggest that a larger concentration (10 equivalents) of the imine **146** might result in equilibration of complexes between the epoxide **135** and the imines **144** and **146** which would favour the formation of at least some of the cross product **148**. Under these conditions, the reaction failed to yield any cross product, consistent with the zwitterionic mechanism proposed in this work (Scheme 29).



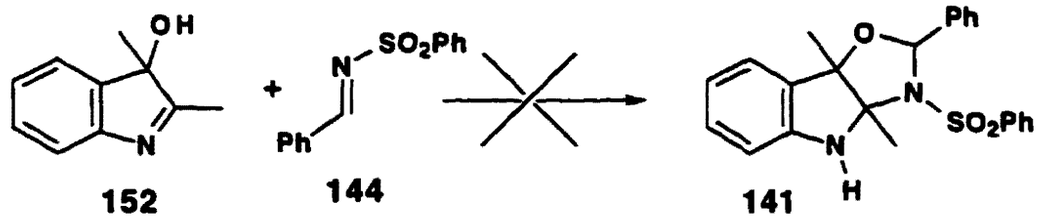
Scheme 41

Further experiments which were carried out to probe these mechanistic possibilities included the attempted reaction of **152**, which might be generated from the epoxide *in situ*, with the N-sulfonylimine **144**. The hydroxy indolenine **152** was prepared by the method of Dave[90] (Scheme 42). The adduct **141**, expected from the one step mechanism, was not observed on reaction of the hydroxy indolenine **152**

with the imine **144** (Scheme 43). The failure of this reaction to form the adduct suggests that the two step mechanism involving an indole intermediate **150** (e.g. Scheme 36) is not in operation.

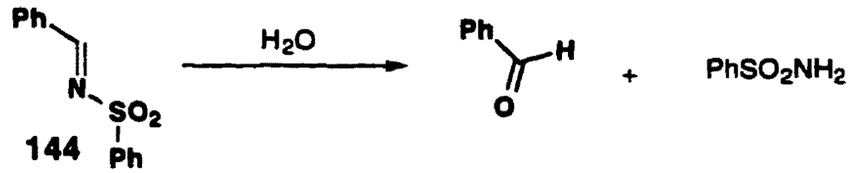


Scheme 42: Synthesis of the hydroxy indolenine 152 by the method of Dave.[90]



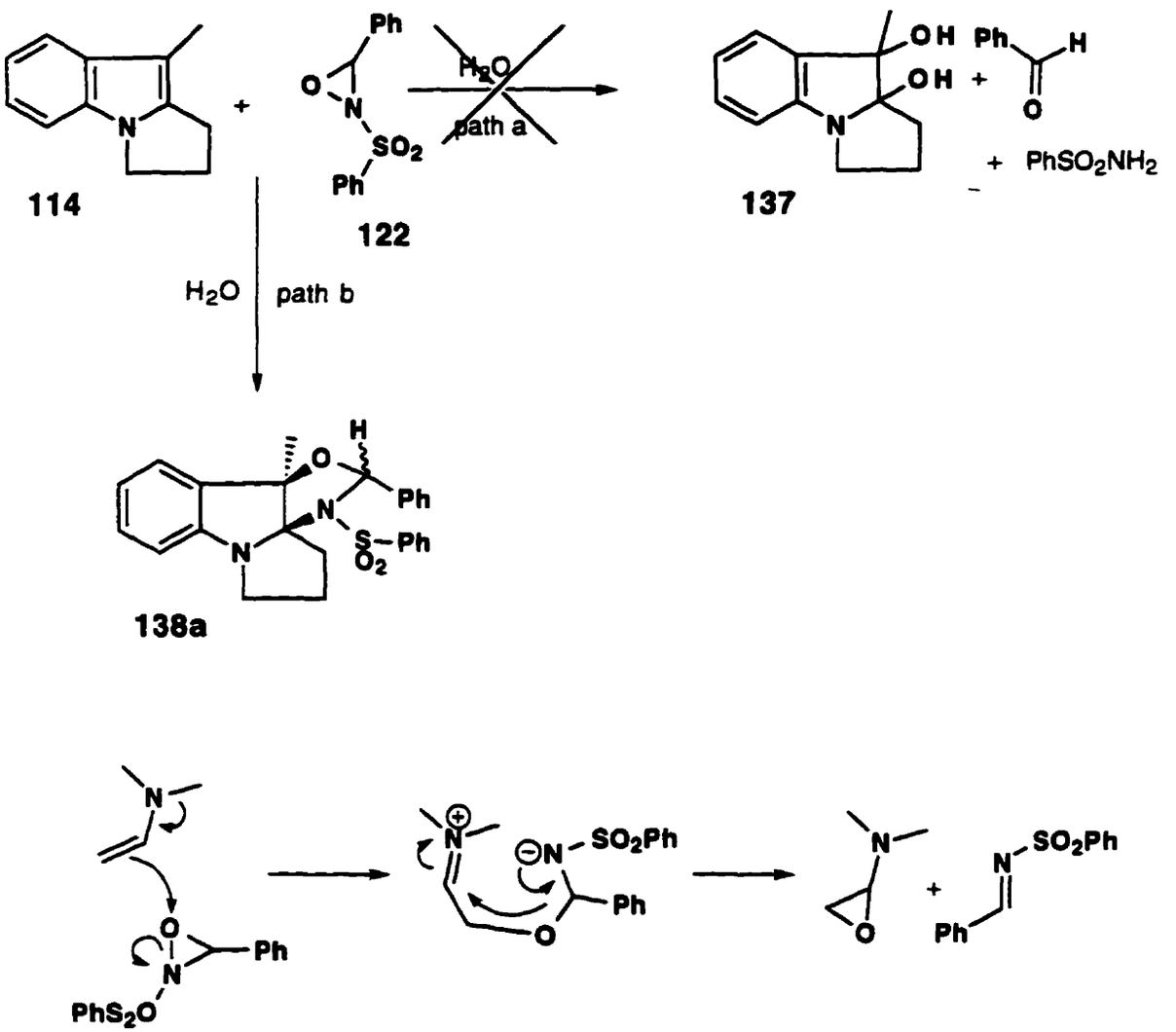
Scheme 43

Yet another observation which argues against the mechanism shown in Scheme 33 is based on the fact that N-sulfonylimines hydrolyze rather rapidly to yield the benzaldehyde and benzenesulfonamide (Scheme 44).



Scheme 44: Hydrolysis of the imine 144.

As a result, the presence of an excess of water might be expected to hinder the reaction shown in Scheme 33. In practice the reaction of indole **114** with Davis' reagent in THF containing a large excess of water proceeded smoothly to yield the addition product **138a** just as was observed in the absence of water (Scheme 45)



Scheme 45

In conclusion, the likely mechanism for the formation of the adduct is the ionic mechanism (Scheme 29) via the zwitterionic intermediate. It also seems likely that enamines and enolates, which are expected to be more nucleophilic than indoles, react with Davis' reagent via an ionic mechanism (Scheme 45).

The above results also suggest that the mechanism requires further investigation. Also, the results obtained in this work, as well as that in the literature, may represent extremes and that reaction of many compounds with Davis' reagent may progress by a mechanism between the two extremes. Examination of the *ab initio* orbital studies revealed that the authors[87-89] utilized a simplified analog of Davis' reagent due to the intensive nature of the calculations. This simplified model, lacking the phenylsulfonyl group and the phenyl group, may not be a sufficiently accurate model (Figure 52).

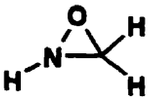
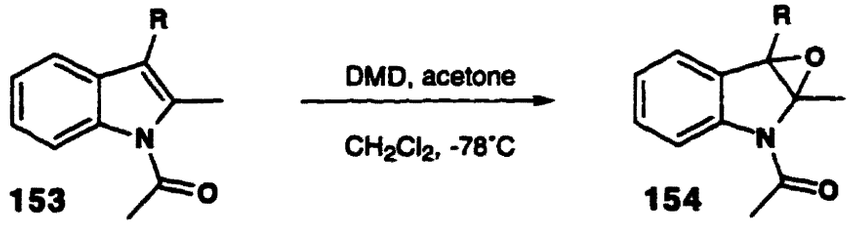


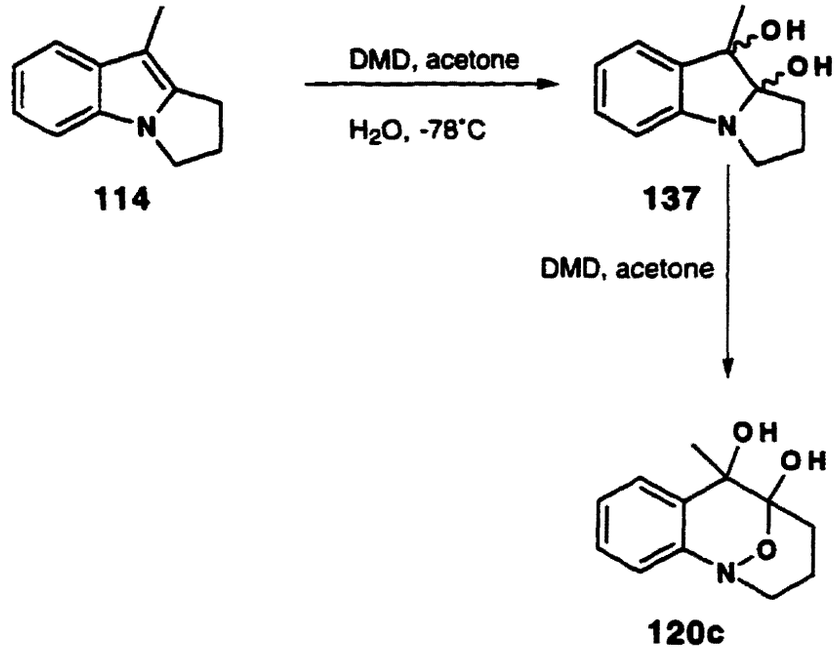
Figure 52

Our intention originally had been to develop a method for the oxidative ring expansion of mitomycin-like structures to structures related to FR-900482. The successful development of a two step method, naturally lead to the investigation of more efficient methods. However, the anomalous reaction of Davis' reagent with indoles directed efforts away from this aim. It may still be possible to develop a single step transformation of pyrrolo[1,2-a]indole **114** to the ring expanded product **137** by utilizing other oxidants such as dimethyldioxirane as the oxidant instead of Davis' reagent.

Work by Adam *et al.* [91] and by Zhang and Foote[92] has shown that a variety of N-acylindoles **153** can be efficiently oxidized to the indole epoxide **154** with dimethyldioxirane (DMD) in acetone at -78°C (Scheme 46). Under these conditions, it should be possible to oxidize pyrrolo[1,2-a]indole **114** to the epoxide which under aqueous conditions might yield **137** (Scheme 47). Further oxidation might then provide the desired ring expanded product **120c**. Currently, work in this area is being explored in this laboratory.



Scheme 46: Oxidation of N-acylindole 153 with dimethyldioxirane.



Scheme 47: Oxidation of pyrrolo[1,2-a]indole 114 with dimethyldioxirane.

Chapter 3: Synthetic Studies Toward Prekinamycin

The proposal that the kinamycins (**3**) undergo bioreductive activation[10] similar to that established some time ago for the mitomycins (**1**)[10,15,36] and more recently for FR-900482 (**2**)[13,45] prompted us to pursue synthetic studies related to the kinamycins in parallel with our studies related to FR-900482 (**2**).

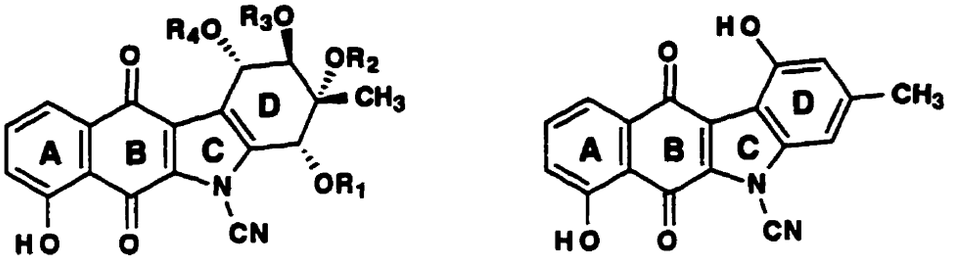


Figure 53

Since prekinamycin (**77**) had been proposed as a key intermediate in the biosynthesis of the kinamycins[62-65,67,93], it was felt that it would serve as a suitable preliminary target in the development of synthetic methodology which might be adapted to the total synthesis of the kinamycin antibiotics.

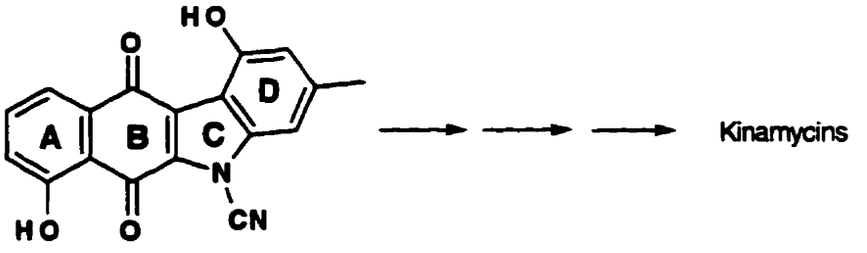


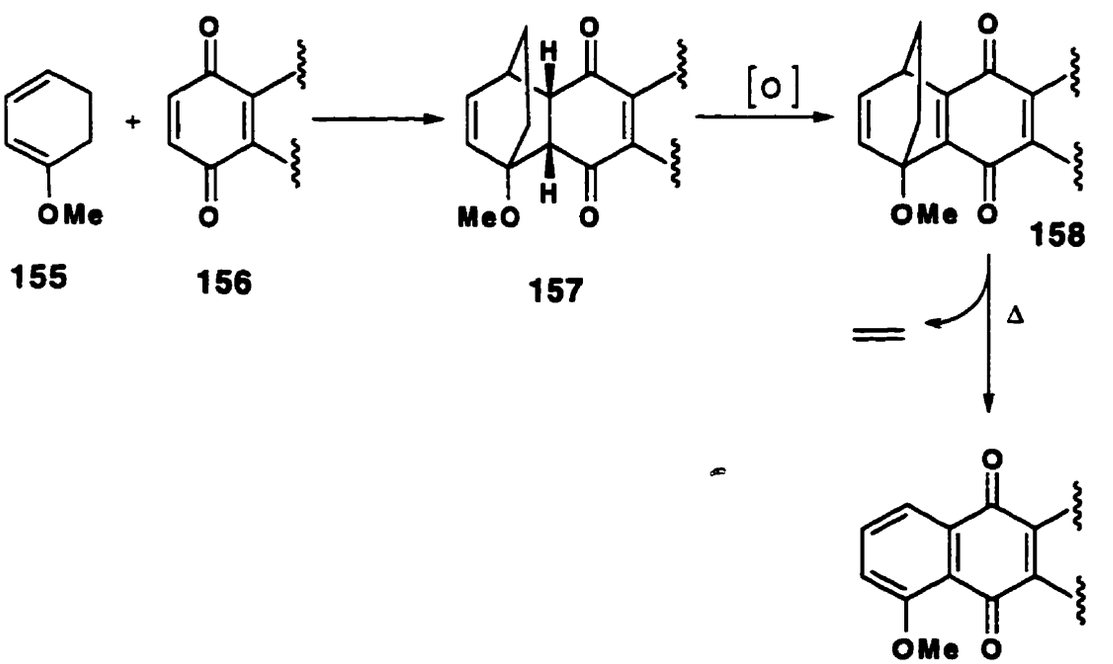
Figure 54: **Prekinamycin is a key intermediate in the biosynthesis of the kinamycin antibiotics.**

Previous model studies in this laboratory established that the A-ring of the kinamycin system might be constructed through a regioselective Diels-Alder

reaction between an N-cyanoindole-4,7-dione and a suitable diene such as 1-methoxy-1,3-cyclohexadiene (Scheme 48).

The use of 1-methoxy-1,3-cyclohexadiene (**155**) as a Diels-Alder diene for construction of naturally occurring quinones was first reported by Birch and Butler[94] and has since been employed by others in natural products synthesis. A notable example is the synthesis of daunomycinone by Kelly and co-workers.[95]

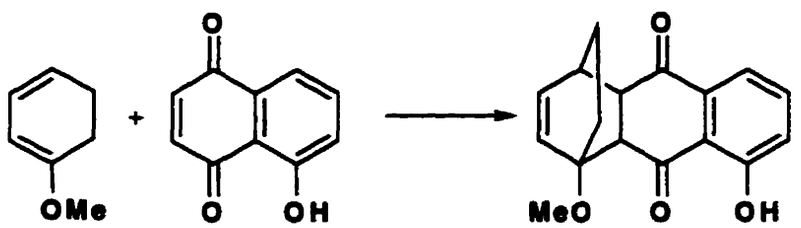
The introduction of a methoxy substituted fused benzenoid ring using this approach involves Diels-Alder cycloaddition with a *p*-quinone **156** as a dienophile. The adduct **157** so produced is stable but can be induced to eliminate ethylene thermally after oxidation to the *p*-quinone system **158** (Scheme 48).



Scheme 48

The key to the utility of this approach in natural product synthesis is the regioselectivity of the cycloaddition process. A high degree of regioselectivity

has been observed with a number of unsymmetrical quinones such as juglone below[96] (Scheme 49).

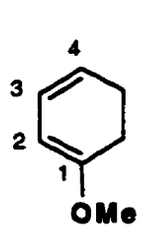


155 **159**

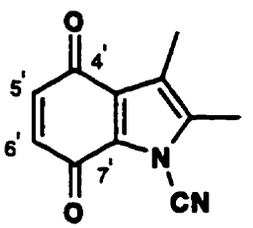
Scheme 49: Reaction of 155 with juglone (159).

It was not clear at the outset of this study whether or not the cycloaddition would occur with the desired regioselectivity and it was anticipated that the preparation of selectively halogenated analogues of **160** might be necessary to control the regioselectivity as has been done by Boisvert and Brassard[97] for the cycloaddition of other quinones. MOPAC calculations were carried out for the dione **160** and the diene **155** using the AM1 Hamiltonian with full geometry optimization. The molecular orbital (m.o.) coefficients so obtained for the HOMO of the diene **155** and for the LUMO of the dienophile **160** were then analyzed in the context of frontier molecular orbital (FMO) interactions. Primary orbital interactions were assessed employing the m.o. coefficients of the HOMO of **155** at the termini of the diene system (C(1) and C(4)) and of the LUMO of **160** at the termini (C(6') and C(5')) of the dienophile. As shown in Figure 55 below, the difference in the coefficients at C(1) and C(4) of **155** as well as at C(6') and C(5') of **160** is sufficiently small that a prediction of regioselectivity was not possible on this basis alone. However, when secondary orbital interactions are considered, namely interactions of the HOMO of the diene **155** (C(2) and C(3)) with the LUMO of the dienophile **160** at the carbonyl carbons (C(7') and C(4')), a more significant difference in coefficients is noted and a regiochemical preference for the desired isomer is predicted based on an assumption that the

predominant regioisomer will arise from a transition state involving interaction of the larger of the secondary orbital coefficients for the diene (C(2) of **155**) and the dienophile (C(7') of **160**).



155

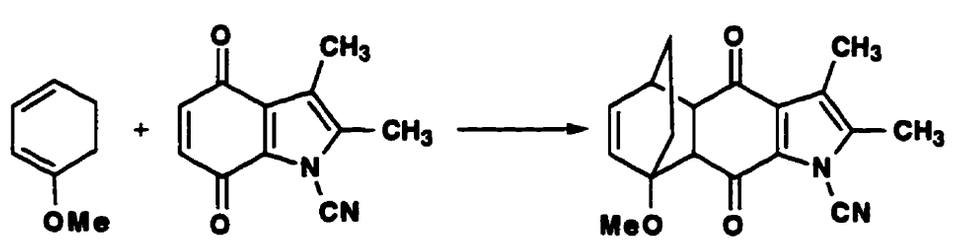


160

	HOMO		LUMO
1	-0.4905	4'	+0.3117
2	-0.4343	5'	+0.3443
3	+0.3794	6'	-0.3180
4	+0.4940	7'	-0.3584

Figure 55

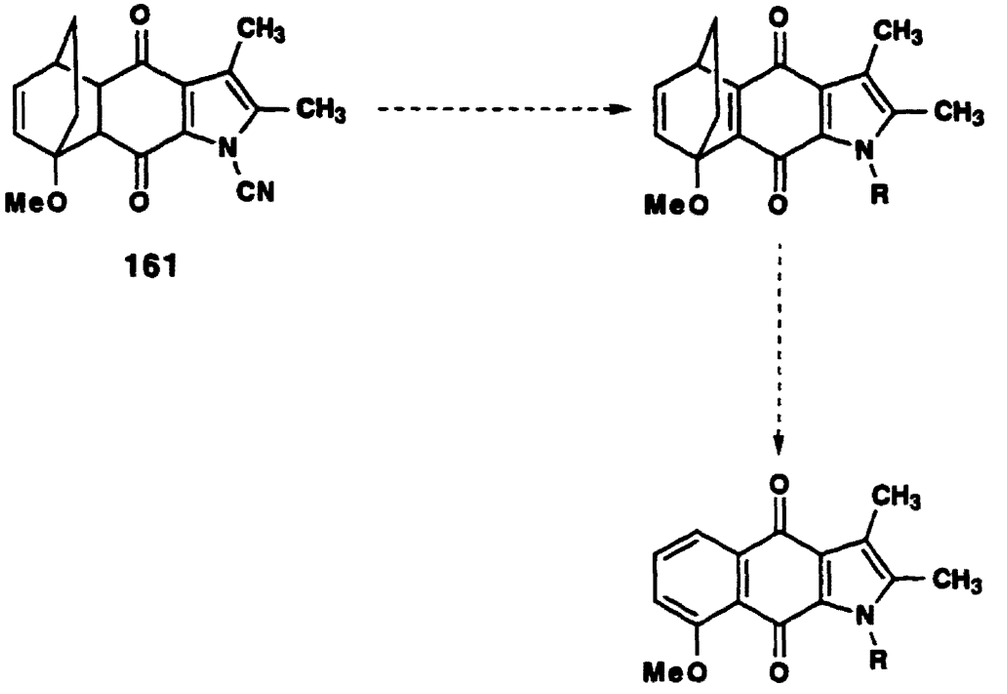
In practice, the N-cyano-2,3-dimethylindole-4,7-dione, **160**, was found to react with complete regioselectivity to generate the adduct **161** (Scheme 50) in agreement with the prediction outlined above.



155 **160** **161**

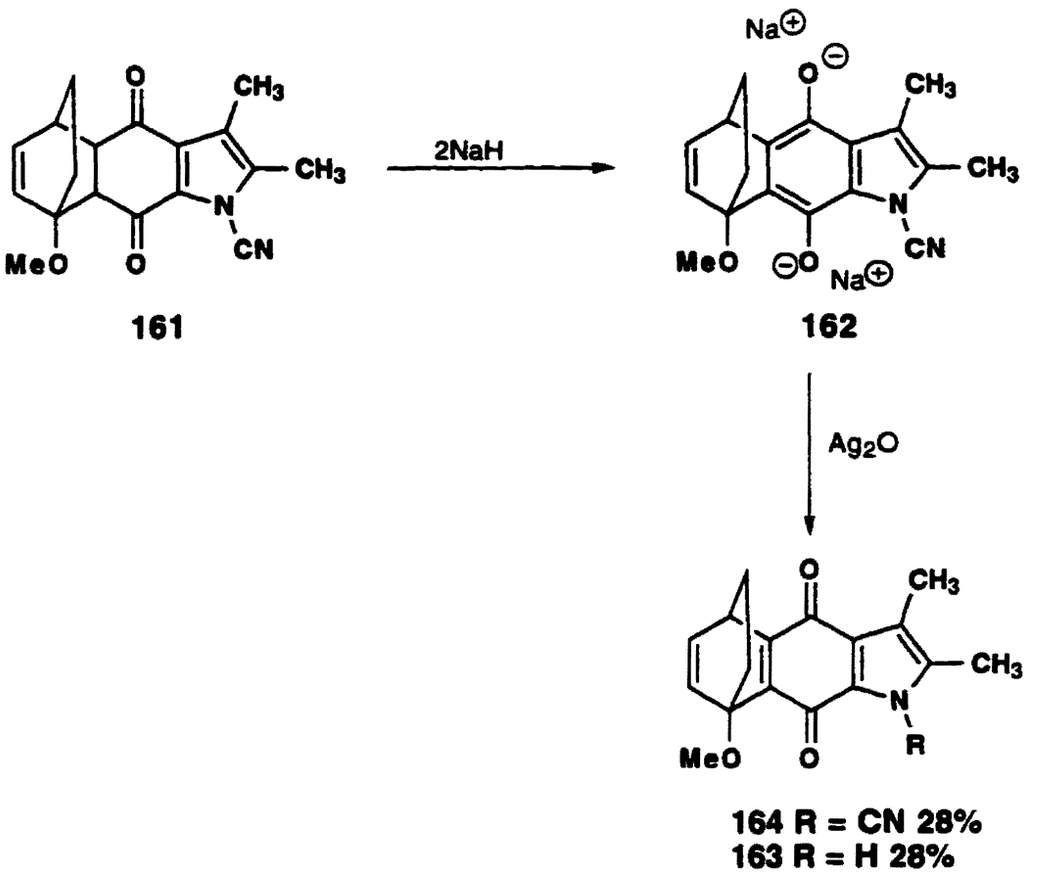
Scheme 50

Aromatization of the A ring in this strategy required an oxidation of the 1,4-diketone **161** to a *p*-quinone which could then be induced to undergo a retro Diels-Alder expulsion of ethylene upon heating in a process analogous to that described above (Scheme 51).



Scheme 51

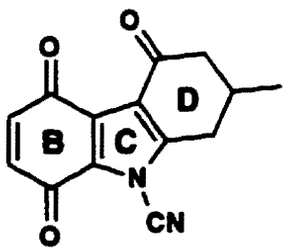
The oxidation procedure involved generation of the dienolate of **162** by treatment of **161** with two equivalents of strong base (NaH in this case) followed by reaction with silver oxide (Ag_2O). In the model study with the dione **161**, the enolate formation/oxidation sequence was only partly successful in that a substantial degree of decyanation was observed (Scheme 52).



Scheme 52

Although, cyanation of **163** to form **164** was a feasible approach to improving the yield, it was clear when the present study began that this particular step of the sequence would require some modification if this approach to the kinamycins was to be an efficient synthetic strategy. Furthermore, the fact that potentially enolizable functionality might be present in the D-ring precursor suggested that the B-ring oxidation strategy would require some revision.

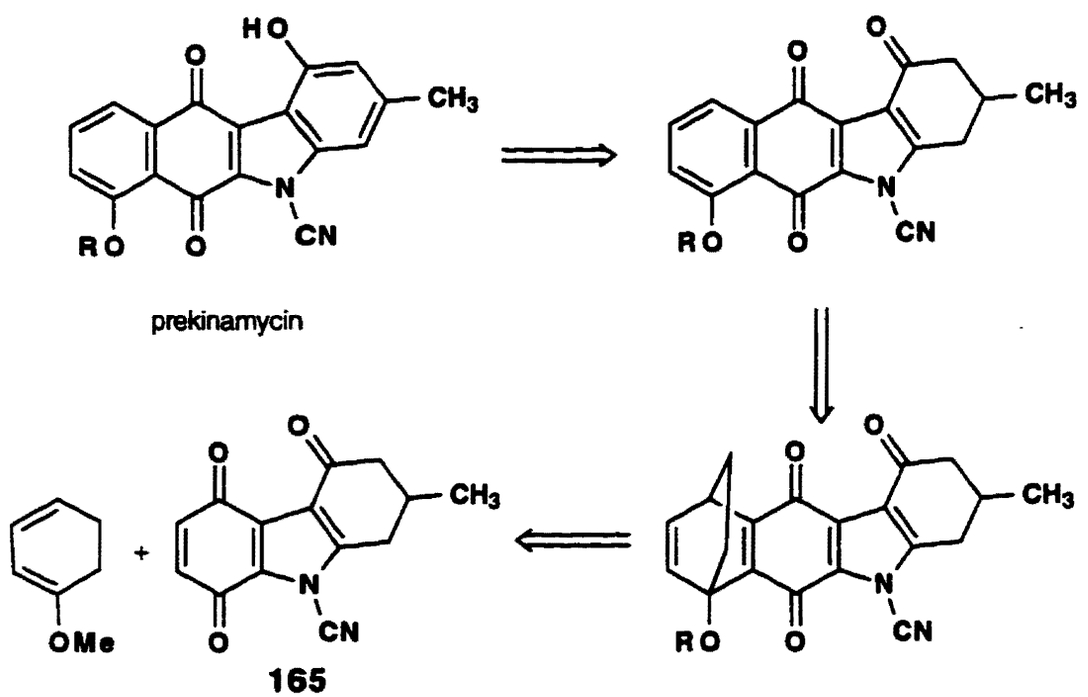
For the present study, it was decided that by analogy with the model study outlined above, the construction of prekinamycin system might be effected via a quinone such as **165** which incorporates a D-ring precursor appropriately fused to the B, C-ring synthon (Figure 56).



165

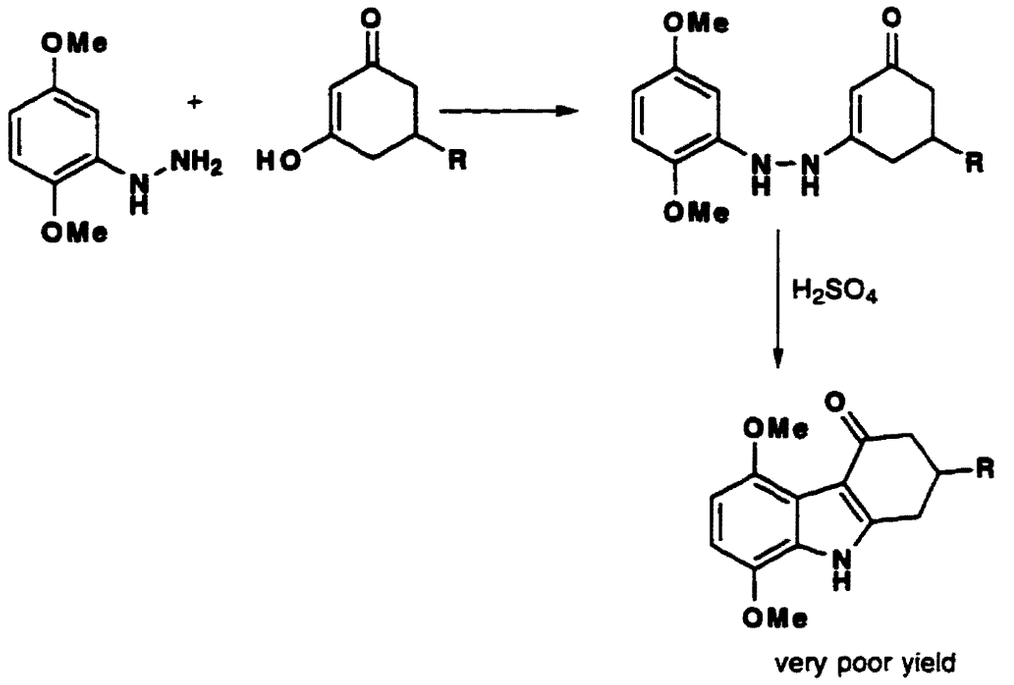
Figure 56

A retro synthetic analysis of the synthetic strategy toward prekinamycin employed in this work appears below (Scheme 53).



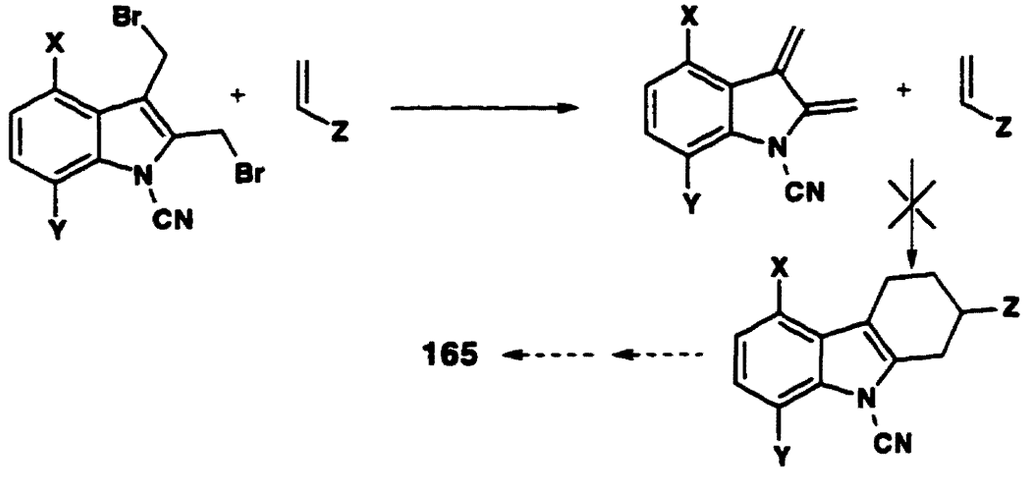
Scheme 53

A number of potential strategies to **165** were considered including the Fisher Indole synthesis approach outlined in Scheme 54. Preliminary studies by G. Weeratunga in this laboratory demonstrated that the yields in the cyclization step were very poor.



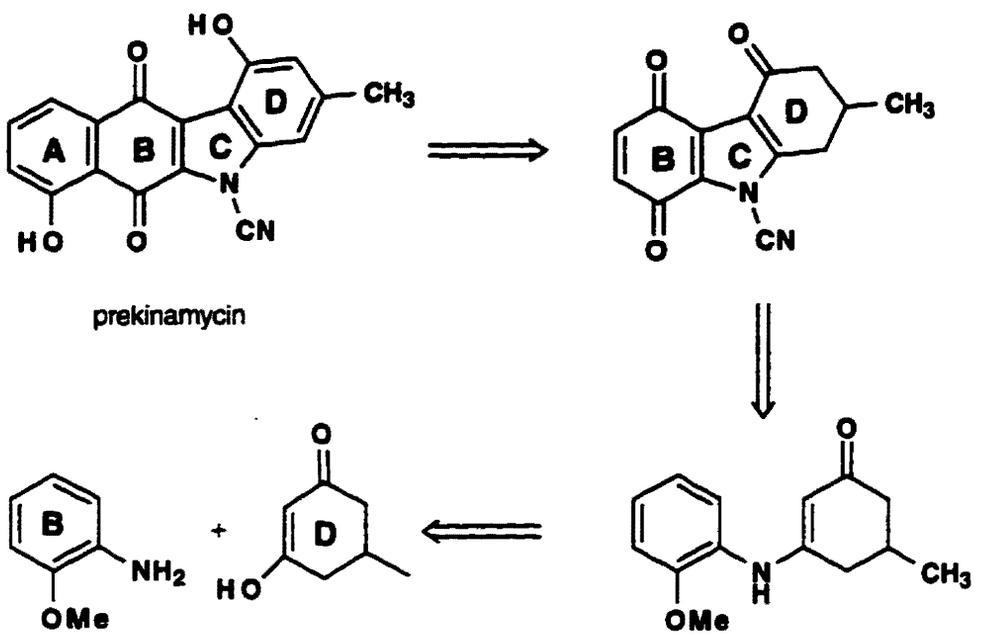
Scheme 54

An alternative approach involving construction of the D-ring from an acyclic B, C ring precursor via an indole-2,3-quinodimethane was also briefly explored by O. Jakiwczk in this laboratory (Scheme 55).[98] The tendency of the N-cyano-indole-2,3--quinodimethane to dimerize rather than undergo Diels-Alder trapping with an appropriate dienophile made the approach unacceptable (Scheme 55).



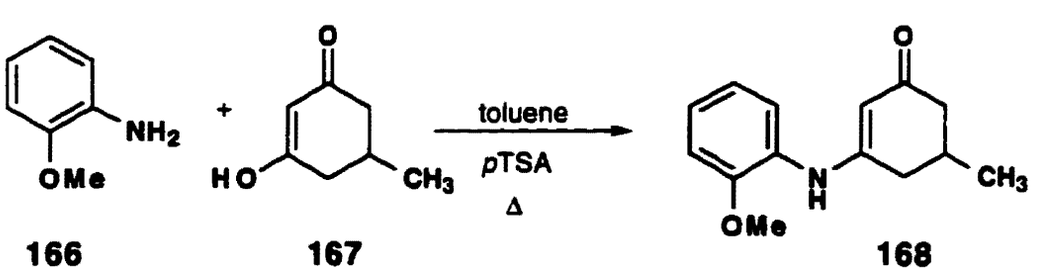
Scheme 55

In the present study the construction of the BCD ring synthon was pursued via a Heck-type palladium catalyzed cyclization.[53,99] A retro synthetic analysis of the strategy appears below (Scheme 56).



Scheme 56

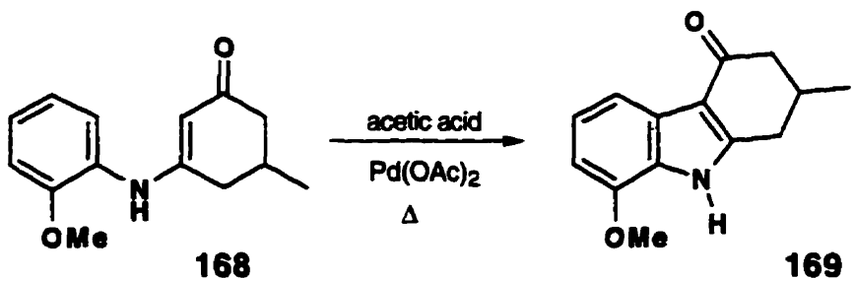
Acid catalyzed condensation of *o*-anisidine **166** with commercially available 5-methyl-1,3-cyclohexanedione which exists essentially completely in the enol form **167** gave the enaminoketone **168** in 86% isolated yield (Scheme 57).



166 **167** **168**

Scheme 57

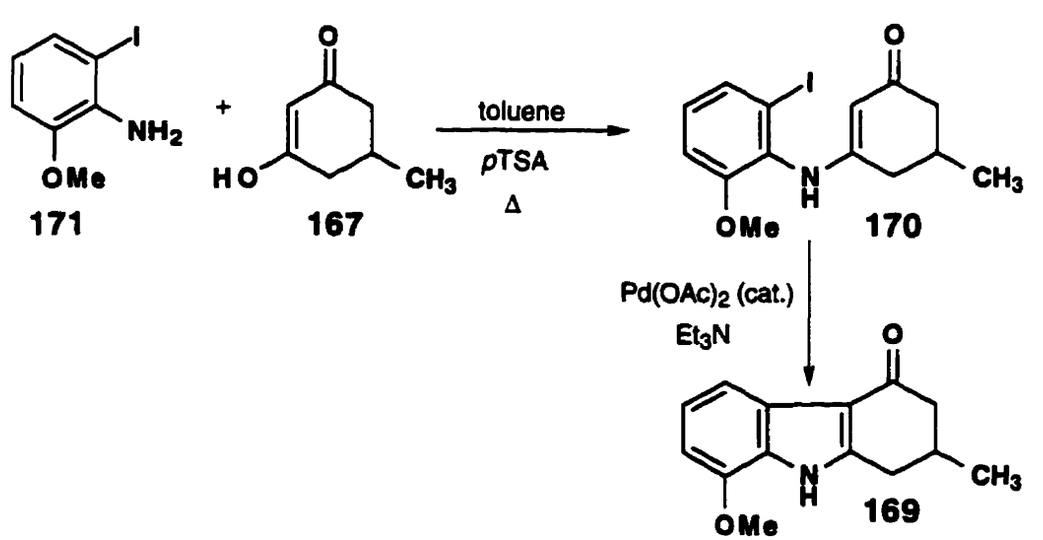
After some experimentation it was found that heating the enamine **168** with an equivalent of palladium acetate in refluxing acetic acid produced the desired tricyclic system **169** in 64% isolated yield (Scheme 58).



168 169

Scheme 58

Although this sequence provided adequate quantities of **169** for the present synthetic purpose, it was recognized that this synthetic step was less than ideal given the expense associated with the use of an equimolar amount of palladium acetate in larger scale reactions. It was planned that refinements of this step would be pursued at a later stage once the remainder of the synthetic route from **169** to prekinamycin was explored. In particular, it was intended that the iodoenamine **170** would be produced from 3-iodo-o-anisidine (**171**) which has been prepared by Clive and coworkers[100] in their synthetic studies aimed at Fredericamycin. Cyclization of **170** should, in principle, be possible with a catalytic amount of palladium acetate, since no overall change in oxidation state of the palladium occurs in this cyclization, unlike the situation with **168** which cyclizes to **169** with overall reduction of Pd^{2+} catalyst to Pd^0 (Scheme 59).

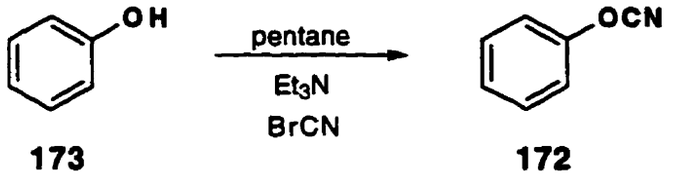


171 167 170 169

Scheme 59

Previous studies in this laboratory (H. Damude, unpublished observations) have shown that oxidation of N-unsubstituted methoxyindoles leads to dimeric products which have not been fully characterized. As a result, N-cyanation of **169** was carried out prior to oxidation to the quinone.

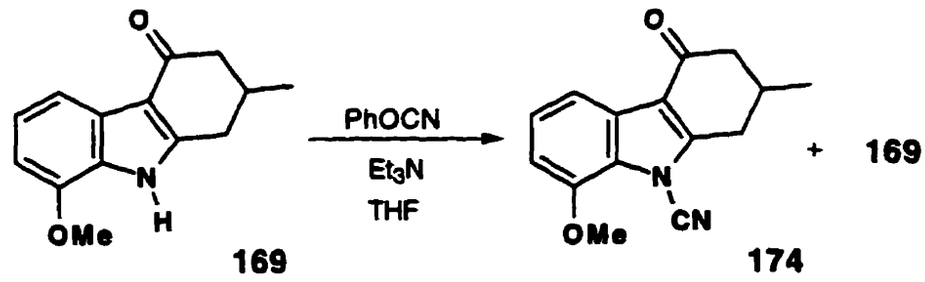
Previous work in this laboratory had established that cyanation of 2,3-dialkylindoles with cyanogen bromide gave poor yields of the N-cyanoindole accompanied by highly coloured byproducts possibly arising from initial electrophilic attack at the β-carbon of the indole ring to yield 3-bromo (or 3-cyano)indolenines known to decompose to similarly coloured oligomeric products. On the other hand, phenyl cyanate (**172**), produced from phenol (**173**) and cyanogen bromide as shown below (Scheme 60), was found to react smoothly with N-sodio indoles, produced by reaction of the 2,3-dialkylindole with sodium hydride, to give good yields of the corresponding N-cyanoindole.



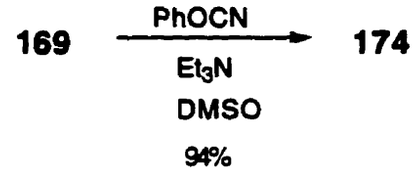
173 **172**

Scheme 60: Preparation of phenyl cyanate

In the present study, the increased acidity of the N-H of the 4-keto-1,2,3,4-tetrahydrocarbazole **169** led us to explore the use of a much weaker base, triethylamine, in the cyanation process. With THF as the solvent, this procedure gave low yields of the N-cyanoindole accompanied by a substantial amount of recovered starting material (Scheme 61). The use of a more polar aprotic solvent, DMSO, however, gave an excellent (94%) yield of the N-cyano product **174** (Scheme 62).

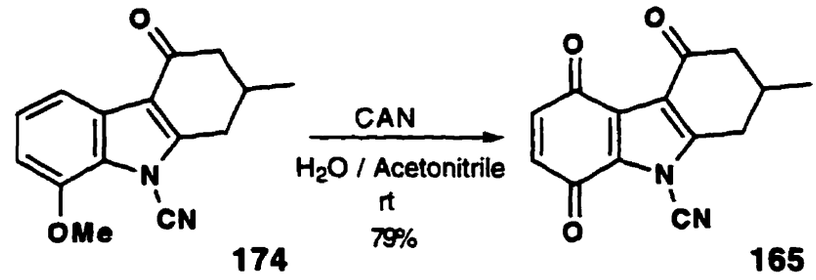


Scheme 61



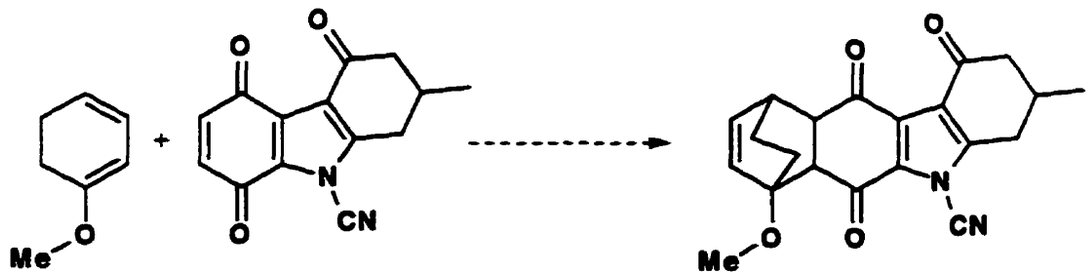
Scheme 62

The oxidation of indole **174** to the indoloquinone **165** was effected smoothly with ceric ammonium nitrate in aqueous acetonitrile (Scheme 63).



Scheme 63

The success of the remainder of the synthesis depended critically on the degree of regiochemical control which was to be observed in the cycloaddition of **155** and **165**. It was hoped that the presence of the keto functionality in **165** would not perturb the m.o. coefficients in the LUMO of **165** relative to those observed in **160** so as to diminish or reverse the desirable regioselectivity observed for the model reactions of **160** and **155** described above.



155 **165** **175**

Scheme 64

To confirm this, MOPAC calculations with full geometry optimization using the AM1 parameter set were performed on both the indoloquinone **165** and the diene **155**. The calculations were executed on a SGI 4D25TG workstation using MOPAC 6.0 as contained in the molecular modeling program SYBYL 6.1 (Tripos Associates). The coefficients obtained from these calculations were employed in frontier molecular orbital (FMO) analysis to predict the regioselectivity of the reaction.

The stereo representation of the structure of **155** submitted for geometry optimization appears in Figure 57. The structure of **155** was energy minimized with the Maximin2 Force Field in the Sybyl program prior to submission for MOPAC geometry optimization and coefficient calculation.

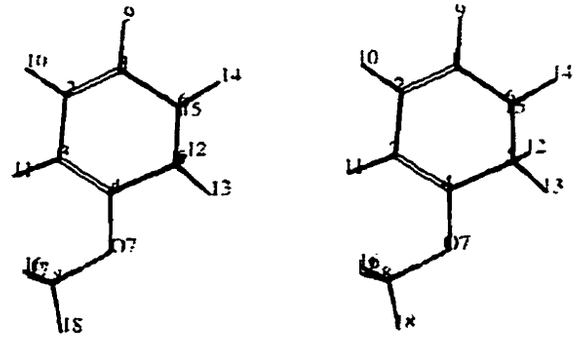


Figure 57: **Stereo representation of 155 prior to MOPAC geometry optimization.**

A stereo representation of **165** before geometry optimization appears in Figure 58. Note that **165** was also energy minimized with Maximin2 prior to submission for MOPAC calculations.

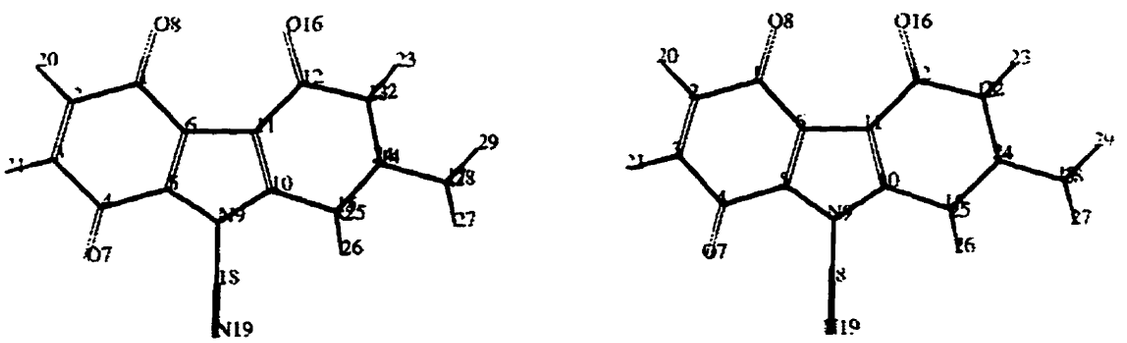
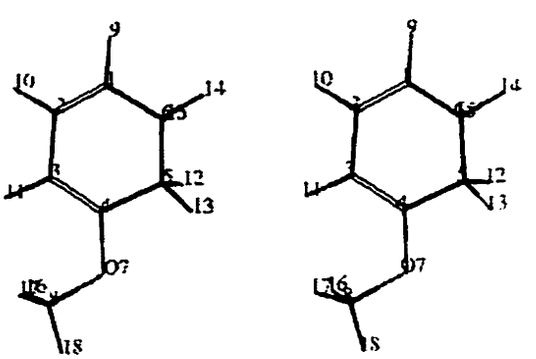
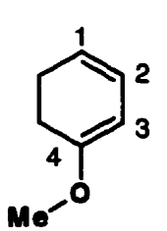


Figure 58: Stereo representation of 165 before MOPAC geometry optimization.

The geometry optimized stereo structure of diene **155** with the HOMO coefficients for the relevant carbons appears in Figure 59 and the geometry optimized stereo structure of **165** with the LUMO coefficients for the relevant carbons appears in Figure 60.

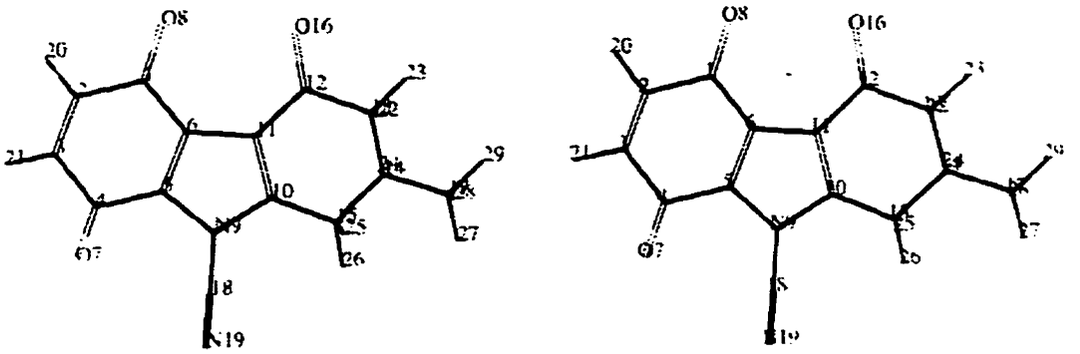


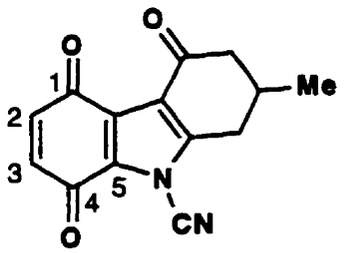


155

Carbon#	HOMO Coefficients
1	0.49664
2	0.34271
3	-0.48735
4	-0.42759

Figure 59: **Geometry optimized stereo structure of diene 155 with the HOMO coefficients for the relevant carbons.**





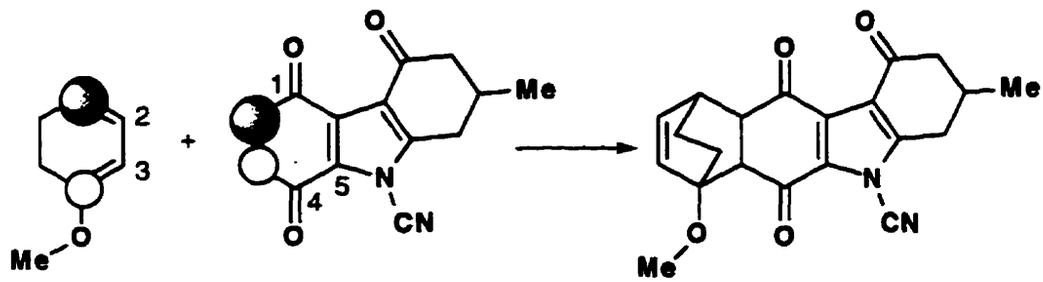
165

Carbon#	LUMO Coefficient
1	0.28931
2	0.33905
3	-0.29886
4	-0.36156

Figure 60: **Geometry optimized stereo structure of quinone 184 with the LUMO coefficients for the relevant carbons.**

In considering only the primary interactions in FMO analysis, the coefficients are those (C(1) and C(4)) of the HOMO of the diene **155** (0.49664 and -0.42759, respectively) (Figure 59) and those (C(2) and C(3)) of the LUMO

of the quinone **165** (0.33905 and -0.29886, respectively) (Figure 60). Matching the large-large and small-small coefficients as predicted by FMO analysis results in the production of the Diels-Alder reaction with the desired regioselectivity (Scheme 65). Since the difference between the large and small coefficients is quite small for both the diene and the quinone, however, the first order FMO analysis predicts that the regiochemical preference would not be large.

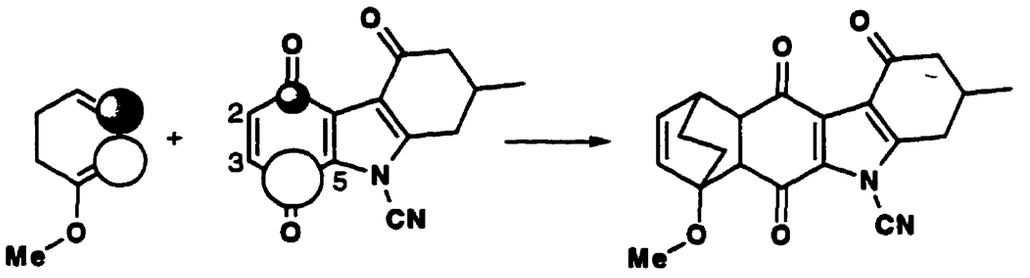


155 **165** **175** (Major)

Scheme 65: **Considering primary orbital interactions only in the FMO analysis.**

This observation led us to include secondary orbital interactions in the FMO analysis. The coefficients appropriate for secondary orbital analysis are those (C(2) and C(3)) of the HOMO of the diene **155** (0.34271 and -0.48735, respectively) (Figure 59). These two coefficients show a much greater difference than was observed for the coefficients employed in analysis of the primary orbital interactions. In the quinone the appropriate coefficients are those at C(1) and C(4) of the LUMO (0.28930 and -0.36156, respectively) (Figure 60). Again, there is a larger difference between the coefficients involved in secondary interaction than was observed with the coefficients involved in primary orbital interactions. Matching the large-large and small-small coefficients involved in secondary orbital interactions, leads to the prediction that the Diels-Alder reaction would be expected to proceed predominantly with

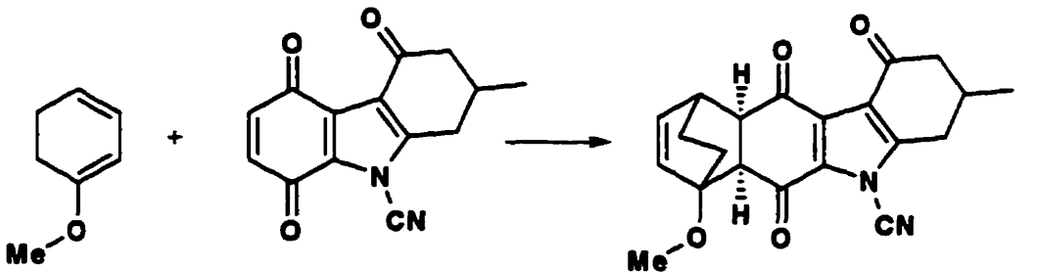
the desired regio-isomer (Scheme 66). Hence, it is predicted that the effects of the primary and secondary orbital interactions reinforce one another. Since the effects of primary orbital interactions and of secondary orbital interactions lead to the same prediction of regiochemical preference, we were confident that the regiochemical control found in the model reaction of **155** and **160** would also be observed for the reaction of **155** and **165**.



155 **165**

Scheme 66: Considering secondary orbital interactions only in FMO analysis

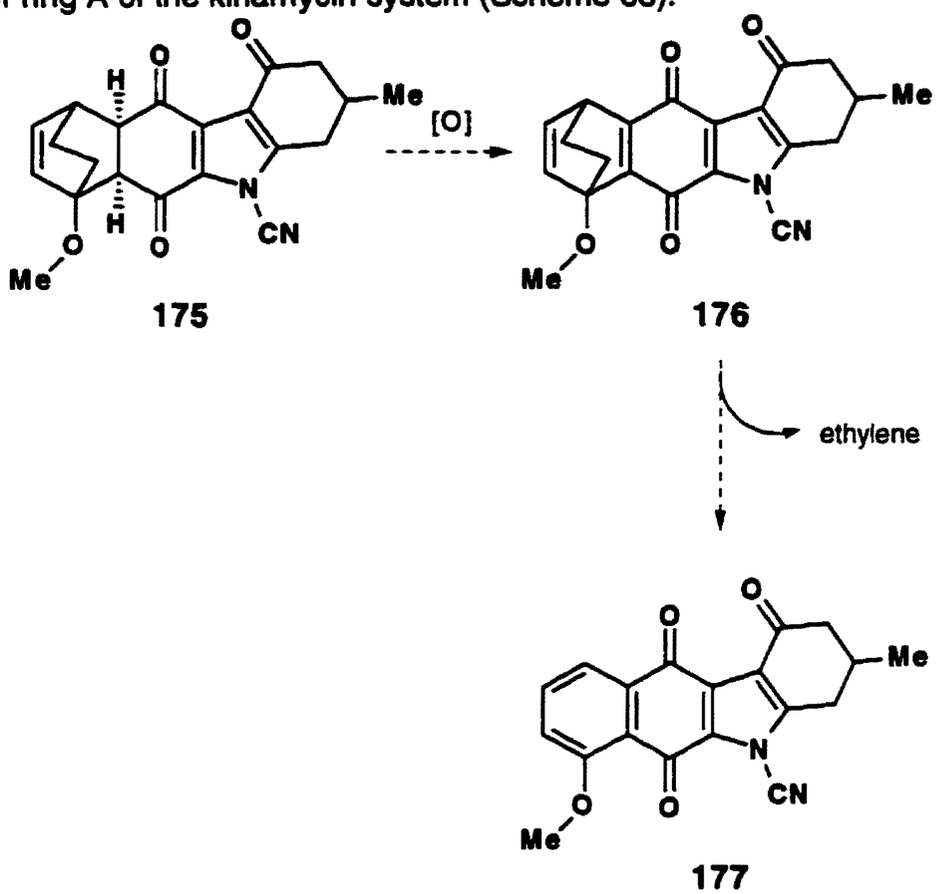
In practice, the diene **155** was observed to react with quinone **165** to give, after recrystallization from THF/hexane, an off-white solid in 89% yield (Scheme 67). The IR spectrum showed a strong band at 2257 cm^{-1} corresponding to the cyano group and the mass spectrum showed a molecule ion of 364. This product was assumed to be a mixture of diastereomers **175**; but, the regioselectivity of the reaction was not established unambiguously at this point in the study.



155 **165** **175**

Scheme 67

The next stage of the synthetic plan involved the conversion of the 1,4-dione **175** into the corresponding p-quinone **176** in preparation for the thermal expulsion of ethylene to give **177** which incorporates the desired aromatized form of ring A of the kinamycin system (Scheme 68).

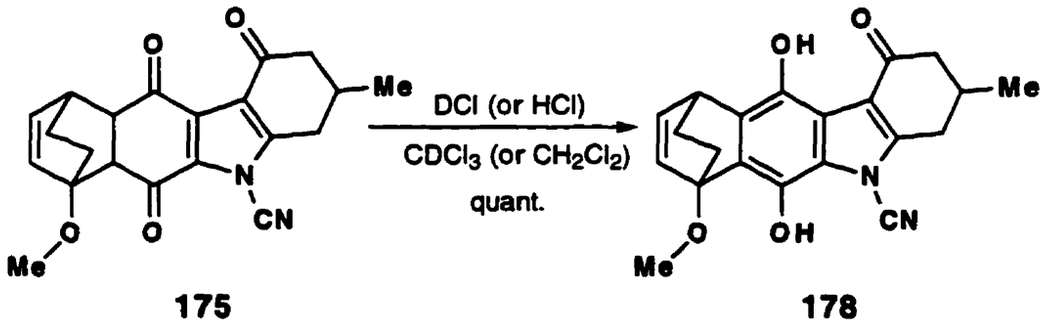


Scheme 68

As indicated earlier (see page 92), this oxidation process proved to be problematic in that treatment of the dione with two equivalents of NaH followed by oxidation with silver oxide yielded a substantial amount of decyanated product in addition to the desired N-cyanoindoloquinone. We expected that we would be forced to vary the reaction conditions (e.g. using lower temperature and/or a different strong base) to improve this process. During the course of spectroscopic characterization of **175**, however, it was discovered that some,

but not all, samples of **175** in $CDCl_3$ underwent complete conversion to a new less polar product isomeric with **175** as indicated by ^1H NMR, TLC and mass spectrometric analysis. The appearance of two one-proton singlets at 9.80 and 9.05 ppm in the ^1H NMR of this product as well as a band at 3307 cm^{-1} in the IR spectrum were compatible with the assumption that this new isomeric product was the hydroquinone **178** (Scheme 69).

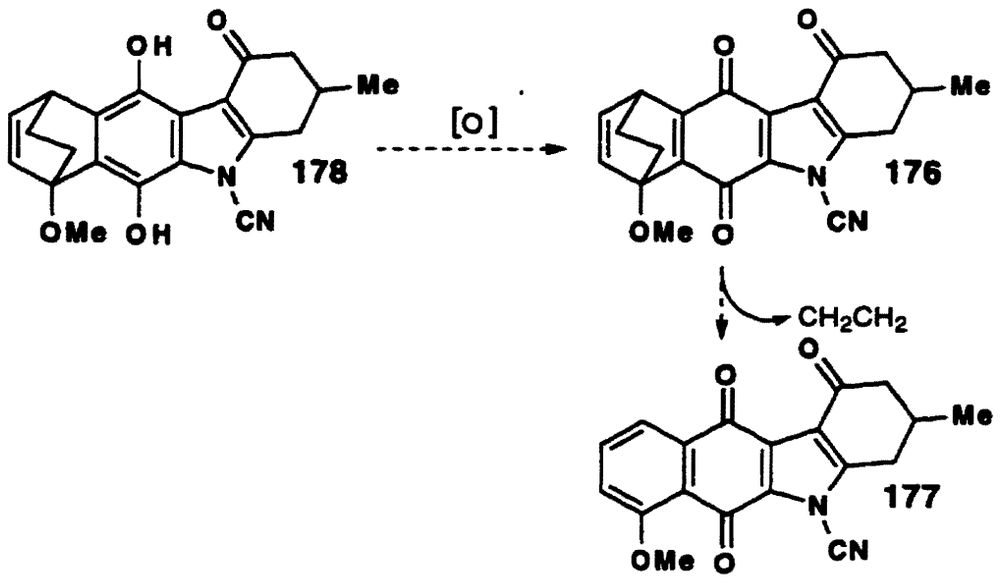
The variability in the tendency of $CDCl_3$ solutions to catalyze this transformation was traced to the use of $CDCl_3$ from different containers and strongly suggested that the process being observed was an acid catalyzed bis-enolization mediated by traces of DCl present from the air oxidation of $CDCl_3$. It was found that this same transformation could also be effected with anhydrous HCl in CH_2Cl_2 solution (Scheme 69). The essentially quantitative formation of **178** was potentially very useful, since, if oxidation of **178** to **176** could be effected smoothly while avoiding enolate formation, the decyanation problem observed in the oxidation of the model might be avoided in the present sequence. This tendency to enolize was not observed in the model studies with **160**.



175 **178**

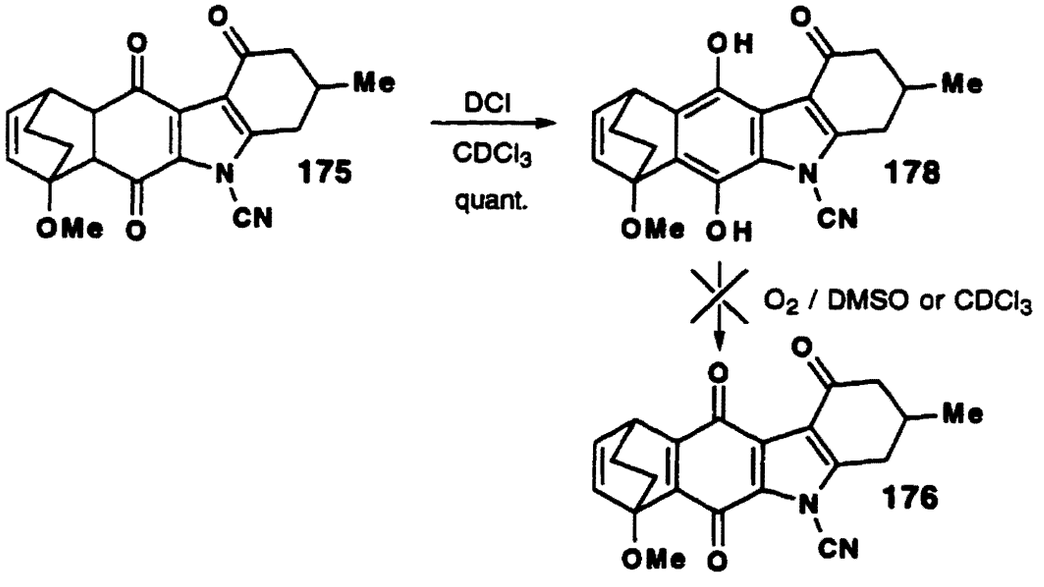
Scheme 69

Conversion of the hydroquinone **178** to the quinone **176** followed by thermolysis could give the appropriately substituted aromatic system **177**, under relatively mild conditions (Scheme 70).



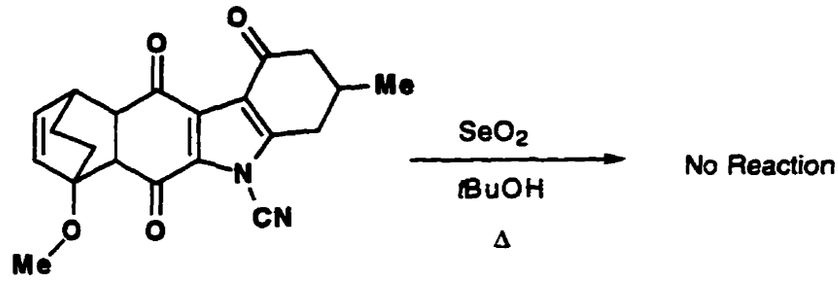
Scheme 70

Attempts at coupling the enolization of the diketone **175** with oxidation of the hydroquinone **178** in an oxygen atmosphere, in either deuterochloroform or in DMSO failed to generate the quinone **176** (Scheme 71). The diketone was successfully transformed to the hydroquinone; however, the hydroquinone **178** remained unchanged even when oxygen was bubbled through the reaction mixture (Scheme 71).



Scheme 71

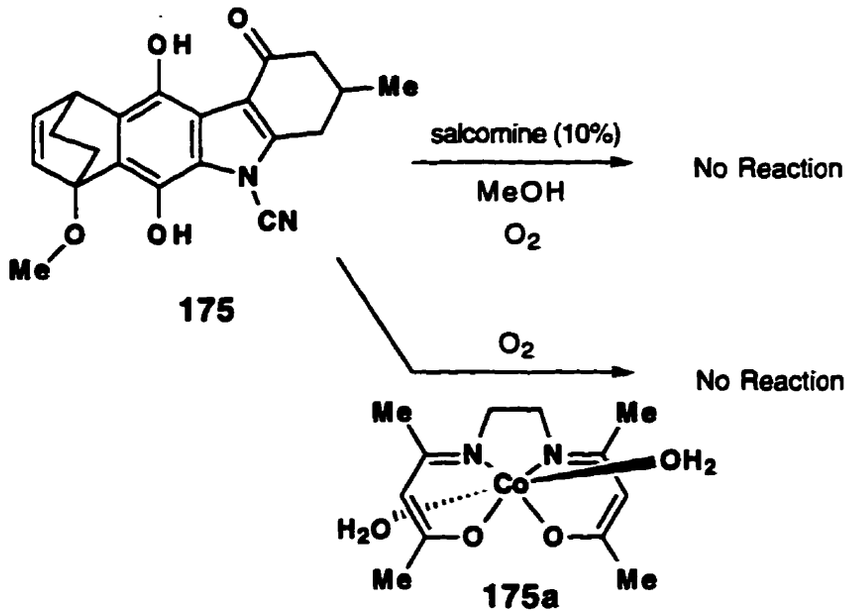
In parallel with studies aimed at generating the quinone **176** via oxidation of the hydroquinone **178**, were studies aimed at producing the quinone **176** directly from the diketone **175**. To this end, the diketone **175** was refluxed in *t*-butanol in the presence of selenium dioxide, which had no observable effect on the substrate (Scheme 72).



175

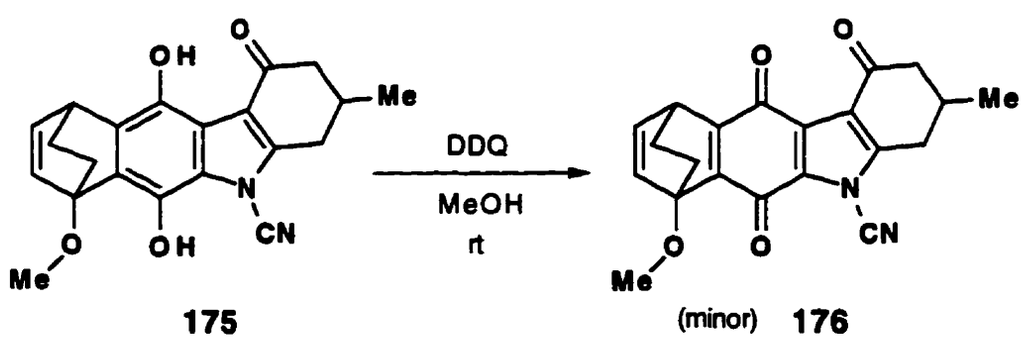
Scheme 72

It is well known that certain cobalt complexes such as salcomine will oxidize substituted phenols and hydroquinones to quinones under mild conditions.[101-103] These cobalt complexes are appealing as oxidants since only a catalytic amount is necessary, making isolation of the product relatively simple. The hydroquinone **175** was stirred at room temperature in the presence of 10 mol% of salcomine in methanol with an oxygen atmosphere. Unfortunately, no reaction was observed. Replacement of salcomine with another cobalt complex **175a**[102], known to oxidize hydroquinones, also had no discernible effect (Scheme 73).



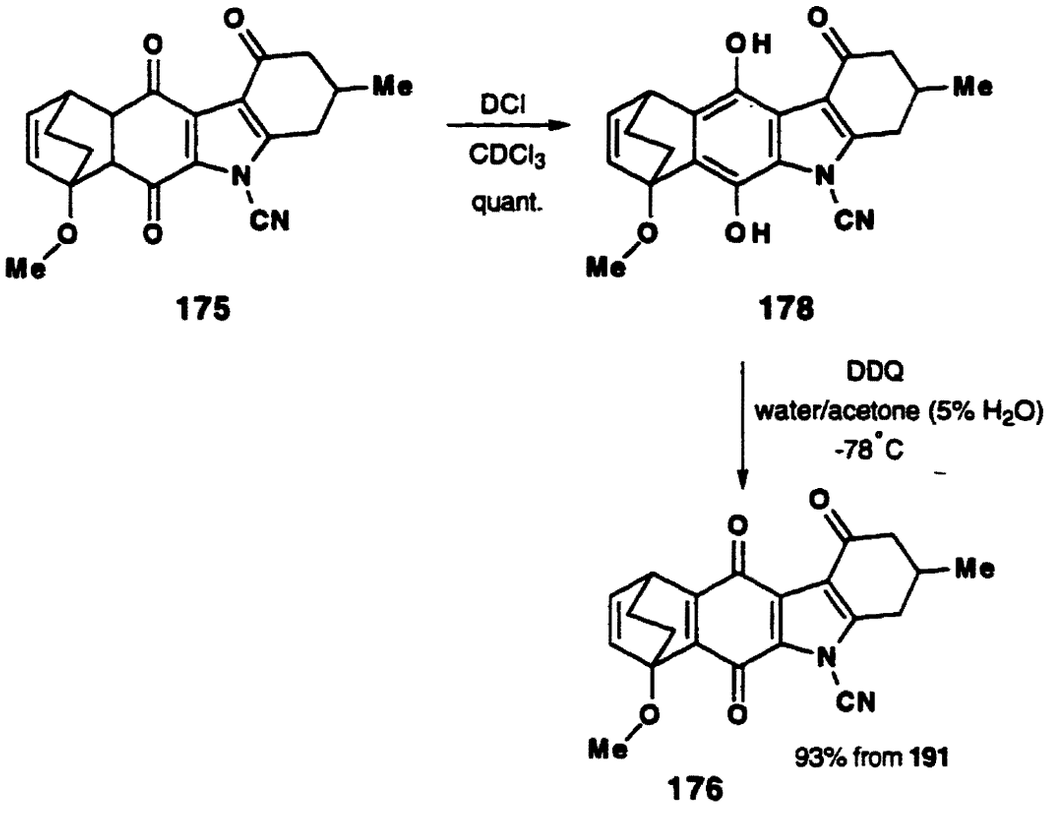
Scheme 73:

Eventually it was found that reaction of the hydroquinone **175** with DDQ in methanol at room temperature yielded a mixture of products (Scheme 74) from which the desired quinone **176** could be isolated as a minor product (22%) (Scheme 74).



Scheme 74

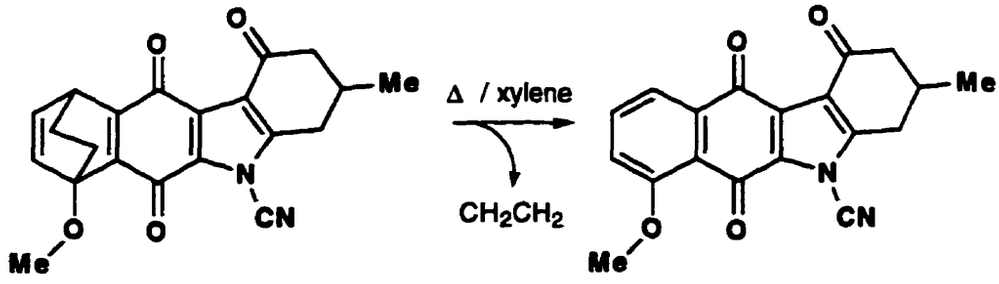
Further study revealed, however, that the yield could be markedly improved by utilizing a water/acetone mixture (5% water in acetone) as the solvent and carrying out the reaction at -78°C.)[25] Under these conditions the quinone **176** was obtained as a bright yellow solid in 93% isolated yield from the diketone **175** (Scheme 75).



175 178 176

Scheme 75

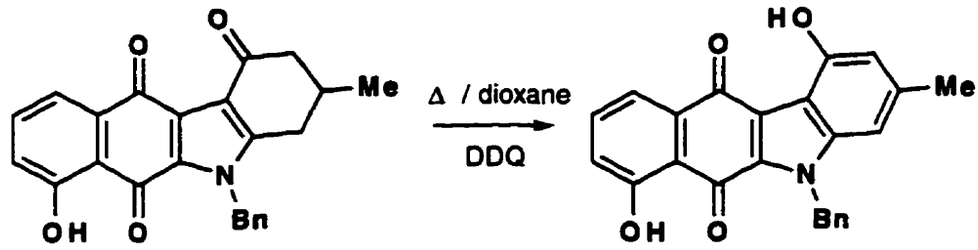
Refluxing the quinone **176** in xylene resulted in aromatization of the A ring with a concomitant loss of ethylene as expected based on the model studies described above (Scheme 76). Recrystallization of the product from THF/hexane yielded **177** as a bright yellow solid in 94% yield from **176**. The mass spectrum showed an M^+ ion of 334. The observation of a strong singlet at 2256 cm^{-1} in the IR spectrum of **177** indicated that the cyano substituent had remained intact. The following signals, observed in the aromatic region of the ^1H NMR spectrum: 7.89 (dd, J=7.7, 1.1 Hz, 1H), 7.73 (dd, J=8.4, 7.7 Hz, 1H) and 7.34 (dd, J=8.5, 0.9 Hz), were consistent with the structure shown.



176 **177**

Scheme 76

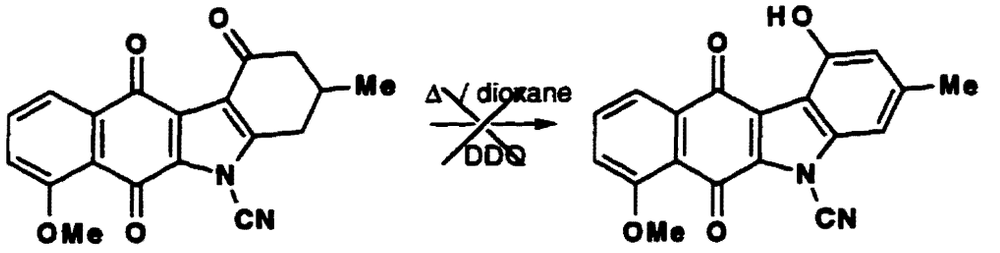
Attention was then turned to the aromatization of the D ring. During the course of this work O'Sullivan *et al.* [104] reported that in their approach to the prekinamycin ring system the related system **179** could be converted to **180** (Scheme 77). However, removal of the N-benzyl protecting group was not reported. It was felt that refluxing in dioxane in the presence of DDQ would also effect the desired aromatization of **177**.



179 **180**

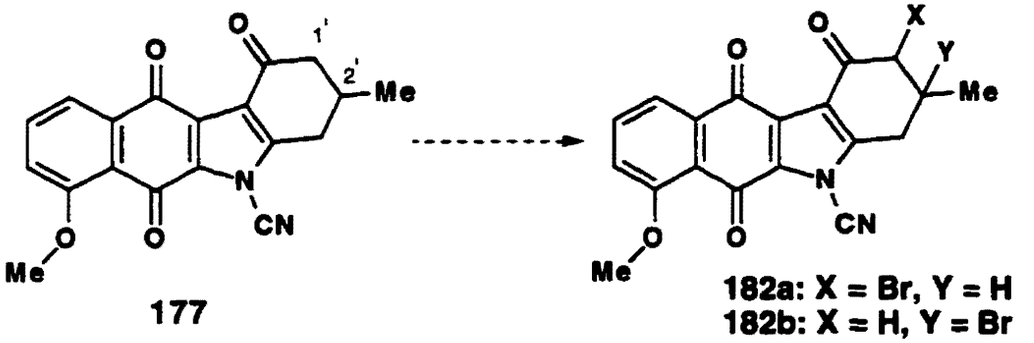
Scheme 77

Unfortunately, under identical reaction conditions **177** remained unchanged suggesting that the strongly electron withdrawing cyano substituent was hindering the aromatization of the D ring which may require hydride transfer to DDQ generating a carbocation intermediate (Scheme 78). Attention was then turned to the possibility that D-ring aromatization might be achieved by first introducing a halogen atom (e.g. bromine) somewhere in the D-ring to give **182**, followed by E2 elimination and tautomerization of **183** to the phenol **181**, as shown in Scheme 79.



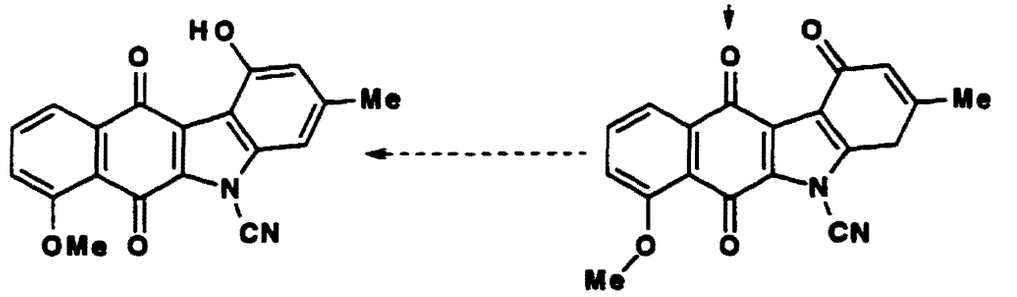
177 181

Scheme 78



177

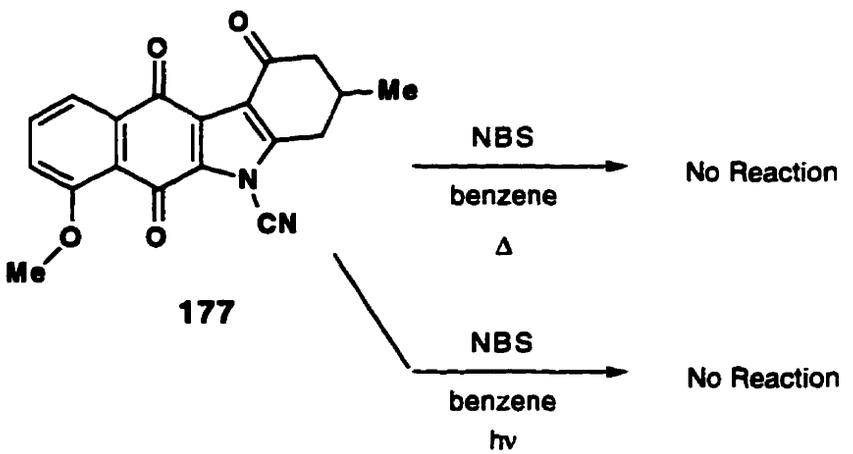
182a: X = Br, Y = H
182b: X = H, Y = Br



181 183

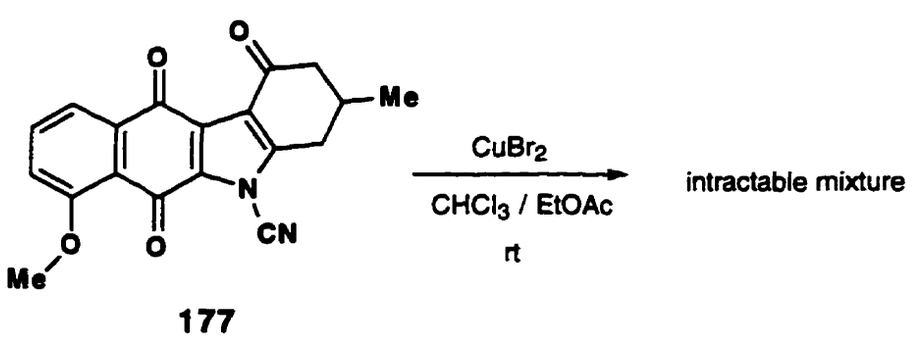
Scheme 79: Proposed strategy for D-ring aromatization.

However, halogenation attempts with NBS in refluxing benzene or with NBS under photolytic conditions failed to yield any halogenated material (Scheme 80).



Scheme 80

Halogenation of **177** with copper(II) bromide under conditions reported to yield halogenated ketones suitable for aromatization in the synthesis of polyaromatic natural products (personal communication from S. J. Gould), in a mixture of chloroform and ethyl acetate at room temperature yielded an intractable mixture of products (Scheme 81).



Scheme 81

As a result of constraints in material supply, **174** was utilized as a model of **177** in many of the following reactions (Figure 61).

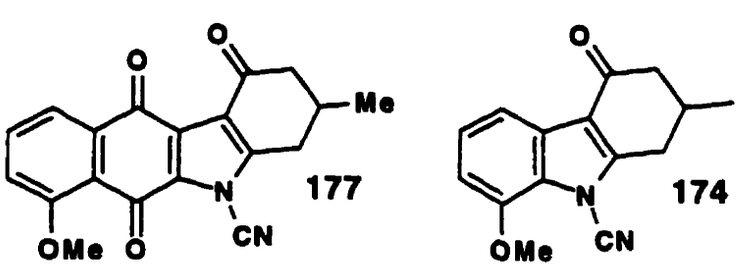
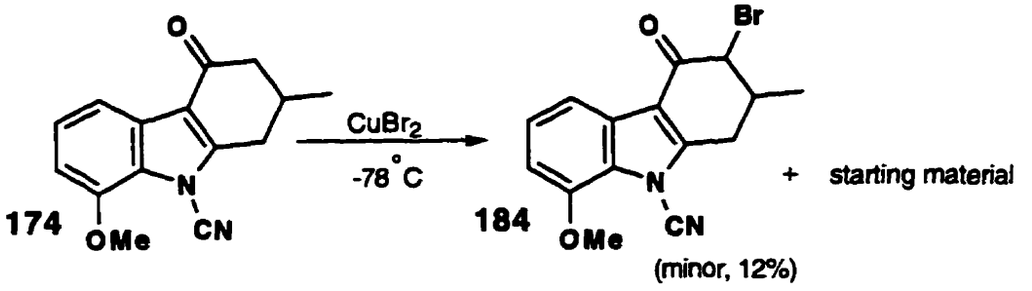


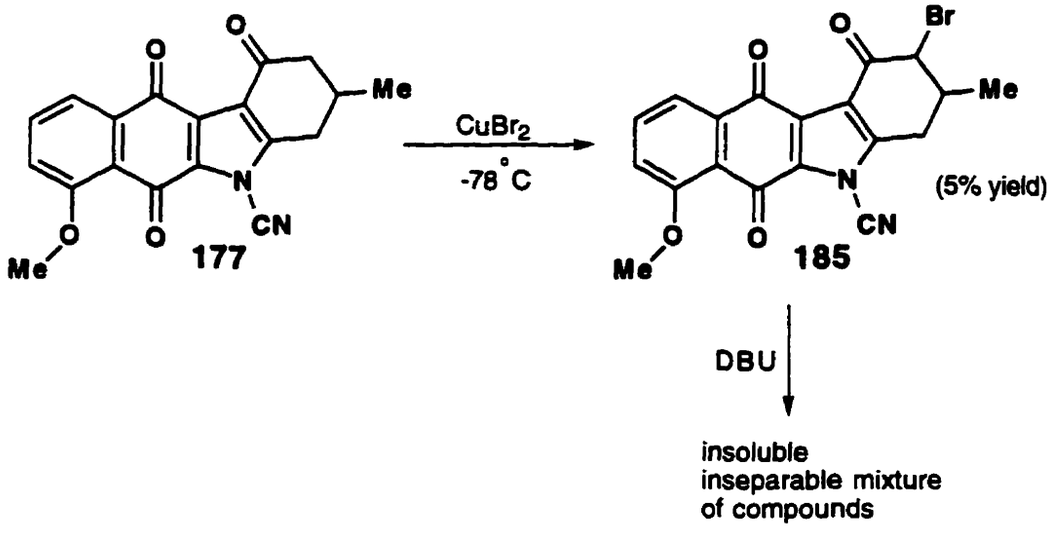
Figure 61

Reaction of **174** with cupric bromide at -78°C resulted in a cleaner reaction but yielded only a small amount of the desired halogenated product **184** along with unchanged starting material (Scheme 82).



Scheme 82

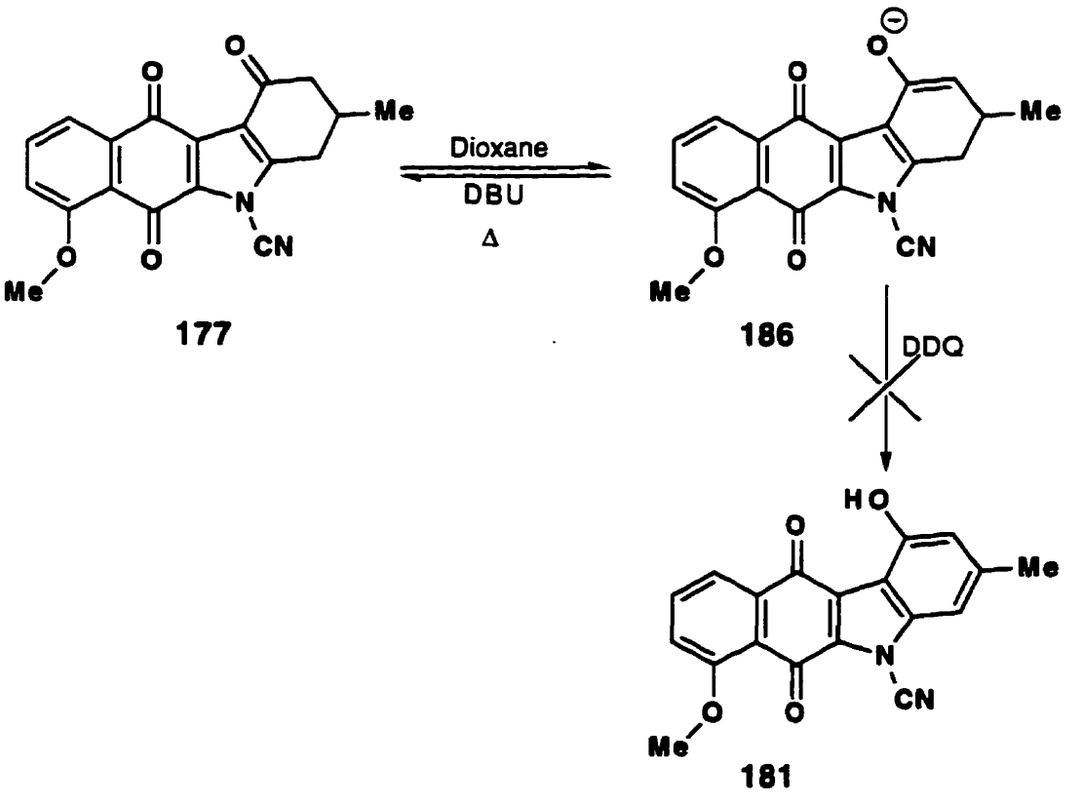
Reaction of **177** with cupric bromide under the same conditions gave a 5% yield of the desired halogenated material **185** (Scheme 83). This halogenated compound was then subjected to reaction with a non-nucleophilic base, DBU, to yield an extremely insoluble product which was judged to be a mixture of compounds by TLC analysis. The formation of highly insoluble materials suggests that the desired aromatization might have occurred, but that the phenolic hydroxyl group might require some form of protection *in situ* to make the system more soluble.



Scheme 83

It was expected that the phenol **181** might exhibit low solubility properties since prekinamycin has been reported to be very poorly soluble in all organic solvents. As a result, it was possible that at least some of the insoluble product was the desired product. However, since only small amounts of **184** and **185** were available as a result of the poor yield in the bromination step, further exploration of the approach was abandoned.

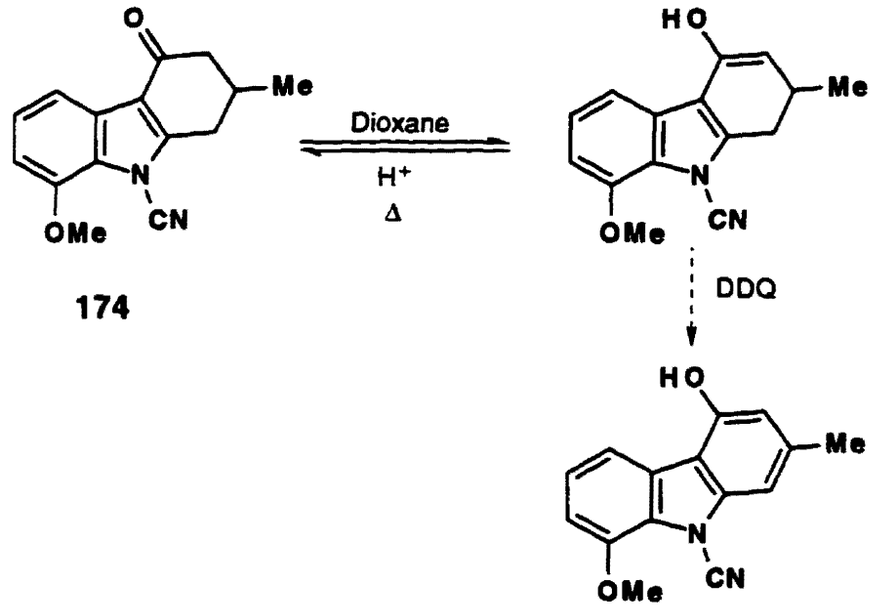
As an alternative approach to aromatization, it was felt that heating of **177** with DDQ in the presence of a weak base might favour an equilibrium with the enolate of **186** which might then more easily react in a hydride transfer reaction with DDQ leading to the formation of the stable aromatic system of prekinamycin (Scheme 84). In practice heating **177** in dioxane at reflux with DDQ and DBU left the starting material unchanged (Scheme 84).



177 **186** **181**

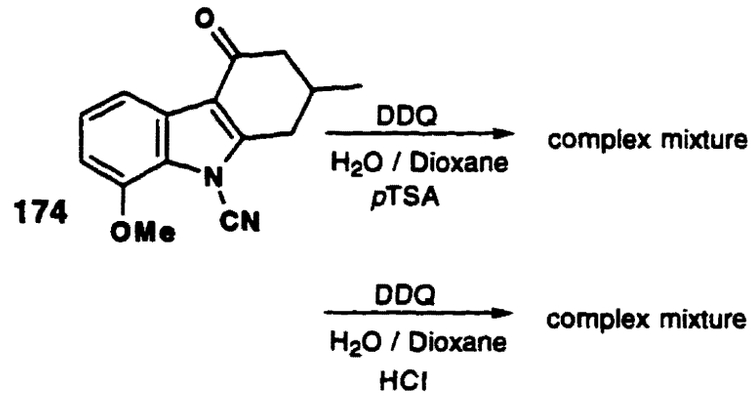
Scheme 84

The possibility that the enol generated *in situ* with acid catalysis, might be aromatized more easily was then explored (Scheme 85). The model compound **174** was stirred at room temperature in a mixture of water and dioxane containing *p*TSA monohydrate. It was felt that any enol formed in the reaction mixture would aromatize when DDQ was added. Under these conditions a complex mixture of products was obtained. Alteration of the conditions by including hydrochloric acid instead of *p*TSA had no discernible effect on the product distribution as indicated by TLC.



174

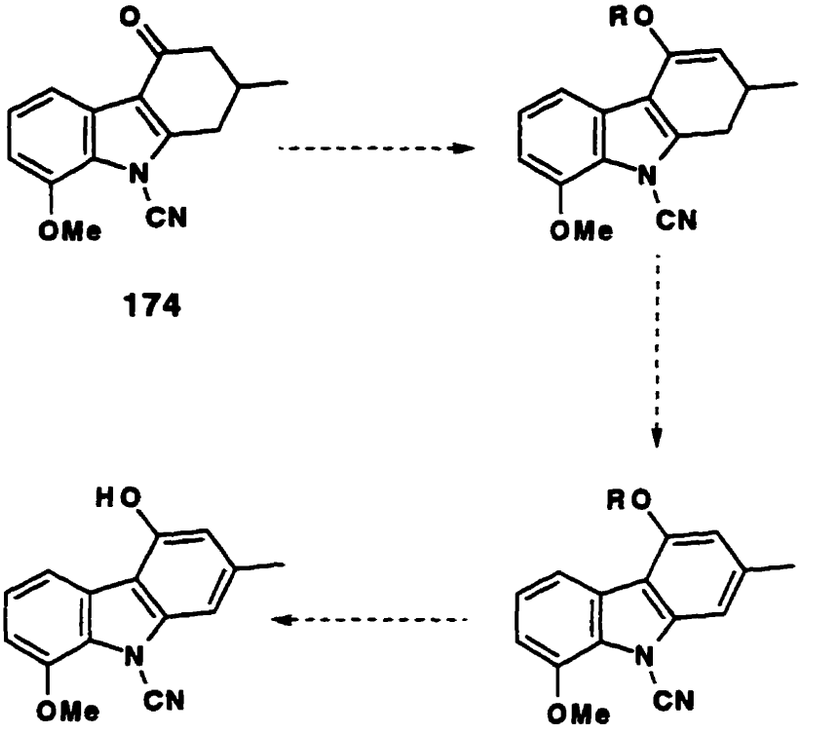
Scheme 85



174

Scheme 86

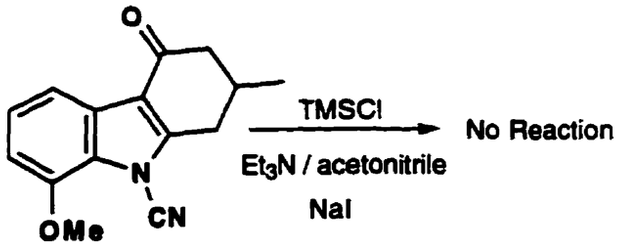
Attention was then turned to the possibility that the desired transformation might yet be effected if carried out in a stepwise manner involving trapping of the enol intermediate which might then be aromatized under mild conditions (Scheme 87).



174

Scheme 87

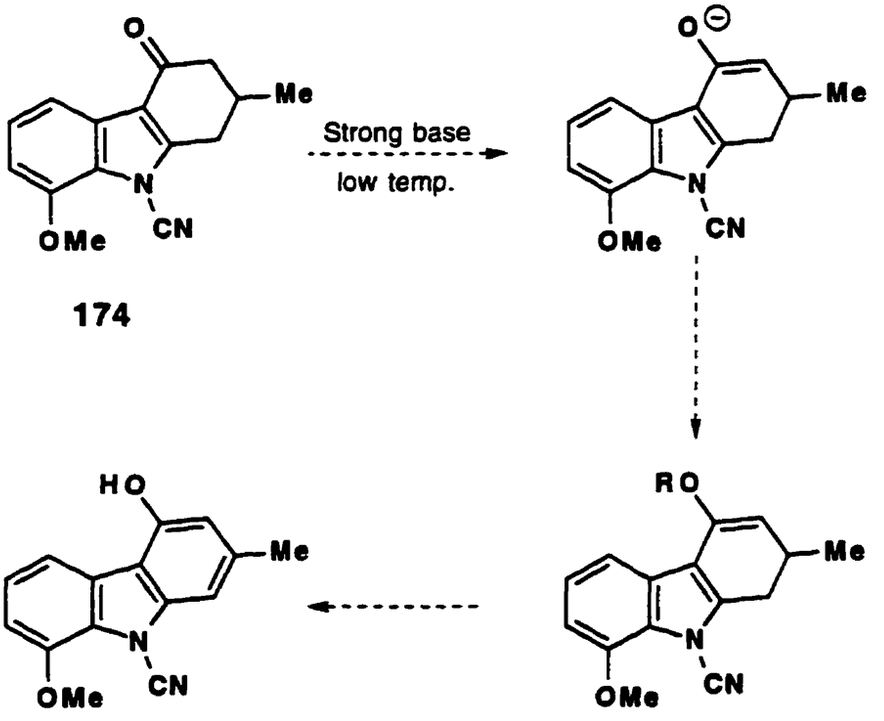
One such possibility was to trap the enol as a silyl ether which could be easily converted to the phenol after aromatization. In this vein, the model compound **174** was treated with TMSCl with triethylamine and sodium iodide (Scheme 88). However, under these conditions the starting material remained unchanged.



174

Scheme 88

Another plausible method for formation of the enol of **174** involved the utilization of a strong base at low temperatures, which would yield an enolate which might then be trapped (Scheme 89). Once trapped, the enol could then be aromatized with subsequent deprotection.

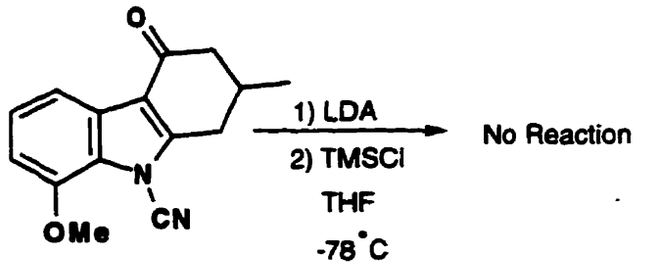


174

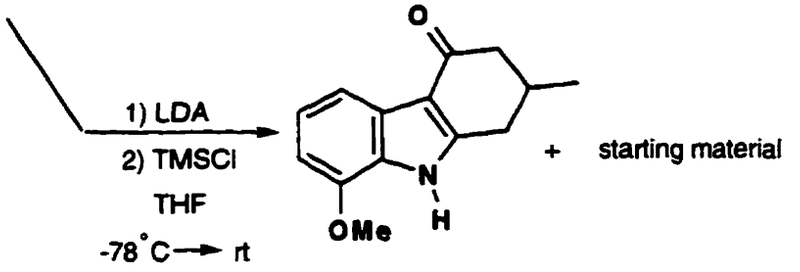
Scheme 89

It was felt that LDA would serve as a suitable base for formation of the enol which could be trapped with TMSCl. Under these conditions, only starting material was isolated from the reaction mixture. However, when the reaction

was carried out at -78°C and then brought up to room temperature to stir, unchanged starting material as well as decyanated material was obtained.



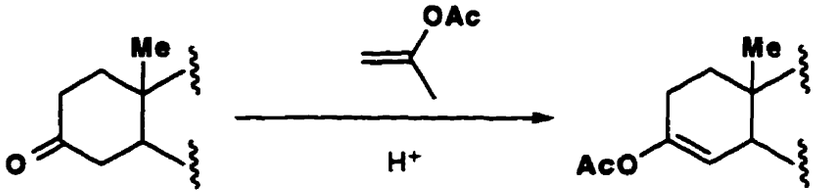
174



169

Scheme 90

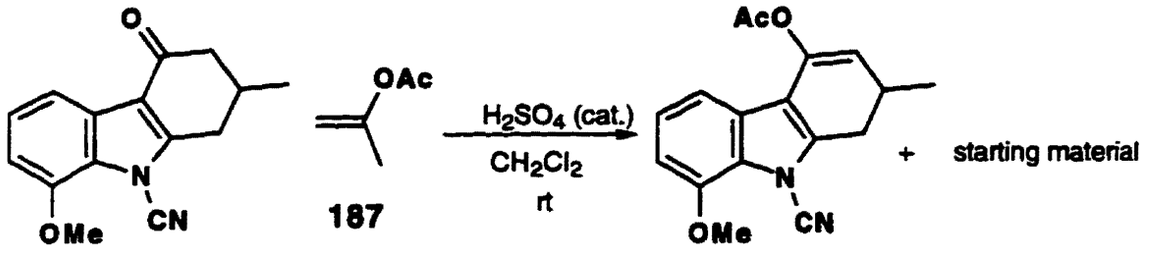
The failure to generate the TMS enol ether under basic conditions led us to consider the possibility of the use of acid catalysis to form the enol acetate rather than a TMS enol ether. Isopropenyl acetate (**187**) in the presence of an acid catalyst is known to react with ketones to form enol acetates.[105]



Scheme 91

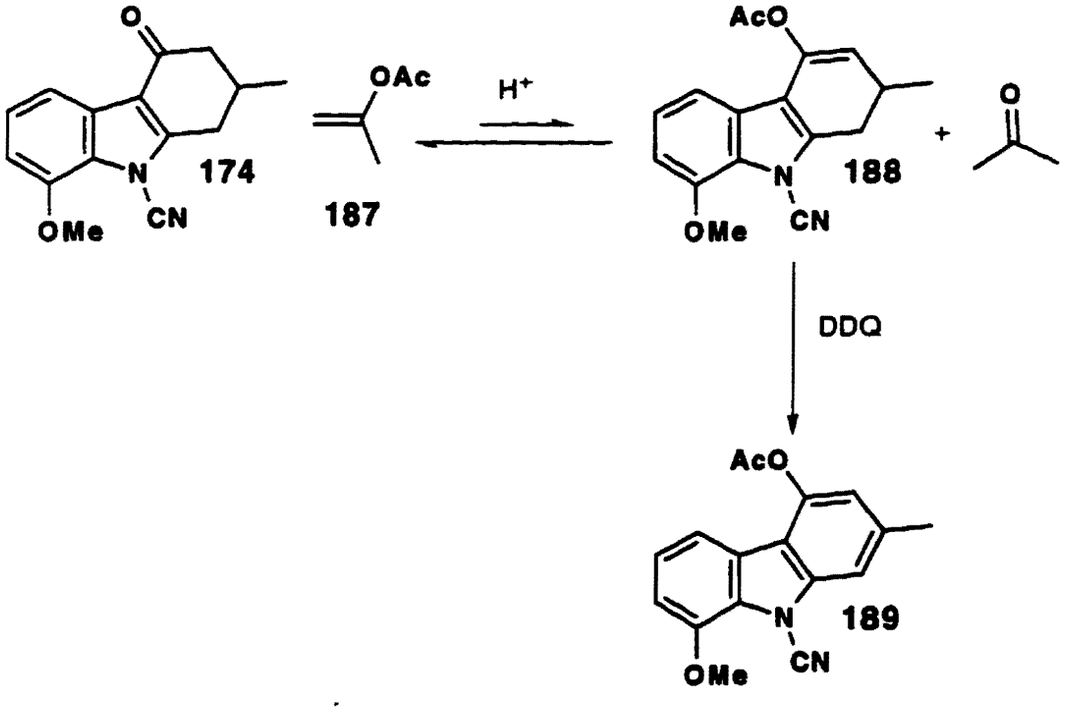
Reaction of the model system **174** with isopropenyl acetate (**187**) in methylene chloride with a catalytic amount of sulfuric acid (12 M) yielded a mixture of starting material as well as **188** (~2%) (Scheme 92). Warming of the reaction mixture did not alter the product distribution dramatically. Extension of reaction

times also had no effect on the product distribution. This behaviour was suggestive of an equilibrium in which the starting material was favoured (Scheme 93).



Scheme 92

Although complete formation of the enol acetate was not achieved, it was felt that this process could still be useful for our purpose if DDQ was reacted with the enol acetate as it was produced *in situ* (Scheme 93).

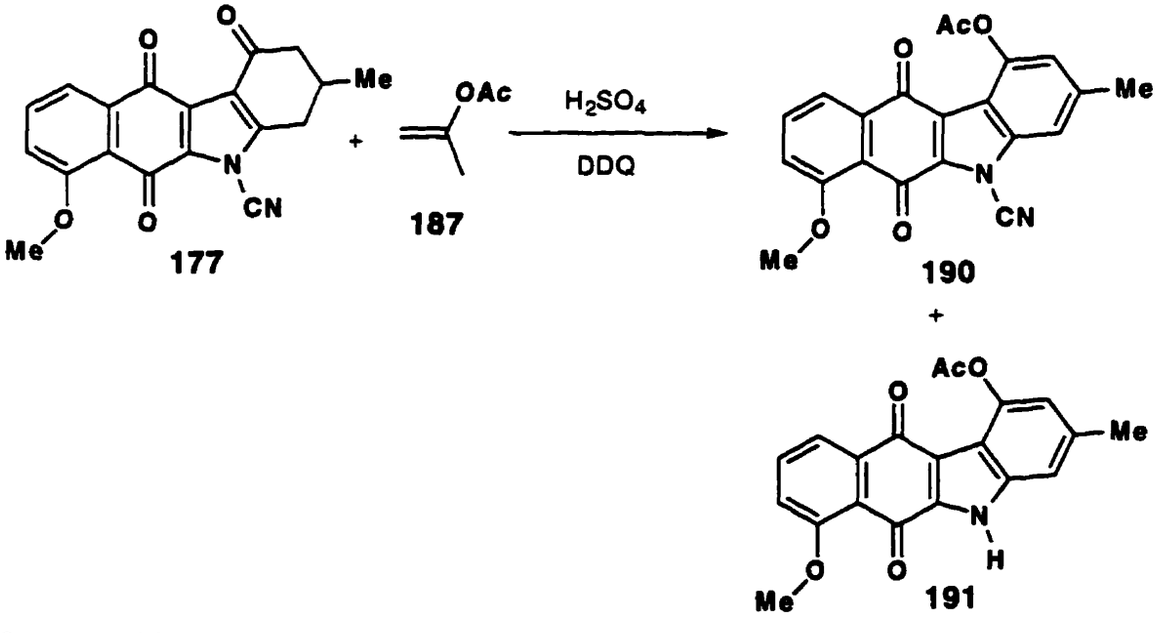


Scheme 93

Reaction of the model compound **174** in isopropenyl acetate as the solvent with a catalytic amount of sulfuric acid and an equivalent of DDQ at

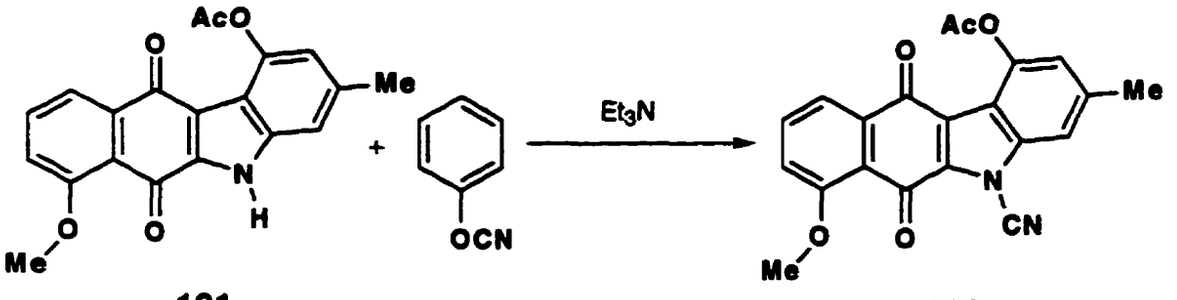
room temperature, yielded cleanly a product for which the ^1H NMR spectrum included three singlets at 4.06, 2.58 and 2.51 ppm, with integrations of three protons each. The low resolution mass spectrum which showed a molecule ion of 280 and the elemental analysis were both consistent with the aromatized system **189** (Scheme 93). The IR spectrum showed bands at 2250 and 1678 cm^{-1}.

Under the same conditions, the fully substituted system **177** yielded two products. The major product (61%) was a bright yellow solid for which the mass spectrum showed a M^+ ion of 374. The proton NMR contained three proton singlets at 4.04 ppm, 2.56 ppm, and 2.53 ppm. The spectroscopic data was consistent with the desired aromatic ring system of prekinamycin **190** (Scheme 94). The minor product (32%) lacked the IR signal attributed to the cyano functionality and had a signal at 3252 cm^{-1} indicative of an indole N-H. Furthermore, the mass spectrum showed an M^+ ion of 348. The structure was assigned as the aromatized decyanated material **191** (Scheme 94).



Scheme 94

Reaction of the decyanated material **191** with phenyl cyanate and triethylamine yielded **190** in 88% isolated yield (Scheme 95).



191 **190**

Scheme 95

The formation of **190** rather than the corresponding phenol proved to be useful since the solubility properties of **190**, unlike those expected for the phenol, were well suited for purification and spectroscopic characterization.

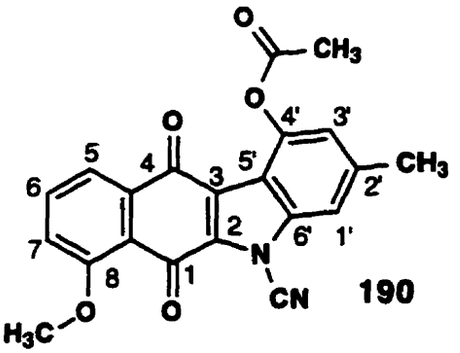
The synthesis of **190** in nine steps and 21% overall yield from 5-methylcyclohexane-1,3-dione essentially represented the achievement of our goal in this area; namely, the development of a synthetic strategy for the construction of the structure assigned to the prekinamycin ring system which might then be adapted to the preparation of the more complex kinamycin antitumour antibiotics.

At this stage of the study it was expected that the total synthesis of prekinamycin itself would be achieved in one step by demethylation and deacylation of **190** with a suitable Lewis acid catalyst such as BBr_3. However, we were dismayed to find that the spectroscopic characteristics (^1H & ^{13}C NMR, IR) of **190**, as prepared in this laboratory, were very different from those reported for prekinamycin diacetate.[61] These observations led us, initially, to question the structure assigned to our synthetic product and, eventually, to propose a revised structure for the natural product and for all the kinamycins. These analyses are described in detail in the next chapter.

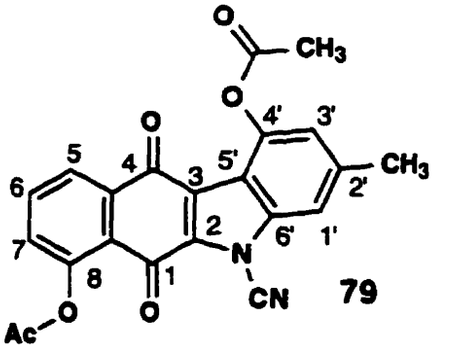
Chapter 4: Spectroscopic Comparison of 190 with the Diacetate Derivative of Prekinamycin

As indicated in Chapter 3, the pleasure in having achieved the synthesis of **190** was relatively short-lived since it was soon recognized that the differences in physical and spectroscopic properties between **190**, as prepared in this laboratory, and prekinamycin diacetate, as described by Gould and coworkers[61], were incompatible with the minor differences in the structures assigned to them.

For example, the kinamycins are described as purple solids and the diacetyl derivative of prekinamycin is dark red. The synthetic product **190**, on the other hand, is a bright yellow solid. Furthermore, comparison of the ^{1}H NMR spectrum of **190**, synthesized in this laboratory, with that of the proton spectrum of the diacetyl[61] derivative of prekinamycin shows marked differences. The ^{1}H NMR signals for **190** and **79** are summarized below (Figure 62).



190



79

Assig.	Signal (190)	Assig.	Signal (79)
2'(CH3)	2.53 (3H, s)	2'(CH3)	2.46 (3H, s)
4'(OAc)	2.56 (3H, s)	4'(OAc)	2.49 (3H, s)
8 (OCH3)	4.04 (3H, s)	8'(OAc)	2.48 (3H, s)
1'	7.04 (1H, br s)	1'	6.84 (1H, d, J = 1.2 Hz)
5 or 7	7.37 (1H, dd, J = 1.1, 8.5 Hz)	7	7.14 (1H, dd, J = 1.1, 7.4 Hz)
3'	7.47 (1H, br s)	3'	6.95 (1H, br. s)
7 or 5	7.75 (1H, dd, J = 1.1, 8.5 Hz)	5	7.52 (1H, dd, J = 1.1, 7.2 Hz)
6	7.86 (1H, dd, J = 7.7, 8.5 Hz)	6	7.34 (1H, dd, J = 7.4, 7.0 Hz)

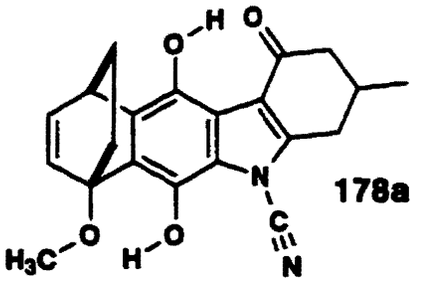
Figure 62: Proton NMR signals and assignments for 190 and prekinamycin diacetate.

It was expected that the signals for protons in the A ring of **190** and **79** would differ somewhat, since the C8 hydroxy protecting groups are different. However, the C4'-OH protecting groups are the same in these structures and it was unlikely that signals for the D-ring protons would be affected greatly by the differences in the C8-OH protecting groups in the structures. Suprisingly, the signals in the D-ring of **190** and **79** are considerably different. The signals for C1' and C3' of structure **190** appear at 7.04 ppm and 7.47 ppm, respectively, whereas, for the corresponding carbons of **79**, the signals appear at 6.84 ppm and 6.95 ppm.

In addition, there are large differences in the ^{13}C spectra of the two compounds.[61] In particular, the cyano functionality gives rise to a signal at 105 ppm for **190**, whereas the cyano moiety was assigned to a signal at 83.71 ppm in the diacetyl derivative **79**.[61] These significant differences clearly could not be explained by the minor differences in protecting groups in the A ring.

Clearly, the assignment of structure **190** to our synthetic product was incompatible with the previous assignment of structure **79** prekinamycin diacetate.

It was widely recognized that the structures of the kinamycins were based on extensive spectroscopic analysis and correlations with the structure and spectroscopic properties of kinamycin C, a derivative of which had been analyzed by single crystal X-ray diffraction. As a result, our first thoughts concerning this dichotomy were directed at the possibility that the Diels-Alder reaction in our synthetic sequence had occurred with a different regioselectivity than was predicted based on our model study and on FMO analysis. To explore this possibility, attempts were made to obtain suitable crystals of intermediates, subsequent to the Diels-Alder reaction, for X-ray crystallography. Surprisingly, the only intermediate that yielded suitable crystals was **178** (Figure 63), which is a diastereomeric mixture (Figure 64). The diastereomeric forms appear to exhibit equal occupancy of sites in the crystal lattice and negligible differences in atomic co-ordinates for the B, C and D ring atoms. The co-ordinate data for the X-ray structure of **178** appears in Appendix B, page 272. The X-ray structure clearly demonstrated that the Diels-Alder reaction had progressed with the expected regioselectivity.



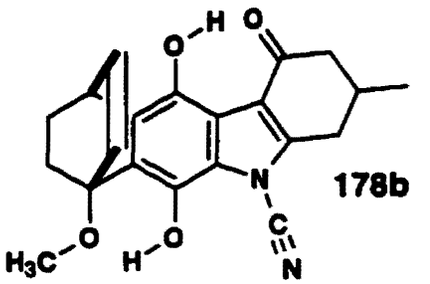


Figure 63

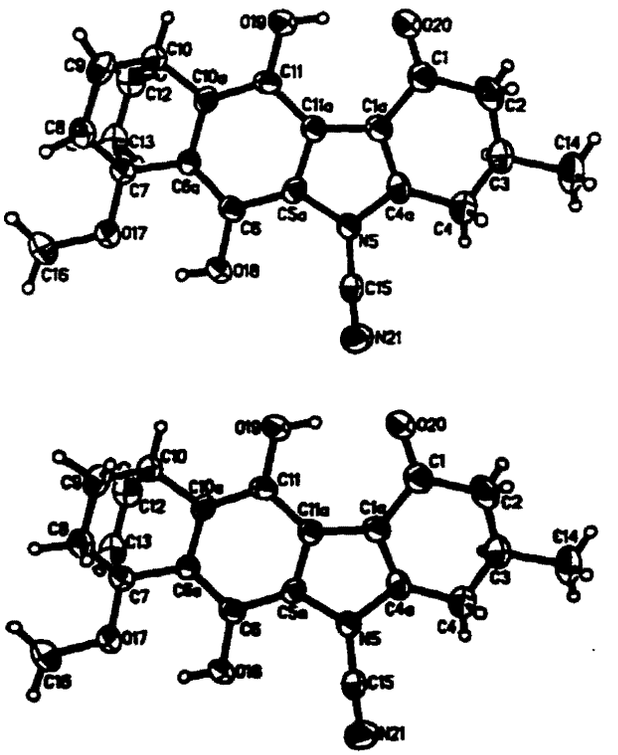


Figure 64: ORTEP plots of the two diastereomeric forms of 178.

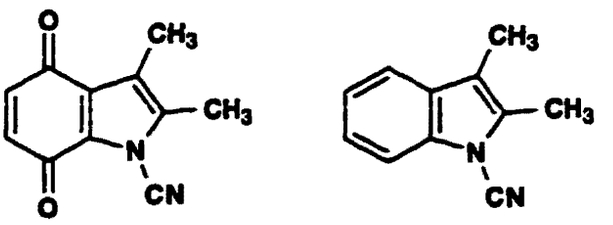
As a result, we were confident that the structure **190** assigned to our synthetic end product was indeed correct and we were thus forced to consider

the possibility that the structures of prekinamycin and its diacetyl derivative had been misassigned. To explore this possibility further, a careful analysis of the spectroscopic data previously reported for the kinamycins and those of the N-cyanoindoles and N-cyanoindoloquinones prepared in this laboratory in model studies and in the present synthetic investigation was undertaken.

The ^{13}C resonance of each of the N-cyano group of 22 N-cyano indoles prepared unambiguously in this laboratory, falls in the range from 104 ppm to 109 ppm; whereas, the ^{13}C signal assigned to the N-cyano group of the kinamycins including prekinamycin, falls in the range from 78.5 ppm to 83.7 ppm. In addition, the range for the stretching frequency of the N-cyano group is 2237 to 2259 cm^{-1} in the IR spectrum for the N-cyanoindoles prepared in this laboratory, whereas the IR bands assigned to the N-cyano group of the kinamycins range from 2119 to 2170 cm^{-1}. It was clear that the most significant differences between **190** and prekinamycin diacetate **79** occur in the region of the cyanamide functionality and, hence, further structural analysis was focused in this area.

4.1 ^{15}N and ^{13}C NMR Experiments

Our suspicion that the kinamycins might not be N-cyanoindoles was further supported by the results of analysis of ^{15}N chemical shifts of model compounds **160** and **192** prepared previously in model studies in this laboratory (Figure 65).



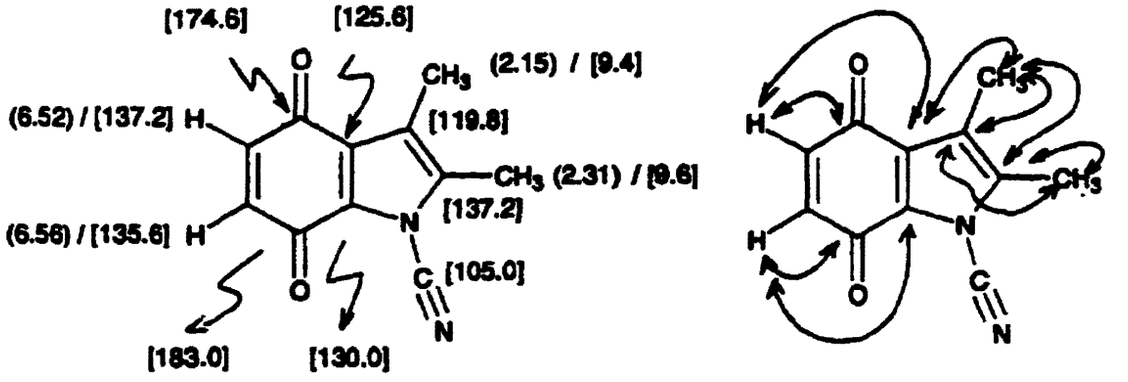
160 **192**

Figure 65

The connectivities of **160** were established by $^{1}H/^{13}C$ long-range HMQC experiments, the results of which are shown as double headed arrows in (^{1}H chemical shift) [^{13}C chemical shift]

Figure 66. The ^{13}C and ^{1}H assignments also appear in (^{1}H chemical shift) [^{13}C chemical shift]

Figure 66. The structure of **192** was established with complete certainty by a single crystal X-ray diffraction analysis on crystals produced from a solution of **192** in chloroform. An ORTEP plot is shown in Figure 67. The X-ray data appears in Appendix B, page 281.



(^{1}H chemical shift) [^{13}C chemical shift]

Figure 66: **^{1}H / ^{13}C long-range HMQC experiments established connectivities and assignments for 160.**

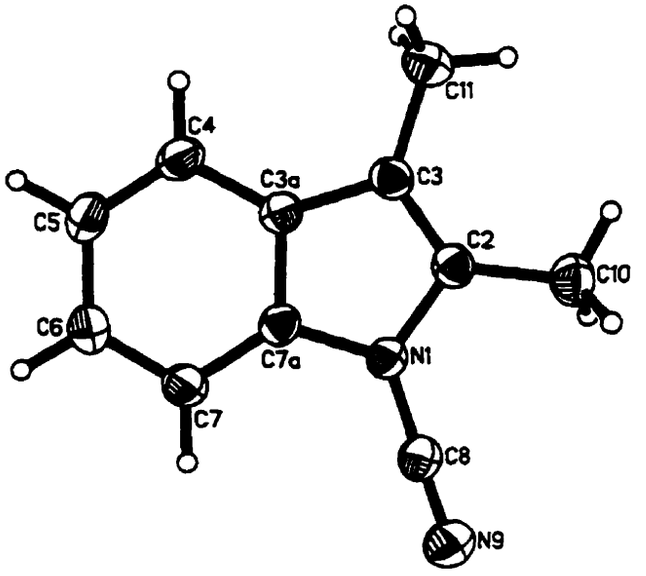
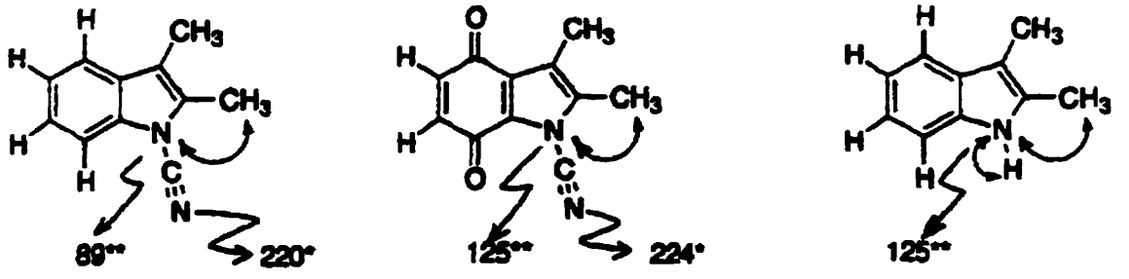


Figure 67: ORTEP plot of N-cyano-2,3-dimethylindole.

Once the structure assignments of **160** and **192** were firmly established, attention was turned to ^{15}N NMR experiments. The object of gaining further spectral data was solely for comparison with published ^{15}N NMR data for ^{15}N enriched kinamycin D produced biosynthetically in the presence of ^{15}N labelled ammonia.[65] The following ^{15}N NMR experiments were performed on a Bruker AMX-500 NMR spectrometer at 50.69 MHz in deuterochloroform. The chemical shifts were determined relative to neat nitromethane and were transformed to the ammonia scale by setting the nitromethane signal to +380 ppm.

^{1}H / ^{15}N HMQC experiments allowed the detection of some signals indirectly while others were observed directly. The direct and indirect resonances with heteronuclear correlations are shown in Figure 68.



192 160

* observed directly

** observed by ^{1}H / ^{15}N HMQC (observed heteronuclear correlations are indicated with double headed arrows)

Figure 68: Direct and indirect observation of ^{15}N NMR signals relative to ammonia of model compounds.

The ring and cyano nitrogens of **160** give rise to signals at 125 ppm and 224 ppm, respectively and those for N-cyano-2,3-dimethylindole (**192**) appear at 89 and 220 ppm respectively. By comparison, the signals assigned to the corresponding nitrogens in ^{15}N enriched kinamycin D appear at 241.6 ppm and 344.5 ppm.[65]

It was clear, based on the significant spectral differences between the N-cyanoindoles synthesized in this laboratory and the kinamycins, that the kinamycins do not possess the N-cyano functionality. A re-examination of the literature concerning the assignment of structures to the kinamycins proved to be very instructive in the course of structural reassignment.

4.2 Structure assignment of the kinamycins

The structures of the kinamycins were originally assigned, in part, by chemical and spectroscopic analysis.[8] The structure was then completely assigned by an X-ray crystallographic study of the *p*-bromobenzoate derivative of kinamycin C (Figure 69).[55]

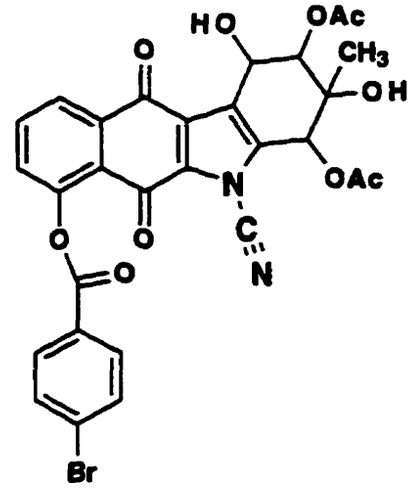


Figure 69: The structure of kinamycin C *p*-bromobenzoate.

However, close examination of the report of the X-ray study revealed that the data set established connectivities of all but a linear three atom fragment **X-Y-Z** (Figure 70). The data quality was such that Furusaki and coworkers[55] were unable to unambiguously assign the last three atoms, two nitrogens and a carbon based solely on the crystallographic analysis. Two possible molecular arrangements were considered feasible; namely, an N-cyano (N-C-N) or N-isocyano (N-N-C) group. The final assignment of the **X-Y-Z** fragment as a cyanamide, N-C-N, was based on earlier[8] chemical analysis. It was expected that, if the kinamycins were cyanamides, hydrolysis with aqueous base would result in the formation of ammonia (Scheme 96), whereas, if the kinamycins were isonitriles, aqueous hydrolysis would result in the formation of formic acid (Scheme 96). Hydrolysis of deacetylkinamycin C with 30% KOH gave a positive Nessler's reagent test for ammonia and a negative chromotropic acid test for formic acid. As a result, the kinamycins were assigned as cyanamides rather than isocyanamides.[8,55]

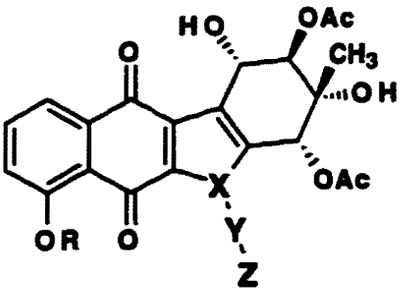
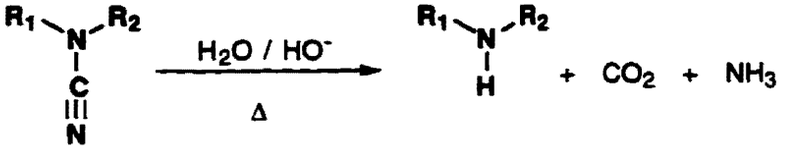
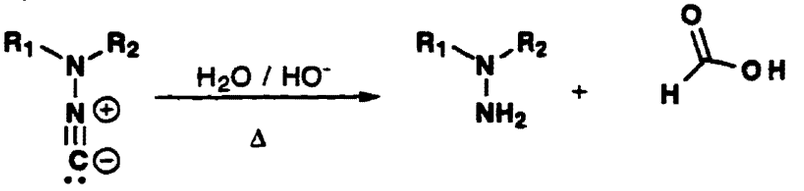


Figure 70

1) X-Y-Z = N-C-N



2) X-Y-Z = N-N-C



Scheme 96

Since $^{1}H/^{13}C$ HETCOR experiments on kinamycin D reported by Gould and co-workers[61] confirmed the connectivities established by X-ray studies, only the three atom fragment, **X-Y-Z**, required reconsideration. Our studies described above clearly eliminated the possibility that the kinamycins were cyanamides. The second possibility for the **X-Y-Z** fragment, an isocyanamide, was ruled out by chemical tests. Furthermore, comparison of the ^{13}C resonance assigned to the **X-Y-Z** groups of the kinamycins (78.5 to 87.3 ppm) with those reported in the literature for isocyanides (150 to 170 ppm)[106] confirmed the conclusion arrived at by Omura *et al.*[8] that the kinamycins are not isocyanides. The only structural possibility which remained for the linear three atom fragment

was a diazo group. That is, the connectivity in the X-Y-Z group is C-N-N and not N-C-N as originally assigned.

That Omura and co-workers[8] did not consider the diazo group as a possible structural feature is not surprising since, in general, diazo compounds are considered to be relatively unstable. Diazo groups, however, can be strongly stabilized by resonance interactions such as those indicated for the known diazo compounds shown in Figure 71 (**193-197**). An interesting recent example of a naturally occurring resonance stabilized diazo compound is lagunamycin (Figure 72).[107]

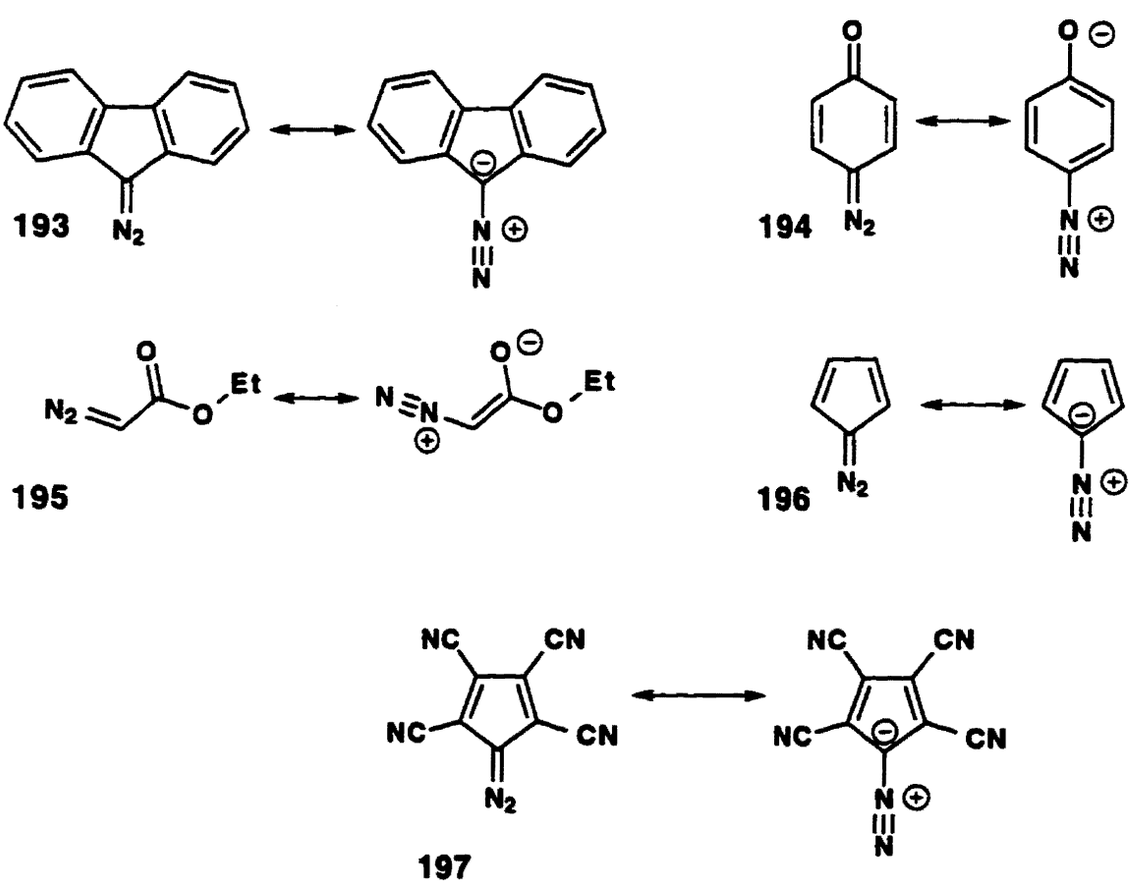
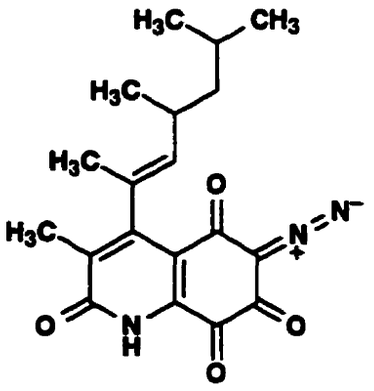


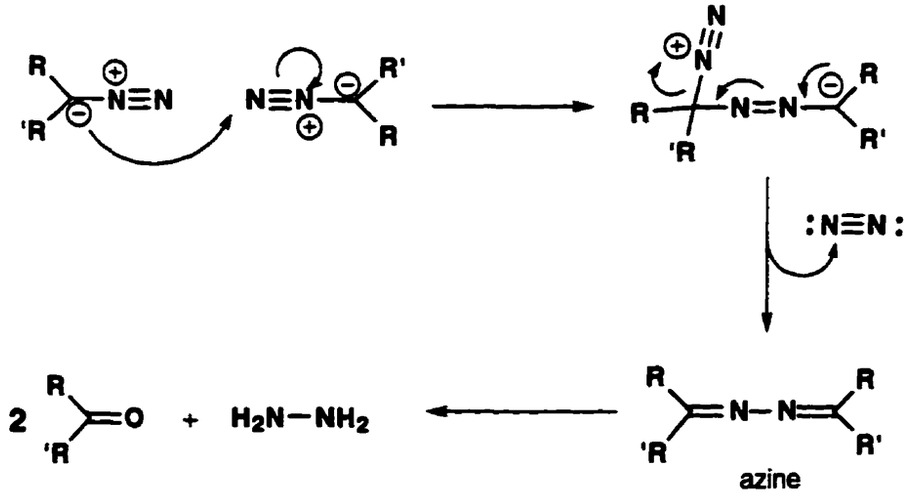
Figure 71



lagunamycin

Figure 72

Given this revised structural assignment to the kinamycins, it is necessary to reconsider the interpretation of the chemical tests used to distinguish between the existence of an isocyanamide or cyanamide functionality in the kinamycins. The negative test for formic acid in the hydrolysate from kinamycin C is clearly compatible with either an N-cyano or diazo group.[108] The apparent formation of ammonia upon hydrolysis, on the other hand, is not as readily reconciled with the diazo structure (Scheme 97).



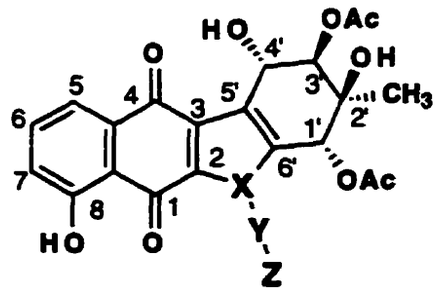
azine

Scheme 97

It is known, however, that diazo compounds can be induced to form azines as shown in Scheme 97. Alkaline hydrolysis of the azine would be expected to liberate hydrazine. Nessler's reagent tests for dilute solutions of hydrazine or ammonia have been shown in this laboratory to be qualitatively indistinguishable. It is then possible that the positive Nessler's reagent test given by the hydrolysate of deacetylkinamycin C may have been from hydrazine formed from an azine byproduct rather than free ammonia.

Interestingly, re-examination of the long-range $^{1}H/^{13}C$ HETCOR experiment with kinamycin D reported by Gould and co-workers[57] shows a weak previously unassigned correlation between C(1')-H and the ^{13}C signal at 78.5 ppm which is in agreement with the diazo compound **199** but not the cyanamide structure **65** or the isocyanamide structure **198** (Figure 73). Additionally, loss of a 28 mass unit fragment in the published mass spectrum of prekinamycin diacetate is consistent with the presence of a diazo group. The presence of a cyanamide or isocyanamide functionality would be expected to result in a 26 mass unit fragmentation pathway in the mass spectrum.

The spectroscopic characteristics of the kinamycins are perfectly compatible with those expected for a diazoquinone system **199**, is indicated by comparison with the spectroscopic characteristics of the known stablized diazo compounds in Figure 71.



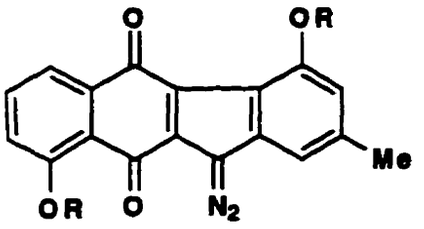
65 X=N, Y=C, Z=N
198 X=N, Y=N, Z=C
199 X=C, Y=N, Z=N

Figure 73

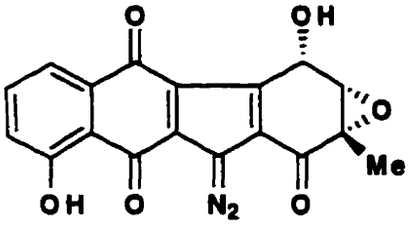
The ^{13}C signal of diazo carbons for a variety of model diazo compounds, including diazofluorene (**193**), 1,4-benzoquinone 1-diazide (**194**), ethyl diazoacetate (**195**), diazocyclopentadiene (**196**) and diazotetracyanocyclopentadiene (**197**), falls in the range of 63 to 93 ppm which encompasses the range of 78.5 to 83.7 ppm observed for the kinamycins. The IR stretching frequency observed for the kinamycins ranges from 2119 to 2159 cm^{-1} whereas that for the diazo groups of the model compounds, is in the range 2065 to 2200 cm^{-1}.

As indicated previously the ^{15}N NMR signals for ^{15}N enriched kinamycin D ring nitrogen and external nitrogen are 241.6 ppm and 344.5 ppm, respectively.[65] These values are far removed from 125 ppm and 224 ppm observed for the corresponding nitrogens of the model compound **160**. They do, however, correspond well with expected signals of the internal (227 to 287 ppm) and terminal (332 to 441 ppm) nitrogens of diazo compounds.[109] Furthermore, the coupling constants published for ^{15}N doubly labelled kinamycin D ($J_{N\text{-}N}$ = 3.4 Hz, $^{1}J_{C\text{-}N}$ = 21.2 Hz, $^{2}J_{C\text{-}N}$ = 5.4 Hz) agree with those observed for doubly labelled ethyl diazoacetate ($J_{N\text{-}N}$ = 5.7 Hz, $^{1}J_{C\text{-}N}$ = 20.4 Hz, $^{2}J_{C\text{-}N}$ = 3.7 Hz).[109] Thus the spectroscopic evidence suggests overwhelmingly that the kinamycins are diazo compounds, rather than cyanamides. For the

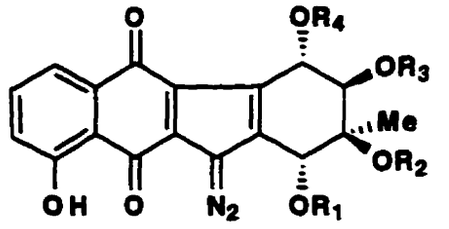
sake of clarity the revised structures for some of the known kinamycins are shown below (Figure 74).



R = H, prekinamycin
R = Ac, prekinamycin diacetate



keto-anhydrokinamycin

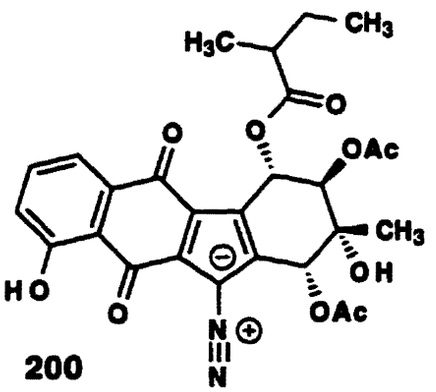


Kinamycin	R_1	R_2	R_3	R_4
A	Ac	Ac	Ac	Ac
B	H	Ac	H	H
C	Ac	H	Ac	Ac
D	Ac	H	Ac	H
E	Ac	H	H	H
F	H	H	H	H

Figure 74: Revised structures of the kinamycins

4.3 Independent Structural Revision of the Kinamycins by Gould and Co-Workers[110]

Upon completion of the synthetic studies and resultant revision of the structure of the kinamycins described above our findings were communicated to Professor Gould at the University of Oregon prior to publication. At that time we were informed that Professor Gould and his co-workers had independently arrived at the same structural revision through a very careful X-ray crystallographic analysis of the (S)-2-methylbutyric acid ester of kinamycin D (**200**) (Figure 75).[110]

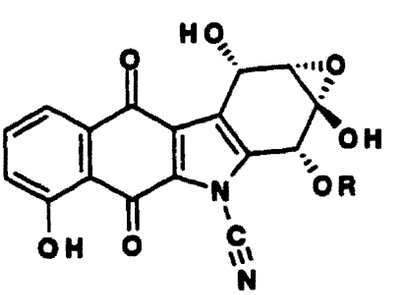


200

Figure 75

In that study, the choice between the three possible connectivities for the linear three atom fragment (X-Y-Z) of the kinamycin system was based on comparison of the fit of the possible structures to the data as indicated by R values (5.69% for N-C-N, 5.73% for N-N-C and 5.18% for C-N-N).[110]

The two research groups then agreed to disclose their independent conclusions as back to back publications.[110,111] Another structural report concerning the kinamycins which is somewhat interesting in light of the discussion above is that published by Chang and co-workers[59,60] just prior to the appearance of the papers describing the revised structure. These workers describe the isolation of six new kinamycin analogues including the epoxides **201** and **202** (Figure 76).



201 R = $COCH(CH_3)_2$
202 R = Ac

Figure 76

The structure of **201** was determined based not only on spectroscopic comparison with other kinamycins but also by a single crystal X-ray diffraction study. Since the authors had no reason to suspect that the structures of the other kinamycins had been misassigned there was no obvious reason for them to undertake a detailed comparison of the "goodness" of fit of the data to the three possible structures based on permutations of two nitrogens and one carbon in the linear three atom grouping in their X-ray structure. The R factor in this study was a perfectly acceptable 6.2% for the N-C-N structural assignment.

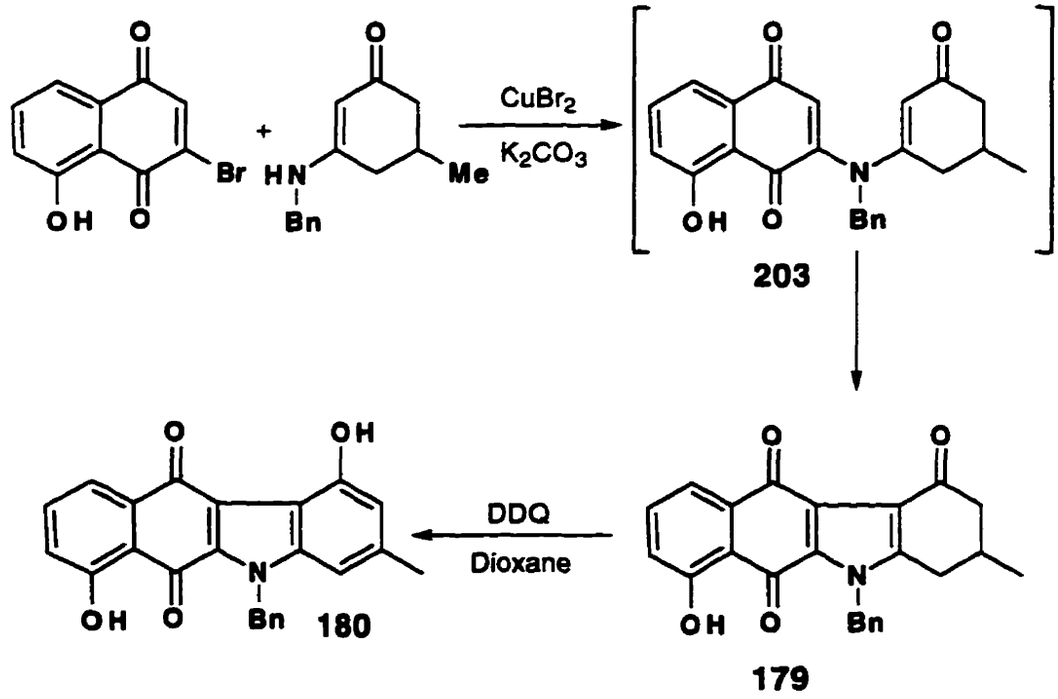
Another study related to the synthesis of the kinamycins which is worthy of comment at this point in this discussion is the work of Echavarren and co-workers.[112] Prior to the disclosure of the true structure of the kinamycins, Echavarren and co-workers reported a synthesis of prekinamycin, at least, a synthesis of the structure originally assigned to prekinamycin. This report is of significance in a number of ways. First, it was the observation by Echavarren[112] that the spectroscopic characteristics of his synthetic product did not agree with those reported by Gould and co-workers[57,61] for the natural product and that led the group in Oregon to re-examine the structure of the kinamycins as described above. The synthetic study by Echavarren was also of significance to our structural and synthetic study since we discovered that the spectroscopic data reported not only disagreed with that of the natural product but also *disagreed with that which we obtained for our synthetic product*, the structure of which we established firmly.

A possible explanation for the discrepancy between the spectroscopic data and structural assignments reported by Echavarren and co-workers and those observed in the present study is presented in the next section.

4.4 Other Synthetic Approaches to the Structure Originally Assigned to the Kinamycins

When studies aimed at the synthesis of the kinamycins were initiated in these laboratories, there were no reports in the literature of synthetic efforts directed at this class of natural products. Some research related to the synthesis of benzo[b]carbazoles had been disclosed but examples of the synthesis of N-cyanocarbazoles or N-cyanoindoles were unknown.

During the course of our research, two synthetic studies in the kinamycin area were disclosed in the literature. One of these reported by O'Sullivan and co-workers, involves the oxidative cyclization of the anilinoquinone **203**, employing potassium carbonate and cupric bromide, and was briefly mentioned above in Chapter 3, page 110, in the context of methods for D ring aromatization.



Scheme 98:

In contrast to our synthetic approach in which the A ring is added after the construction of a suitable BCD ring synthon, the O'Sullivan synthesis involves

the coupling of an AB ring synthon with a D ring precursor followed by a cyclization to construct the full ABCD skeleton of the kinamycins. A potential pitfall in this approach to prekinamycin is the need to remove the N-benzyl protecting group in order to introduce the N-cyano group present in the structure **77**, originally assigned to the natural product. N-Benzylindoles are known to be somewhat resistant to standard N-debenzylation methods and this difficulty may be the cause of the failure of these workers to report a simple extension of their synthetic approach beyond **180** to the structure assigned to the natural product.

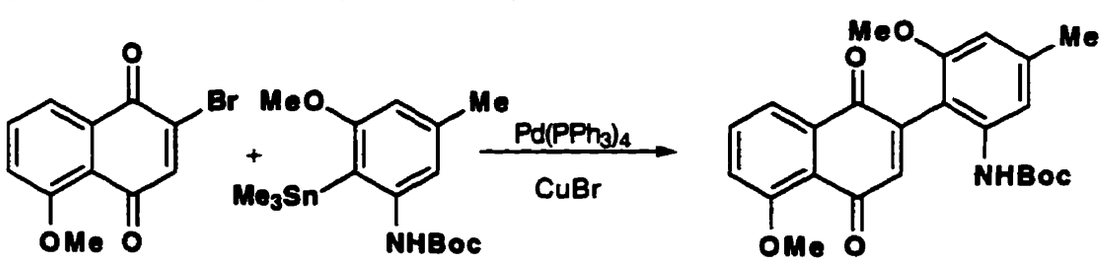
Another approach to the originally assigned prekinamycin structure, which was reported to have yielded the full target structure, is that of Echavarren and co-workers.[112] These authors pointed out that the spectroscopic characteristics of their end product, to which they assigned the structure previously proposed for prekinamycin,[61] differed substantially from those previously reported for the natural product and suggested that the structures of the kinamycins might "require further examination". This report had some influence on the research efforts which eventually led to the structural revision for the kinamycins which are described above in Chapter 4.

It was this report which first led the group in Oregon to have serious doubts about the validity of the structure previously assigned to the kinamycins and which served as the impetus for the careful X-ray crystallographic work outlined above. In our laboratory the paper by Echavarren and co-workers appeared at a time when we had already constructed **190** and were ourselves questioning the structures assigned to the kinamycins. Whereas the Echavarren paper eventually led to enlightenment in the research group at Oregon, this same paper created considerable confusion in our own laboratory. The confusion arose as a consequence of the fact, that, although our group and that Echavarren had both reached the conclusion, through synthetic studies,

that the structures of the kinamycins were in error, the spectroscopic characteristics reported by the Echavarren group were *not only incompatible with those reported for the natural product but also incompatible with those recorded for our synthetic materials.* Since the structure of the synthetic product **190** prepared in our laboratory was based on sound spectroscopic analysis of all synthetic intermediates and on an unambiguous assignment of structure **178** by an X-ray crystallographic study, we eventually were led to conclude that the report of the synthesis of prekinamycin by Echavarren *et al.*[112] included misassignments of structures to the synthetic products. Presented below is an outline of the synthesis of prekinamycin as presented by Echavarren *et al.*[112] followed by a possible alternative interpretation which may explain the differences in the spectroscopic characteristics of the synthetic products of that study and of those prepared in the present project.

4.5 A Re-examination of the Echavarren Synthesis of Prekinamycin

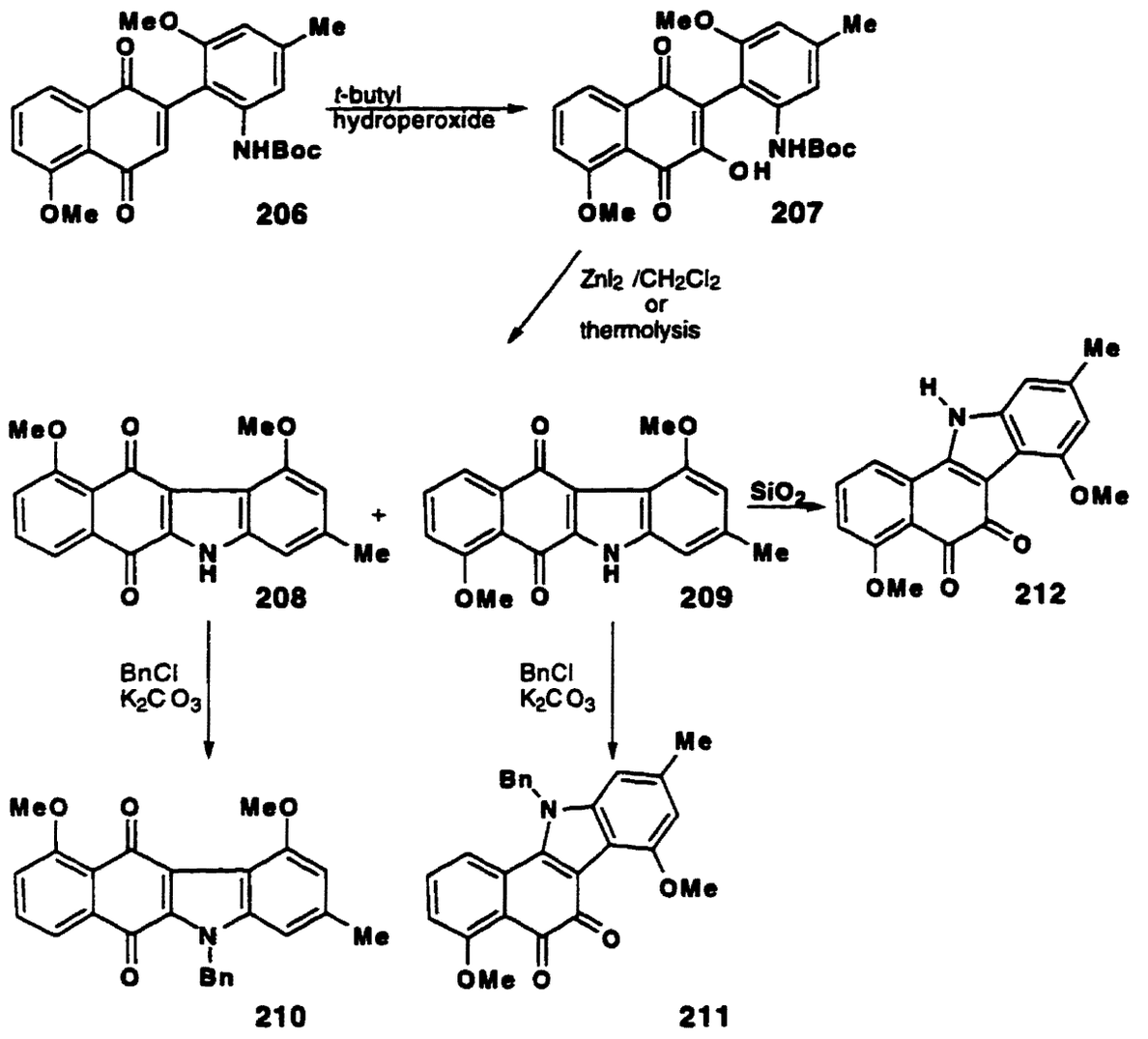
The key to the Echavarren synthesis was the coupling of a bromojuglone **204** and an aryl stannane **205** with $Pd(PPh_3)_4$ - CuBr in dioxane to give **206** in 65% yield (Scheme 99).



204 **205** **206**

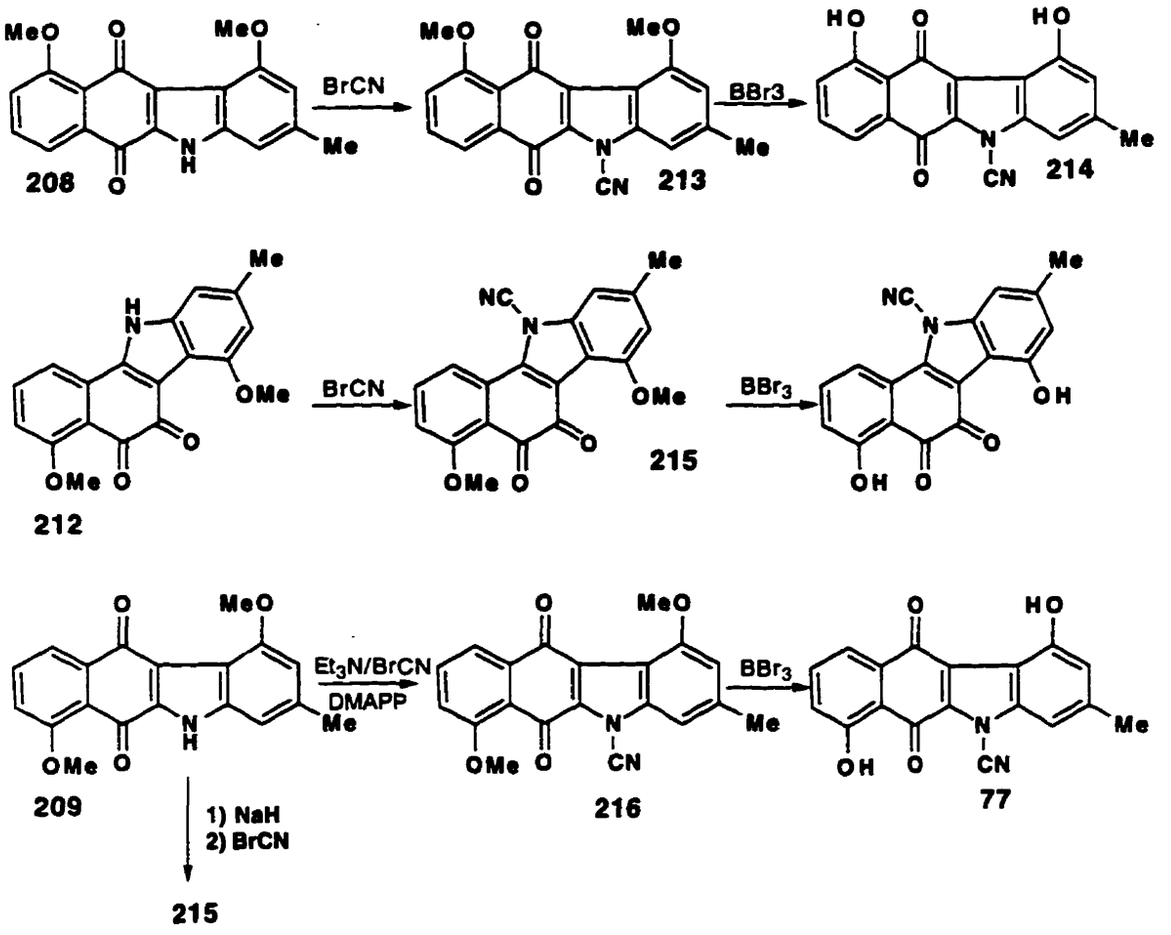
Scheme 99: The key to the Echavarren synthesis.

The quinone **206** was hydroxylated with *t*-butyl hydroperoxide (Scheme 100). Removal of the protecting group with ZnI_2 in methylene chloride was reported to result in cyclization to give **209** only as a minor product. The major product was reported to be **208** formed in a 6:1 ratio relative to **209** (Scheme 100). This remarkable, apparent rearrangement was also observed under purely thermolytic conditions to yield **208** and **209** in a 1:1 ratio. Benzylation of **208** with benzyl chloride and potassium carbonate was reported to give **210**. However, benzylation of **209** under the same conditions was reported to give **211** (Scheme 100). Furthermore, **209** was reported to undergo a similar rearrangement to the *o*-quinone **212** upon exposure to silica gel (Scheme 100).



Scheme 100

The amine **208** was reported to undergo smooth cyanation with cyanogen bromide and potassium carbonate in DMF to give **213** and the methyl ether protecting groups were removed to give **214** (Scheme 101). Cyanation of the ortho quinone **212**, under the same conditions, gave **215**. On the other hand cyanation of **209** proved to be quite problematic in that the reaction was very sluggish. Conversion to what was proposed to be **216** could be effected only in variable yields (30-76%) by sonicating a suspension of **209** in CH_2Cl_2 in the presence of Et_3N and DMAP. The use of NaH as a base was reported to give the N-cyano-*o*-quinone **215**.

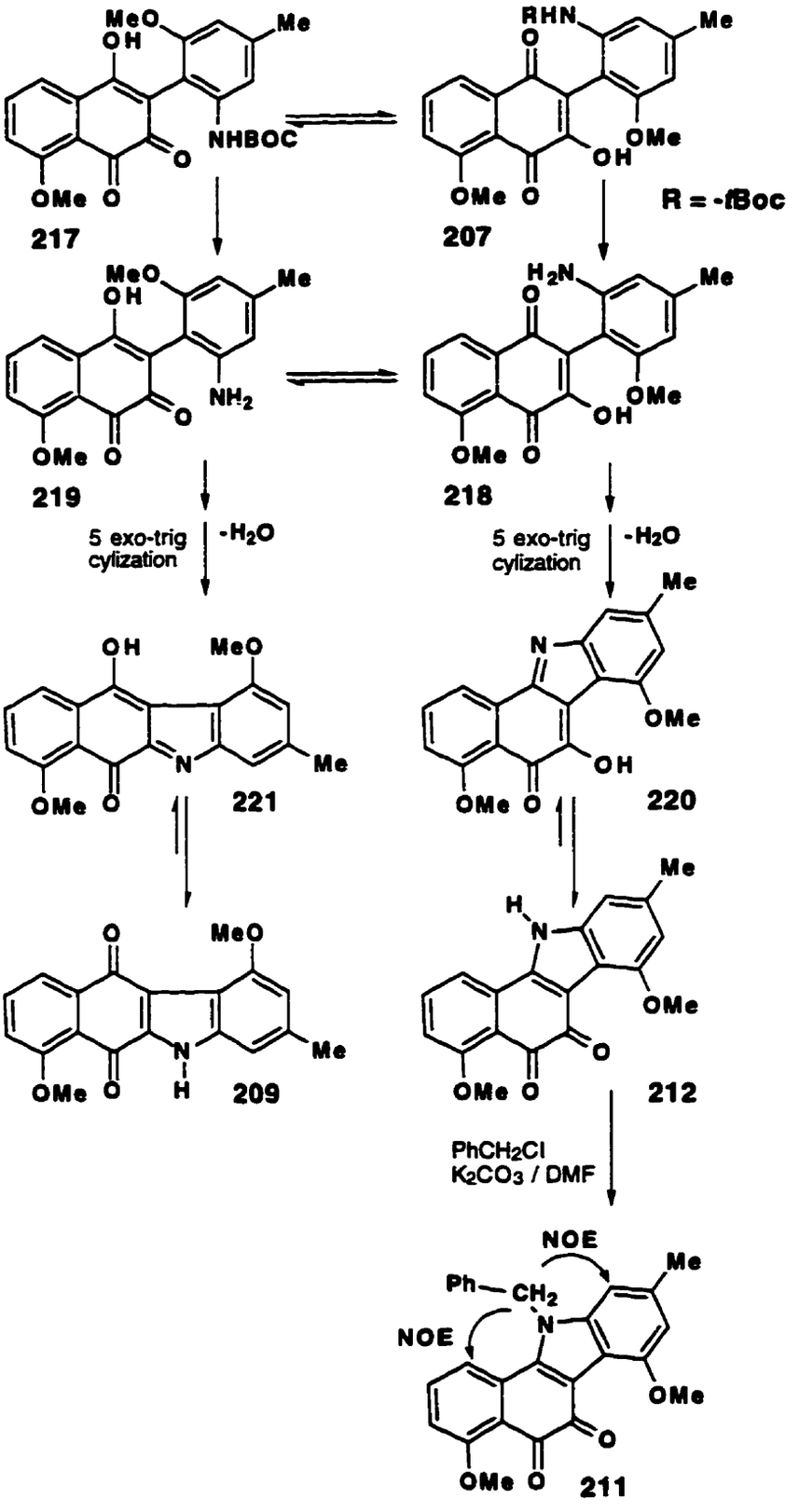


Scheme 101

Demethylation of **216** gave a product suggested by the authors to be **77**. However, the spectroscopic characteristics were substantially different from those reported for prekinamycin and, thus, Echavarren and co-workers decided that "the natural product identified as **77** has a different structure". This report was troubling to us in that the spectroscopic characteristics of the N-cyano carbazoles prepared by the Spanish group were substantially different from those observed in our laboratory. Most notably, the ^{13}C resonances assignable to the N-cyano carbon were reported to be in the 115-123 ppm range whereas those observed for N-cyanoindoles in this laboratory were in the range 104 to 109 ppm.

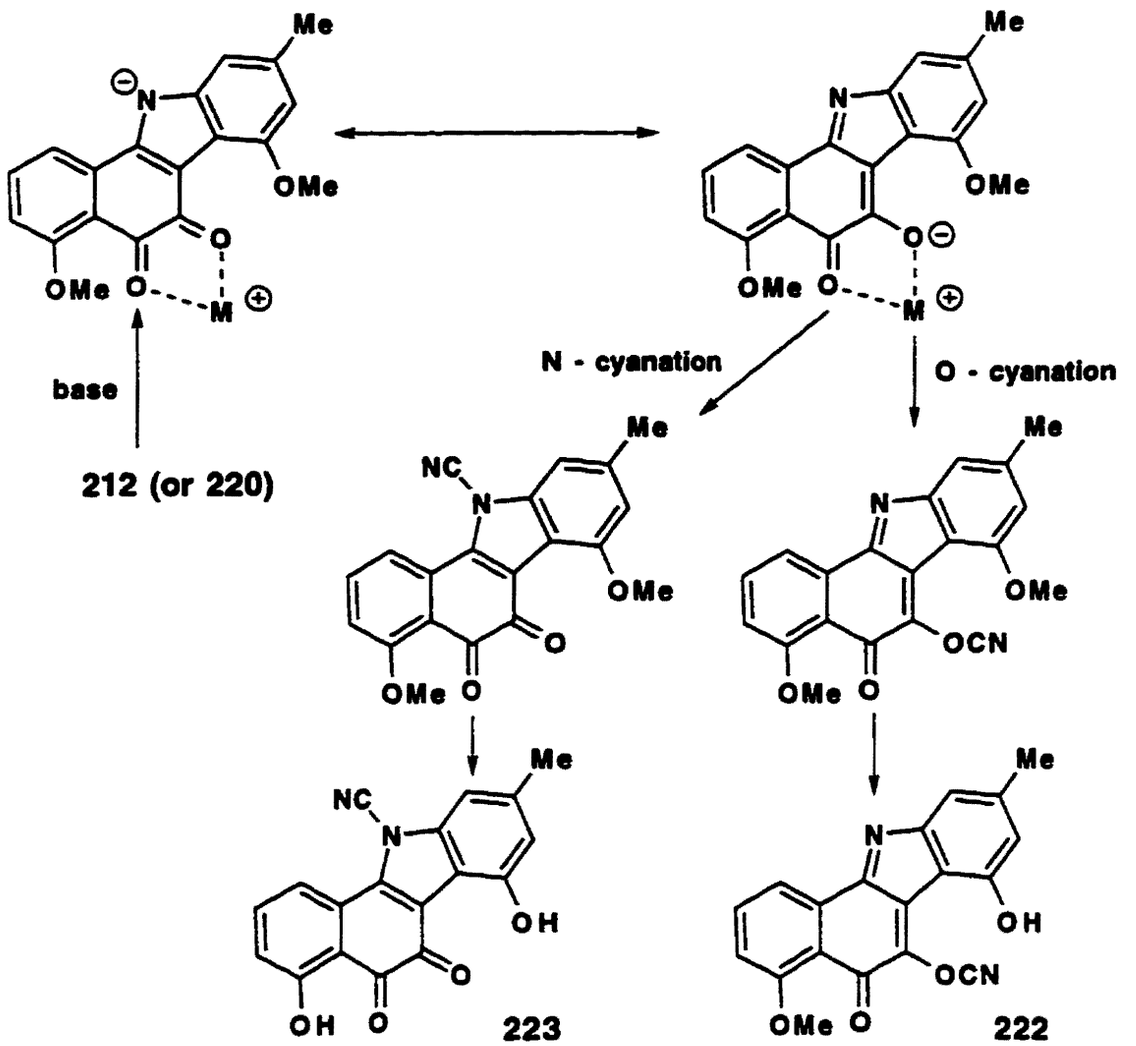
We were thus led to a reconsideration of the structural assignments made the Echavarren group. After some thought it is possible to reinterpret the experiments reported by Echavarren in such a way as to avoid the necessity to postulate the very unusual rearrangements apparently observed in that study and in such a way as to explain the discrepancies between the spectroscopic data reported by that group for N-cyanocarbazoles and data obtained for apparently very similar groups in this laboratory.

The alternative analysis is based on the recognition of the existence of two, *a priori* reasonable, cyclization modes for **207** which do not involve skeletal rearrangement. In particular, it was recognized that **207** could reasonably be expected to exist in equilibrium with an *o*-quinone tautomer **217** (Scheme 102). Deprotection of the N-*t*BOC protected amino group would yield **218** in equilibrium with **219**. Intramolecular cyclization involving the amino group and a carbonyl group of **218** would yield **220** whereas an analogous dehydrative cyclization of the *o*-quinone **219** would be expected to yield **221**. Both cyclizations are favourable 5-exo-trig processes. The product **221** would be expected to exist in equilibrium with **209** which has the same structure as was assigned previously to the minor component in the cyclization of **207**. In this reformulation **209** corresponds to the major product (**208** in Scheme 100). The minor product is now proposed to be **220** (**209** in Scheme 100). The observed isomerization of "**209**" to an *o*-quinone **212** in the presence of SiO_2 is now reformulated simply as tautomerization of **220** to **212**. The formation of an o-quinone product upon N-benzylation of the minor product, which required the postulation of an unusual rearrangement in the original interpretation, now arises quite naturally through N-benzylation of the anion generated by deprotonation of **220** or its tautomer **212**.


MeO
OH
Me
NHBOC
OMe O
O
217
RHN
Me
OMe
OH
OMe O
O
207
R = -fBoc
MeO
OH
Me
NH2
OMe O
O
219
H2N
Me
OMe
OH
OMe O
O
218
5 exo-trig cylization
-H2O
5 exo-trig cylization
-H2O
OH
MeO
N
Me
OMe O
221
Me
N
OMe
OH
OMe O
220
O
MeO
N
H
Me
OMe O
209
Me
H
N
OMe
O
OMe O
212
PhCH2Cl
K2CO3 / DMF
NOE
Ph—CH2
N
Me
NOE
OMe
O
OMe O
211

Scheme 102:

The interpretation of cyanation of the minor product "**209**", which was reported to give **216** (see Scheme 101), in variable yield, upon reaction with BrCN and Et_3N / DMAP in CH_2Cl_2, but, very mysteriously, the N-cyano-*o*-quinone **215** when NaH was used as base, also requires revision. In this alternative analysis, these results can be interpreted as a competition of N-cyanation and O-cyanation of the anion derived from **212** (or **220**) (Scheme 103). It is possible that under heterogeneous conditions the counter ion is tightly associated with the *o*-quinoid oxygen atom of the anion making the nitrogen atom more accessible for reaction with a electrophile whereas when NaH is used as base in a polar aprotic solvent the association of the anion with the cation is looser and reaction at oxygen predominates.



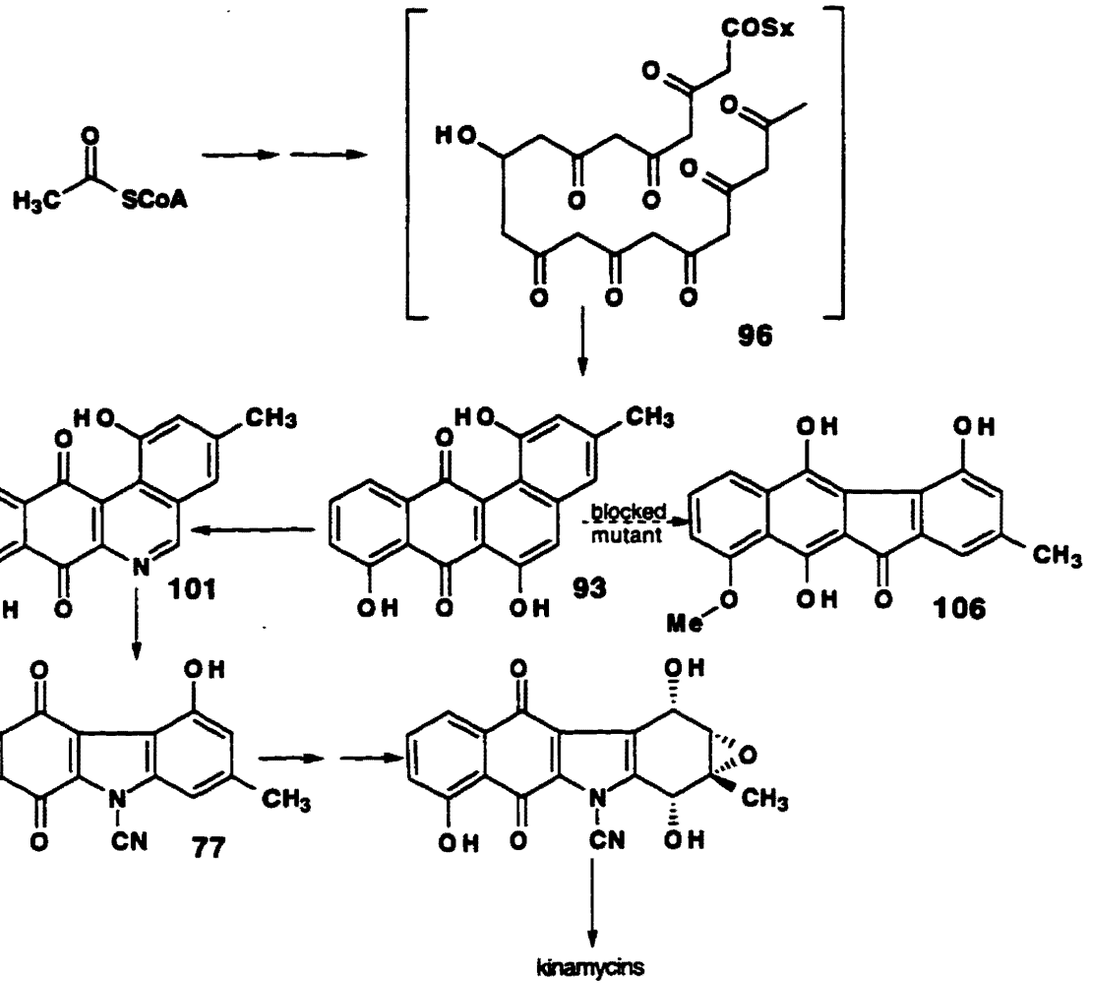
Scheme 103

Thus, it is possible to propose a chemically reasonable reinterpretation of the results reported by Echavarren and co-workers which may explain the discrepancy between the spectroscopic characteristics of synthetic products prepared in that laboratory and related compounds prepared in this laboratory. The compound prepared in the Spanish laboratory and proposed to possess the N-cyanobenzo[b]carbazole structure originally suggested for prekinamycin is very likely the *O*-cyano-*p*-iminoquinone **222**, explaining the discrepancy between the ^{13}C chemical shift of the cyano carbon in **222** and **190**.

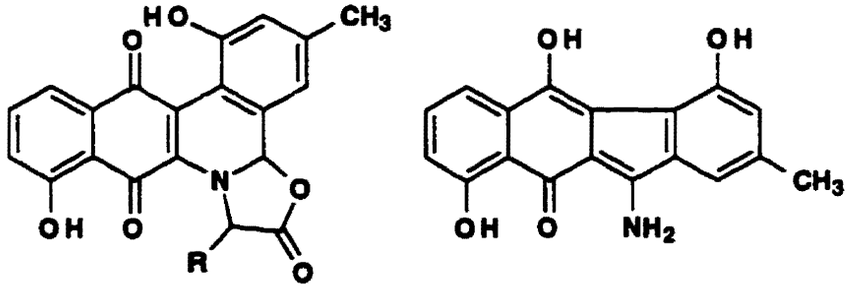
4.6 Significance of the Structural Revision of the Kinamycins to Currently Accepted Biogenetic Mechanisms

Extensive work by Gould and co-workers[61-65,67-70,93,110,113,114], prior to the structural revisions described above, had established that the kinamycins are acetate derived natural products likely arising via the polyketide intermediate **96** (Scheme 104). Dehydrorabelomycin (**93**) was shown through isotopic labeling experiments to be a key intermediate in the pathway to the kinamycins. The isolation of phenanthroviridine aglycone (**101**) from the same species led to the reasonable suggestion that it was also an intermediate in the formation of the N-cyanobenzo[b]carbazole ring system.

Structurally related to phenanthroviridine are the jadomycins isolated by Ayer and co-workers[115] from *Streptomyces venezuelae* (Figure 77). Research with a mutant bacterial strain blocked in kinamycin biosynthesis resulted in the isolation of kinafluorenone (**106**) which was assumed to be a shunt metabolite produced from dehydrorabelomycin (**93**). The stealthins[116] (**225**) represent yet another class of fluorene derivatives related to the kinafluorenones[70] (**106**) (Figure 77).



Scheme 104: The accepted biosynthetic pathway to the kinamycins.



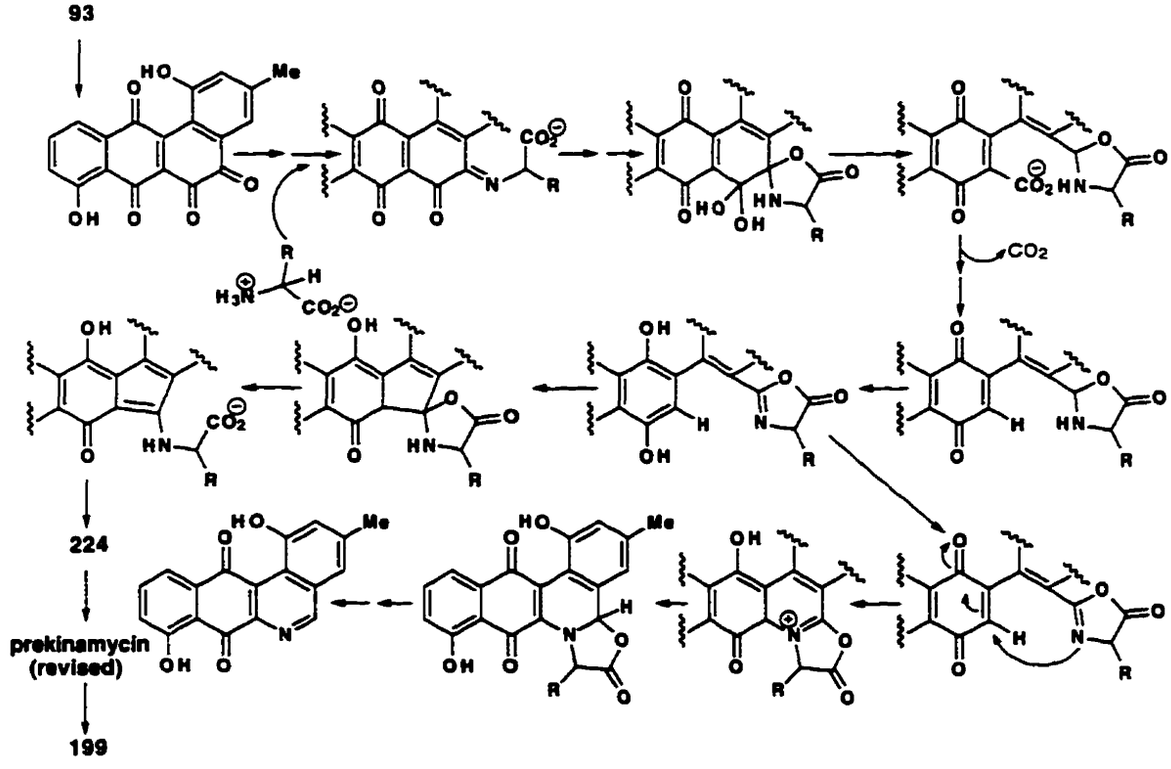
Jadomycin **224** Stealthins **225**

Figure 77

The recognition that the kinamycins are derivatives of diazofluorene and not of N-cyanocarbazole requires that the biosynthetic hypothesis be re-

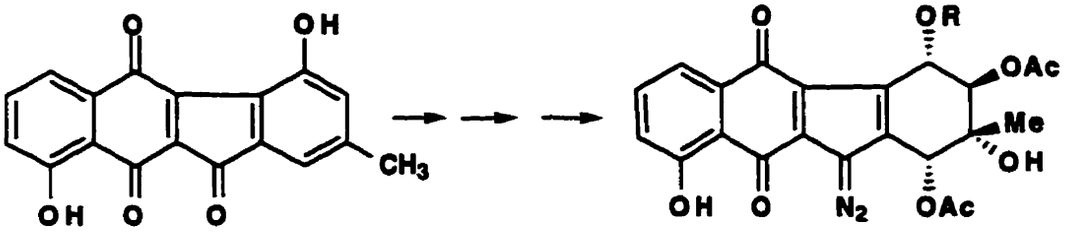
examined. In particular, the proposal that phenanthroviridine aglycone (**101**) is an intermediate in kinamycin biosynthesis is no longer chemically reasonable. In addition, the status of fluorenones such as kinafluorenone, which are considered shunt metabolites, requires some re-evaluation. That is, the likelihood that such compounds are true intermediates in the pathway to the kinamycins must be considered.

A modified biogenetic hypothesis which defines possible relationships of dehydrorabelomycin not only to kinamycins but also to the jadomycins, phenathroviridine aglycone, kinafluorenone and the stealthins is shown in Scheme 105. The validity of the proposals defined in Scheme 105 remains to be tested experimentally.



Scheme 105

More recent work by Gould and co-workers has revealed that the fluorenone, kinobscurinone (**226**) is an intermediate in the biosynthesis of kinamycin C and kinamycin D (Scheme 106).[93]



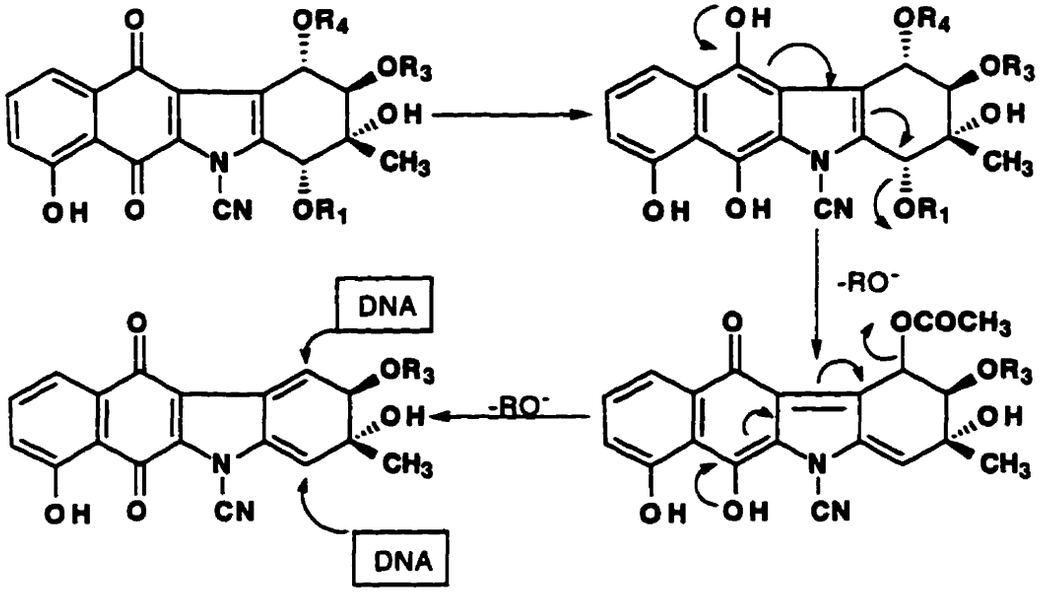
kinobscurinone **226**

Kinamycin	R
C	Ac
D	H

Scheme 106

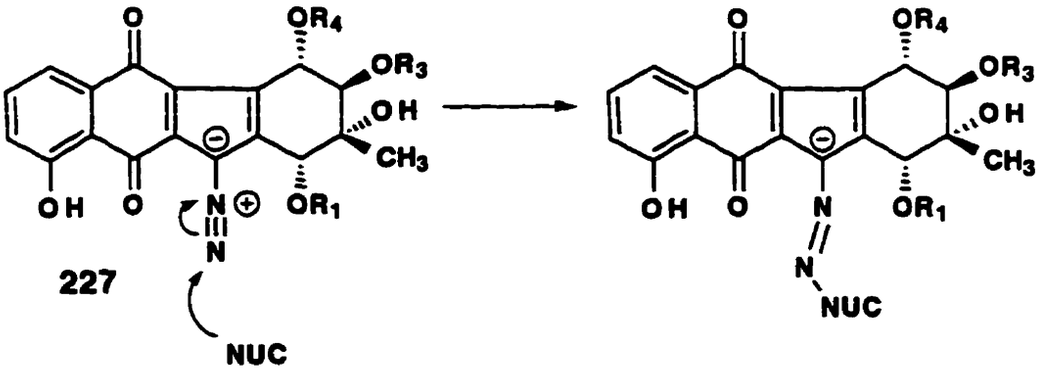
4.7 Significance of the Structural Revisions of the Kinamycins in Relation to the Proposed Mechanism of Biological Activity

Interest in this laboratory in the kinamycins as synthetic targets arose initially as a consequence of the possibility that these compounds might be bioreductively activated antitumour antibiotics related in mechanism of action to the mitomycins. This possibility which was first enunciated in print by Moore[10] who proposed that the kinamycins might effect DNA alkylation within the hypoxic environment of solid tumours is roughly shown in the scheme below (Scheme 107).



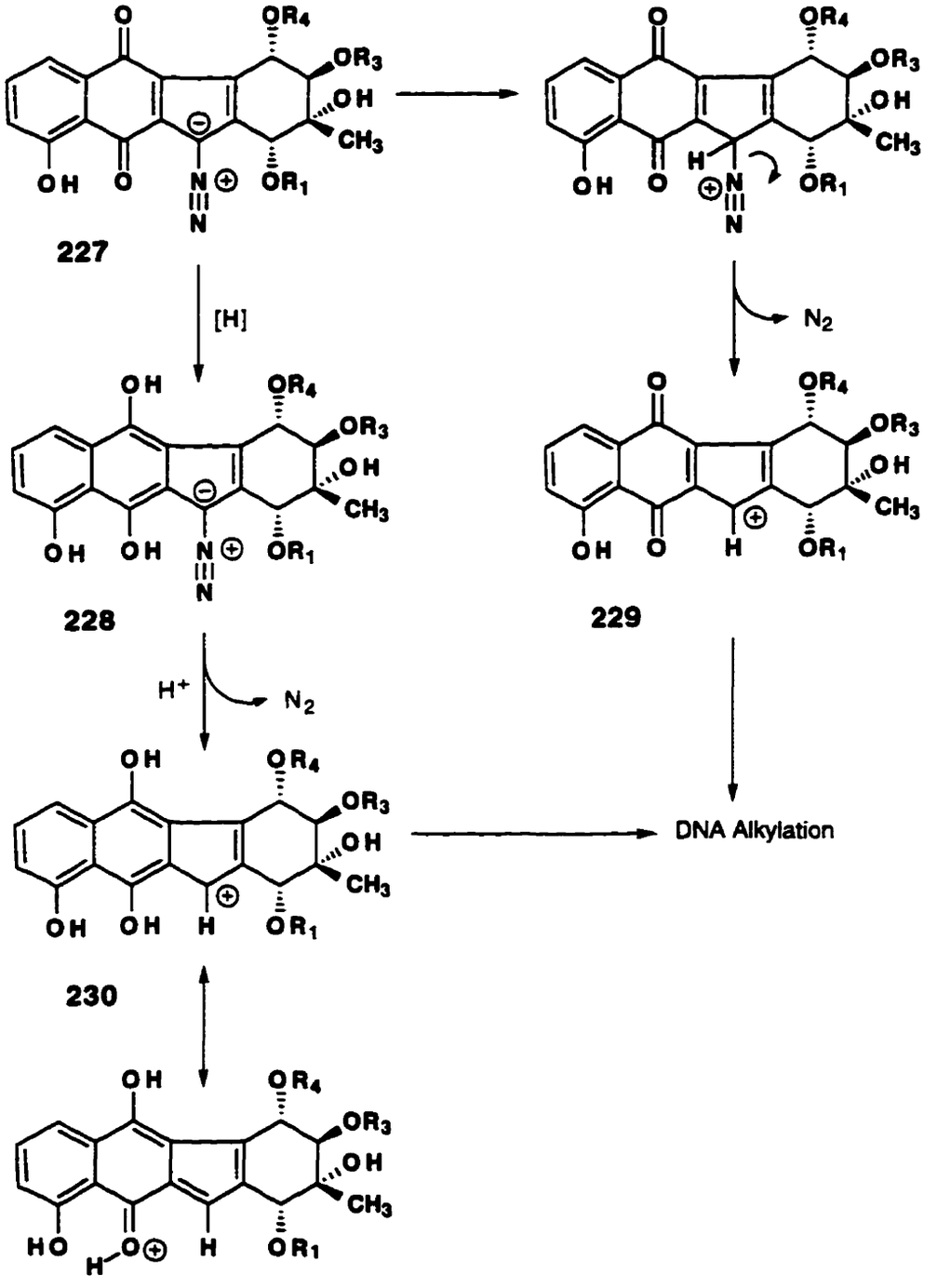
Scheme 107:

The recognition of the presence of a potentially reactive diazo group in the kinamycins suggests that alternative mechanisms of biological activity should be considered. The disclosure of the revised structure of the kinamycins by this laboratory[111] and by that of Gould and co-workers[110] has stimulated some experimental work to probe possible mechanisms for the biological activity of the kinamycins. Arya and Jebaratnam have recently reported that 9-diazofluorene and β-naphthylphenyl diazomethane can effect oxidative cleavage of DNA *in vitro* in the presence of cupric acetate, suggesting that analagous behaviour of the kinamycins *in vivo* should be considered as possible mechanisms for the observed antitumour and antibacterial activities.[117] It should be noted, however, that the kinamycins are more highly stabilized diazo compounds than are diazofluorene or diaryldiazomethanes. As a result, other possible mechanisms of action should be considered. For example, the diazonium ion-like character shown in **227** suggests that a nucleophilic attack perhaps by a suitable base in DNA, might occur as shown to initiate DNA modification (Scheme 108).



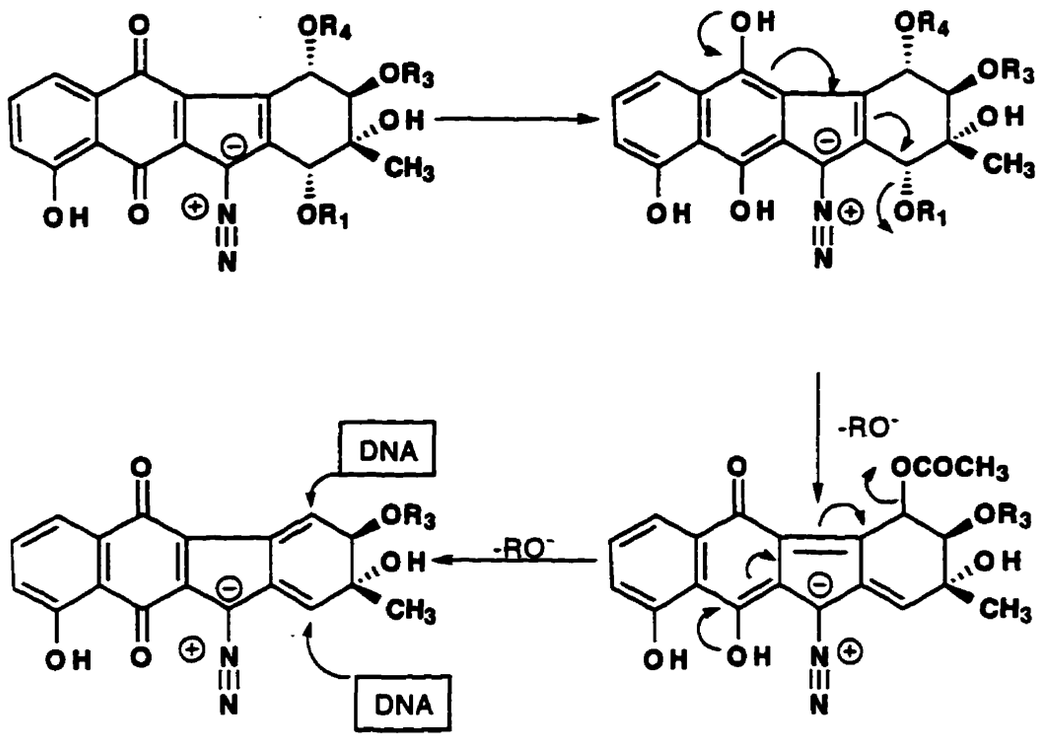
Scheme 108

Alternatively, protonation might lead to deazotization and formation of a reactive carbocation-type alkylating agent either from the hydroquinone form **228** produced by bioreduction or from **227** (Scheme 109). The carbocation **229** and **230** may possess some antiaromatic character resulting from their resemblance to the 4n π electron cyclopentadienyl cation system. However, in **230** resonance stabilization as shown might make the energetics for formation of the carbocations somewhat more favourable.



Scheme 109

It should also be noted that the diazofluorene structure for kinamycins is isoelectronic with the N-cyanocarbazole structure suggesting that a bioreductive activation/DNA alkylation pathway similar to that originally suggested by Moore[10], remains a viable hypothesis (Scheme 110).

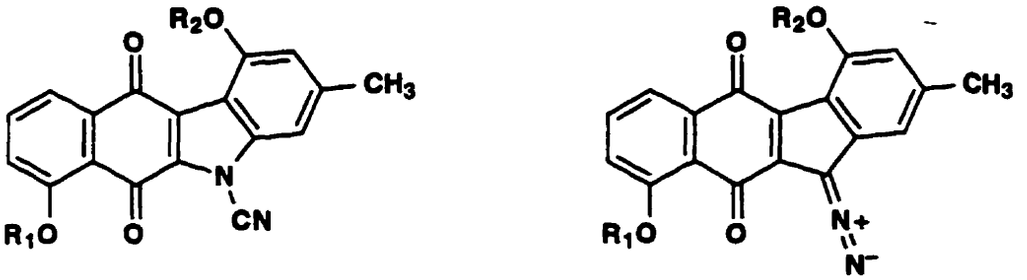


Scheme 110

Hopefully, the novelty of the revised structures of the kinamycins will attract sufficient attention to warrant further experimental exploration of the mechanism of biological activity of these unusual natural products.

Chapter 5: Synthetic Studies Toward the Revised Structure of Prekinamycin

In light of the structure revision of the kinamycins, attention was turned to developing methodology for the total synthesis of the revised structure of prekinamycin (Figure 78). It was felt that the present synthetic route toward **190** could not be adapted easily for the synthesis of **231** or **232**; hence, other strategies would have to be considered.

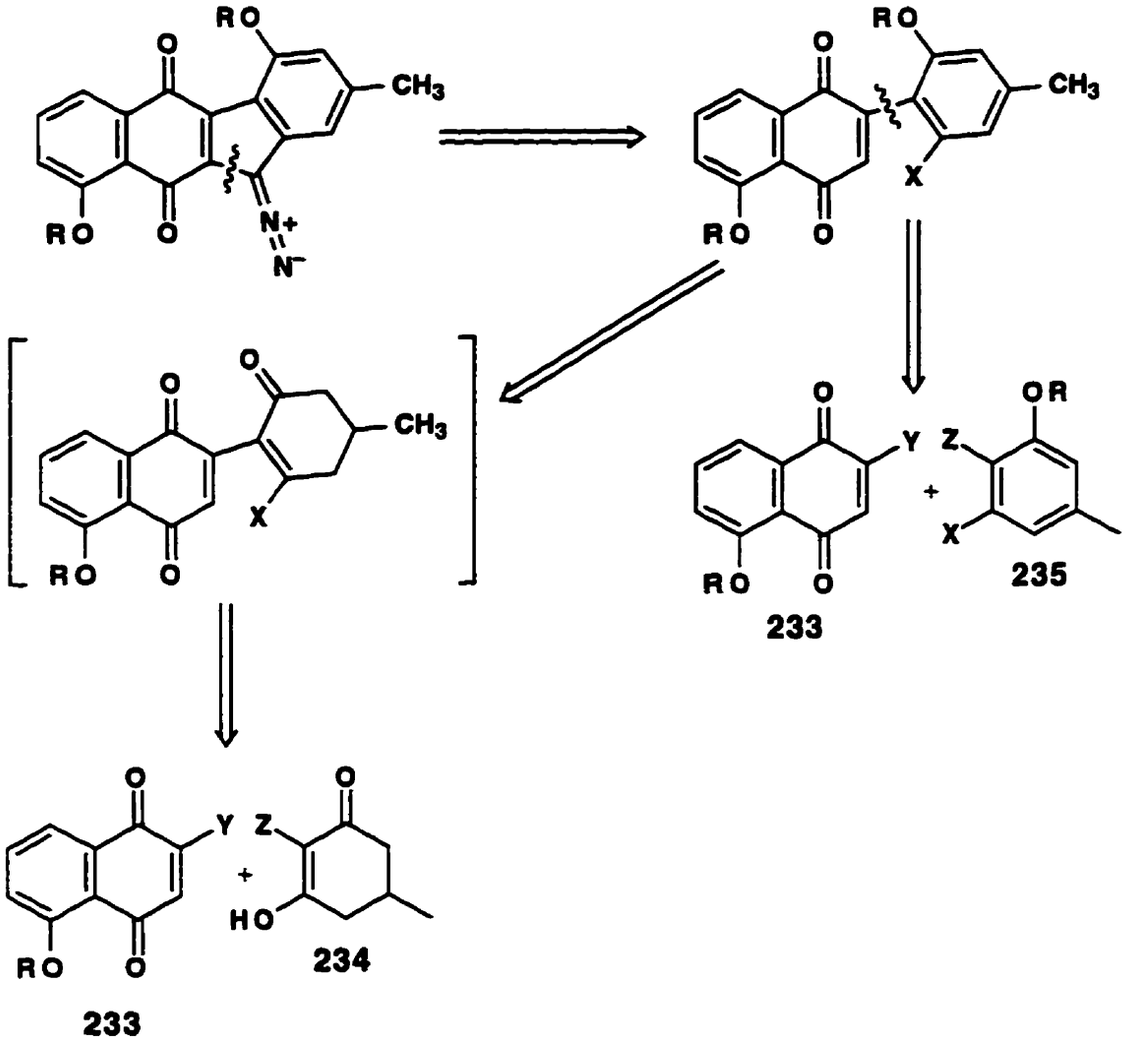


77 $R_1 = R_2 = H$
190 R_1 = Me, R_2 = Ac

231 $R_1 = R_2$ = Ac
232 R_1 = Me, R_2 = Ac

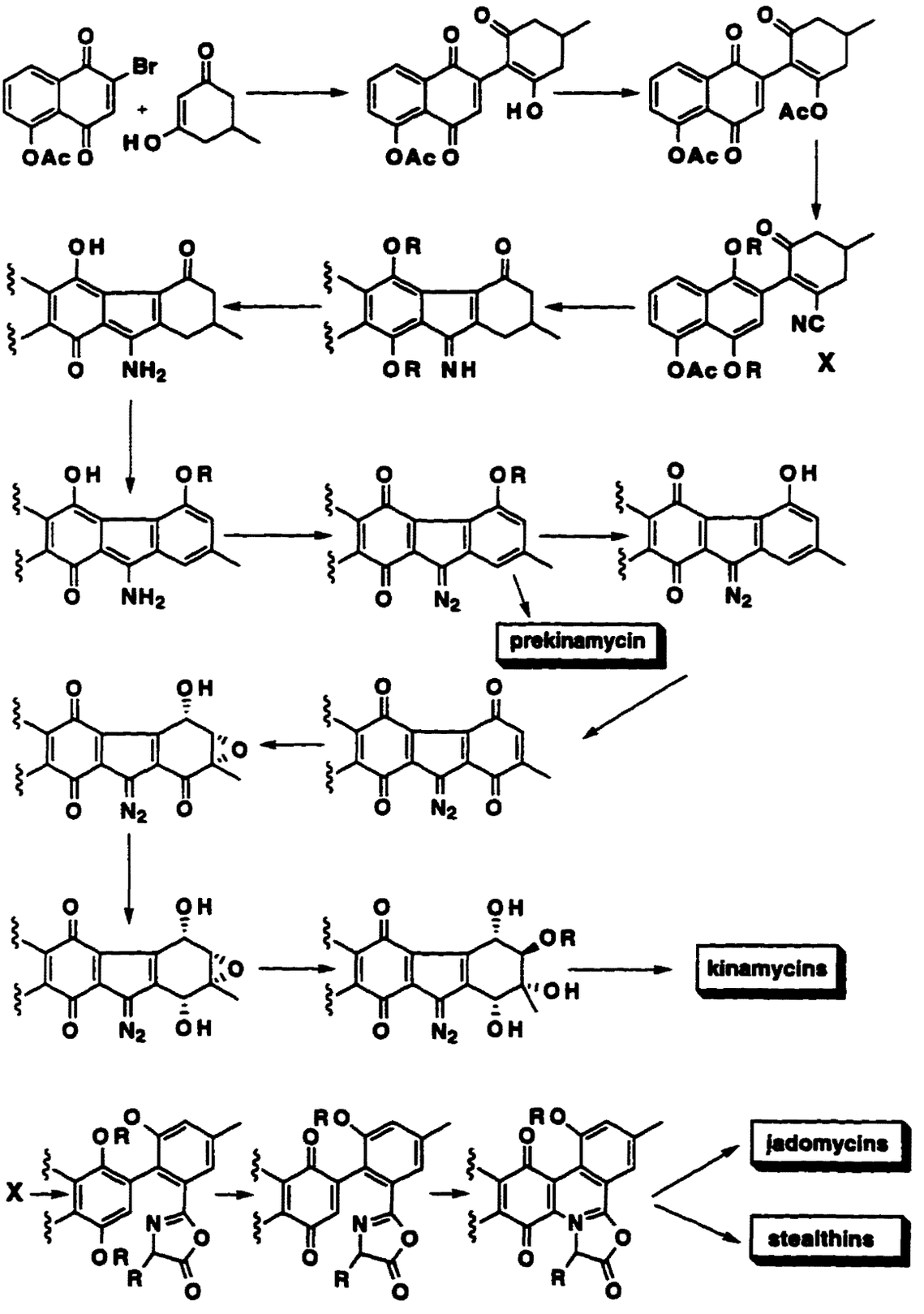
Figure 78

Our initial study in this area was based on the partial retrosynthetic analysis shown in Scheme 111. In this approach the tetracyclic framework was to be constructed by coupling an AB ring synthon **233** with a D-ring precursor **234** or **235** which might be in an aromatic or partially saturated form as shown. The C ring construction was to follow, perhaps by an electrophilic attack on ring B, in reduced hydroquinone form, by a suitably activated one carbon group X attached to the D ring component.



Scheme 111: One possible strategy to the revised structure of prekinamycin.

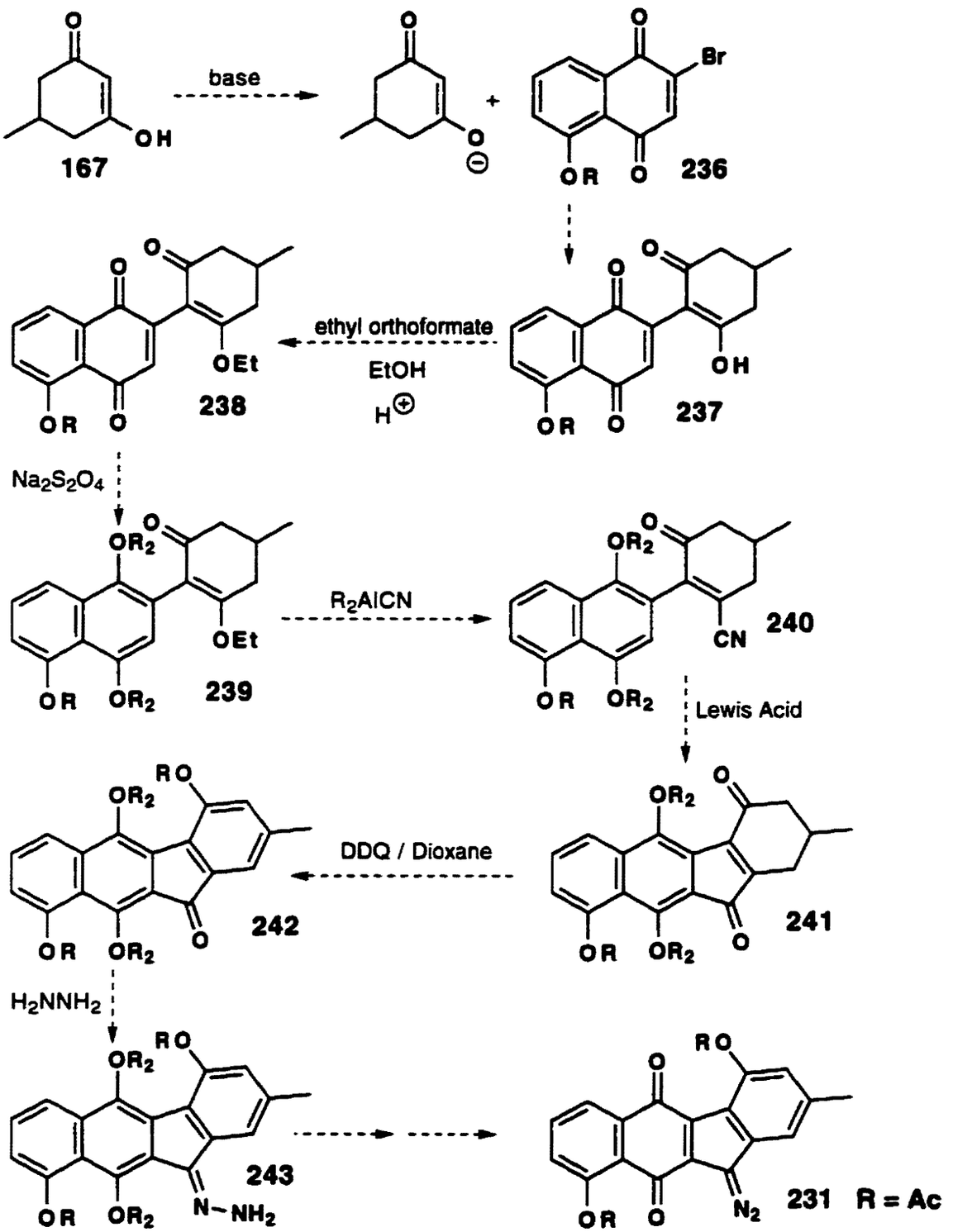
It was hoped that such an approach might be extended into a strategy to all of the natural products which are biosynthetically related to the kinamycins. An overview of this biogenetic inspired strategy is presented in Scheme 112 below.



Scheme 112

The focus of this study was on exploring the feasibility of this approach to the construction of the benzo[b]fluorenone ring system which might be constructed as shown in Scheme 113.

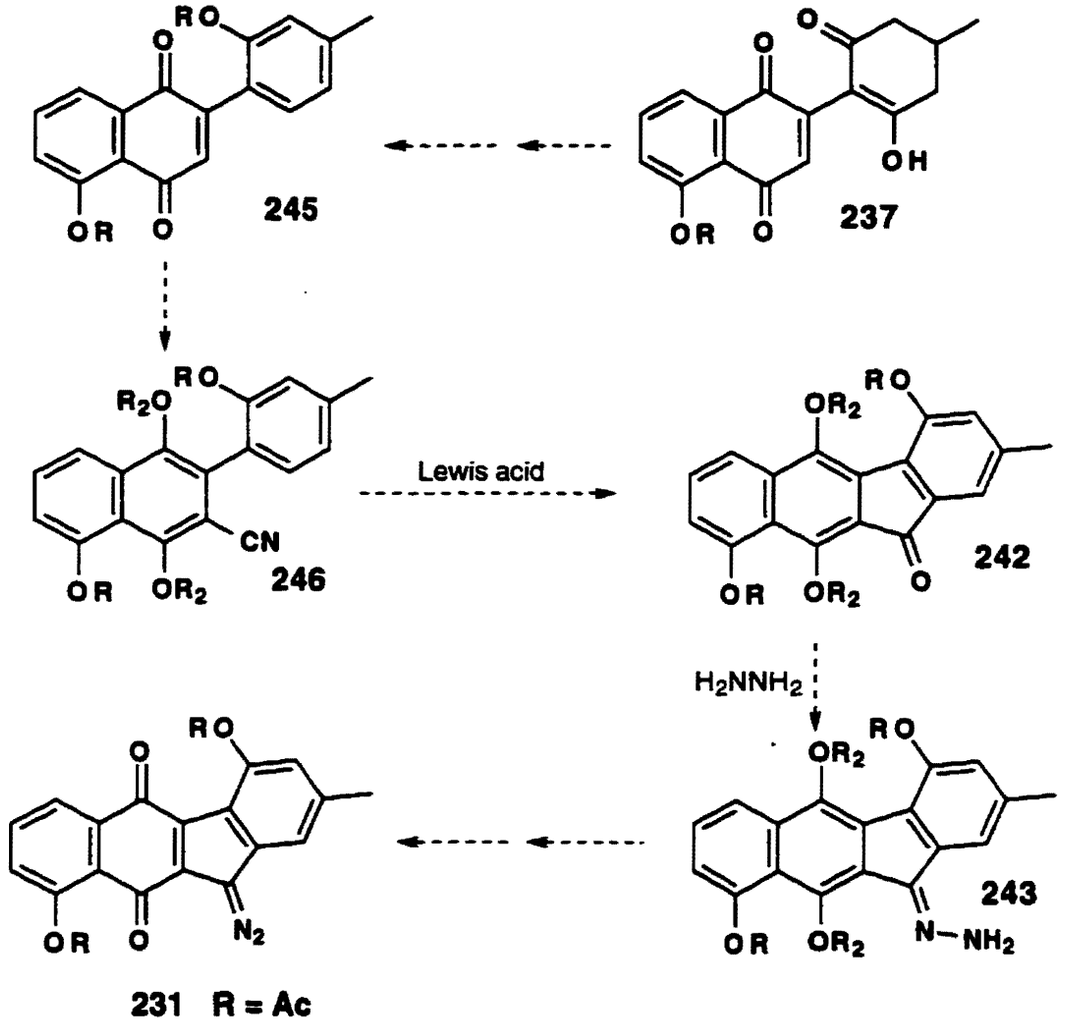
It was proposed that **167**, used in the synthesis of **190**, could serve as one of the starting materials in the synthesis of **231** (Scheme 113). Treatment of **167** with a base could potentially generate a nucleophile to react with the substituted naphthoquinone **236**, affording the adduct **237** expected to exist as the enol shown.[118-122] Systems such as these are easily converted to the enol ether by an acid catalyzed reaction with ethyl orthoformate in ethanol. Reduction of **238** with dithionite[42] followed by protection of the hydroquinone was expected to afford **239**. This reaction was to be followed by a hydrocyanation with diethylaluminum cyanide to give **240**.[123-125] Treatment of system **240** with a Lewis acid[124,126] to give the ketone **241** was to be followed by reaction with DDQ to afford the aromatized fluorenone **242**. Reaction of **242** with hydrazine followed by deprotection would yield the hydroquinone/hydrazone **243** (R_2 = H). Mild oxidation[101-103,127,128] of the hydroquinone to the quinone and of the hydrazone to the diazo group, in either a one or two step sequence, would give the prekinamycin ring system.



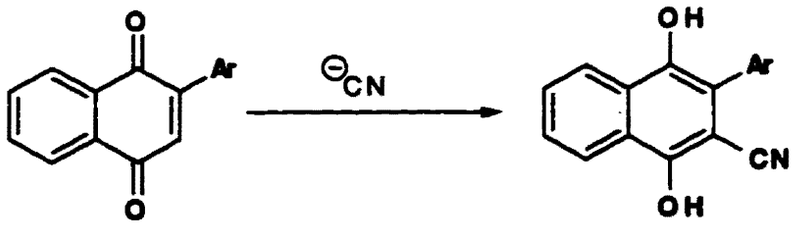
Scheme 113: One possible strategy toward 231.

Alternatively, the ketone **237** might be aromatized in the precursor to the D-ring (Scheme 114). Hydrocyanation of quinones such as **244** has been

shown to afford cyano-hydroquinones (Scheme 115).[129] Thus, cyanation of the quinone **245** should afford the cyanohydroquinone which could be protected to afford **246**. Lewis acid catalyzed cyclization would give **242** and functional group manipulation as described before in Scheme 113 would give the prekinamycin system.



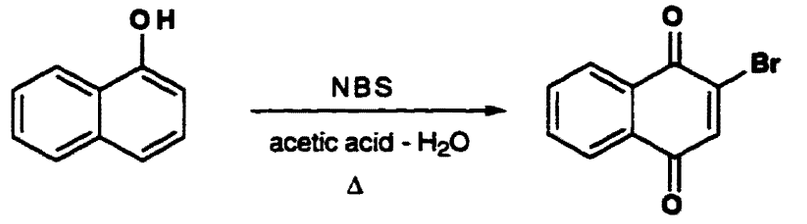
Scheme 114



244

Scheme 115

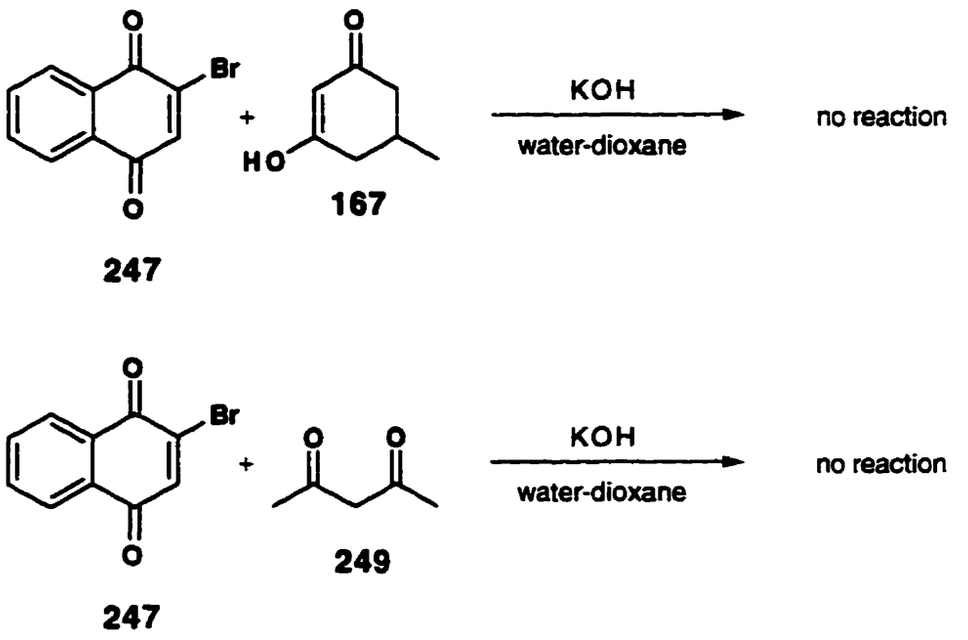
To this aim the model compound **247** was prepared by the method of Heinzman and Grunwell.[130] Reaction of α-naphthol **248** with NBS in acetic acid-water affords the naphthoquinone **247**. It was felt that this quinone would serve as a suitable model to explore the coupling reaction.



248 **247**

Scheme 116

However, the reaction of this bromonaphthoquinone **247** and **167** in potassium hydroxide in aqueous dioxane failed to yield the desired adduct (Scheme 117). Furthermore, the naphthoquinone **247** also failed to react with the diketone **249** under the same conditions (Scheme 117).

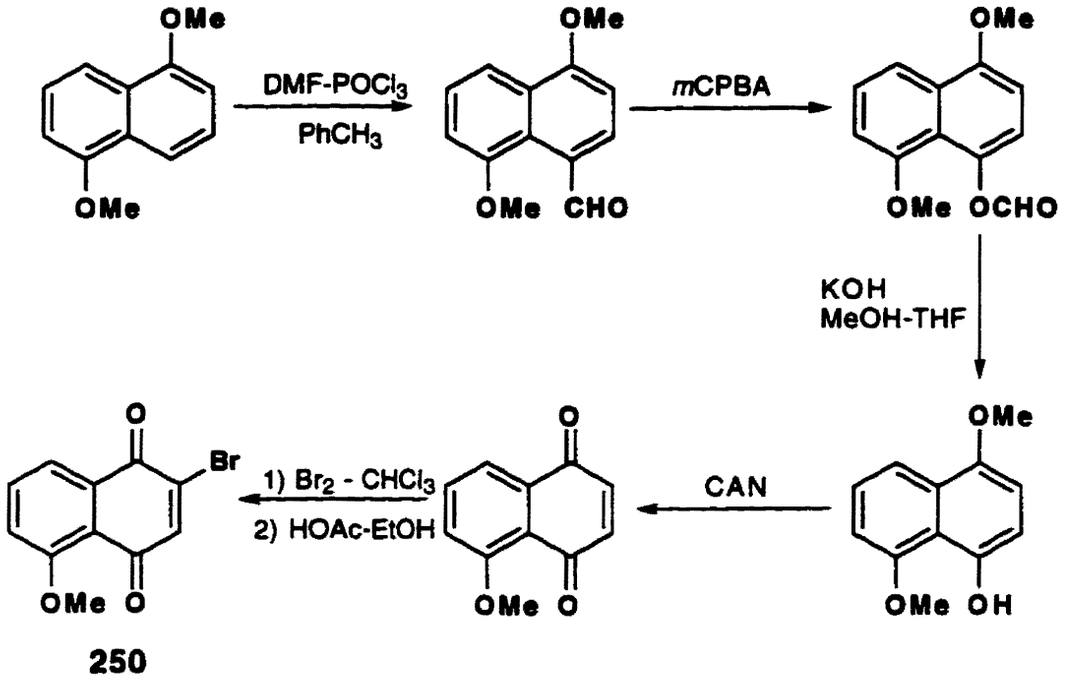


Scheme 117

The reaction of the naphthoquinone and the dione was repeated on a very small scale in methylene chloride utilizing triethylamine as the base. The TLC and the ^{1}H NMR spectrum indicated the presence of a mixture of products; however, the proton NMR spectrum did show signals that correponded to a compound incorporating the naphthoquinone and the dione components. On the strength of this, it was felt that further exploration of this chemistry with the more highly substituted system required in the synthesis of **231** would be more desirable. A number of approaches to the desired C-2 halogenated, C-5 oxygenated naphthoquinone have been reported in the literature.[131,132]

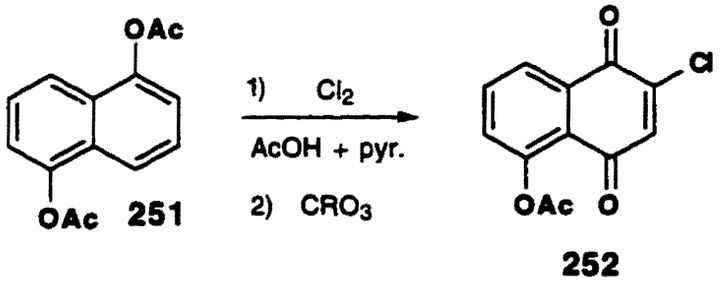
One synthesis of **250** utilizes 1,5-dimethoxynaphthalene as the starting material, yielding the desired bromonaphthoquinone in five steps (Scheme 118).[133] Thomson[132] began with diacetoxy-naphthalene **251** which was chlorinated with molecular chlorine and oxidized with chromium trioxide to afford the chlorosubstituted system **252** (Scheme 119). A more appealing method by Heinzman and Grunwell[130] begins with the readily available dihydroxy naphthalene **253** (Scheme 120). The dihydroxy compound is

protected as the diacetate and reacted with NBS in aqueous acetic acid to afford the desired system **254**.



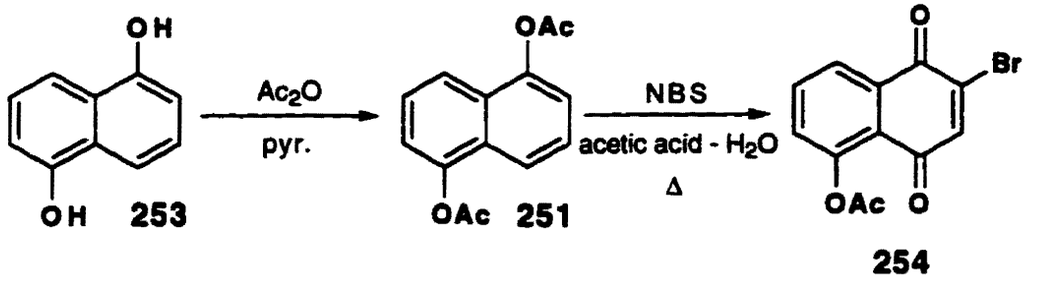
250

Scheme 118: Synthesis of 250 in five steps from 1,5-dimethoxy-naphthalene.



252

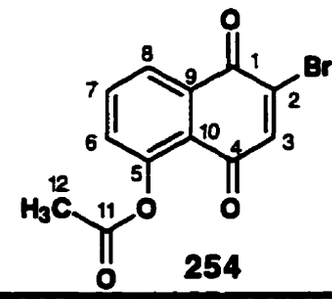
Scheme 119



254

Scheme 120

Following the published procedure a product presumed to be the desired system **254** was obtained in 90% yield as a yellow-green solid. The system assigned as **254** was found to be unexpectedly unreactive under a variety of conditions. Furthermore, synthesis of a second batch yielded material which was spectroscopically different from material obtained in the first batch. Qualitatively the spectra of the two batches appeared to be correct (that is, appeared to have the correct number of protons). The material from the second batch was produced at higher temperatures (10-15°C) with a slightly higher proportion of water and with a longer reaction time. The signals in the ^{13}C NMR spectrum for material isolated from both batches as well as the data published by Heinzman and Grunwell[130] is shown in Figure 79. The ^{13}C assignments made by Heinzman and Grunwell were based on assignments originally made by Kobayashi *et al.*[134]



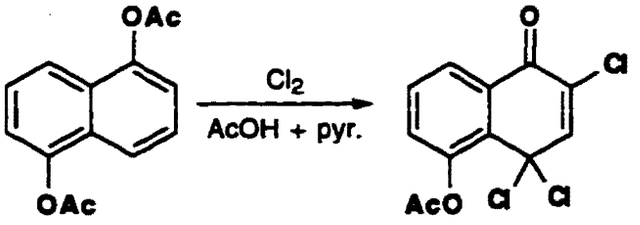
254

Carbon Assign.	Published† ^{13}C signals	batch 1 ^{13}C Signals	batch 2 ^{13}C Signals
4	180.9	-	180.8
1	177.5	174.9	-
11	169.2	167.9	169.2
5	149.9	148.6	149.8
3	141.5	134	141.3
2	138.5	130.9	138.4
7	134.9	129.9	134.9
9	132.7	126.7	132.5
6	130.4	124.9	130.2
8	126.4	119.9	126.3
10	123.3	41.7	123.2
12	20.99	21.6	20.96

†results published by Heinzman and Grunwell [130]

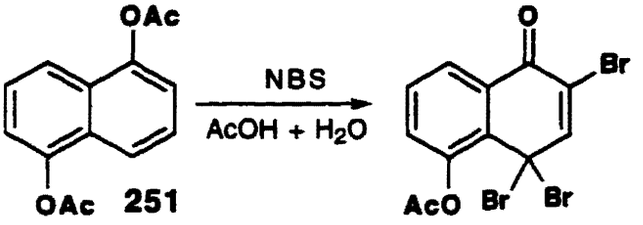
Figure 79: ^{13}C NMR data published[130,134] for 254 as well as ^{13}C data for bromination products obtained in this study.

Material obtained from the second batch correlates well with the published results, whereas material obtained from the first batch shows significant differences. It was found that material from the first batch could be converted to **254** by refluxing in acetic acid/water for a short while. An examination of the literature in this area revealed that Thomson[132] had obtained the trichloro compound **255** when 1,5-diacetoxynaphthalene was treated with chlorine in acetic acid and pyridine (Scheme 121). It seemed possible that material from the first batch was **256** the bromo analog of **255** (Scheme 122).



255

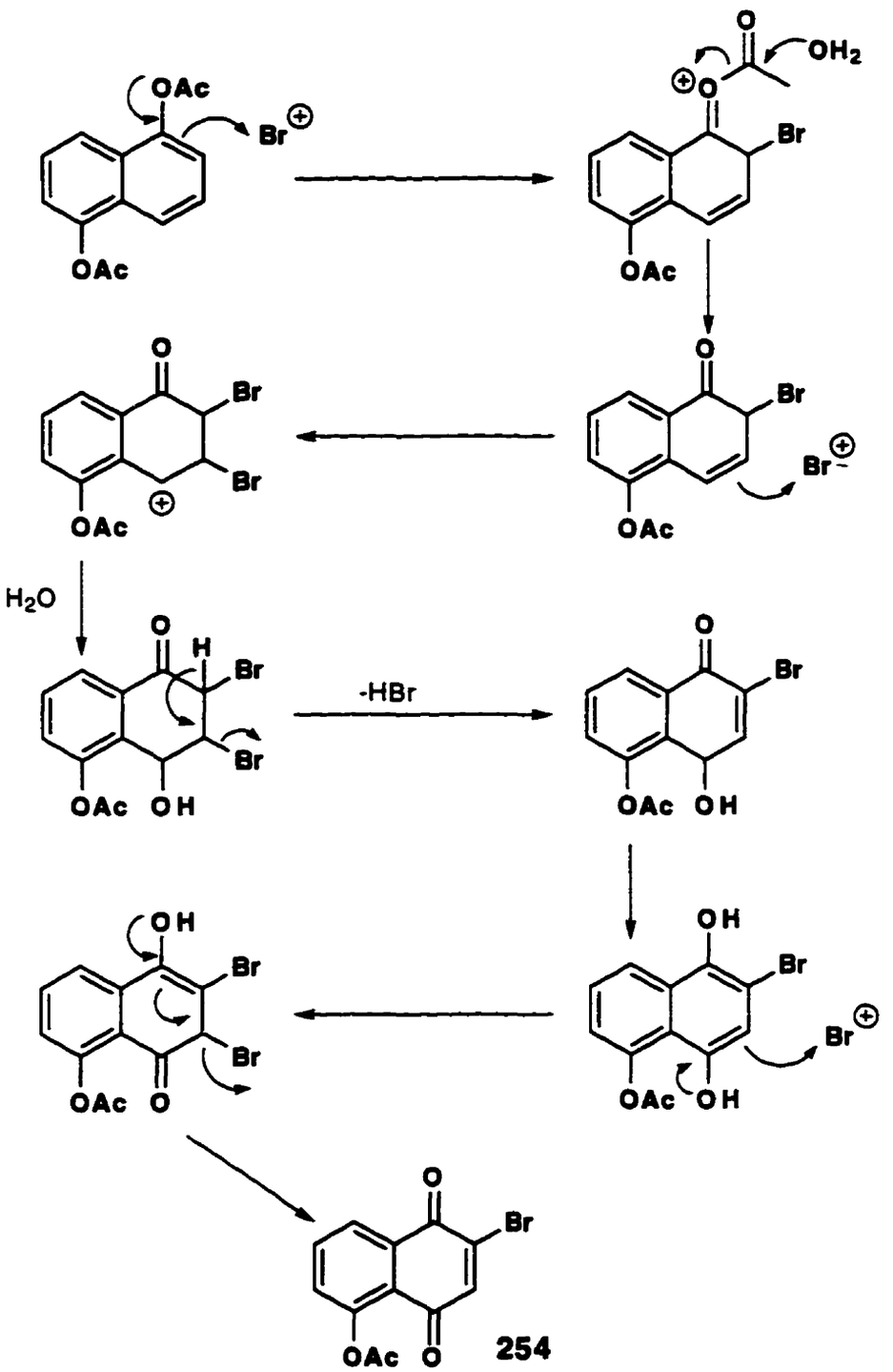
Scheme 121



251 **256**

Scheme 122

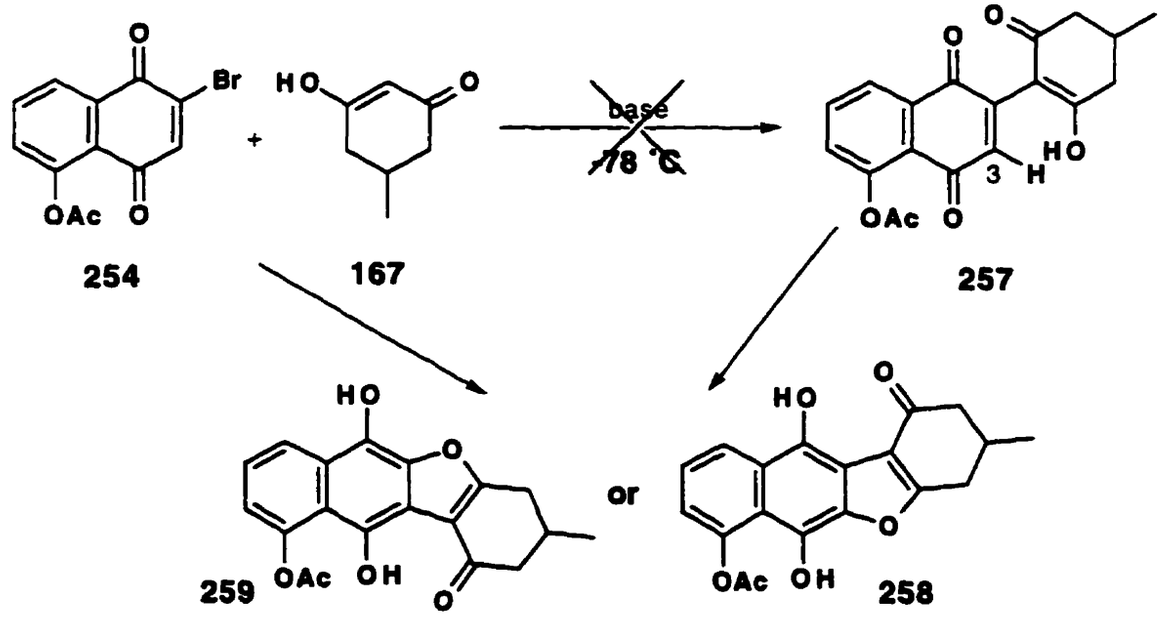
Extension of reaction times and temperatures resulted in the isolation of **254** which suggests that **256** may be a stable intermediate in the reaction. However, the mechanism proposed by Heinzman *et al.* [130] for the transformation of **251** to **254** does not show such an intermediate (Scheme 123).[130] It is also possible that, under the proper conditions, **256** is formed instead of **254** by another pathway which is not in operation in the presence of a greater proportion of water and at higher temperatures. In any event, it is clear that mechanism of the formation of **254** and for that matter **256** needs to be investigated further.



Scheme 123: The mechanism proposed for the formation of 254.[130]

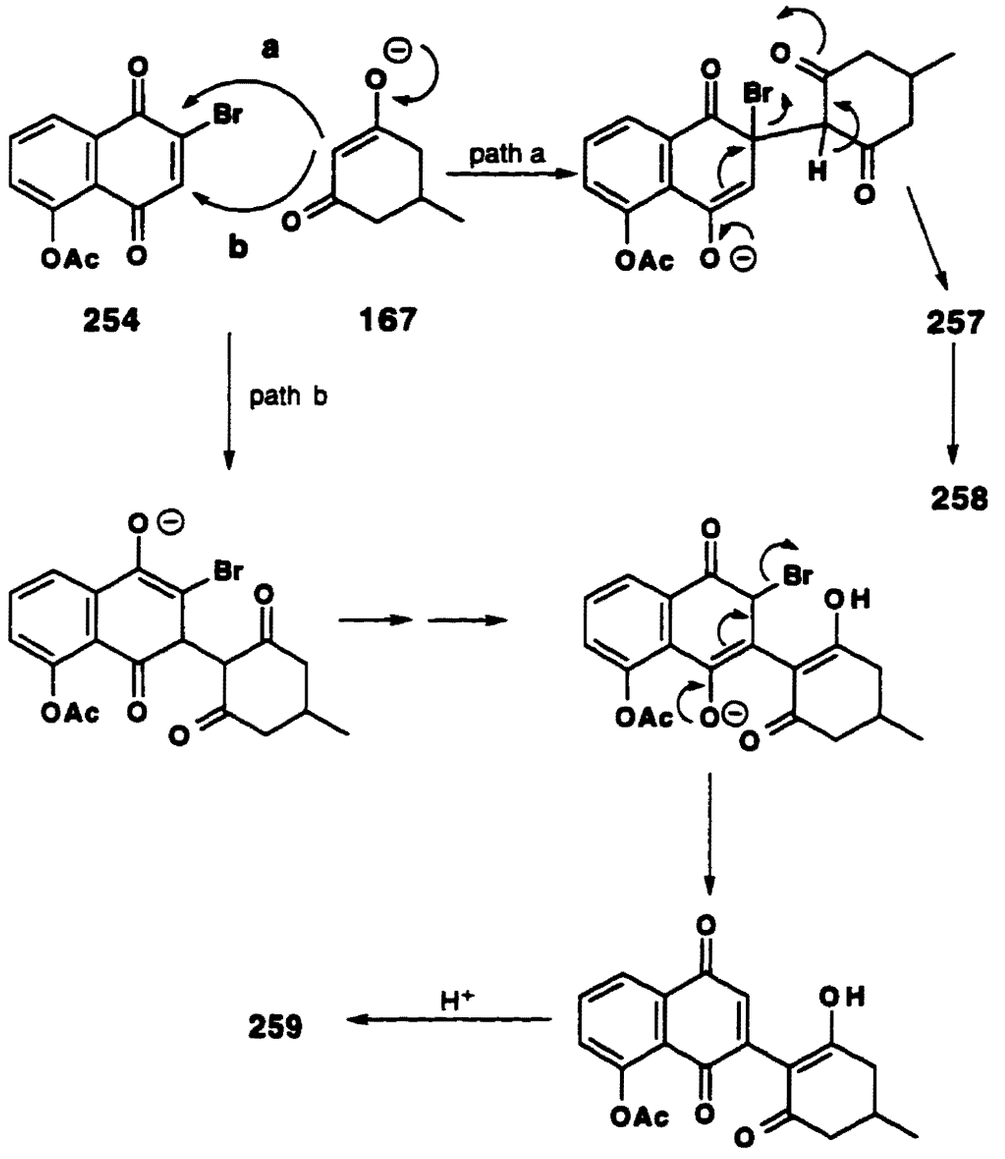
Reaction of **254** with **167** at -78°C utilizing diisopropylethylamine as the base yielded a mixture of products as indicated by TLC analysis. Isolation of the products from the reaction medium proved to be difficult. Quenching of the

reaction mixture with water followed by extraction with organic solvents led to the formation of dye-like materials. These products were extremely difficult to extract from the aqueous layer. The extent of the colour of the aqueous layer varied with repetition and with the addition of acid. The addition of acid was found to be necessary for extraction into the organic layer. The extent to which the products were extracted into the organic layer varied with the acid concentration. Also, the colour of the extract varied with exposure to air. The major product which was eventually isolated appeared to be an addition product, although lacking a signal assignable to vinyl hydrogen at C3 in the ^{1}H NMR spectrum (Scheme 124). Both the naphthoquinone and dione components appeared to be present in the isolated compound. The M^+ ion found for the major component was 340 which does support **257** or either one of **258** or **259** but the lack of a signal assignable to the C(3)-H in the ^{1}H NMR spectrum is incompatible with structure **257** and compatible with either **258** or **259**.



Scheme 124: Reaction of 254 with 167 utilizing diisopropylethylamine as the base at -78 °C.

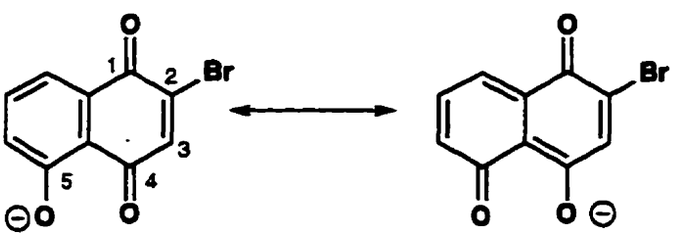
Since **258** was not isolated unless the aqueous phase was acidified, it is possible that **257** was formed to some extent but cyclized to **258** upon acidification. An alternative structure **259** is also compatible with the available spectroscopic data and might arise via an alternative pathway b (Scheme 125).



Scheme 125

Michael addition via path a is normally favoured for such bromonaphthoquinones. Examples of path b type addition-elimination have been reported for compounds in which the aromatic ring bears a hydroxyl group

at C-5 expected to be ionized under basic conditions (Scheme 126).[135] Resonance of the type shown deactivates the system with respect to nucleophilic attack at C-2 resulting in competing attack at C-3.

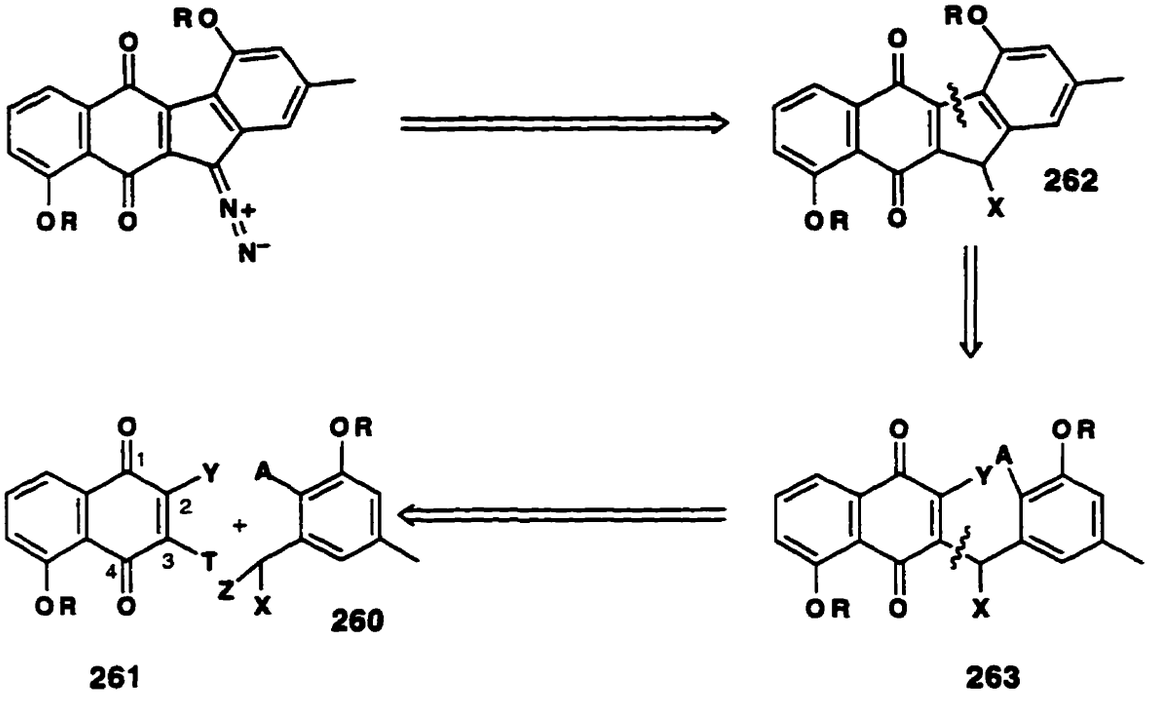


Scheme 126

The difficulty in isolation of products may be due in part to the acidity of the enolic OH in **257** which may readily ionize increasing the water solubility of **257** and creating the possibility for air oxidation of the resultant anion. These difficulties were sufficiently frustrating and other potential strategies were sufficiently attractive that this approach to the kinamycin ring system was abandoned in the present study. If future work is to be pursued along these lines some strategy for trapping the enolate from **257** in organic soluble and air insensitive form (e.g. as the O-silyl enol ether) will have to be devised. The product distribution was unaffected by alterations in the reaction conditions such as utilizing diisopropylethylamine at room temperature, triethylamine at -78°C or at room temperature or using ethanol or dioxane instead of methylene chloride.

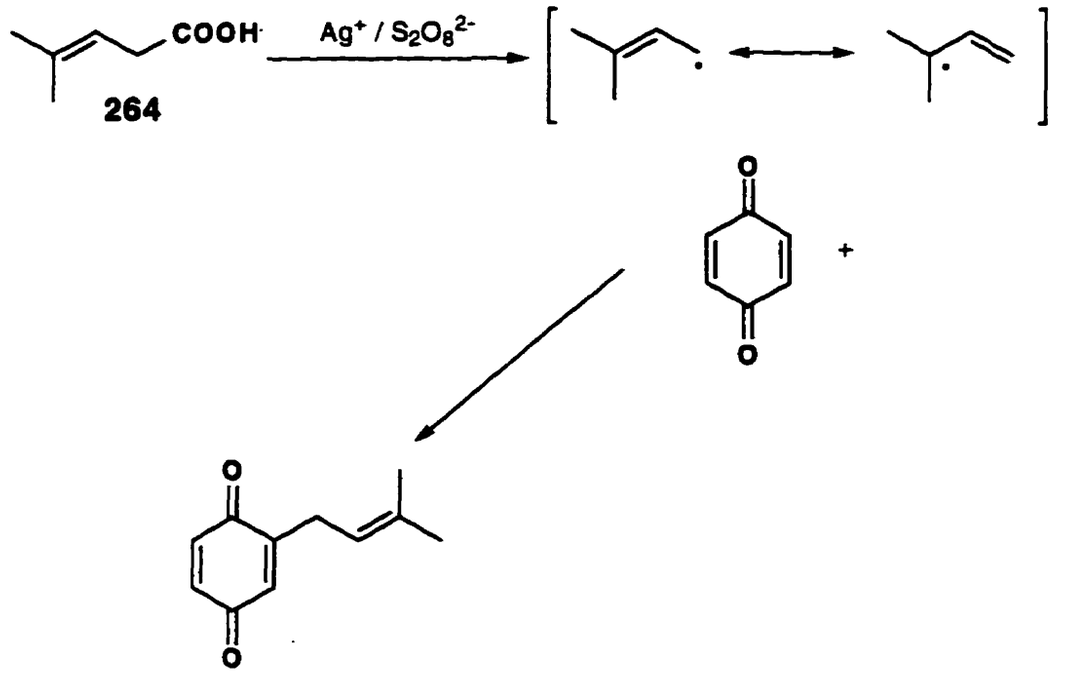
An alternative approach to construction of the kinamycin ABCD ring system which can also make use of the 2-bromojuglone system as an AB ring synthon is illustrated in retrosynthetic fashion in Scheme 127. In this strategy the D ring synthon **260** possesses all of the carbon atoms necessary for construction of the complete CD rings onto the AB ring precursor **261**. The prekinamycin precursor **262** might be constructed from a precursor such as

263 so that the aryl-quinone ring bond linking the B and D rings would be the last bond formed in constructing the tetracyclic carbon skeleton. The precursor **263** in turn is viewed as a molecule constructed by coupling the exocyclic carbon of the D-ring precursor **260** to C-3 of the naphthoquinone system **261**.



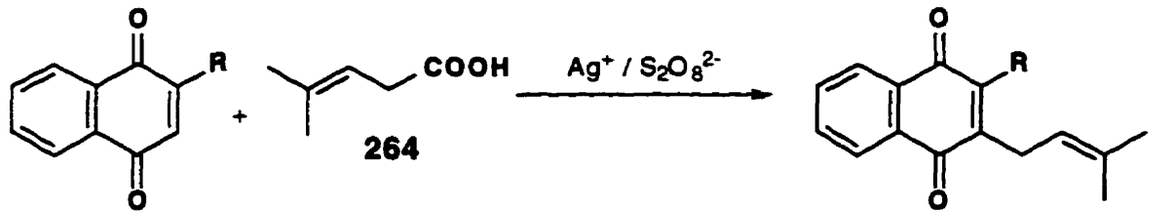
Scheme 127: An alternative strategy to Scheme 111.

Free radical chemistry suitable for effecting such a coupling has been described in the literature. Work by Jacobsen and Torssell[136,137] has shown that acids can be coupled with quinones in moderate to good yields. Oxidative decarboxylation of a carboxylic acid with silver ions and persulfate generates free radicals which couple with substituted quinones (Scheme 128). One example is the attachment of an isoprenyl group to a benzoquinone system through the oxidative decarboxylation of the acid **264** (Scheme 128).



Scheme 128

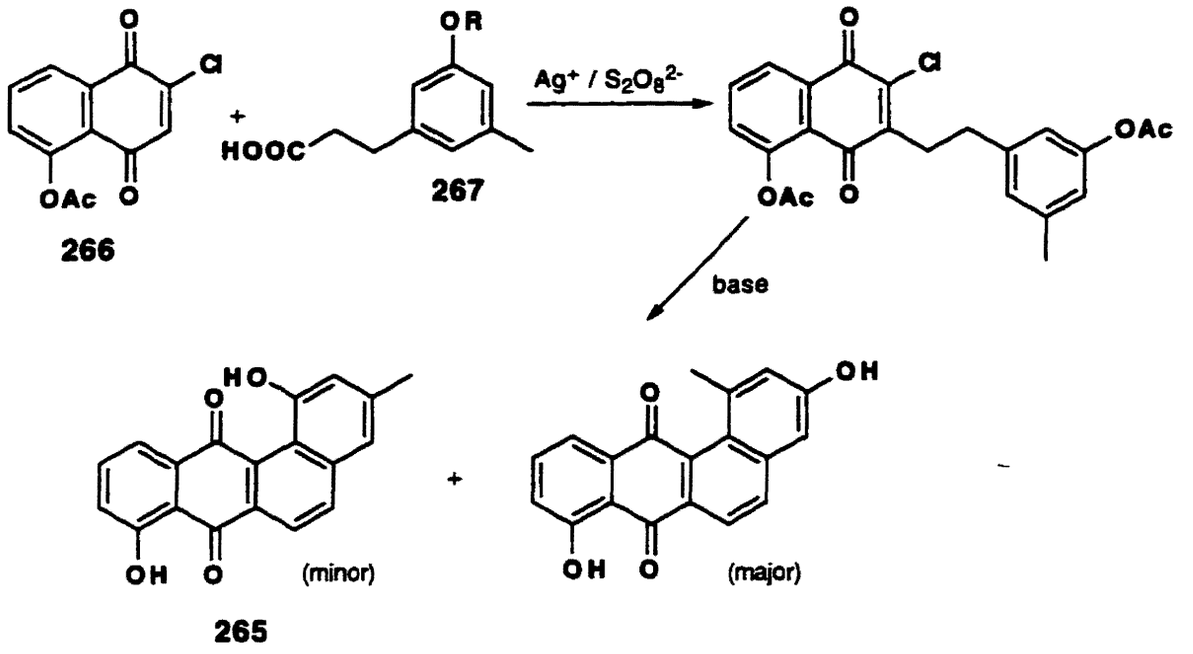
It has also been shown that substituents on naphthoquinones can have a directing effect on the coupling reaction i.e. a substituent at the 2-position of the naphthoquinone will direct the coupling to the 3- position (Scheme 129).



R = CH_3
R = $OCOCH_3$

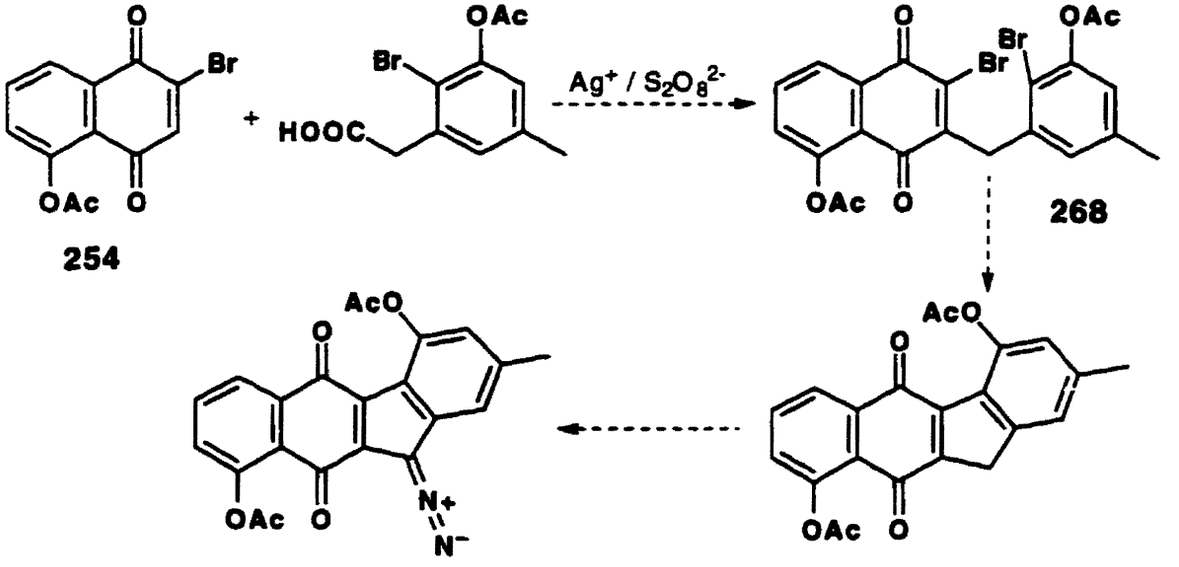
Scheme 129

This methodology has been utilized by Brown and Thomson[138] in the synthesis of tetrangulol (**265**) (Scheme 130). The chloronaphthoquinone **266** was coupled, by the method of Jacobsen and Torssell[136,137], with a substituted aromatic acid **267**. Treatment with base afforded tetrangulol **265** as a minor product via an intramolecular Michael addition-elimination sequence.



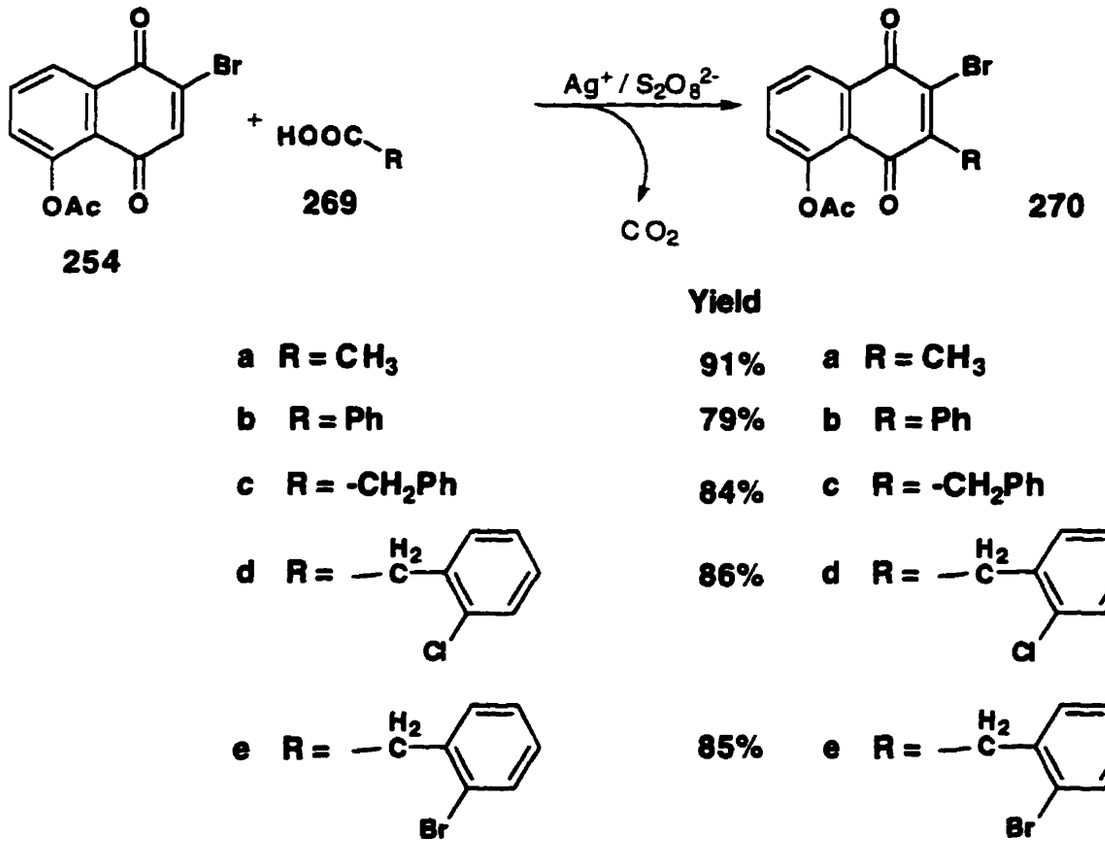
Scheme 130

With this precedent in mind, it seemed that reaction of 2-bromonaphthoquinone **254** with a substituted aromatic acid might provide a convergent method to the desired adduct **268** as outlined in Scheme 131. It was intended that the bond forming process which would close ring C would be effected by some transition-metal catalyzed process.[53,54,99,139-142]



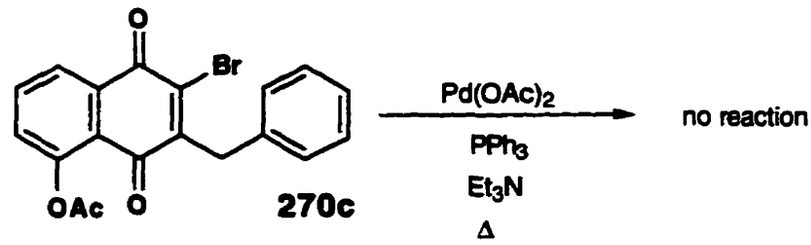
Scheme 131

Before pursuing this strategy in earnest, it was decided that the decarboxylative coupling of some readily available carboxylic acids to the bromojuglone derivative **254** should be studied. In practice it was found that acetic acid, benzoic acid, phenylacetic acid, *o*-chlorophenylacetic acid and *o*-bromophenylacetic acid (**269a-e**, respectively) all reacted smoothly to give the corresponding C-3 substituted 2-bromojuglone derivatives (**270a-e**) as shown in Scheme 132.



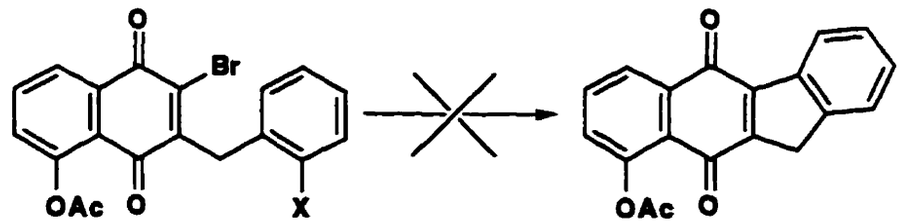
Scheme 132

Each of the benzylated quinones shown in Scheme 132(i.e. **270c-e**) was examined as a model for discovering reaction conditions suitable for cyclization to the benzo[b]fluorene system. For example, cyclization of compound **270c** was attempted using Heck-like reaction conditions ($Pd(OAc)_2/PPh_3/Et_3N$) without success (Scheme 133).



Scheme 133

Although it was recognized that this process might proceed more readily if the aromatic ring possessed a π-electron donating substituent, this approach was not studied in detail since it was felt that in the synthesis of prekinamycin, a selectively halogenated aryl system would be more appropriate for the cyclization to ensure proper regiochemistry in the C ring construction. As a result, the halogenated models **270d** and **270e** were studied in more detail. The chlorosubstituted system **270d** was studied first since it was prepared before the bromo analogue **270e** because of the availability of the precursor acid in this laboratory. Palladium catalyzed coupling attempts with Pd/C in acetonitrile or toluene were unsuccessful (Scheme 134).[53,99,142,143] Ullman[54,144,145] type coupling utilizing copper powder in DMF at room temperature also failed to effect the desired transformation, whereas Ullman reaction in refluxing DMF yielded an intractable mixture of compounds.

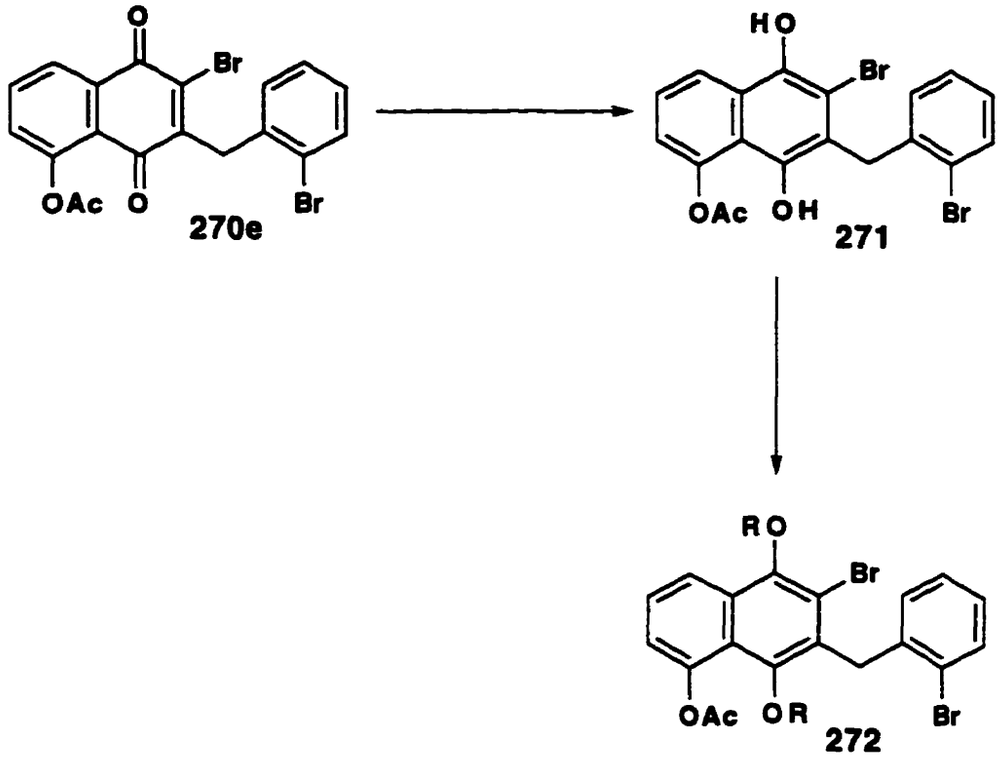


270d X = Cl
270e X = Br

Scheme 134

Attempted nickel promoted cyclization of **270e** with nickel bromide in the presence of triphenyl phosphine and zinc in DMF resulted in no reaction

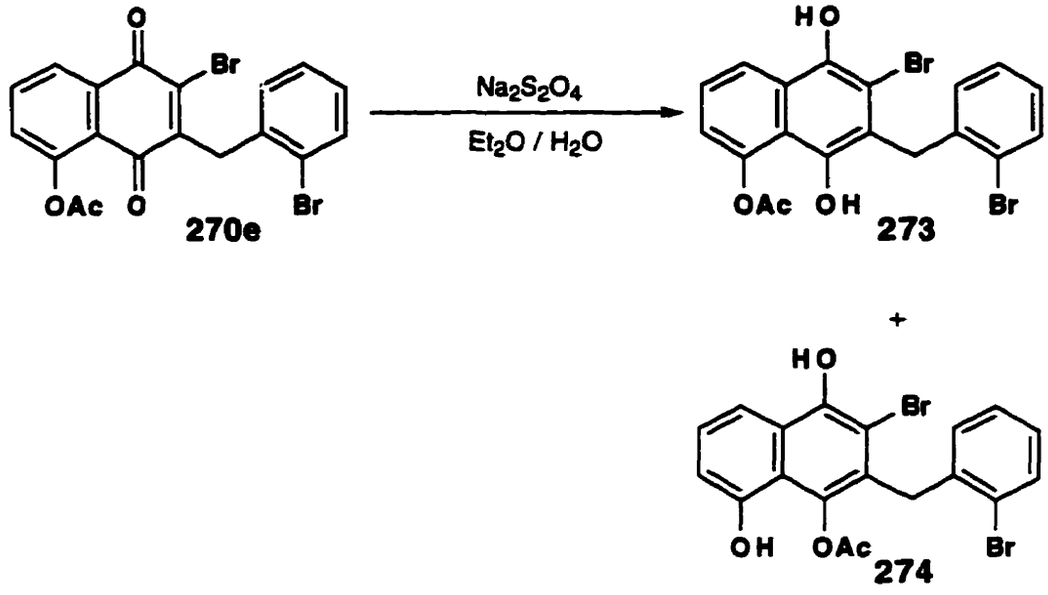
(Scheme 134). Also, Ullman coupling with copper at room temperature showed no reaction while at reflux a mixture of a large number of compounds was obtained. It was felt that this system was probably also too π electron deficient for these methods and that reduction to the hydroquinone **271** followed by protection of the hydroxy groups might afford a system **272** more suitable for these methods of coupling (Scheme 135).



Scheme 135

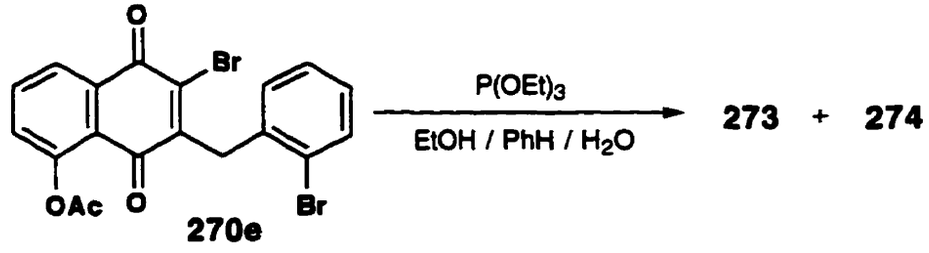
To this end, the bromo compound **270e** was reduced with sodium dithionite in ether-water. The ^{1}H NMR of the product showed that a mixture of two very similar compounds in a ratio of 2 to 1 had been produced. The mass spectrum of the mixture showed an M^+ ion of 466. The proton NMR showed two acetate signals at 2.25 and 2.41 ppm. The other signals in the proton spectrum also appeared to be doubled. The doubling of signals in the spectrum was attributed

to an intramolecular acetyl transfer reaction which gave **273** and **274** (Scheme 136).



Scheme 136

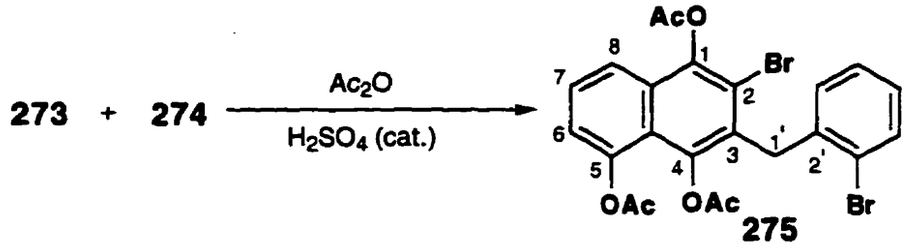
Reduction with triethyl phosphite in aqueous ethanol and benzene also yielded the same mixture **273** and **274** (Scheme 137).[146]



Scheme 137

The mixture of **273** and **274** was acetylated with acetic anhydride with a catalytic amount of sulfuric acid to afford the triacetate **275** (Scheme 138). The M^+ ion in the mass spectrum was found to be 548. The proton NMR shows three proton singlets at 2.24, 2.35 and 2.52 ppm and the aromatic region was substantially simplified. However, the signal assigned to the CH_2 of the bridge appears as two broad humps in the proton spectrum (Figure 80). This

observation suggested that the rotation about the Ar-CH_2 bond is slow on the NMR time scale. In the ^1H NMR spectrum at 250K the broad signals at 4.2 and 4.5 ppm (Figure 81) appear as a sharper AB quartet. Interestingly, one of the acetyl groups has now become broader and appears as an apparent doublet. Furthermore, the set of signals at 6.8 ppm has also broadened at 250K. It is possible that the complex behaviour may result from one or both of two hindered rotations, one about the C_4-O bond and one about the C_3-$C_{1'}$ bond, although hindered rotation about the C_1-O and C_5-O bonds might also be considered.



Scheme 138

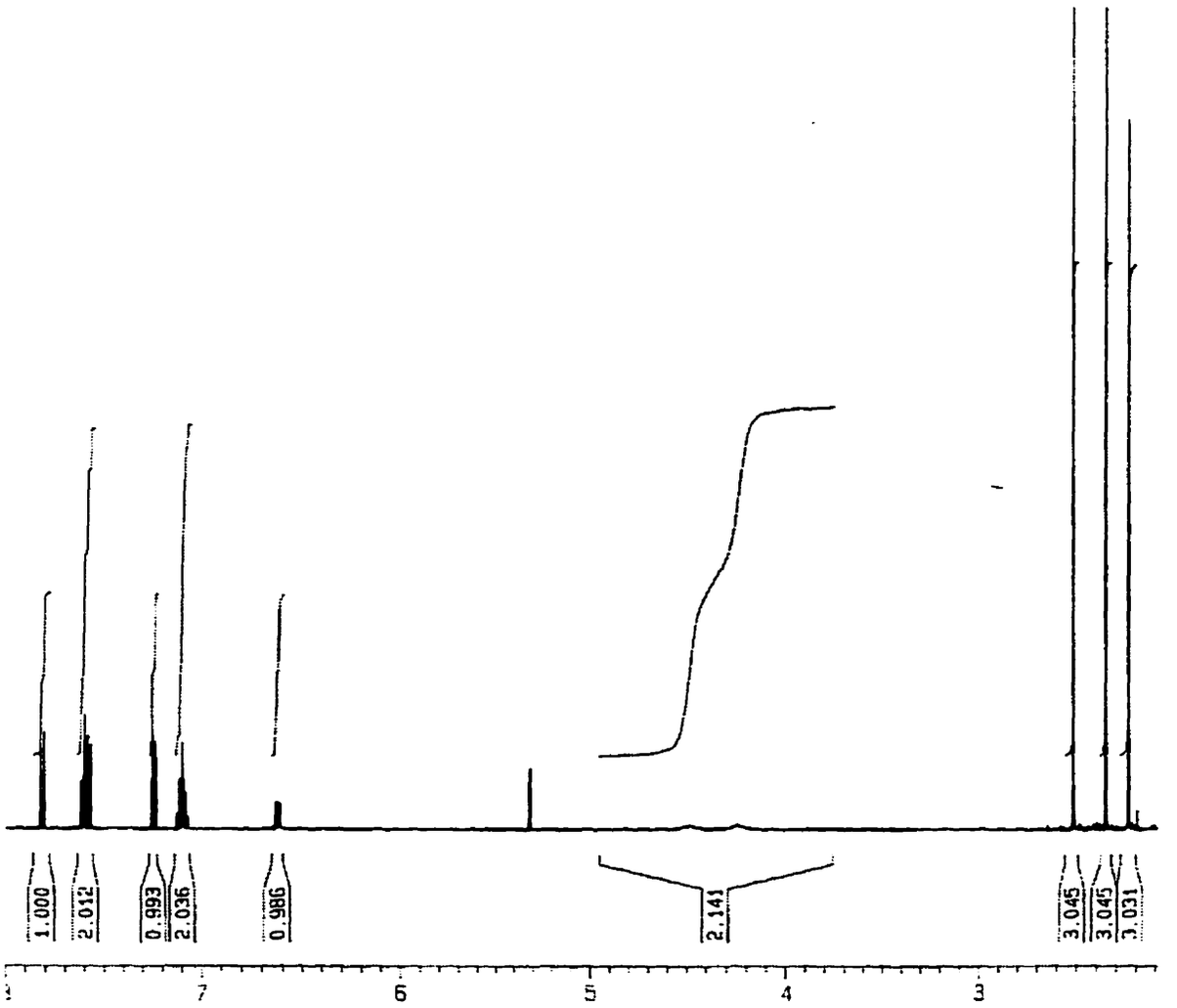


Figure 80: **^{1}H NMR (AMX-500) spectrum of 275 in CD_2Cl_2 at room temperature.**

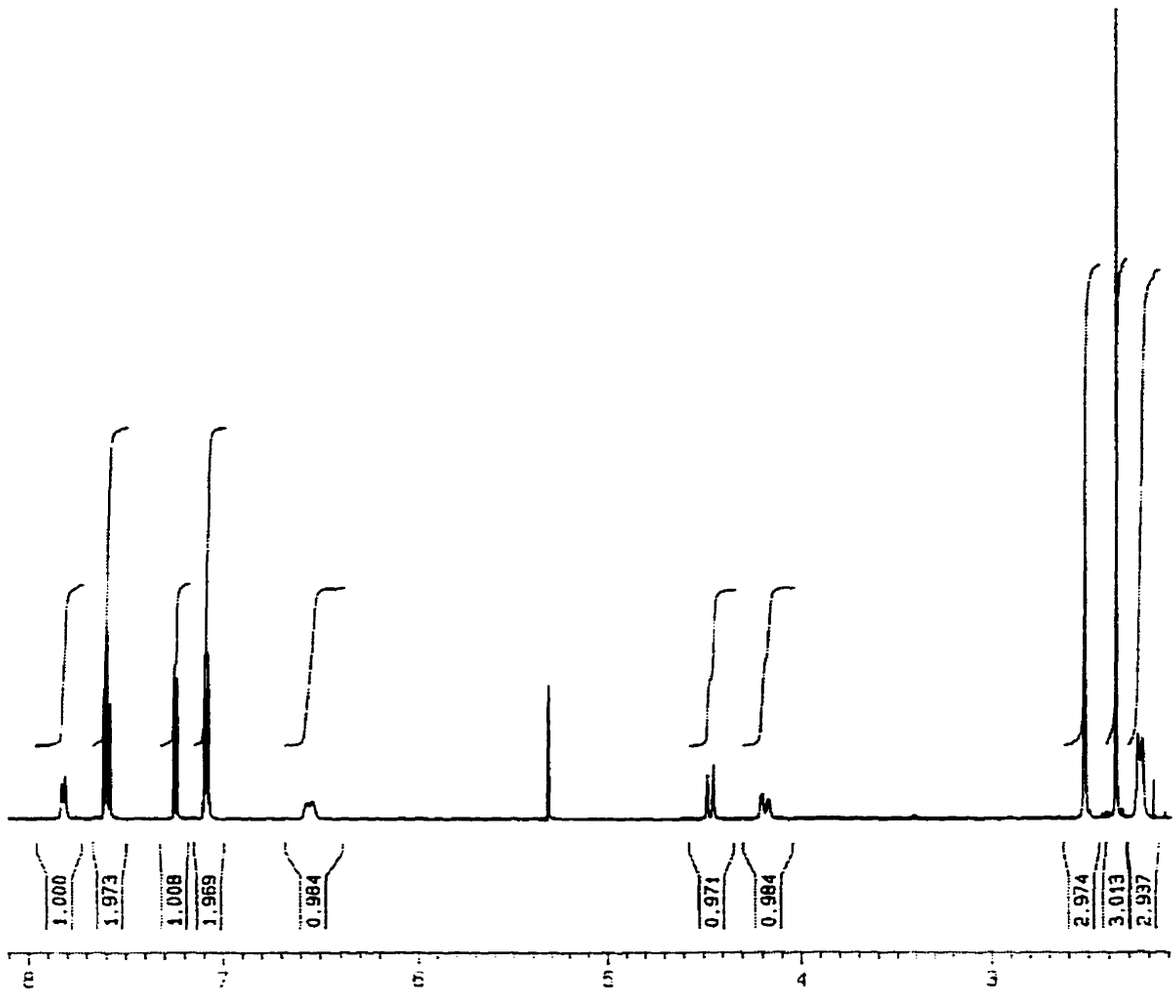
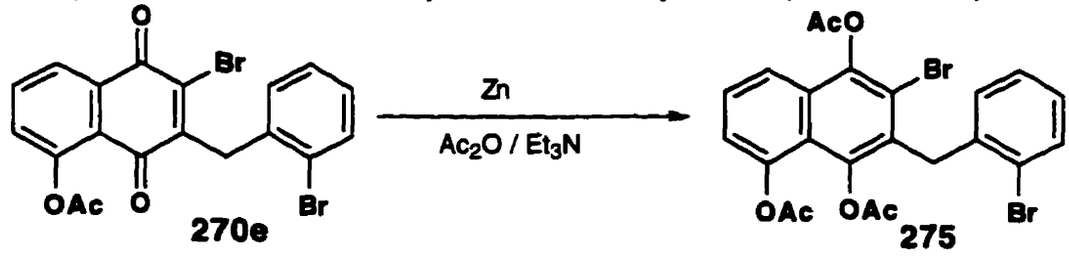


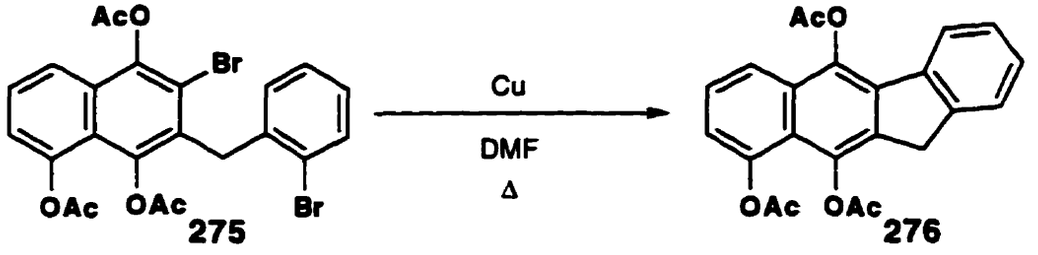
Figure 81: ^{1}**H NMR (AMX-500) spectrum of 275 in CD_2Cl_2 at 250K**

Later, it was found that the reduction and acetylation could be accomplished in a single step with zinc in acetic anhydride and triethylamine (Scheme 139).



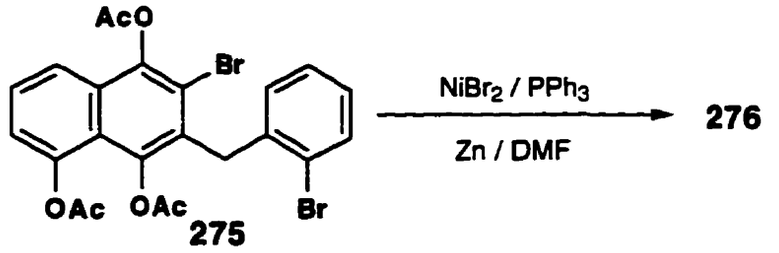
Scheme 139

Since, the system **275** was less π electron deficient, it was felt that it might now be amenable to the metal promoted coupling reactions. Reaction under Ullman conditions failed to give the desired coupling (Scheme 140).



Scheme 140

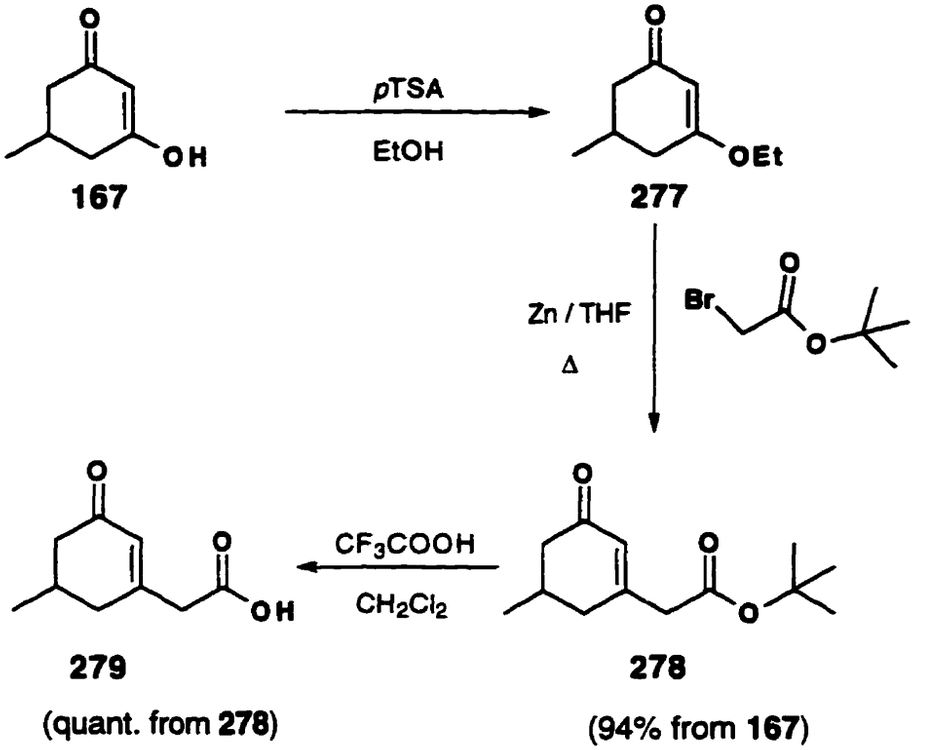
Eventually it was found that reaction with nickel bromide, triphenyl phosphine and zinc in DMF did yield the desired coupled product **276**, albeit in only a modest yield of 35% (Scheme 141).



Scheme 141

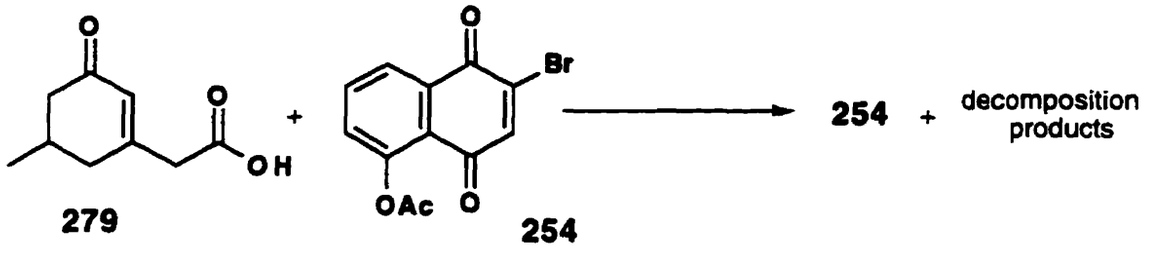
Thus, this model study demonstrated the feasibility of construction of the desired tetracyclic carbon framework based on the retrosynthetic analysis shown in Scheme 127 (page 173). No further attempts were made at optimizing the yield of this conversion. Instead attention was turned to the construction of the benzylic acid precursor suitable for building the full prekinamycin structure by this approach. The ketone **167** was considered to be a suitable starting material for the synthesis of the fully substituted system (Scheme 142). The enol ether **277** was formed from **167** in ethanol with a catalytic amount of *p*TSA. A Reformatsky[147] reaction with *t*-butyl bromoacetate

afforded the protected acid **278** in 94% isolated yield from **167**. Deprotection with trifluoroacetic acid yielded **279**.



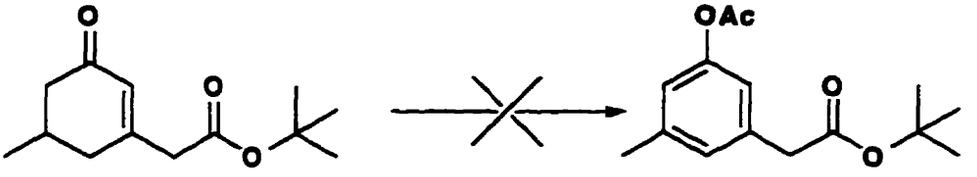
Scheme 142: The acid 279 was generated from 167 in 3 steps.

It was thought that it might be possible to couple the acid **279** and the naphthoquinone **254** prior to aromatization with silver nitrate and ammonium persulfate, since the method has shown considerable flexibility in the nature of the substrates to be coupled. Reaction of the acid **279** with the naphthoquinone **254**, however, yielded only unchanged **254** as well as decomposition products from the acid (Scheme 143).



Scheme 143

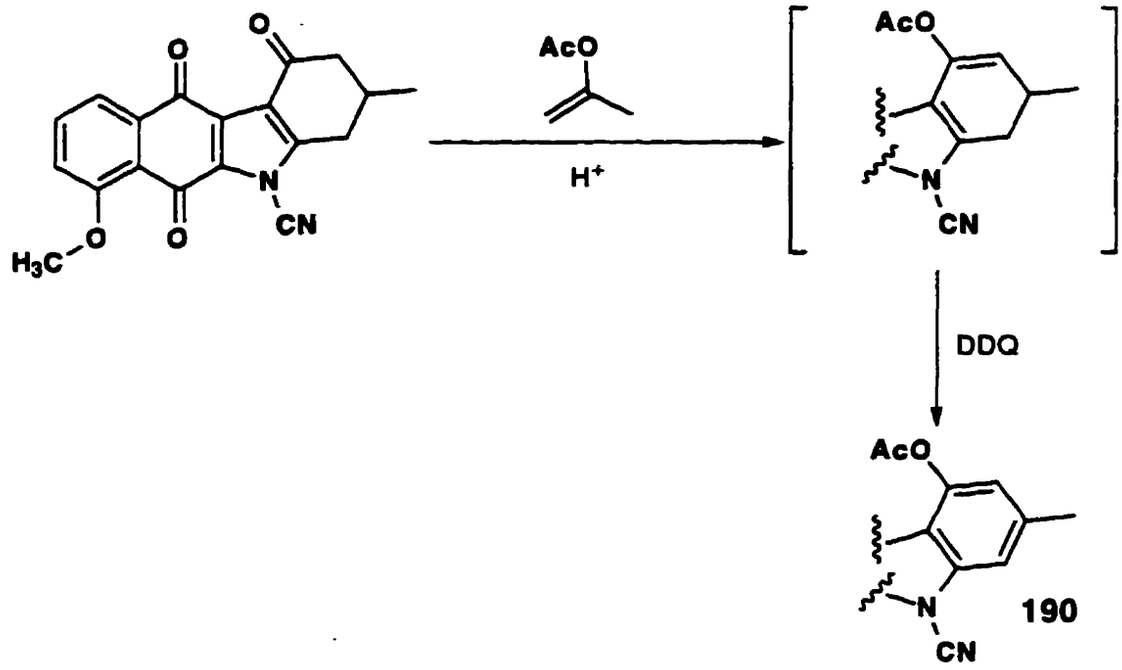
This suggested that radical addition to **279** might be competing to the exclusion of radical addition to **254**. Thus, it was decided that the acid must be aromatized prior to the coupling reaction with the naphthoquinone **254**. Reaction of **278** with DDQ in refluxing dioxane yielded decomposition products (Scheme 144). The reaction was repeated at room temperature again yielding a mixture of products. The ^{1}H NMR spectrum of the reaction mixture showed no sign of the desired aromatized product. Furthermore, the use of chloroanil at reflux also failed to effect the aromatization of **278**. Reaction of **278** with palladium on carbon left the starting material unchanged (Scheme 144).



278

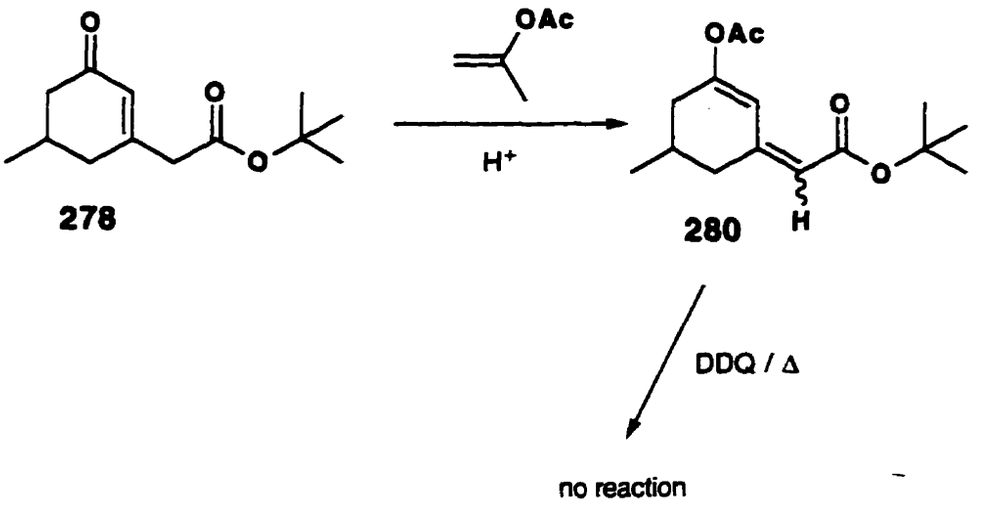
Scheme 144

It was felt that the **278** might more readily aromatize, if a second double bond could be introduced into the system and that the conditions developed earlier in the synthesis of **190** might be suitable (Scheme 145).



Scheme 145

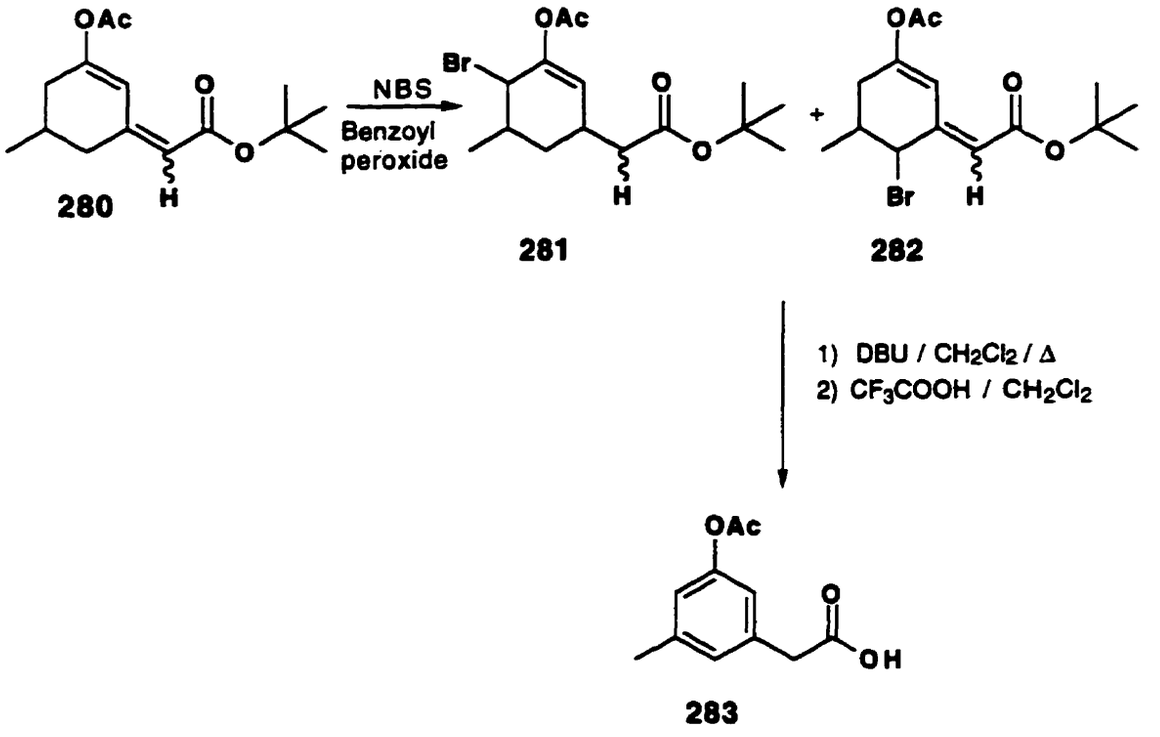
Initially, the enol acetate formation and aromatization with DDQ were carried out in a stepwise manner. To this end, the ester **278** was reacted with isopropenyl acetate in the presence of a catalytic amount of p-toluenesulfonic acid (Scheme 146). The conjugated system **280**, containing an exocyclic rather than an endocyclic double bond, was isolated as a mixture of E and Z isomers. It was not expected that the exocyclic double bond in **280** would make this system more agreeable to aromatization than **278**. In practice, reaction of **280** with DDQ in *t*-butanol at reflux temperatures left the starting material unchanged (Scheme 146).



278 280

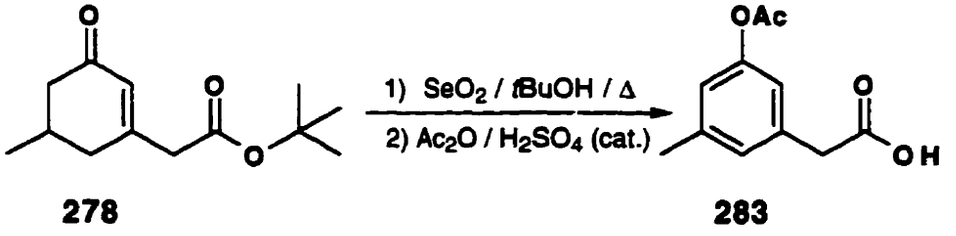
Scheme 146

The focus of this work was then turned to the introduction of a suitable leaving group into **280** which when eliminated with a weak base would yield the desired aromatized system. Thus, **280** was reacted with NBS in the presence of a catalytic amount of benzoyl peroxide to afford a mixture of monobrominated products believed to be **281** and **282** (Scheme 147). Heating the mixture of **281** and **282** in refluxing methylene chloride in the presence of DBU effected elimination and isomerization to yield the aromatic system which was isolated as the acid **283** after treatment with trifluoroacetic acid (Scheme 147). The overall yield of this two step process was 46%.



Scheme 147

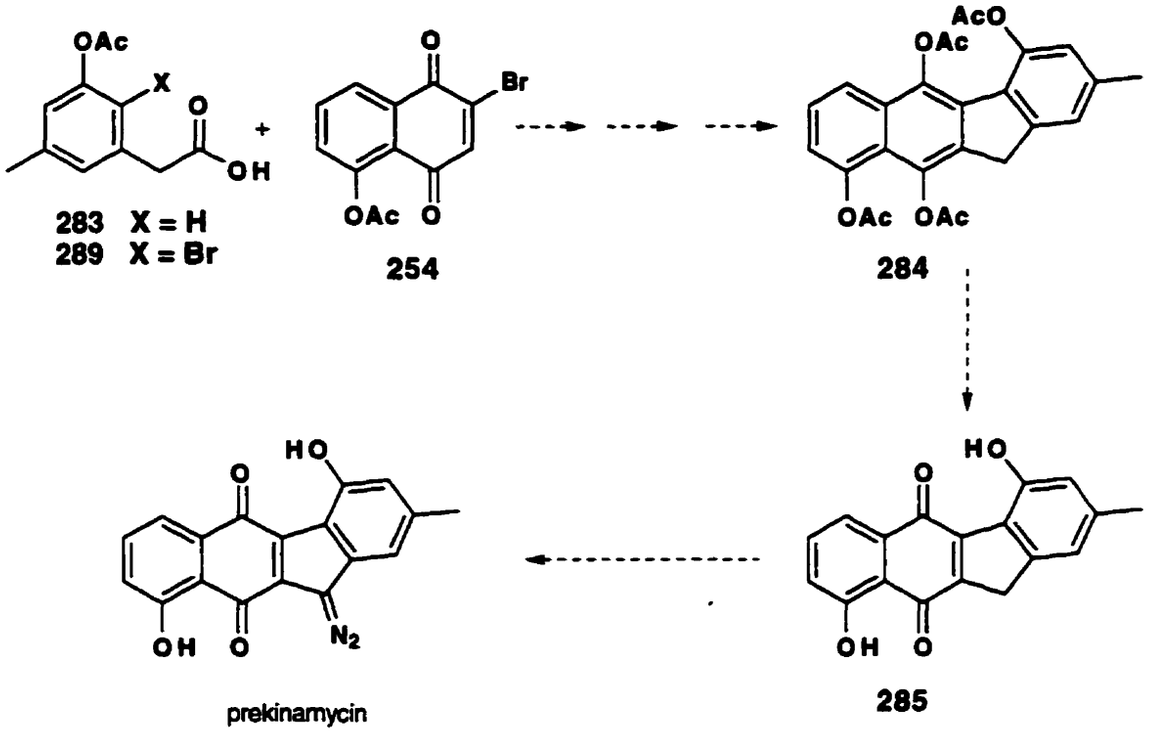
It was found later that **283** could be produced directly from **278** in 71% isolated yield (Scheme 148). The acid **283** was produced by reaction of **278** with selenium dioxide in *t*-butanol at reflux temperatures followed by acetylation with acetic anhydride in the presence of a catalytic amount of sulfuric acid.



Scheme 148

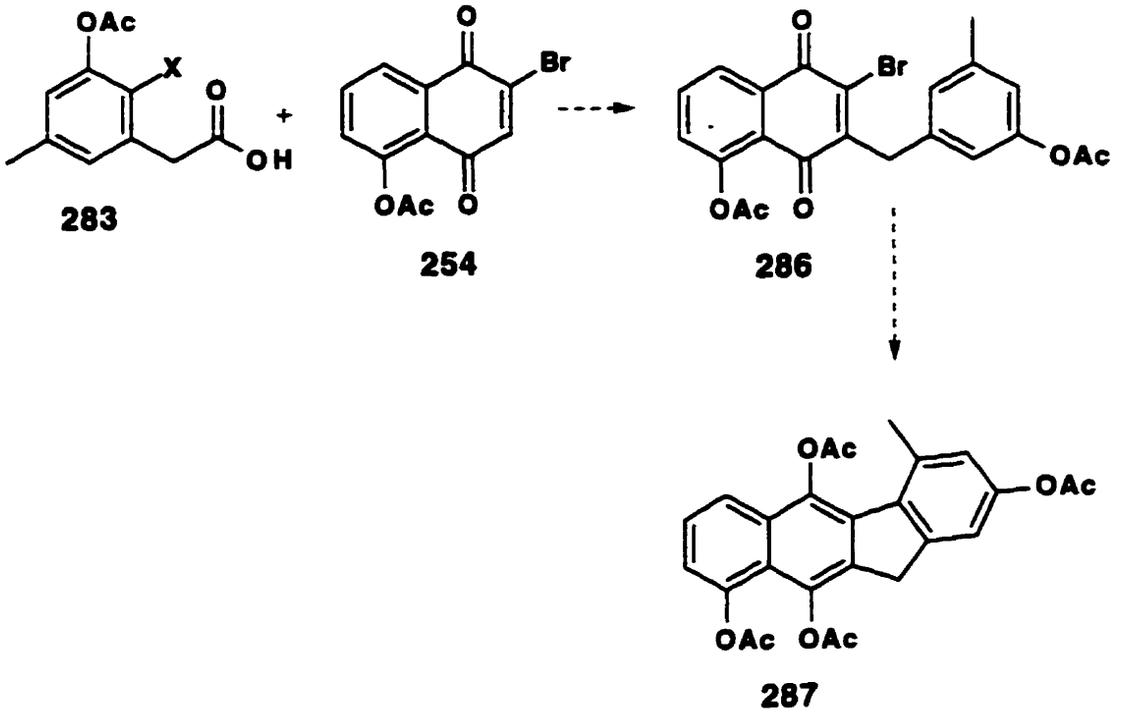
Future work in this area will require the assembling, by the methodology developed in this section, of the substituted components (**283** and **254**) to produce the revised structure of prekinamycin (Scheme 149). It is hoped that the acid **283** and the quinone **254** can be coupled, by the method developed

in this section, to give **284**. Deprotection and mild oxidation, utilized earlier in the synthesis of the N-cyano prekinamycin, should yield **285**. Diazo transfer[108,148], utilizing diazo transfer reagents such as p-toluenesulfonylazide,[148,149] azidotris(diethylamino)phosphonium bromide,[150] mesyl azide[151] or an azidinium salt[152], to the methylene group of **285** may complete the synthesis and provide prekinamycin.

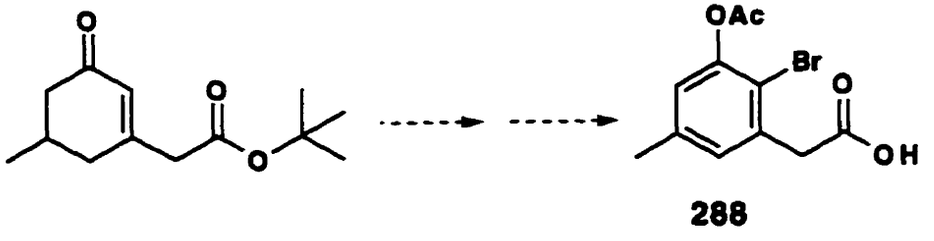


Scheme 149: Possible synthetic route to the revised structure of prekinamycin based on methodology developed in this section.

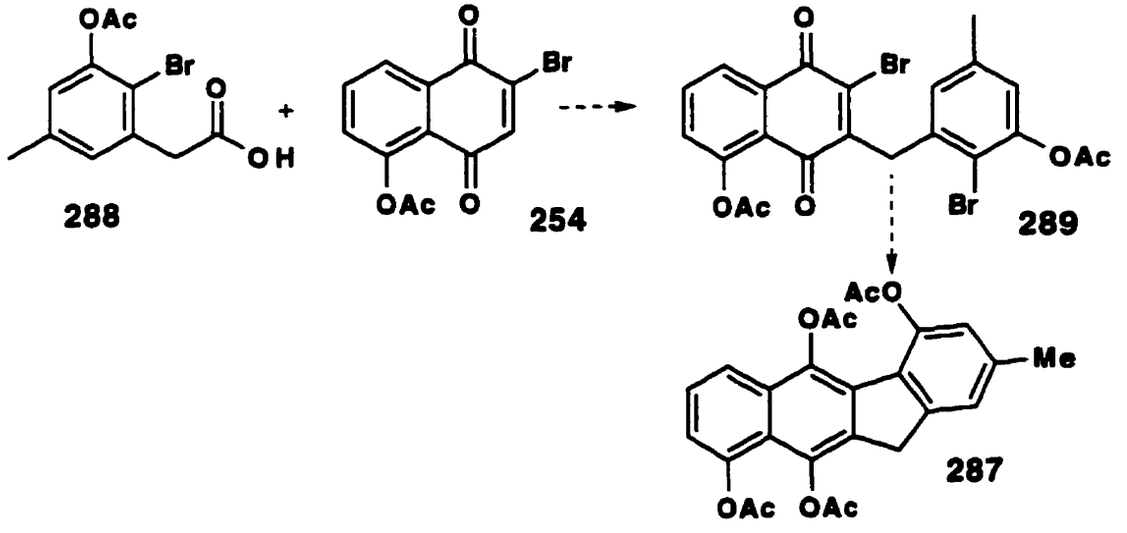
If, however, the Heck-type coupling reaction to give **284** progresses with the opposite regiochemistry (Scheme 150) than is required for the synthesis of the revised structure of prekinamycin, then it may be necessary to generate the bromo-substituted aromatic acid **289** (Scheme 151) to direct the regiochemistry of the coupling reaction (Scheme 152) using the nickel promoted chemistry utlized earlier in the synthesis of **276**.



Scheme 150



Scheme 151:



Scheme 152

5.1 Summary of Results in the Area of the Kinamycins

1) A synthetic route toward the structure originally assigned as prekinamycin acetate methyl ether (**190**) in 21% yield from *o*-anisidine was developed.

2) Comparison of the physical and spectroscopic properties of **190**, prepared in this laboratory, and prekinamycin diacetate (**79**) revealed significant differences which could not be explained by minor differences in the structures assigned to them.

3) These differences led to a very careful examination of the spectroscopic properties, including ^{1}H NMR , ^{13}C NMR , IR and in some cases X-ray crystallographic studies, of intermediates in the synthesis of **190**, N-cyanoindoles and N-cyanoindolediones, prepared in this laboratory. Comparison with published spectroscopic data for the kinamycins led to the conclusion that the kinamycins were not cyanamides.

4) Examination of the original structural assignment based on a X-ray crystallographic study of the *p*-bromobenzoate of kinamycin C revealed that the X-ray data was such that a three atom fragment could not be unambiguously assigned and that the cyanamide part structure was assigned on the basis of an earlier chemical test.

5) The diazo structural feature was not considered in this chemical test and comparison of the spectroscopic properties of known diazo compounds with that of the kinamycins led to the conclusion that the kinamycins were not cyanamides. The structures of the kinamycins, including prekinamycin, were revised from derivatives of N-cyanocarbazoles to derivatives of diazofluorene.

6) Revision of the structures of the kinamycins to derivatives of diazofluorene from derivatives of N-cyanocarbazoles has significant impact on the understanding of kinamycin biosynthesis and mode of action. A revised biosynthetic pathway leading to the kinamycins as well as to related natural products has now been suggested. Furthermore, possible mechanisms of action in biological systems for these revised structures have been proposed.

7) A synthetic route to the carbon skeleton (**276**) of the revised structure of prekinamycin, lacking substituents in the D-ring, from a substituted naphthoquinone was developed.

8) Also, a synthetic route to an aromatic acid (**283**), which when utilized in the synthetic route described above, would yield the D-ring substitution present in prekinamycin, has been described.

Chapter 6: Experimental

6.1 General Procedures

All reagents were obtained from the Aldrich Chemical Company, Inc. unless otherwise stated. All reactions were carried out in a nitrogen or argon atmosphere. THF was dried by distillation from sodium wire and stored over molecular sieves (4A). Toluene was distilled from sodium wire with sodium benzophenone ketyl as the indicator. DMSO was dried by distillation from sodium hydride under an argon atmosphere. DMF was dried by distillation from calcium hydride. Triethylamine was distilled from powdered potassium hydroxide. Zinc was purified by the method described in Purification of Laboratory Chemicals.[153]

Reactions were monitored by thin layer chromatography using aluminum-backed sheets precoated with silica gel (0.2 mm) or by ^{1}H NMR. The TLC plates were analyzed by an ultraviolet lamp (254 nm) or by staining with phosphomolybdic acid in ethanol. Column chromatography was performed using silica gel (70-230 mesh A.T.S.M., E. Merck). Preparative Layer Chromatography was performed using glass backed plates (20 cm x 20 cm) precoated with silica gel (1000 microns) supplied by Analtech, Inc.

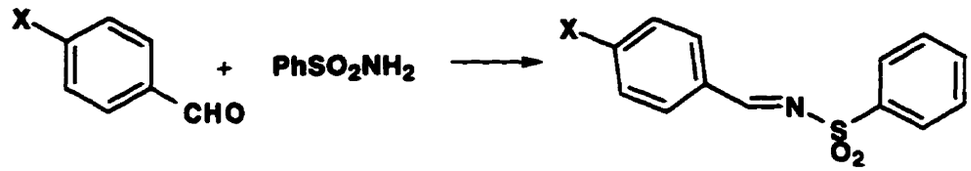
High resolution and low resolution mass spectra were recorded at the McMaster Regional Center for Mass Spectrometry. Electrospray mass spectra were recorded at the University of Waterloo using a VG Quattro II triple quadrupole mass spectrometer (Manchester, U.K.) fitted with an electrospray source run in 50:50 acetonitrile/water with 0.1% acetic acid at a flow rate of 50uL/min via HP 1090 HPLC (the flow source) with a declustering voltage of 3.5KV. Elemental analyses of samples were performed by M-H-W Laboratories in Arizona.

Infrared spectra were determined on a MB-100 Fourier Transform spectrometer using KBr pellets unless otherwise indicated. The relevant peaks are given in cm^{-1}.

^{1}H NMR spectra were obtained on a Bruker AC-200 (200 MHz), AM-250 (250 MHz), or AMX-500 (500 MHz) NMR Spectrometer with deuterochloroform as the solvent and tetramethylsilane as the internal standard, unless otherwise stated. The spectral parameters are listed in the following order: (frequency, solvent) chemical shift in ppm (multiplicity, coupling constant in Hertz, number of protons). ^{13}C NMR spectra were determined on an AC-200 (50.3 MHz), AM-250 (62.9 MHz) or AMX-500 (125.8 MHz) NMR Spectrometer with deuterochloroform as the solvent (triplet centered at 78.0 ppm as the reference) unless otherwise stated. All spectra obtained were broad band decoupled, unless otherwise stated. The spectral parameters are listed in the following order: (frequency, solvent) chemical shifts in ppm. HMQC[154,155] and HMBC[156] experiments were performed on the AMX-500 by Dr. Sandra Mooibroeck. X-ray crystallographic studies were performed by Dr. N. J. Taylor.

6.2 Experimental Procedures

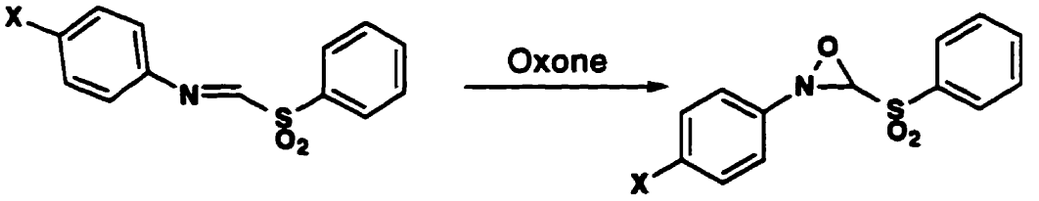
General Procedure for the Synthesis of N-Benzenesulfonylimines[78]



144 X = H
146 X = NO_2

Powdered molecular sieves (4A, 15g), Amberlyst 15 ion exchange resin (0.2 g), benzenesulfonamide (15.7 g, 100 mmol), dry toluene (170 mL) and the aldehyde (101.4 mmol) were added to a 300 mL one necked round bottom flask with a Dean Stark water separator and an argon gas inlet. The reaction mixture was stirred and heated at reflux under an atmosphere of argon until water ceased to separate in the Dean Stark apparatus (approx. 18 h). The reaction mixture was cooled to room temperature and filtered through a sintered glass funnel. The residue was washed with toluene (70 mL) and the solvent was removed *in vacuo* leaving a viscous yellow oil. On standing the viscous oil solidified to a yellow-white solid. The solid was suspended in pentane (80 mL) and collected on a sintered glass funnel. The solid was then recrystallized from ethyl acetate/pentane. The products were spectroscopically identical to material obtained by Davis *et al.*[78] For **144**: ^{1}H NMR (250 MHz, CD_2Cl_2) δ 9.04 (s, 1H), 7.93 (d, J=8.1 Hz, 2H), 7.68-7.49 (m, 8H); For **146**: ^{1}H NMR (250 MHz, CD_2Cl_2) δ 9.12 (s, 1H), 8.32 (d, J=8.7 Hz, 2H), 8.12 (d, J=8.7 Hz, 2H), 8.06 (d, J=8.7 Hz, 2H), 7.73-7.51 (m, 3H).

General Procedure for the Synthesis of Davis' Reagent

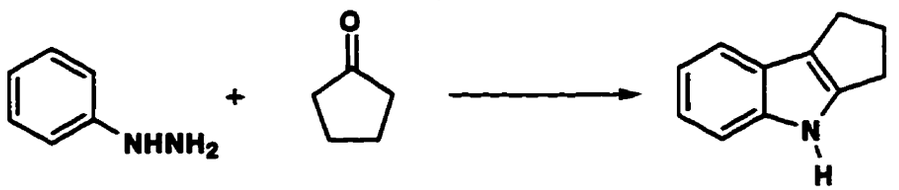


144 X = H
146 X = NO_2

122 X = H
145 X = NO_2

A solution of Oxone (potassium peroxymonosulfate) (6.0 g, 9.8 mmol) in water (50 mL) was added slowly (over 15 min.) to a vigorously stirred mixture of N-benzenesulfonylimine (2.0 g, 8.2 mmol), toluene (80 mL), potassium carbonate (9.5 g, 68.7 mmol) and water (50 mL). The reaction mixture was stirred for 1 h. The solvent was removed *in vacuo* from the organic phase and the aqueous layer was extracted with toluene (3x25 mL). The combined organic extracts were washed with 1% sodium sulfite, dried over magnesium sulfate and the solvent removed *in vacuo* leaving a white solid. The products were spectroscopically identical to material obtained by Davis *et al.*[74,78] **122**: ^{1}H NMR (250 MHz, CD_2Cl_2) δ 8.04 (d, J=7.4 Hz, 2H), 7.80 (d, J=7.4 Hz, 2H), 7.57-7.38 (m, 6H), 5.45 (s, 1H); **145**: ^{1}H NMR (250 MHz, CD_2Cl_2) δ 8.26 (d, J=8.1 Hz, 2H), 8.04 (d, J=7.5 Hz, 2H), 7.8 (d, J=7.5 Hz, 2H), 7.71-7.64 (m, 3H), 5.58 (s, 1H).

Synthesis of 2,3-Cyclopentanoindole 142[157]



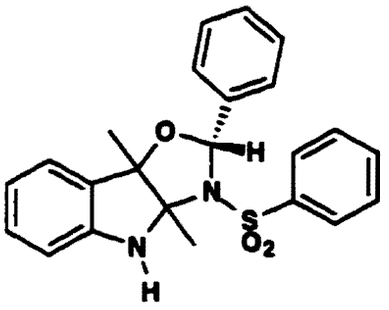
142

A mixture of phenylhydrazine (20 g, 185 mmol) and cyclopentanone (16 g, 167 mmol) was heated on a steam bath for 5 min. To the cooled red viscous liquid was added a solution of water (360 mL) and sulfuric acid (12M, 20 mL). The reaction mixture was then heated on a steam bath for 35 min followed by cooling in an ice bath for 20 min. The reaction mixture was filtered and the filtrate was discarded. The solid was sonicated with hexane for 10 min and filtered. The solvent was removed *in vacuo* from the filtrate leaving a white solid (35%). ^{1}H NMR (500 MHz, CD_2Cl_2) δ 7.93 (s, 1H), 7.38 (d, J=8.8 Hz, 1H), 7.29 (d, J=8.6 Hz, 1H), 7.07-7.01 (m, 2H), 2.87 (t, J=7.5 Hz, 1H), 2.82 (t, J=7.6 Hz, 2H), 2.57-2.51 (m, 2H).

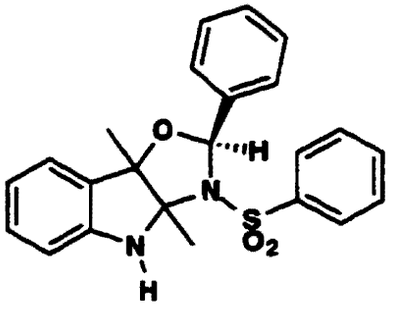
General Procedure for the Reaction of Indoles with 122

To a solution of the indole (7.1 mmol) in THF (8.0 mL) was added dropwise a solution of **122** (14.2 mmol) in THF (10 mL). The solution was allowed to stir at room temperature for 2 h under an argon atmosphere. The solvent was removed *in vacuo* and the residue was purified by column chromatography unless stated otherwise. Both **114** and **140** were also reacted with **122** in the presence of 10% H_2O in THF as the solvent, which produced identical results with that observed for the analogous anhydrous reactions.

Adduct 141



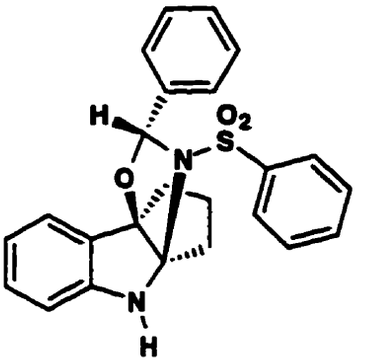
141a



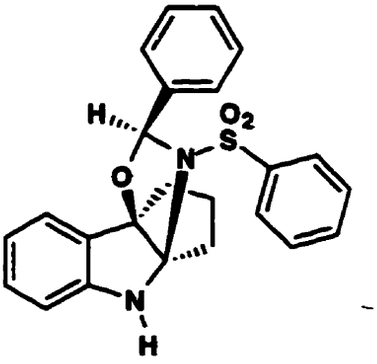
141b

The compound **141** was purified on a column eluting with methylene chloride to give a white solid (74%) The mixture of diastereomers was separated on a column eluting with 15%, 20% ethyl acetate/hexane. The diastereomer **141a** was isolated by column chromatography and provided suitable crystals from THF/toluene for a single crystal X-ray diffraction study (Appendix B, page 252): IR (KBr) 3408 cm^{-1}; ^1H NMR (200 MHz, CD_2Cl_2) (**141a**) δ 7.35-7.06 (m, 12H), 6.83 (t, J=6.4 Hz, 1H), 6.64 (d, J=6.4 Hz, 1H), 5.62 (s, 1H), 5.40 (s, 1H), 1.97 (s, 3H), 1.56 (s, 3H); HRMS calcd for $C_{23}H_{22}N_2O_3S$ 406.1352, found 406.1361; Anal. Calcd. for $C_{23}H_{22}N_2O_3S$: C, 67.96; H, 5.45; N, 6.89. Found: C, 67.71; H, 5.33; N, 6.91.

Adduct 143



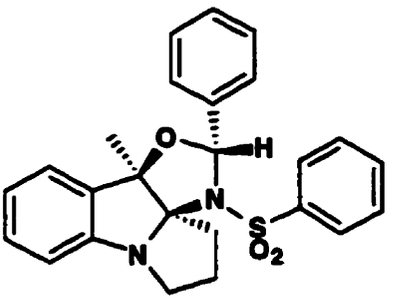
143a



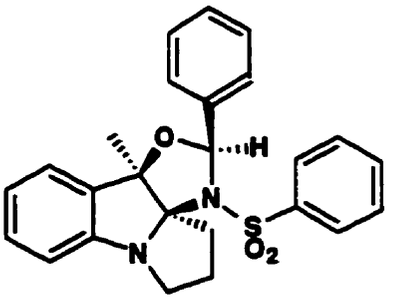
143b

The compound **143** was purified by column chromatography eluting with 30% ethyl acetate/hexane yielding a crystalline white solid (81%). The mixture of diastereomers was separated by repeated recrystallization from 30% ethyl acetate/hexane which provided a single diastereomer, **143b**, as a suitable crystal for a single crystal X-ray diffraction study (Appendix B, page 260): IR (KBr) 3395 cm^{-1}; ^1H NMR (250 MHz, CD_2Cl_2) (one diastereomer) δ 7.37-6.65 (m, 14H), 5.91 (s, 1H), 5.36 (s, 1H), 2.62-2.46 (m, 2H), 2.32-2.23 (m, 2H), 2.05-1.93 (m, 1H), 1.75-1.58 (m, 1H); MS(EI) m/z 418(100%); HRMS calcd for $C_{24}H_{22}N_2O_3S$ 418.1353, found 418.1360; Anal. Calcd. for $C_{24}H_{22}N_2O_3S$: C, 68.88; H, 5.30; N, 6.69. Found: C, 68.62; H, 5.28; N, 6.80.

Adduct 138



138a1



138a2

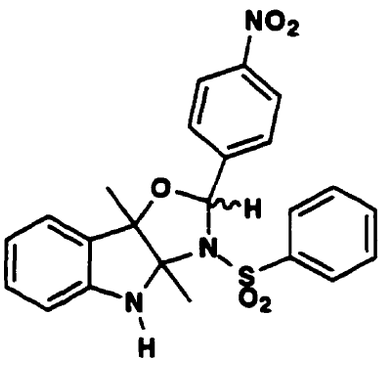
The compound **138** was purified on a column eluting with 30% ethyl acetate/hexane yielding a white crystalline solid (71%): IR (KBr) 3395 cm^{-1}; ^1H NMR (500 MHz, CD_2Cl_2) (mixture of diastereomers)** δ 7.67-7.64 (m, $2H^{AB}$), 7.56-7.54 (m, $2H^{AB}$), 7.49-7.47 (m, $1H^{A}$), 7.40-7.23 (m, $9H^{AB}$), 7.16-7.04 (m, $8H^{AB}$), 7.02-6.97 (m, $2H^{AB}$B), 6.80-6.75 (m, $2H^{AB}$), 6.53-6.51 (m, $1H^{B}$), 6.39 (s, $1H^{B}$), 6.38-6.37 (m, $1H^{A}$), 5.59 (s, $1H^{A}$), 3.84-3.78 (m, $1H^{A}$), 3.63-3.58 (m, $1H^{B}$), 3.29-3.25 (m, $1H^{B}$), 3.15-3.14 (m, $1H^{A}$), 2.83-2.75 (m, $2H^{AB}$), 2.42-2.31 (m, $2H^{AB}$), 2.30-2.23 (m, $1H^{A}$), 1.94-1.73 (m, $3H^{AB}$), 1.50 (s, $3H^{A}$), 1.42 (s, $3H^{B}$); MS(EI) m/z 432(36%); HRMS calcd for $C_{25}H_{24}N_2O_3S$ 432.1509, found 432.1500. Anal. Calcd. for $C_{25}H_{24}N_2O_3S$: C, 69.42; H, 5.59; N, 6.48. Found: C, 69.75; H, 5.28; N, 6.61.

** The signals in the proton NMR spectrum of **143** were assigned based on NOE and selective TOCSY experiments which are described in detail in Page 61, Chapter 2.2.1. Also, assignment A refers to component A (page 70) and assignment B refers to component B (page 70) while AB refers to signals from both diastereomers A and B.

General Procedure for the Reaction of Indoles with 145

To a solution of the indole (7.1 mmol) in THF (8.0 mL) was added dropwise a solution of **145** (14.2 mmol) in THF (10 mL). The solution was allowed to stir at room temperature for 2 h under an argon atmosphere. The solvent was removed *in vacuo* and the residue was purified by column chromatography unless stated otherwise.

Adduct 148

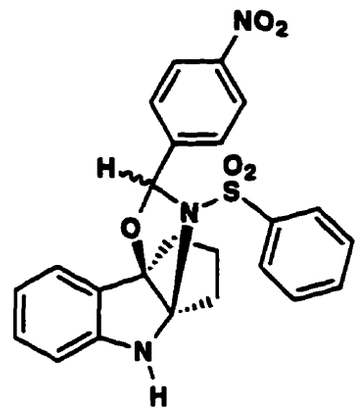


148

Adduct **148** was purified on a column eluting with 30% ethyl acetate/hexane to give a yellow solid (63%): IR (KBr) 3403 cm^{-1}; ^1H NMR (200 MHz, CD_2Cl_2) (mixture of diastereomers**) δ 8.38 (d, J=9.0 Hz, 2H¥), 8.07 (d, J=8.8 Hz, 2H¥), 7.92 (d, J=9.0 Hz, 2H¥), 7.37-6.60 (m, 20H¥π), 6.11 (s, 1H¥), 5.58 (s, 1H¥), 5.51 (s, 1H¥), 5.35 (s, 1H¥), 2.02 (s, 3H¥), 1.58 (s, 6H¥π), 1.45 (s, 3H¥); MS(EI) m/z 161(53%), 141(64%), 451(100%); HRMS calcd for $C_{23}H_{21}N_3O_5S$ 451.1203, found 451.1202.

** ¥ refers to signals from one diastereomer whereas ¥π refers to signals from both diastereomers. Note, the signals in the proton NMR spectrum have not been assigned to any particular diastereomer.

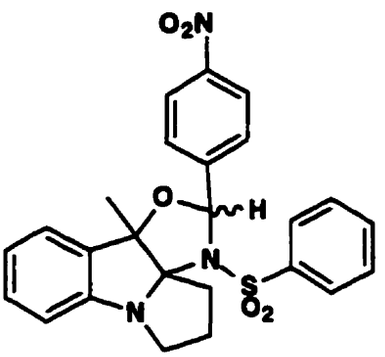
Adduct 149



149

Adduct **149** was purified by preparative layer chromatography eluting with 25% ethyl acetate/hexane to give a yellow solid (54%). The diastereomers were separated by repeated recrystallization from ethyl acetate/hexane: IR (KBr) 3390 cm^{-1}; ^1H NMR (200 MHz, CD_2Cl_2) (one diastereomer) δ 8.38 (d, J=8.4 Hz, 2H), 8.07 (d, J=8.8 Hz, 2H), 7.85 (d, J=8.8 Hz, 1H), 7.49-7.13 (m, 6H), 6.84-6.71 (m, 2H), 5.67 (s, 1H), 5.35 (s, 1H), 3.01-2.97 (m, 1H), 2.56-1.19 (m, 5H); MS(EI) m/z 171(59%), 463(100%); HRMS calcd for $C_{24}H_{21}N_3O_5S$ 463.1203, found 463.1218.

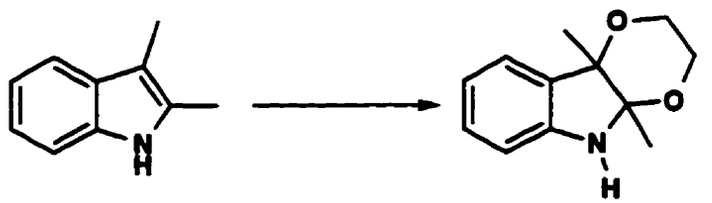
Adduct 147



147

Adduct **147** was purified on a column eluting with 25% ethyl acetate/hexane to give a yellow solid (68%) which was recrystallized from diethyl ether/hexane: IR (KBr) 2962 cm^{-1}. ^{1}H NMR (200 MHz, CD_2Cl_2) δ 8.15 (d, J=8.8 Hz, 4H¥), 7.90-7.82 (m, 3H¥π), 7.65-7.22 (m, 13H¥π), 7.11-7.03 (m, 4H¥π), 6.83-6.73 (m, 2H¥), 6.68 (s, 1H¥), 6.37-6.26 (m, 2H¥), 5.75 (s, 1H¥), 3.86-3.73 (m, 1H¥), 3.57-3.39 (m, 1H¥), 3.19-3.07 (m, 2H¥π), 2.85-2.65 (m, 2H¥π), 2.49-2.25 (m, 3H¥π), 2.03-1.62 (m, 3H¥π), 1.53 (s, 3H¥), 1.26 (s, 3H¥); ^{13}C NMR (50.3 MHz, CD_2Cl_2) δ 151.0, 148.9, 147.9, 147.0, 146.0, 141.8, 140.8, 133.5, 132.8, 132.6, 131.0, 130.8, 129.6, 129.5, 128.7, 128.1, 127.8, 127.5, 123.6, 122.6, 121.6, 120.6, 113.0, 111.3, 100.6, 99.4, 94.2, 92.4, 91.0, 89.3, 52.6, 50.5, 33.7, 29.4, 27.1, 26.3, 24.3, 21.8, 15.5; MS(EI) m/z 185(100%), 336(53%), 477(45%); HRMS calcd for $C_{25}H_{23}N_3O_5S$ 477.1360, found 477.1356.

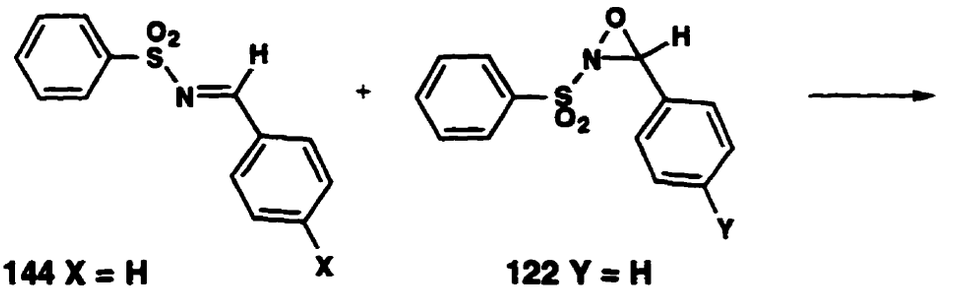
Synthesis of 129 from 2,3-Dimethylindole



129

To a cooled (-5°C) solution of 2,3-dimethylindole (0.511 g, 3.52 mmol) and triethylamine (1 mL) in methylene chloride (20 mL), was added slowly a solution of Br_2 (4.20 mmol) in methylene chloride (6 mL). Ethylene glycol (30 mL) was then added and the solution was allowed to stir for 15 min. A solution of p-toluenesulfonic acid monohydrate in ethylene glycol (100 mmol) was added until an orange colour persisted. The solution was stirred further for 10 min., then basified with 10% NH_4OH (pH 8). The reaction mixture was extracted with methylene chloride. The organic layer was washed with three portions of water (50 mL each), washed with brine (50 mL), dried over magnesium sulfate and concentrated *in vacuo*. The residue was purified by column chromatography on silica gel with elution by 10% ethyl acetate/hexane to give **129** as a white solid (0.583 g, 81%): mp 77-78°C; IR (KBr) 3327 cm^{-1}; ^1H NMR (250 MHz, $CDCl_3$) δ 7.25-7.11 (m, 2H), 6.85 (d, J=5.9 Hz, 1H), 6.66 (d, J=6.2 Hz, 1H), 4.12 (s, 1H), 3.75-3.65 (m, 4H), 1.52 (s, 3H), 1.37 (s, 3H); ^{13}C NMR (50.3 MHz, $CDCl_3$) δ 147.5, 131.0, 128.8, 122.9, 120.0, 110.3, 93.0, 81.4, 61.2, 60.9, 23.2, 17.7; MS(EI) m/z 205; HRMS calcd for $C_{12}H_{15}NO_2$ 205.1103, found 205.1104; Anal. Calcd. for $C_{12}H_{15}NO_2$: C, 70.22; H, 7.37; N, 6.82. Found: C, 70.08; H, 7.51; N, 6.76.

General Procedure for Testing Exchange Between Davis' Reagent and N-Benzenesulfonylimines



144 X = H
146 X = NO_2

122 Y = H
145 Y = NO_2

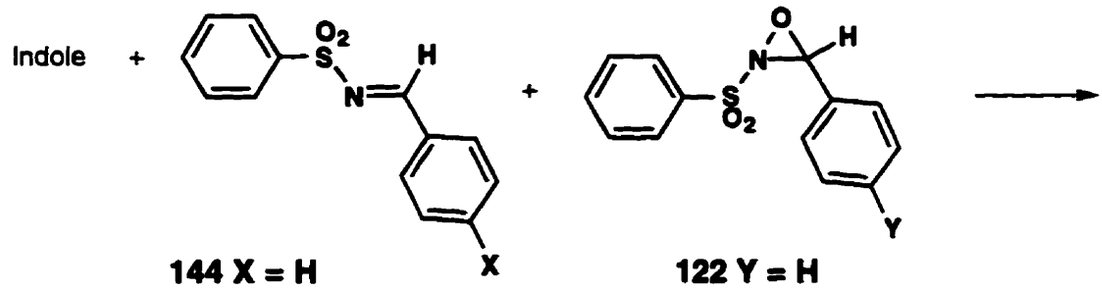
A solution of the imine (0.082 mmol) and oxaziridine (0.082 mmol) in THF (0.5 mL) was stirred at room temperature under a nitrogen atmosphere for 10 h. The solvent was removed *in vacuo*. The residue was analyzed by TLC and ^{1}H NMR. The following experiments were carried out:

a) **144** and **145**

b) **146** and **122**

In both cases, exchange between the imine and the oxaziridine was not observed.

General Procedure for Cross-Over Experiments



144 X = H
146 X = NO_2

122 Y = H
145 Y = NO_2

To a solution of the indole (0.51 mmol) and imine (0.51 mmol) in THF (3.0 mL) was added a solution of oxaziridine (0.51 mmol) in THF (2.0 mL). The reaction mixture was allowed to stir at room temperature and the progress of the reaction was monitored by TLC. Upon detection of complete disappearance of the starting indole by TLC analysis, the solvent in the reaction mixture was removed *in vacuo*. The product composition was analyzed by TLC and compared with authentic material. The product distribution was also analyzed by ^{1}H NMR. The following experiments were carried out:

a) cyclopentanoindole **142** with **144** and **145**

b) cyclopentanoindole **142** with **146** and **122**

c) 2,3-dimethylindole **140** with **144** and **145**

d) 2,3-dimethylindole **140** with **146** and **122**

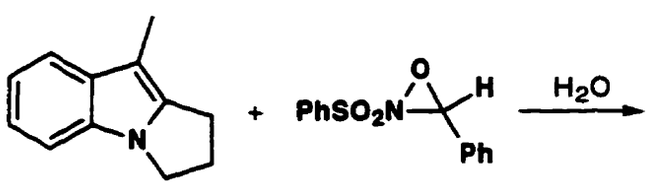
e) pyrroloindole **114** with **144** and **145**

f) pyrroloindole **114** with **146** and **122**

g) 2,3-dimethylindole **140** (0.19 mmol), with **144** (1.9 mmol), with **145** (0.19 mmol)

In all the above experiments (a-f), analysis by TLC as well as analysis of ^{1}H NMR spectra showed no cross-over product formation. A cross-over experiment in which the imine was present in 10 fold excess was also performed (exp. g). Again, the cross product was not observed by TLC or by ^{1}H NMR.

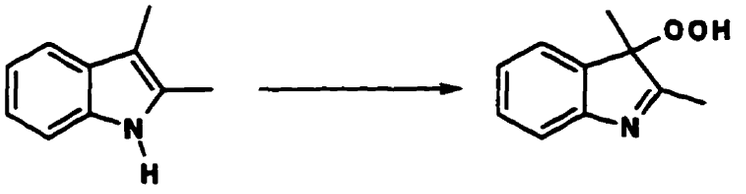
Reaction of pyrrolo[1,2-a]indole 114 with Davis reagent in the Presence of Water



114 **122**

A solution of indole (0.6 mmol), Davis' reagent (0.6 mmol), THF (3.0 mL) and water (1.0 mL) was stirred at room temperature for 3 h under a nitrogen atmosphere. The reaction mixture was diluted with methylene chloride (30 mL). The organic phase was washed with water, brine, dried over sodium sulfate and the solvent removed *in vacuo*. The ^{1}H NMR spectrum of the residue indicated the presence of **138** as well as benzaldehyde and benzenesulfonamide (from hydrolysis of the imine). The ^{1}H NMR spectrum failed to show any indication of the presence of the dihydroxy compound **120c**.

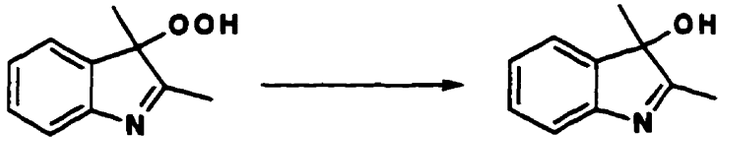
Synthesis of 3-Hydroperoxy-2,3-dimethylindole



140

Oxygen was bubbled through a cold (ice bath) solution of 2,3-dimethyl indole (**140**) (2.0 g, 15 mmol) in petroleum ether (60-80°C fraction, 200 mL) for 12 h with vigorous stirring. The white solid formed in the reaction was filtered and washed with several portions of petroleum ether. The peroxide (2.17 g, 87%) was utilized without further purification.[90]

Synthesis of 2,3-dimethyl-3-hydroxyindolenine

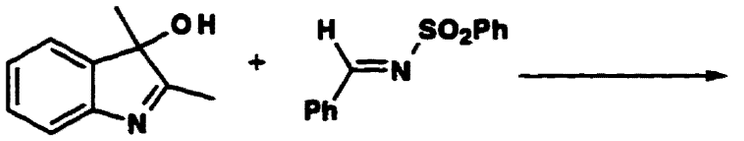


152

Sodium dithionite (0.471 g of 85%) was added to a solution of the hydroperoxide (0.2 g, 1.2 mmol) in ether (6 mL) suspended with aqueous NaOH (2N, 3.5 mL). The mixture was stirred at room temperature for 1.5 h and then diluted with ether (10 mL). The aqueous layer was discarded and the organic layer was washed

with water, brine and the solvent removed *in vacuo*. The product **152** (85%) was utilized without further purification.[90]

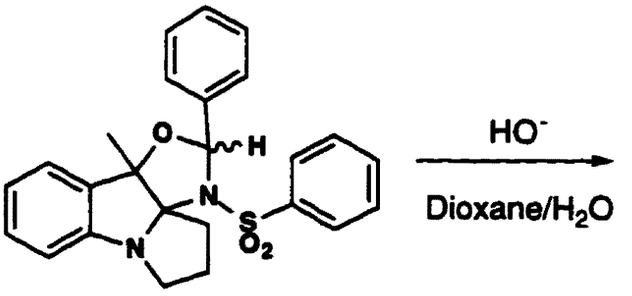
Reaction of 3-hydroxy-2,3-dimethylindolenine with 144



152 **144**

A solution of indolenine **152** (0.065 g, 0.4 mmol) and imine **144** (0.0989 g, 0.4 mmol) in THF (2.0 mL) was stirred at room temperature under an argon atmosphere for 3 h. The solvent was removed *in vacuo*. TLC and ^{1}H NMR analysis showed only starting materials.

Reaction of 138 with aqueous base



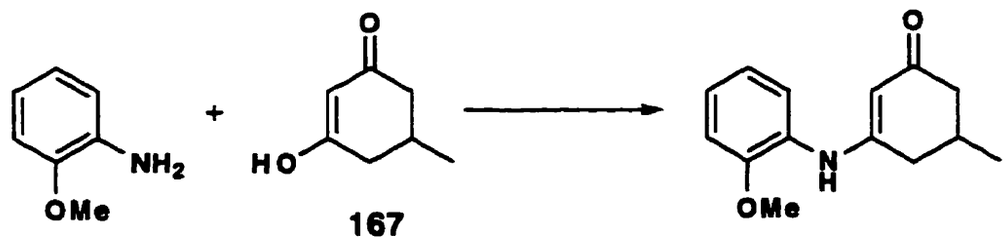
138

A solution of **138** (0.0103 g, 0.024 mmol) in dioxane (0.5 mL) and water (0.5 mL) containing sodium hydroxide (1M, 0.5 mL) was heated at reflux for 3 h. The reaction mixture was diluted with water and extracted with ethyl acetate. The organic phase was washed with water, brine and the solvent was removed *in vacuo*. TLC and ^{1}H NMR analysis showed only starting material present.

Reaction of 138 with aqueous acid

The above reaction was repeated with sulfuric acid (1M, 0.5 mL) instead of sodium hydroxide and again only starting material was observed by TLC and ^{1}H NMR analysis.

Synthesis of Anilinoketone 168

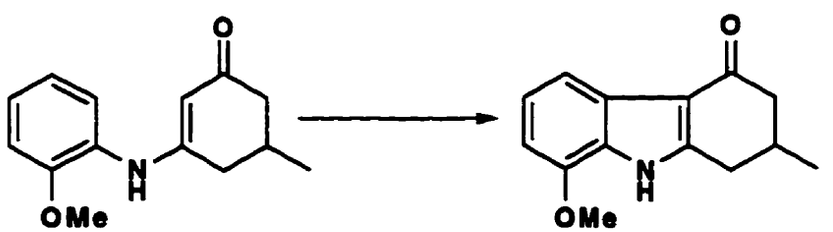


166 **167** **168**

A solution of *o*-anisidine, **166**, (8.95 mL, 79.4 mmol), 5-methylcyclohexane-1,3-dione, **167**, (10.0 g, 79.4 mmol) and p-toluenesulfonic acid monohydrate (1.0 g, 5.3 mmol) in toluene (200 mL) was heated at reflux for 6 h. The solvent was removed *in vacuo* leaving a bright yellow solid. A solution of the residue in

methylene chloride was washed with water, brine and dried over magnesium sulfate. The solvent was removed *in vacuo* leaving a residue which was recrystallized from methylene chloride/hexane to give **168** as a pale yellow solid (15.85 g, 86%): mp 142.5-144°C; *Rf* 0.21 (4:1 ethyl acetate/hexane); IR (KBr) 3240, 1544(br) cm^{-1}; ^1H NMR (500 MHz, CD_2Cl_2) δ 7.33 (dd, J=7.6, 1.6 Hz, 1H), 7.12-7.08 (m, 1H), 6.95-6.92 (m, 2H), 6.46 (br. s, 1H), 5.57 (d, J=1.0 Hz, 1H), 3.84 (s, 3H), 2.44 (ddd, J=11.3, 8.9, 1.5 Hz, 1H), 2.35-2.19 (m, 3H), 2.01 (dd, J=11.3, 4.7 Hz, 1H), 1.08 (d, 6.4 Hz, 3H); ^{13}C NMR (125.8 MHz, CD_2Cl_2) δ 199.4, 162.4, 153.1, 129.9, 126.8, 124.8, 122.1, 113.0, 101.5, 55.0, 46.9, 40.1, 31.5, 22.5; MS(EI): m/z 231 (100%), 189 (44%), 174 (24%); HRMS calcd for $C_{14}H_{17}NO_2$ 231.1260, found 231.1259; Anal. Calcd. for $C_{14}H_{17}NO_2$: C, 72.70; H, 7.41; N, 6.06. Found: C, 72.75; H, 7.50; N, 6.06.

Synthesis of 4-keto-1,2,3,4-tetrahydrocarbazole 169

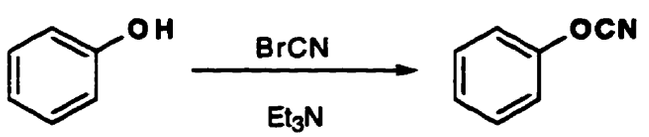


168 **169**

A mixture of **168** (4.11 g, 17.8 mmol), palladium acetate (4.4 g, 19.6 mmol) and glacial acetic acid (450 mL) was heated at reflux with stirring for 7 h. The reaction mixture was cooled to room temperature and filtered through celite. The solvent was removed from the filtrate *in vacuo* leaving a brown solid. The residue was recrystallized from methylene chloride to give **169** as a tan solid (4.12 g, 64%): mp 262-263°C; *Rf* 0.6 (8:2 ethyl acetate/hexane); IR (KBr) 3015, 1613 cm^{-1}; ^1H NMR

(250 MHz, DMSO-d_6) δ 7.51 (d, J=7.7 Hz, 1H), 7.05 (dd, J=7.7, 7.9 Hz, 1H), 6.75 (d, J=7.9 Hz, 1H), 6.41 (br. s, 1H), 3.91 (s, 3H), 2.99 (dd, J=3.1, 16 Hz, 1H), 2.66-2.17 (m, 4H), 1.10 (d, J-6.0 Hz, 3H); ^{13}C NMR (62.9 MHz, DMSO-d_6) δ 192.5, 151.1, 145.7, 125.8, 125.7, 122.2, 112.8, 111.8, 103.5 55.2, 46.1, 31.1, 30.6, 20.8; MS(EI) m/z 229(100%), 187(73%); HRMS calcd for $C_{14}H_{15}NO_2$ 229.1104, found: 229.1103; Anal. Calcd. for $C_{14}H_{15}NO_2$: C, 73.34; H, 6.59; N, 6.11. Found: C, 73.44; H, 6.65; N, 6.09.

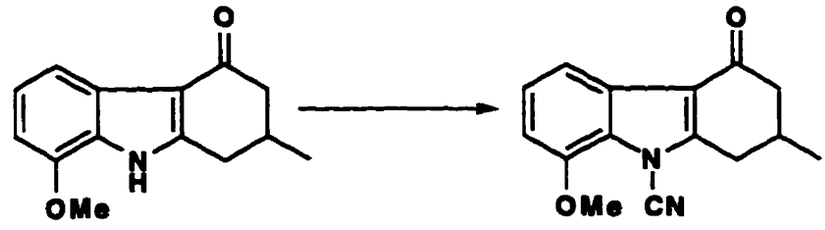
Synthesis of Phenyl Cyanate[158] (172)



173 **172**

Triethylamine (19.6 mL, 140 mmol) was added slowly to a cooled solution of cyanogen bromide (14.2 g, 134 mmol), phenol (12.5 g, 133 mmol), pentane (67 mL) and diethyl ether (27 mL). The temperature was kept below 30°C during the addition. The reaction mixture was allowed to stir at 0°C for 1 h. The white solid formed in the reaction was removed by filtration and washed with pentane (3 x 40 mL). The filtrate and washings were combined and the solvent removed *in vacuo* leaving a pale yellow oil (13.1 g, 83%). IR (Neat) 2275 cm^{-1}.

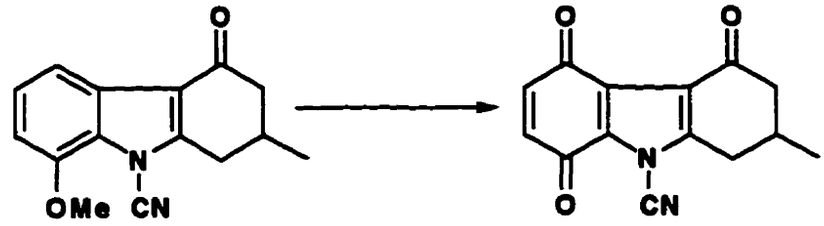
Synthesis of 9-cyano-4-keto-8-methoxy-1,2,3,4-tetrahydrocarbazole 174



169 **174**

To a solution of **169** (3.97 g, 17.3 mmol) and phenyl cyanate (3.0 mL) in dry dimethyl sulfoxide (60 mL) was added dry triethylamine (5.4 mL, 38.0 mmol). This mixture was allowed to stir overnight under an argon atmosphere. The reaction was diluted with water (100 mL) and extracted with ethyl acetate (3x50 mL). The extracts were combined and washed with water, brine and dried over magnesium sulfate. The residue was then purified by column chromatography eluting with methylene chloride to yield **174** as a white solid (4.11 g, 94%): mp 165-166°C; *Rf* 0.47 (2:3 ethyl acetate/hexane); IR (KBr) 2245, 1666 cm^{-1}; ^{1}H NMR (250 MHz, $CDCl_3$) δ 7.70 (d, J=8.0 Hz, 1H), 7.27 (t, J=8.0 Hz, 1H), 6.82 (d, J=8.0 Hz, 1H), 3.97 (s, 3H), 3.10 (dd, J=4.1, 16.7 Hz, 1H), 2.72-2.29 (m, 4H), 1.25 (d, J=6.2 Hz, 3H); ^{13}C NMR (62.9 MHz, CDCl3) δ 193.3, 151.5 156.6, 126.4, 125.6, 124.5, 117.1, 114.3, 107.1, 106.1, 55.9, 46.1, 30.8, 29.7, 21.1; MS(EI) m/z 254(100%), 212(58%); HRMS calcd for $C_{15}H_{14}N_2O_2$ 254.1056, found: 254.1049; Anal. Calcd. for $C_{15}H_{14}N_2O_2$: C, 70.85; H, 5.55; N, 11.02. Found: C, 70.99; H, 5.54; N, 10.89.

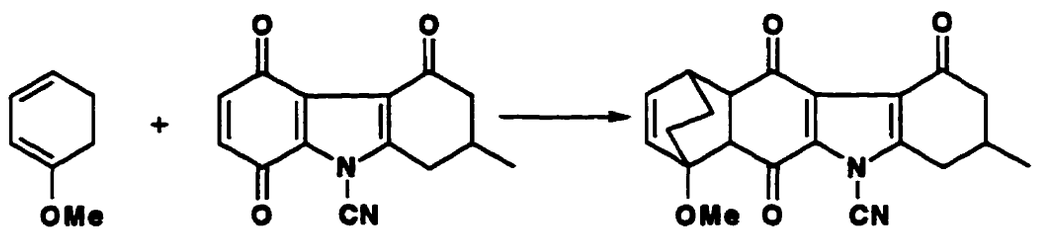
Synthesis of 9-cyano-4-keto-1,2,3,4-tetrahydrocarbazole-5,8-dione 174



174 **165**

To a cooled solution of **174** (3.6 g, 14.3 mmol) in acetonitrile (300 mL) was added slowly a cooled solution of ceric ammonium nitrate (50.2 g, 91.5 mmol) in water (150 mL). The solution was allowed to stir at room temperature overnight. Water (500 mL) was added and the solution was extracted with ethyl acetate (3 portions). Removal of the solvent *in vacuo* from the dried organic phase yielded a residue which was recrystallized from acetone/water to give a yellow solid (2.8 g, 79%): mp 200°C (decomp.); *Rf* 0.55 (4:1 ethyl acetate/hexane); IR (KBr) 2258, 1689, 1667 cm^{-1}; ^1H NMR (200 MHz, $CDCl_3$) δ 6.82 (d, J=10.4 Hz, 1H), 6.75 (d, J=10.4 Hz, 1H), 3.18 (dd, J=17, 3.7 Hz, 1H), 2.3-2.7 (m, 4H), 1.25 (d, J=6.1 Hz, 3H); ^{13}C NMR (62.9 MHz, $CDCl_3$) δ 189.5, 179.3, 175.6, 152.2, 138.8, 134.3, 132.5, 120.5, 102.9, 96.2, 46.9, 30.3, 29.8, 20.8; MS(EI) m/z 254(37%), 212(100%), 187(44%), 184(34%); HRMS calcd for $C_{14}H_{10}N_2O_3$ 254.0692, found 254.0698; Anal. Calcd. for $C_{14}H_{10}N_2O_3$: C, 66.14; H, 3.96; N, 11.02. Found: C, 66.09; H, 4.24; N, 10.72.

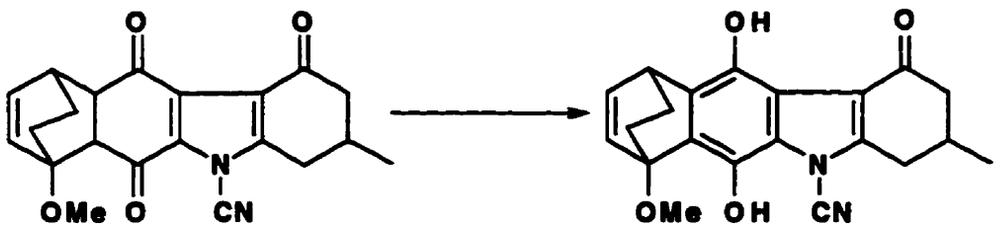
Synthesis of the Diels-Alder adduct 175



155 **165** **175**

To a solution of the quinone **165** (2.35 g, 9.3 mmol) in DMF (40 mL) was added 1-methoxy-1,3-cyclohexadiene (3.06 g, 27.8 mmol). The solution was stirred overnight, diluted with water and extracted with several portions of ethyl acetate. The combined organic extracts were washed with water, brine and dried over sodium sulfate. The solvent was removed *in vacuo* leaving a dark brown solid. The residue was recrystallized from THF/hexane to give the adduct **175** as an off-white solid (3.0 g, 89%): mp 166°C (decomp.); *Rf* 0.23 (3:2 ethyl acetate/hexane): IR (KBr) 2257, 1702, 1675 cm^{-1}; ^1H NMR (200 MHz, CD_2Cl_2) δ 6.15-6.02 (m, 2H), 3.47 (s, 3H), 3.42 (s, 1H), 3.23-3.05 (m, 2H), 2.7-1.4 (m, 9H), 1.19 (d, J=6.1 Hz, 3H); MS(EI) m/z 364(13%), 336(44%), 256(27%), 110(100%); HRMS calcd for $C_{21}H_{20}N_2O_4$ 364.1424, found 364.1463; Anal. Calcd. for $C_{21}H_{20}N_2O_4$: C, 69.22; H, 5.53; N, 7.69. Found: C, 69.14; H, 5.70; N, 7.50.

Preparation of hydroquinone 178

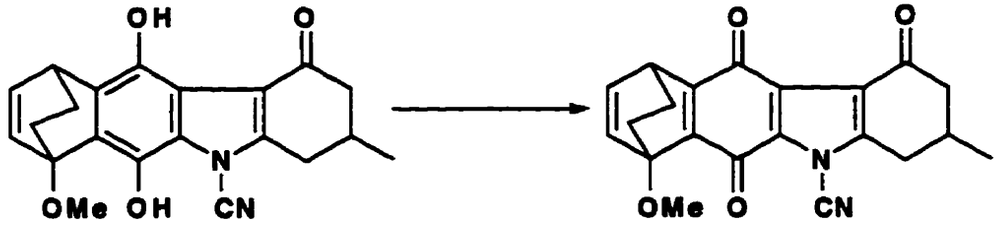


175 **178**

To a cooled (ice bath) solution of the adduct **175** (0.099 g, 0.27 mmol) in methylene chloride (10 mL) was added $CDCl_3$** (1 mL). The solution was brought up to room temperature and allowed to stir for 3 h. The reaction was monitored by TLC until completion. The solution was washed with water and dried over sodium sulfate. Removal of the solvent *in vacuo* produced the hydroquinone **178** as a solid residue which was analytically pure and was used directly in the oxidation step described below. A suitable crystal for an X-ray diffraction study (Appendix B, page 272) was obtained form THF/toluene: *Rf* 0.57 (2:3 ethyl acetate/hexane); IR (KBr) 3307, 2249, 1637 cm^{-1}; ^1H NMR (250 MHz, $CDCl_3$) δ 9.80 (s, 1H), 9.05 (s, 1H), 6.66 (dd, J=1.1, 8.3 Hz, 1H), 6.55 (dd, J=6.2, 8.3 Hz, 1H), 4.45-4.32 (m, 1H), 3.68 (s, 3H), 3.13 (dd, J=3.6, 16 Hz, 1H), 2.75-2.33 (m, 4H), 2.12-2.03 (m, 1H), 1.72-1.52 (m, 3H), 1.25 (d, J=6.2 Hz, 3H); ^{13}C NMR (50.3 MHz, CD_2Cl_2) δ 197.16, 152.38, 137.37, 135.43, 134.32, 133.09, 126.45, 125.36, 122.57, 118.08, 112.27, 106.46, 87.12, 45.16, 32.76, 31.56, 31.45, 30.02, 28.54, 25.97, 20.91; MS(EI) 364; HRMS calcd for $C_{21}H_{20}N_2O_4$ 364.1424, found 364.1411; Anal. Calcd. for $C_{21}H_{20}N_2O_4$: C, 69.22; H, 5.53; N, 7.69. Found: C, 69.00; H, 5.69; N, 7.49.

This reaction was first detected during attempts to record NMR spectra of the adduct **178 in $CDCl_3$. The catalytic effect was observed with many but not all samples of $CDCl_3$ and is undoubtedly the result of the presence of traces of DCl. The suitability of a given sample of $CDCl_3$ for this reaction was determined in very small scale transformations of **175** to **178** monitored by TLC analysis. Preliminary experiments indicate that this reaction can also be effected cleanly in 2 h by addition of a saturated solution of HCl in CH_2Cl_2 (0.05 mL) to a solution of **175** (2.2 mg) in CH_2Cl_2 (0.5 mL).

Synthesis of quinone 176

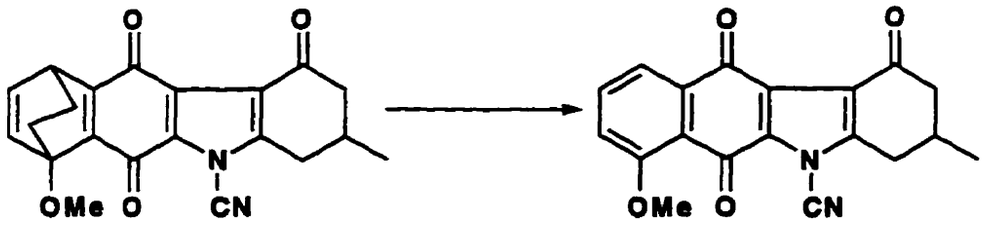


178 **176**

To a cooled (-78°C) solution of the hydroquinone **178** (obtained from the reduction step above) in 20:1 acetone:water (5 mL) was added slowly a solution of DDQ (0.709 g, 0.31 mmol) in 20:1 acetone:water (15 mL). The reaction was stirred at -78°C for 1.5 h. The solvent was removed *in vacuo* and the residue was dissolved in methylene chloride. The organic layer was washed with water and dried over sodium sulfate. Byproducts derived from DDQ were removed by stirring the organic layer with alumina. The suspension was filtered and the solvent was removed from the filtrate *in vacuo*. Recrystallization of the solid residue from acetone gave **176** as a bright yellow solid (0.092 g, 93% from **175**): mp 216°C (decomp.); *Rf*

0.64 (4:1 ethyl acetate/hexane); IR (KBr) 2259, 1694, 1661 cm^{-1}; ^1H NMR (200 MHz, CD_2Cl_2) δ 6.59 (dd, J=7.7, 1.0 Hz, 1H), 6.38 (dd, J=7.7, 6.1 Hz, 1H), 4.43-4.38 (m, 1H), 3.13 (dd, J=16.1, 4.3 Hz, 1H), 2.72-2.26 (m, 4H), 1.82-1.26 (m, 4H), 1.20 (d, J=6.1 Hz, 3H); ^{13}C NMR (62.9 MHz, CD_2Cl_2) δ 190.2, 176.3, 173.0, 152.5, 151.7, 144.0, 135.6, 133.7, 131.7, 122.8, 120.4, 103.8, 85.4, 55.8, 47.4, 34.5, 31.4, 30.7, 30.1, 25.2, 20.9; MS(EI) m/z 334(62%) [M-28], 292(36%), 264(75%), 237(100%); Anal. Calcd. for $C_{21}H_{18}N_2O_4$: C, 69.60; H, 5.00; N, 7.73. Found: C, 69.41; H, 5.22; N, 7.56.

Synthesis of ketone 177

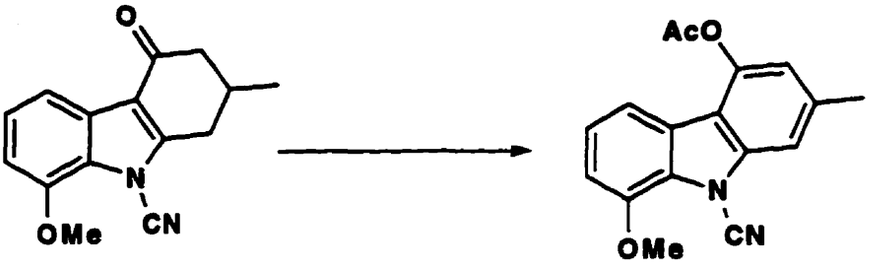


176 **177**

A solution of the quinone **176** (0.503 g, 1.4 mmol) in toluene was heated at reflux for 3.5 h and was stored at 4°C overnight. The precipitate which was formed was collected by filtration and washed with a small quantity of toluene. The reddish solid was recrystallized from acetone/hexane to give **177** as a bright yellow solid (0.434 g, 94%): *Rf* 0.33 (4:1 ethyl acetate/hexane); IR (KBr) 2256, 1697, 1658 cm^{-1}; ^1H NMR (250 MHz, $CDCl_3$) δ 7.89 (dd, J=7.7, 1.1 Hz, 1H), 7.73 (dd, J=8.4, 7.7 Hz, 1H), 7.34 (dd, J=8.5, 0.9 Hz, 1H), 4.05 (s, 3H), 3.21 (dd, J=17.0, 3.9 Hz, 1H), 2.41-2.81 (m, 4H), 1.27 (d, J=6.2 Hz, 3H); MS(EI) m/z 334(61%), 292(31%), 264(59%),

237(100%); HRMS calcd for $C_{19}H_{14}N_2O_4$ 334.0954, found 334.0978; Anal. Calcd. for $C_{19}H_{14}N_2O_4$: C, 68.26, H, 4.22; N, 8.38. Found: C, 68.43; H, 4.07; N, 8.19.

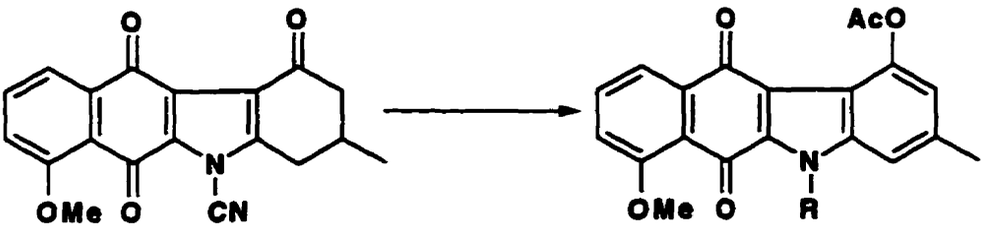
Synthesis of 189



174 **189**

To a cooled (ice bath) solution of ketone **174** (0.100 g, 0.3 mmol and DDQ (0.071 g, 0.3 mmol) in isopropenyl acetate (25 mL) was added one drop of sulfuric acid (12 M). The mixture was allowed to stir at ice bath temperature for 2 h and equilibrated to room temperature overnight. Methylene chloride was added and the organic layer was washed with water, dried over sodium sulfate and the solvent was removed *in vacuo*. The solid residue was purified by preparative layer chromatography eluting 40% ethyl acetate/hexane (0.053 g, 48%): IR (KBr) 2250, 1678 cm^{-1}; ^1H NMR (200 MHz, CD_2Cl_2) δ 7.79 (dd, J=7.8, 1.0 Hz), 7.74 (dd, J=8.2, 7.8 Hz), 7.53 (s, 1H), 7.44 (dd, J=8.2, 1.0 Hz), 7.11 (s, 1H), 4.06 (s, 3H), 2.58 (s, 3H), 2.51 (s, 3H); MS(EI) m/z 280(5.3%), 238(100%). Anal. Calcd. for $C_{17}H_{14}NO_3$: C, 72.85; H, 5.03; N, 5.00, Found: C, 72.50; H, 4.98; N, 4.87.

Synthesis of 190 and isolation of 191



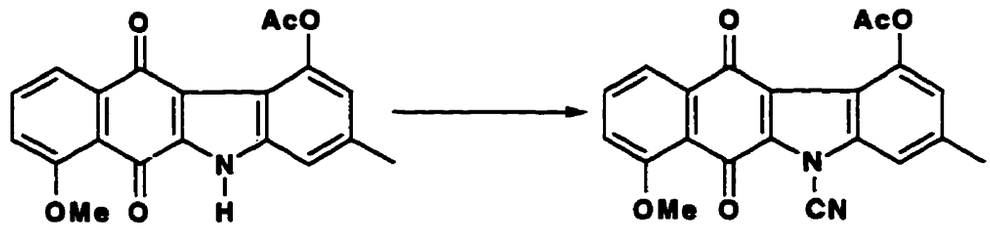
177 **190 R = CN**
191 R = H

To a cooled (ice bath) suspension of ketone **177** (0.110 g, 0.3 mmol and DDQ (0.086 g, 0.36 mmol) in isopropenyl acetate (25 mL) was added one drop of sulfuric acid (12 M). The mixture was allowed to stir at ice bath temperature for 2 h and at room temperature for 12 h. Methylene chloride was added and the solution was filtered to remove small amounts of insoluble material. The precipitate, which was produced in variable amounts, was identified as the decyanated analog of **190**. The filtrate was washed with water, dried over sodium sulfate and the solvent was removed *in vacuo.* The solid residue was recrystallized from methylene chloride and from acetone leaving **190** as a bright yellow solid (0.075 g, 61%): *Rf* 0.59 (4:1 ethyl acetate/hexane); IR (KBr) 2252, 1770, 1668 cm^{-1}; ^{1}H NMR (500 MHz, CD_2Cl_2) δ 7.86 (dd, J=7.6, 1.1 Hz, 1H), 7.75 (dd, J=8.5, 7.7 Hz, 1H), 7.47 (br. s, 1H), 7.37 (dd, J=8.5, 1.1 Hz, 1H), 7.04 (br. s, 1H), 4.04 (s, 3H), 2.56 (s, 3H), 2.53 (s, 3H); ^{13}C NMR (125.8 MHz, CD_2Cl_2) δ 178.8, 175.2, 170.4, 161.1, 146.3, 142.6, 140.7, 137.7, 136.3, 136.2, 122.2, 120.9, 118.6, 116.1, 110.3, 105.0, 56.9, 22.0, 21.6; MS(EI) m/z 374(6.5%), 332(100%); HRMS calcd for $C_{21}H_{14}N_2O_5$ 374.0903, found 374.0912; Anal. Calcd. for $C_{21}H_{14}N_2O_5$: C, 67.38; H, 3.77; N, 7.48, Found: C, 67.33; H, 3.76; N, 7.34.

The decyanated material **191** was isolated by filtration of the reaction mixture of the aromatization of **177**, as described above, and was washed with several

portions of methylene chloride and dioxane to yield a bright yellow solid (0.017 g, 15%). IR (KBr) 3252, 1754, 1651 cm^{-1}; ^1H NMR (200 MHz, $CDCl_3$) δ 7.98-7.60 (m, 3H), 7.39-7.7.22 (m, 2H), 6.80 (s, 1H), 4.06 (s, 3H), 2.52 (s, 3H); MS(EI) m/z 349(5.2%); HRMS calcd for $C_{20}H_{15}NO_5$ 349.0951, found 349.0948.

Cyanation of 191



191 **190**

To a cooled (ice bath) stirred suspension of **191** (0.0326 g, 0.093 mmol) and phenyl cyanate (0.066 g, 0.55 mmol) in dimethyl sulfoxide (1.5 mL) was added slowly triethylamine (30 μL, 0.205 mmol). The reaction mixture was allowed to equilibrate to room temperature and was stirred overnight. The reaction mixture was diluted with ethyl acetate and washed with water, brine, dried over sodium sulfate and solvent removed *in vacuo*. The residue was recrystallized from methylene chloride to give **190** a bright yellow solid (0.0307 g, 88%) which was spectroscopically and chromatographically identical to **190** as prepared above.

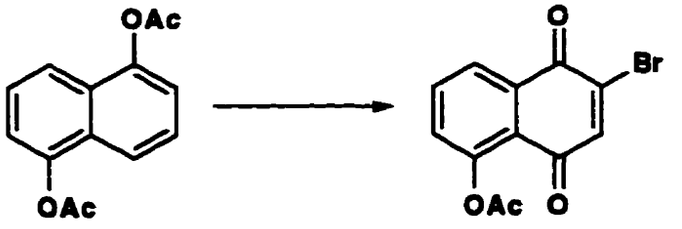
Acetylation of 1,5-dihydroxynaphthalene



253 **251**

Acetic anhydride (29.5 mL, 312 mmol) was added slowly to a cooled solution (ice bath) of 1,5-dihydroxynaphthalene (**253**) (20.2 g, 126 mmol) in methylene chloride (400 mL) and pyridine (25.2 mL, 312 mmol) and the solution was stirred at ice bath temperature for an additional five minutes and then equilibrated to room temperature over 2 h. The reaction mixture was diluted with methylene chloride, washed with several portions of water and brine, dried over sodium sulfate and the solvent was removed *in vacuo*. The residue was recrystallized from ethyl acetate/hexane leaving **251** as an off white solid (25.8 g, 85%): *Rf* 0.51 (40% ethyl acetate/hexane); IR (KBr) 1751 (br. s) cm^{-1}; ^{1}H NMR (250 MHz, $CDCl_3$) δ 7.84 (d, J=8.6 Hz, 2H), 7.54 (dd, J=8.6, 7.5 Hz, 2H), 7.33 (d, J=7.5 Hz, 2H), 2.50 (s, 6H); ^{13}C NMR (62.9 MHz, $CDCl_3$) δ 170.1, 147.6, 129.0, 126.9, 120.2, 119.7, 21.8.

Synthesis of 254

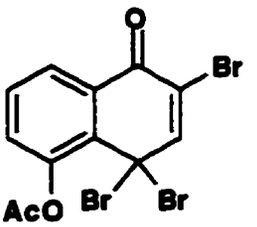


251 **254**

To a cooled solution of N-bromosuccinimide (50.1 g,) in acetic acid (700 mL) and water (1000 mL) was added a warm solution of **251** (17.0 g, 69.7 mmol) in acetic acid (700 mL). The reaction mixture was heated to 65-70°C and maintained at this temperature for 45 min. The reaction mixture was then cooled and diluted with water (1000 mL). Solid formed in the reaction was filtered and washed with several portions of water. The solid was then dissolved in methylene chloride (300 mL), washed with water, brine, dried over sodium sulfate and the solvent removed *in vacuo* leaving a yellow solid. The residue was recrystallized from methylene chloride/cyclohexane leaving **254** as a bright yellow solid (18.6 g, 91%).**: *Rf* 0.29 (20% ethyl acetate/hexane); IR (KBr) 1778, 1679, 1663 cm^{-1}; ^1H NMR (250 MHz, CD_2Cl_2) δ 8.12 (dd, J=8.0, 1.1 Hz, 1H), 7.79 (t, J=8.0 Hz, 1H), 7.44 (dd, J=8.0, 1.1 Hz, 1H), 7.40 (s, 1H), 2.40 (s, 3H); ^{13}C NMR (50.3 MHz, $CDCl_3$) δ 180.8, 169.2, 149.8, 141.3, 138.4, 134.9, 132.5, 130.2, 126.3, 123.2, 21.0; MS(CI) m/z 312 $[M+18]^+$.

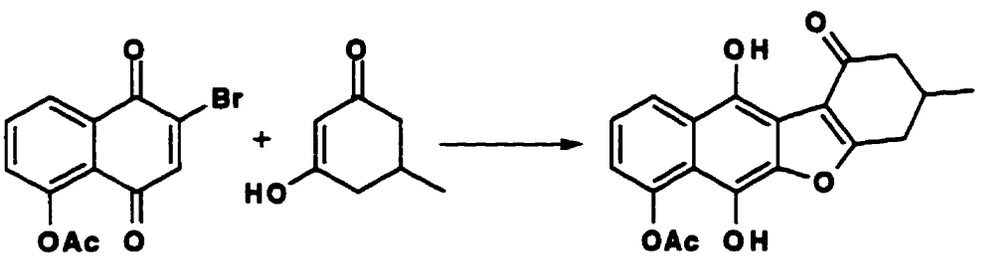
**If the reaction is kept at 50-55°C instead of 65-70°C and the water content was reduced by 30%, then the isolated product has the following properties: ^1H NMR (250 MHz, CD_2Cl_2) δ 8.06 (dd, J=7.5, 1.7 Hz, 1H), 7.99 (s, 1H), 7.68-7.56 (m, 2H),

2.50 (s, 3H); ^{13}C NMR (50.3, $CDCl_3$) δ 174.9, 167.9, 148.6, 134.0, 130.9, 129.9, 126.7, 124.9, 119.9, 41.7, 21.6. This product is believed to be **256** (below).



256

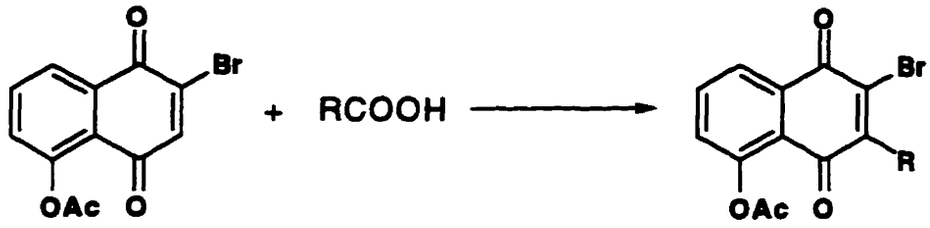
Reaction of 254 with 5-methyl-1,3-cyclohexanedione



254 **167** **258**

To a mixture of quinone **254** (0.979 g, 3.3 mmol), dione **167** (0.419 g, 3.3 mmol) in ethanol was slowly added a solution of diisopropylethylamine (0.96 g, 6.97 mmol) in ethanol (2 mL). The reaction mixture was allowed to stir at room temperature for 2 h. Solid formed in the reaction mixture was filtered off and the filtrate was acidified with dilute HCl (2M) with cooling (ice bath). The product **258** was filtered and dried under high vacuum (0.716 g, 63%): IR (KBr) 3448, 1771, 1698 cm-1; ^1H NMR (200 MHz, CD_2Cl_2) δ 8.15 (dd, J=7.7, 1.3 Hz, 1H), 7.78 (dd, J=8.1, 7.7 Hz, 1H), 7.42 (dd, J=8.1, 1.3 Hz, 1H), 3.23-3.12 (m, 1H), 2.81-2.30 (m, 4H), 2.47 (s, 3H), 1.21 (d, J=6.2 Hz, 3H); MS(EI) m/z 340.

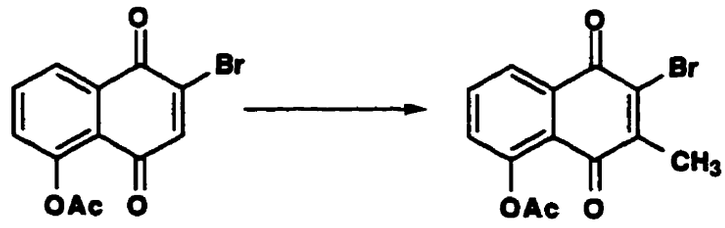
General Procedure for Oxidative Substitution of 254:



254

A solution of quinone **254** (0.3 mmol), the carboxylic acid (0.3 mmol), and silver nitrate (15 mg, 0.08 mmol) in acetonitrile (2.5 mL) was warmed to 60°C. Ammonium persulfate (178 mg, 0.78 mmol) in water (3 mL) was added slowly to the reaction mixture. Upon complete addition of the persulfate solution, the reaction mixture was heated to 95°C and stirred at this temperature for 1 h. The reaction mixture was then cooled to room temperature, diluted with water (20 mL) and extracted with several portions of methylene chloride. The organic phase was dried over sodium sulfate and the solvent removed *in vacuo*.

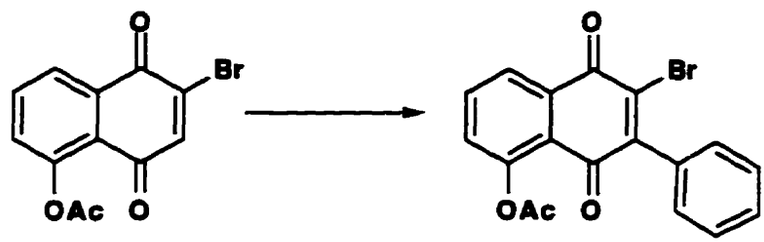
Oxidative Methylation of 254



254 **270a**

The time that the reaction mixture was maintained at 95°C was extended to 2 h and the progress of the reaction was monitored by TLC. The quinone **270a** was purified by column chromatography eluting with 20% ethyl acetate/hexane to give a bright yellow solid (91%): *Rf* 0.28 (20% ethyl acetate/hexane); IR (KBr) 1765, 1672, 1662 cm^{-1}; ^1H NMR (250 MHz, C_6D_6) δ 7.86 (dd, J=7.4, 1.5 Hz, 1H), 6.95-6.83 (m, 2H), 2.21 (s, 3H), 1.95 (s, 3H); ^{13}C NMR (62.9 MHz, C6D6) δ 176.2, 174.1, 168.6, 150.2, 148.8, 141.0, 137.8, 133.2, 129.7, 125.5, 20.8, 17.5; MS(CI) m/z 309 $[M+1]^+$.

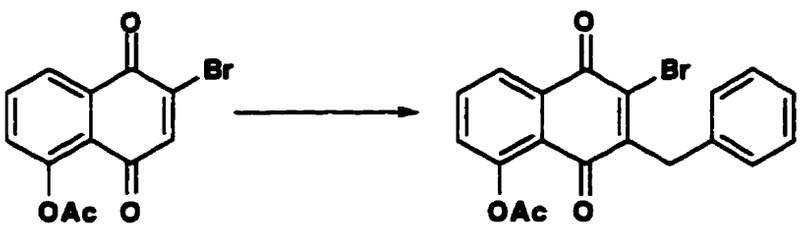
Oxidative coupling of benzoic acid with 254



254 **270b**

The adduct **270b** was recrystallized from ethyl acetate/hexane to give a bright yellow solid (79%): *Rf* 0.58 (40% ethyl acetate/hexane); IR(KBr) 1763, 1674, 1661 cm^{-1}; ^1H NMR (250 MHz, CD_2Cl_2) δ 8.18 (dd, J=7.8, 1.3 Hz, 1H), 7.82 (t, J=8.0 Hz, 1H), 7.52-7.44 (m, 4H), 7.30-7.26 (m, 2H), 2.35 (s, 3H); MS (electrospray) 371.

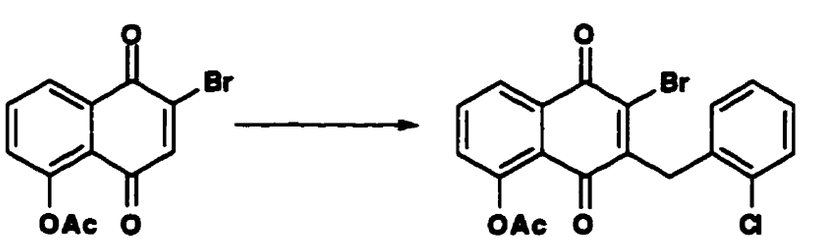
Oxidative coupling of phenylacetic acid with 254



254 **270c**

The adduct **270c** was recrystallized from ethyl acetate/hexane to give a bright yellow solid (84%): *Rf* 0.27 (20% ethyl acetate/hexane); IR (KBr) 1770, 1670 cm^{-1}; ^1H NMR (250 MHz, CD_2Cl_2) δ 8.10 (dd, J=7.8, 1.3 Hz, 1H), 8.41 (dd, J=8.1, 7.8 Hz, 1H), 7.41 (dd, J=8.1, 1.3 Hz, 1H), 7.34-7.18 (m, 5H), 4.18 (s, 2H), 2.42 (s, 3H); ^{13}C NMR (62.9 MHz, $CDCl_3$) δ 181.2, 178.3, 170.2, 151.8, 150.9, 139.5, 137.3, 135.7, 133.7, 131.1, 130.1, 129.6, 127.8, 127.0, 124.0, 37.6, 22.1; MS(EI) m/z 384; HRMS calcd for $C_{19}H_{13}O_4Br$ 383.9997, found 383.9972.

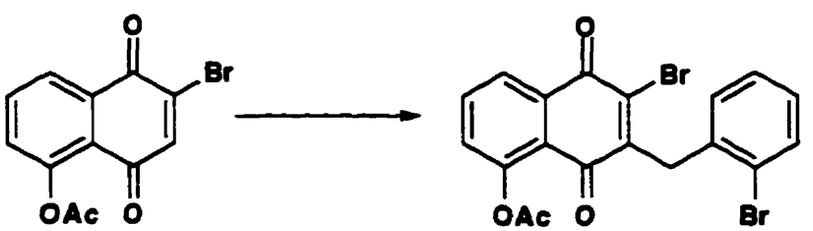
Oxidative coupling *o*-chlorophenylacetic acid with 254



254 **270d**

The adduct **270d** was purified by column chromatography eluting with 20% ethyl acetate hexane yielding a bright yellow solid (86%): *Rf* 0.25 (20% ethyl acetate/hexane); IR (KBr) 1764, 1673 cm^{-1}; ^{1}H NMR (250 MHz, CD_2Cl_2) δ 8.17 (dd, J=7.8, 1.3 Hz, 1H), 7.77 (t, J=8.0 Hz, 1H), 7.43-7.38 (m, 2H), 7.20-7.09 (m, 2H), 6.97-6.93 (m, 1H), 4.27 (s, 2H), 2.40 (s, 3H); ^{13}C NMR (62.9 MHz, $CDCl_3$) δ 180.9, 178.0, 170.1, 151.2, 150.9, 140.9, 135.8, 135.1, 133.7, 131.1, 130.5, 129.7, 128.9, 127.9, 127.0, 124.0, 35.4, 22.0; MS(CI) m/z 419 $[M+1]^+$.

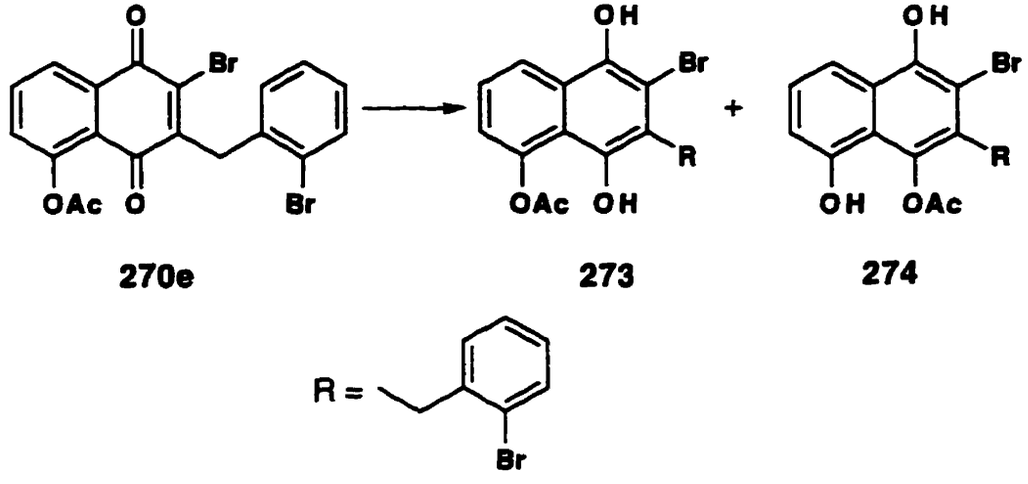
Oxidative coupling of *o*-bromophenylacetic acid with 254



254 **270e**

The adduct **270e** was purified by column chromatography eluting with 20% ethyl acetate hexane yielding a bright yellow solid (85%): *Rf* 0.21 (20% ethyl acetate/hexane); IR (KBr) 1766, 1670 cm^{-1}; ^{1}H NMR (200 MHz, CD_2Cl_2) δ 8.15 (dd, J=7.8, 1.3 Hz, 1H), 7.80 (t, J=7.9 H, 1H), 7.62 (dd, J=7.7, 1.7 Hz, 1H), 7.44 (dd, J=8.0, 1.1 Hz, 1H), 7.23-7.07 (m, 2H), 6.94 (dd, J=7.0, 2.0 Hz, 1H), 4.26 (s, 2H), 2.36 (S, 3H); ^{13}C NMR (62.9 MHz, $CDCl_3$) δ 181.0, 178.0, 170.2, 151.3, 151.0, 141.0, 136.8, 135.8, 133.9, 133.8, 131.2, 129.5, 129.2, 128.6, 127.1, 125.7, 124.0, 38.2, 22.0; MS(CI) m/z 465 $[M+1]^+$.

Reduction of 270e with sodium dithionite



270e **273** **274**

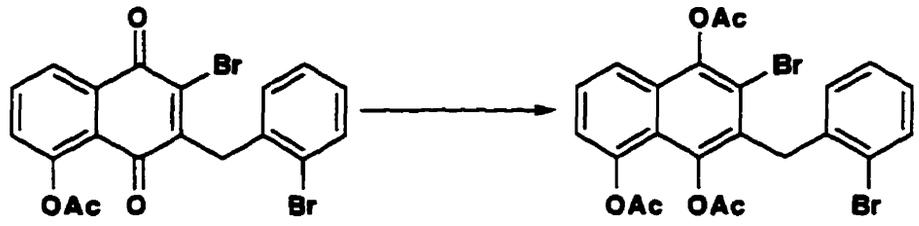
A mixture of **270e** (100 mg, 0.22 mmol), sodium dithionite (77 mg, 0.44 mmol), water (0.6 mL) and ether (0.6 mL) was stirred at room temperature under a nitrogen atmosphere for 30 min. The aqueous layer was discarded and the organic layer was washed with water and brine. The organic phase was dried over sodium sulfate and the solvent was removed *in vacuo* yielding a tan solid (95 mg, 95%): ^{1}H NMR (200 MHz, CD_2Cl_2) δ 8.17 (dd, J=8.5, 1.0 Hz, 1H), 7.87 (dd, J=8.5, 0.8 Hz, 1H), 7.37-7.28 (m, 6H), 7.21-7.05 (m, 4H), 6.91 (dd, J=7.8, 0.7 Hz, 1H), 6.79-6.67 (m, 1H), 4.38 (s, 2H), 4.27 (br s, 2H), 2.41 (s, 3H), 2.25 (s, 3H); MS(EI) m/z 466.

Reduction of 270e with triethyl phosphite

To a solution of quinone (100 mg, 0.22 mmol), benzene (0.5 mL), ethanol (0.5 mL) and water (0.2 mL) was slowly added triethyl phosphite (0.57 mL). After stirring the reaction mixture for 1 h at room temperature, water was added and the aqueous

layer was extracted with ethyl acetate. The organic phase was washed with water, brine and the solvent was removed *in vacuo* to give a tan solid (91 mg, 91%). The product obtained was spectroscopically similar to that obtained by reduction with dithionite.

Reduction of 270e with dithionite followed by acetylation with acetic anhydride



270e **275**

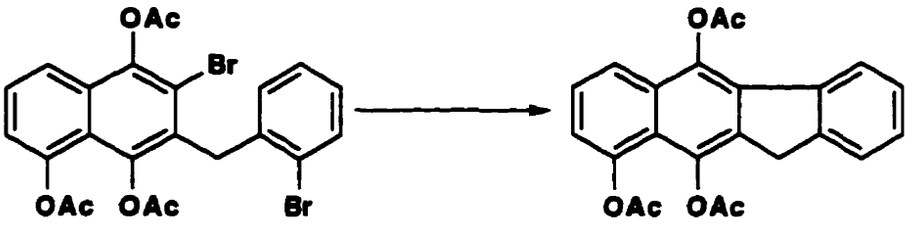
A mixture of quinone **270e** (0.1 g, 0.22 mmol), diethyl ether (0.6 mL), sodium dithionite (77 mg, 0.44 mmol) and water (0.6 mL) was stirred under an atmosphere of nitrogen for 30 min. The aqueous layer was discarded and the organic phase was washed with several portions of water and brine. The organic layer was then dried over sodium sulfate and the solvent removed *in vacuo*. The crude product was dissolved in acetic anhydride (5 mL) to which was added sulfuric acid (2 drops of 12 M). The reaction mixture was stirred at room temperature for 20 min then poured into a mixture of ice water, methylene chloride and sodium bicarbonate, which was stirred vigorously for 30 min. The aqueous and organic layers were separated. The aqueous layer was extracted with several portions of methylene chloride. The organic layers were combined and washed with water, brine and the solvent removed *in vacuo*. The crude product was recrystallized from diethyl ether to give

275 as a white solid (0.092 g, 78%). *Rf* 0.43 (50% ethyl acetate/hexane); IR (KBr) 1769 (br.) cm^{-1}; ^1H NMR (250 MHz, $CDCl_3$) δ 7.78 (dd, J=8.6, 1.1 Hz, 1H), 7.60-7.51 (m, 2H), 7.20 (dd, J=7.5, 1.1 Hz, 1H), 7.14-7.05 (m, 2H), 6.66 (dd, J=7.4, 2.0 Hz, 1H), 4.33 (br., 2H), 2.51 (s, 3H), 2.35 (s, 3H), 2.22 (s, 3H); ^{13}C NMR (50.3 MHz, CD_2Cl_2) δ 169.6, 169.2, 168.4, 145.8, 144.0, 142.6, 137.5, 132.9, 130.7, 129.4, 128.4, 128.0, 124.7, 122.5, 121.8, 120.6, 118.6, 37.3, 21.3, 20.9; MS(EI) m/z 548(4%), 506(4%), 464(8%), 422(28%); HRMS calcd for $C_{23}H_{18}Br_2O_6$ 547.9470, found 547.9469.

Reduction of 270e with zinc in acetic anhydride

A mixture of Zn (0.060 g, 0.92 mmol), quinone **270e** (0.2 g, 0.44 mmol), acetic anhydride (0.765 g, 7.5 mmol, 0.71 mL) and triethylamine (0.133 g, 1.32 mmol) was heated to reflux. The mixture was maintained at reflux for 3 min and then poured into ice water (40 mL). The aqueous layer was then extracted with several portions of methylene chloride. The organic layer was filtered, washed with water, brine and the solvent removed *in vacuo*. The crude product was recrystallized from diethyl ether to give a white solid (0.053 g, 75%) which was spectroscopically identical to material obtained by dithionite reduction followed by acetylation.

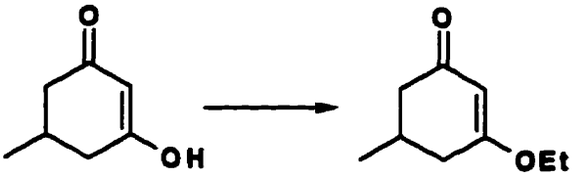
Synthesis of 276



275 **276**

A mixture of triphenyl phosphine (0.032 g, 0.14 mmol), nickel bromide (0.004 g, 0.018 mmol), zinc (0.036 g, 0.55 mmol) and dry DMF (5 mL) was heated to ~60°C. The reaction mixture was kept between 60-70°C until a deep red-brown colour was observed. Into this mixture was then canulated a solution of **275** (0.2 g, 0.36 mmol) in DMF (5 mL). The reaction mixture was kept between 60-70°C for three hours under an argon atmosphere. The reaction mixture was poured into a mixture of ice water and ethyl acetate. The aqueous layer was discarded and the organic layer was washed with cold dilute hydrochloric acid (0.1 N). The organic layer was then washed with several portions of water and brine, filtered, dried over sodium sulfate and the solvent removed *in vacuo*. The product was isolated by preparative layer chromatography using 20% ethyl acetate/hexane to give **276** as a white solid (0.050 g, 35%): *Rf* 0.48 (50% ethyl acetate/hexane); IR (KBr) 1772 cm^{-1}; ^1H NMR (200 MHz, CD_2Cl_2) δ 7.89-7.81 (m, 2H), 7.62-7.40 (m, 4H), 7.20 (dd, J=8.0, 1.1 Hz, 1H), 3.39 (s, 2H), 2.68 (s, 3H), 2.49 (s, 3H), 2.42 (s, 3H); MS(EI) m/z 390; HRMS calcd for $C_{23}H_{28}O_6$ 390.1098, found 390.1086.

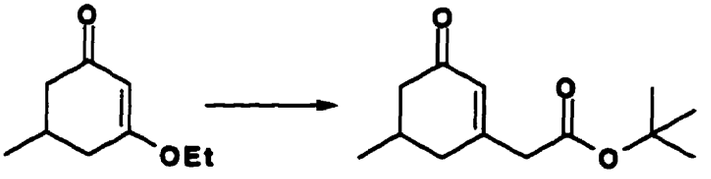
Synthesis of the enol ether 277



167 **277**

A mixture of dione **167** (5.65 g, 45.2 mmol), pTSA (0.219 g, 1.4 mmol), ethanol (25 mL) and benzene (50 mL) was brought to reflux. Water formed in the reaction mixture was removed by azeotropic distillation. The reaction mixture was then washed with 10% sodium hydroxide and with four portions of brine. The reaction mixture was then washed with water until the washings were neutral by pH paper. Benzene was added (25 mL) and the solvent was removed by further distillation leaving a clear colourless oil (6.16 g, 88%) which appeared to be homogeneous by TLC and ^{1}H NMR analysis: *Rf* 0.18 (20% ethyl acetate/hexane); IR (Neat) 1654 cm-1; ^{1}H NMR (250 MHz, CD_2Cl_2) δ 5.28 (s, 1H), 3.91-3.80 (m, 2H), 2.47-1.91 (m, 5H), 1.32 (t, J=7.0 Hz, 3H), 1.05 (d, J=6.0 Hz, 3H); MS(EI) m/z 154.

Synthesis of the ester 278

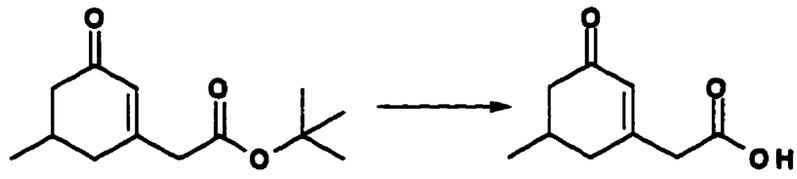


277 **278**

A solution of *t*-butyl bromoacetate (2.1 g, 10.7 mmol) and enol ether **277** (1.1 g, 7 mmol) in dry THF (10 mL) was added slowly to a refluxing mixture of zinc (0.78 g, 12.1 mmol), iodine (1 crystal) and dry THF (10 mL). The reaction mixture was refluxed for 1.5 h then poured into ice water (100 mL) and methylene chloride (15 mL). Cold sulfuric acid (10%) was added to acidify the reaction mixture. The aqueous layer was discarded and the organic layer was washed with water, dried over sodium sulfate and the solvent removed *in vacuo* yielding **278** as a pale

yellow oil (1.5 g, 94%): *Rf* 0.27 (20% ethyl acetate/hexane); IR (Neat) 1727, 1673 cm^{-1}; ^{1}H NMR (250 MHz, C_6D_6) δ 6.01 (s, 1H), 2.75 (s, 2H), 2.3-2.0 (m, 1H), 1.83-1.59 (m, 4H), 1.37 (s, 9H), 0.68 (d, J=6.0 Hz, 3H); ^{13}C NMR (62.9 MHz, CD_2Cl_2) δ 199.3, 168.8, 157.4, 128.2, 81.6, 45.7, 44.9, 38.2, 30.5, 28.1, 21.1; MS(CI) m/z 225 $[M+1]^+$; HRMS(CI) calcd for $C_{13}H_{21}O_3$ $[M+1]^+$ 225.1491, found 225.1488 $[M+1]^+$.

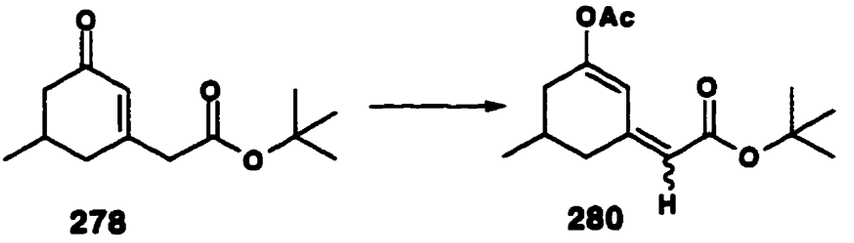
Deprotection of the t-butyl ester yielding the acid 279



278 **279**

To a stirred cooled (ice bath) solution of ester **278** (0.1 g, 0.45 mmol) in methylene chloride was added slowly triflouroacetic acid (0.154 g, 1.35 mmol). The reaction mixture was allowed to equilibrate to room temperature over 1 h. Toluene (50 mL) was added and the solvent was removed *in vacuo* to give **279** as a yellow solid (quantitative): *Rf* 0.08 (40% ethyl acetate/hexane); IR (KBr) 3025, 1730, 1651 cm^{-1}; ^{1}H NMR (250 MHz, CD_2Cl_2) δ 7.95 (br s, 1H), 5.95 (s, 1H), 3.29 (s, 2H), 2.5-2.0 (m, 5H), 1.07 (d, J=6.3 Hz, 3H); ^{13}C NMR (250 MHz, $CDCl_3$) δ 174.3, 156.4, 128.7, 45.3, 43.0, 38.0, 30.2, 21.1; MS(electrospray) m/z 168.

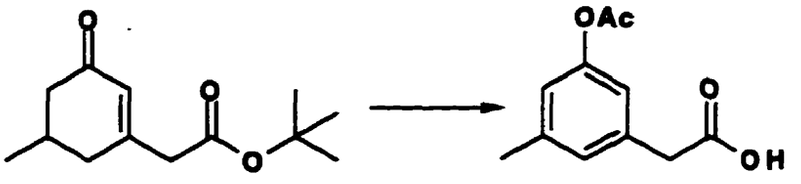
Synthesis of the enol acetate 280



278 **280**

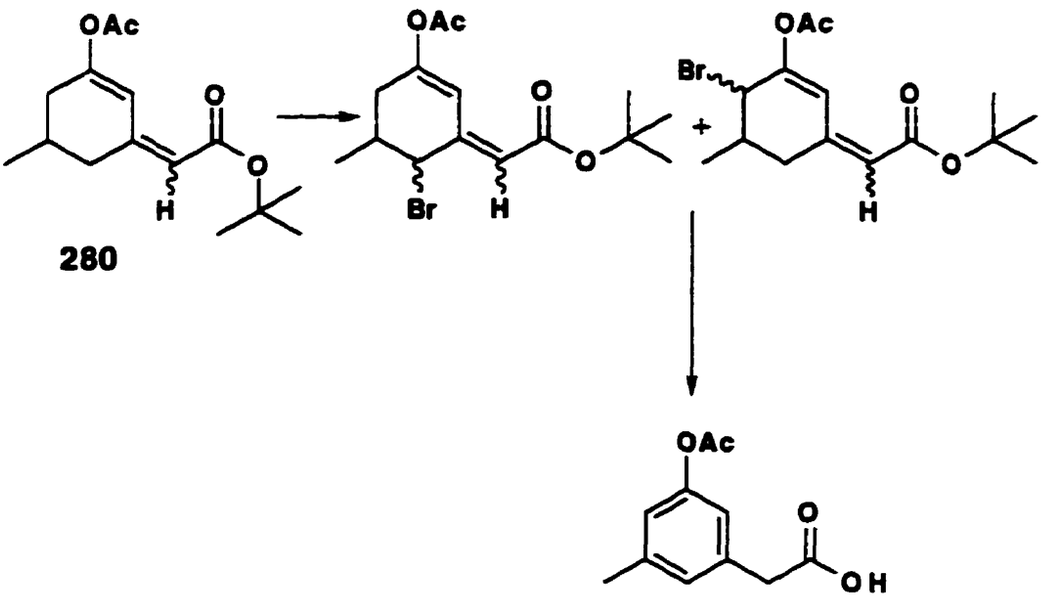
A solution of **278** (0.5 g, 2.2 mmol), isopropenyl acetate (3 mL) and *p*TSA (0.005 g) was allowed to stir at room temperature for 3 h. The reaction mixture was diluted with methylene chloride and washed with several portions of water. The solvent was removed *in vacuo* yielding a viscous oil. The product **280** was purified by column chromatography eluting with 40% ethyl acetate/hexane to give the mixture of E/Z isomers as a clear colourless oil (0.4 g, 75%): *Rf* 0.49 (20% ethyl acetate/hexane); IR (Neat) 1763, 1702 cm^{-1}; ^1H NMR (250 MHz, C_6D_6) δ 8.08 (s), 5.95 (s), 5.76 (s), 5.66 (s), 2.19-1.75 (m), 1.67 (s), 1.63 (s), 1.53 (s), 1.51 (s), 0.79 (d, J=6.6 Hz), 0.70 (d, J=6.2 Hz); MS(EI) m/z 266(2%), 224(17%); HRMS calcd. for $C_{15}H_{22}O_4$ 266.1518, found 266.1534.

Synthesis of the aromatic acid 283



278 **283**

A mixture of the ester **278** (2.253 g, 10.1 mmol) and selenium dioxide (1.241 g, 11.2 mmol) in t-butanol (10 mL) was heated at reflux for 3 h. The reaction mixture was cooled, diluted with t-butanol (50 mL) and filtered through celite. The solvent was then removed *in vacuo* leaving a dark red solid. To the residue was added acetic anhydride (10 mL) and a catalytic amount of sulfuric acid (6 M). This mixture was stirred at room temperature for 3 h. The reaction mixture was then poured into a mixture of ice water, saturated sodium bicarbonate and ethyl acetate. This mixture was stirred vigorously for 1 h with periodic addition of ice. The aqueous phase was discarded and the organic layer was washed with water, brine and the solvent removed *in vacuo* leaving a dark red viscous oil. The residue was purified by column chromatography eluting with 20% ethyl acetate/hexane yielding a pale yellow oil (1.485 g, 71%). *Rf* 0.68 (ethyl acetate/hexane); IR (Neat) ; ^{1}H NMR (250 MHz, $CDCl_3$) δ 6.86 (s, 1H), 6.74 (s, 2H), 3.43 (s, 2H), 2.28 (s, 3H), 2.35 (s, 3H); MS(electrospray) m/z 208.



280

283

A mixture of enol acetate **280** (0.122 g, 0.45 mmol), NBS (0.0862 g, 0.48 mmol) and benzoyl peroxide (cat.) in carbon tetrachloride (3 mL) was heated at reflux for 2 h. The reaction mixture was diluted with carbon tetrachloride (5 mL) and was filtered. The organic layer was washed with water, cold dilute HCl (1%), brine and the solvent was removed *in vacuo*. To the residue was added methylene chloride (5 mL) and DBU (0.146 g, 0.96 mmol). This mixture was heated at reflux for 30 min. and then cooled to ice bath temperature. To this was then added methylene chloride (5 mL) and trifluoroacetic acid (2 mL) and the mixture was stirred at ice bath temperature for 1 h. The reaction mixture was filtered, washed with water, brine and the solvent removed *in vacuo*. The dark residue was purified on a preparative layer plate eluting with 20% ethyl acetate/hexane to give **283** as a pale yellow oil which was spectroscopically identical to material obtained above (38%).

Appendix A

Appendix A: Table of Contents

PROTON NMR SPECTRUM OF 138A 240

EXPANSION 1.0 TO 3.5 PPM 241

EXPANSION 6.0 TO 8.0 PPM 242

TOCSY: IRRADIATION AT 3.61 PPM 243

TOCSY: IRRADIATION AT 3.81 PPM 244

TOCSY: IRRADIATION AT 6.39 PPM 245

TOCSY: IRRADIATION AT 6.53 PPM 246

NOE: IRRADIATION AT 1.42 PPM 247

NOE: IRRADIATION AT 1.50 PPM 247

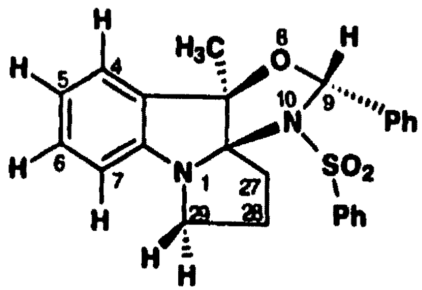
NOE: IRRADIATION AT 5.60 PPM 248

NOE: IRRADIATION AT 6.40 PPM 248

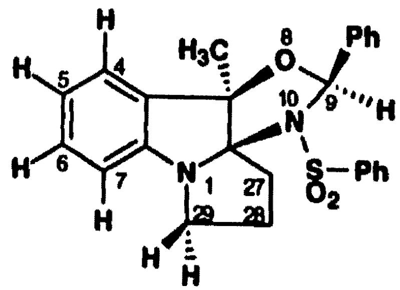
NOE: IRRADIATION AT 6.39 PPM 249

NOE: IRRADIATION AT 6.53 PPM 249

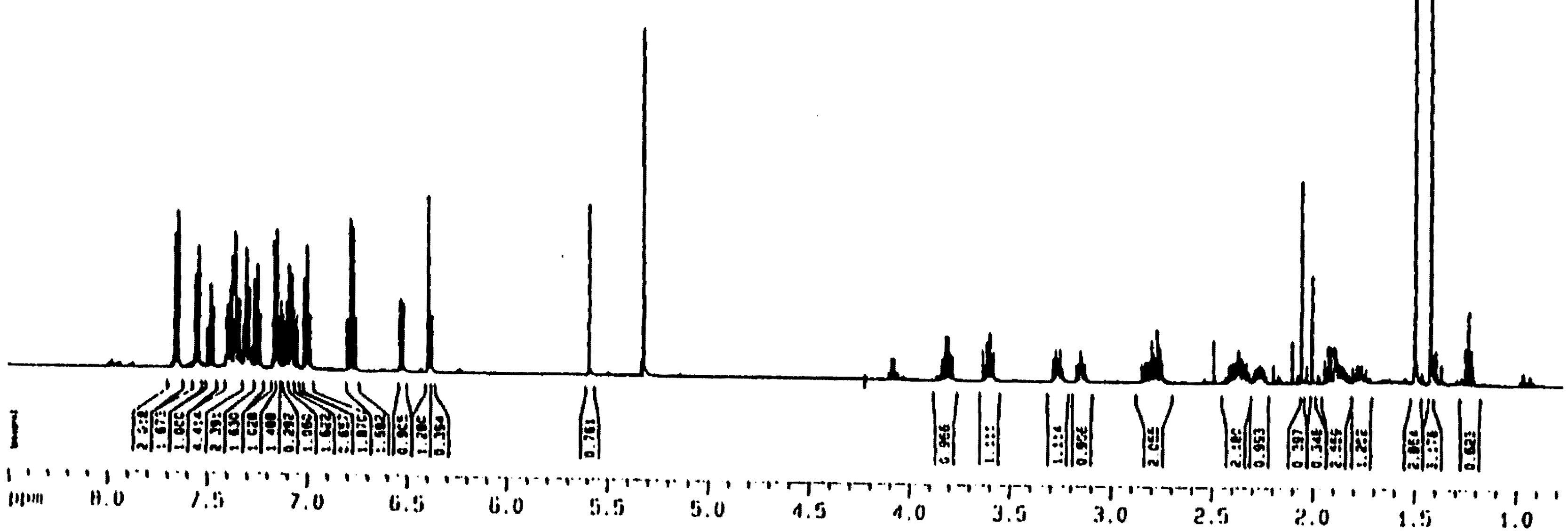
[1]H NMR spectrum of 138a (AMX-500)



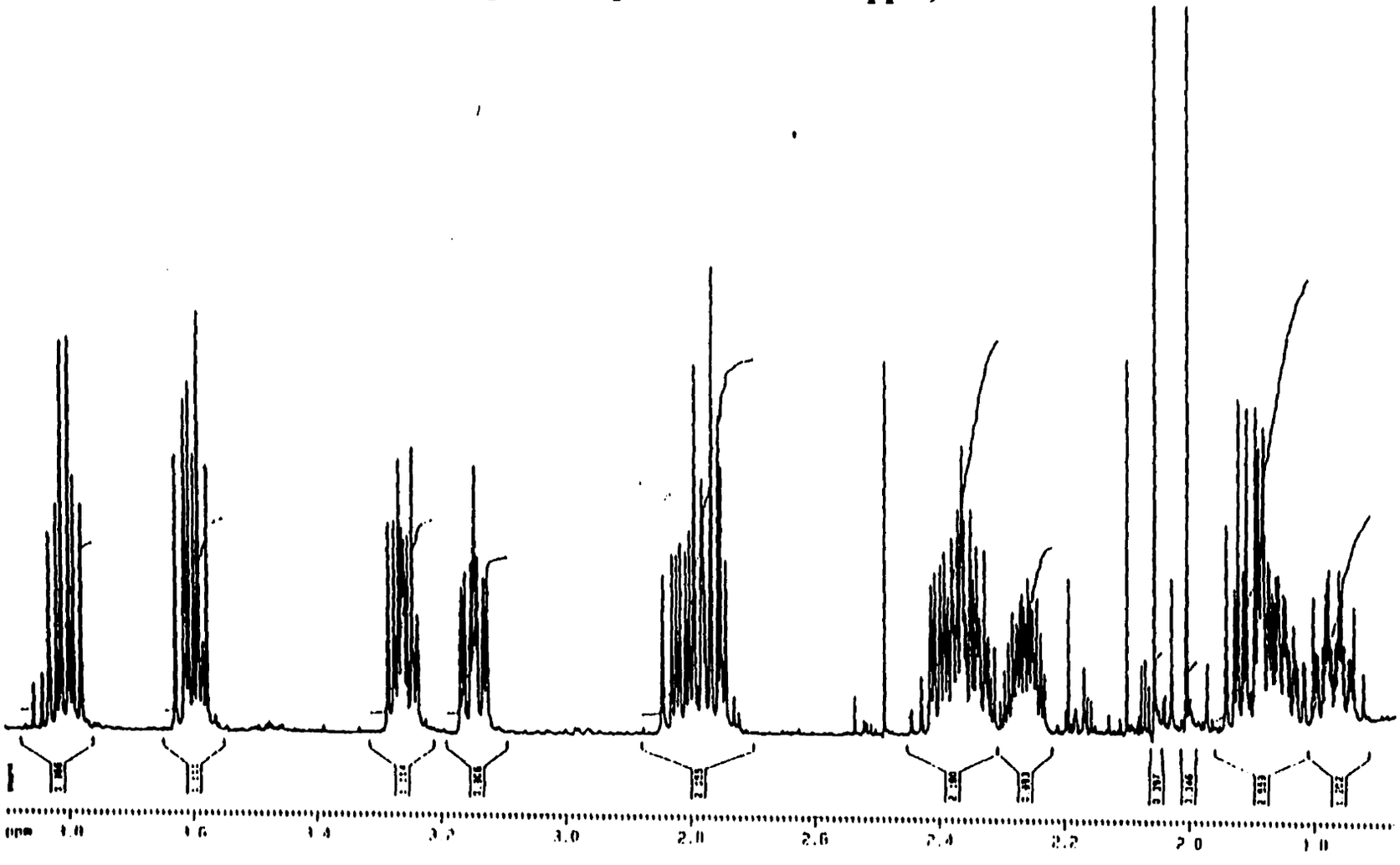
138a1



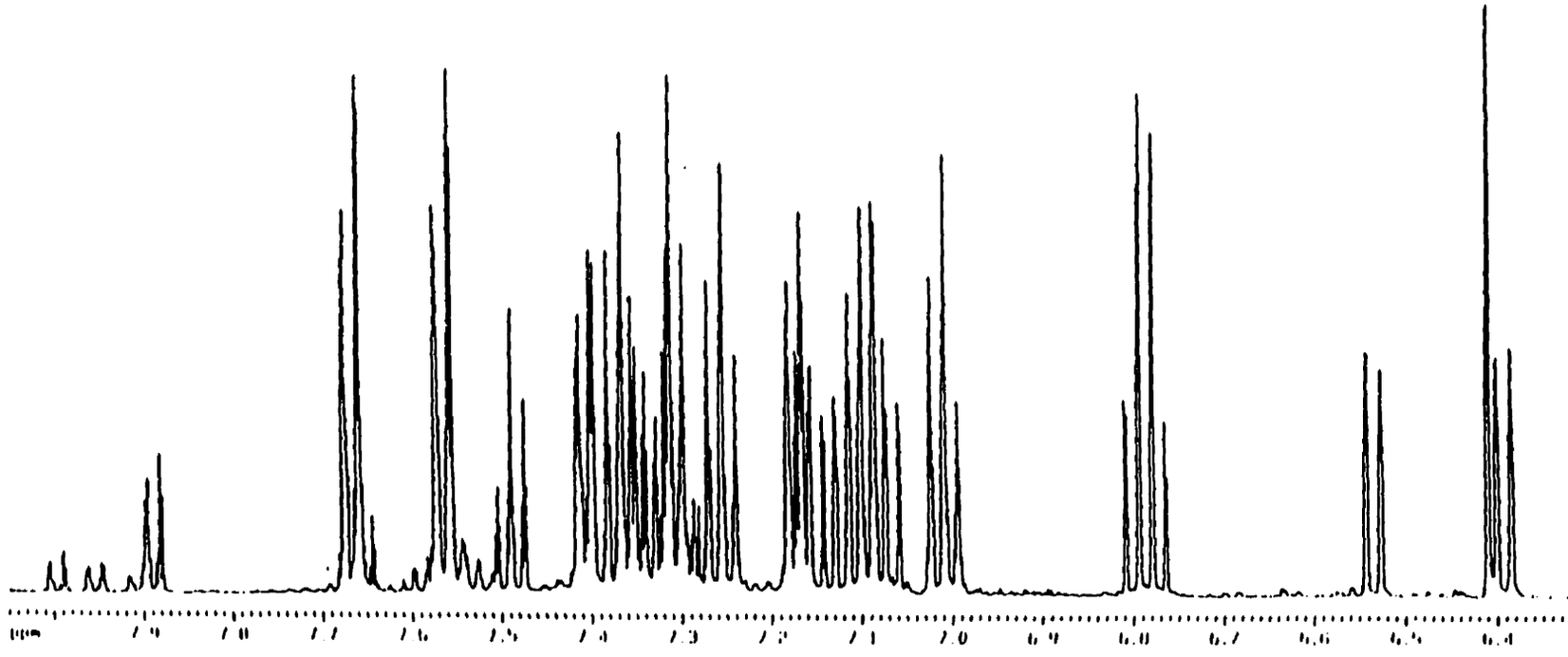
138a2

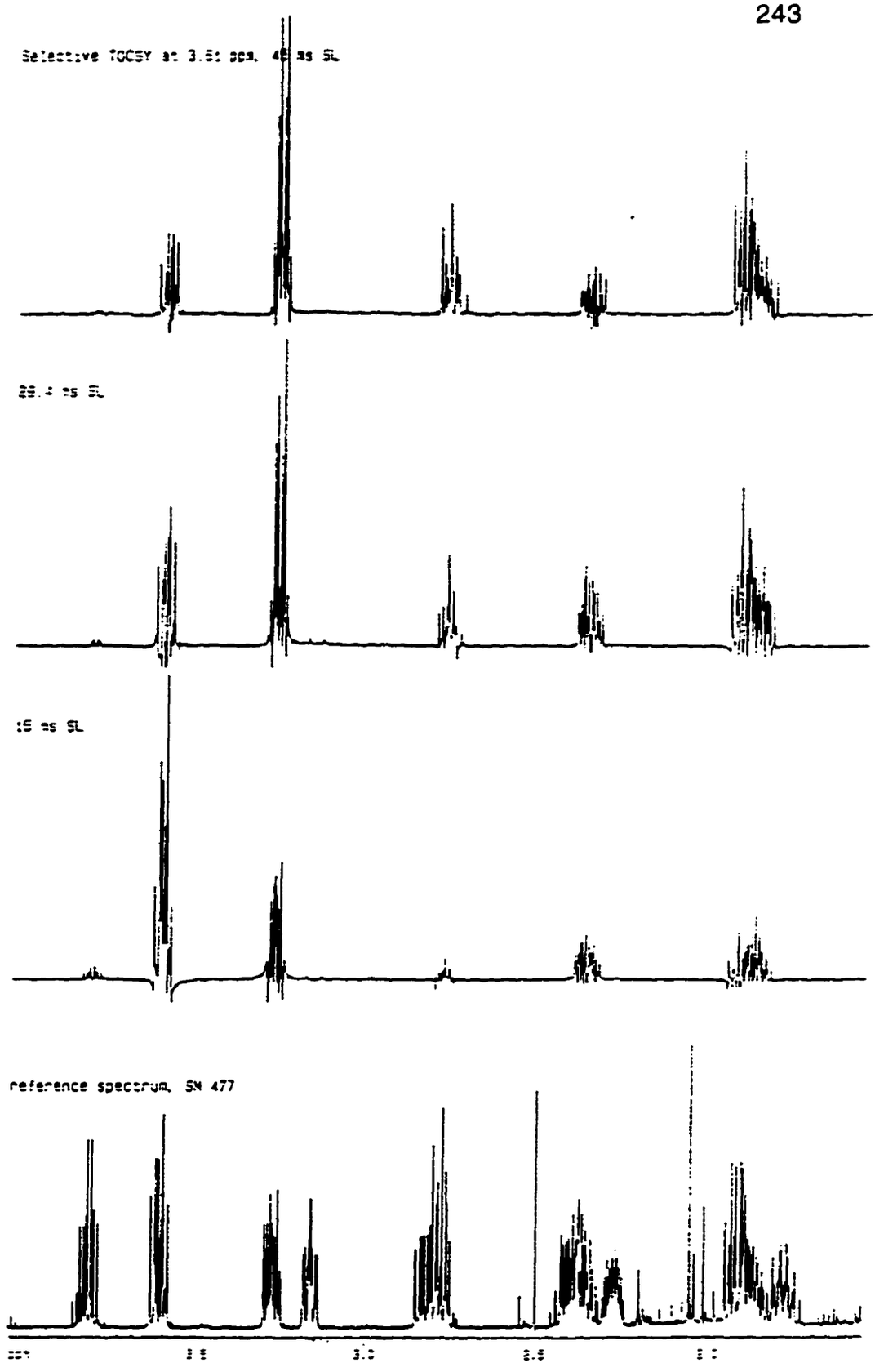


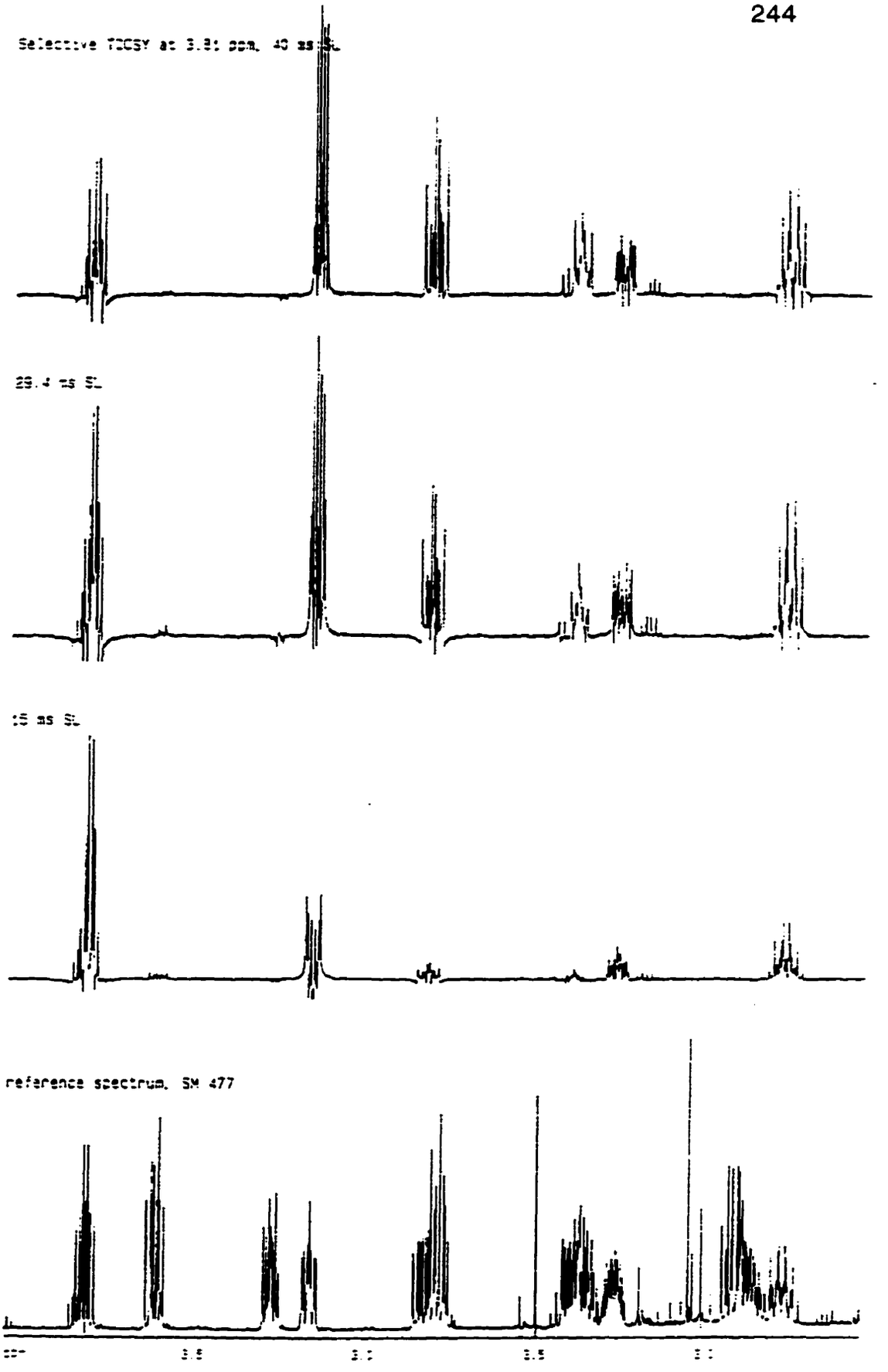
^{1}H NMR spectrum of 138a (AMX-500)
(expansion plot: 1.0 to 3.85 ppm)

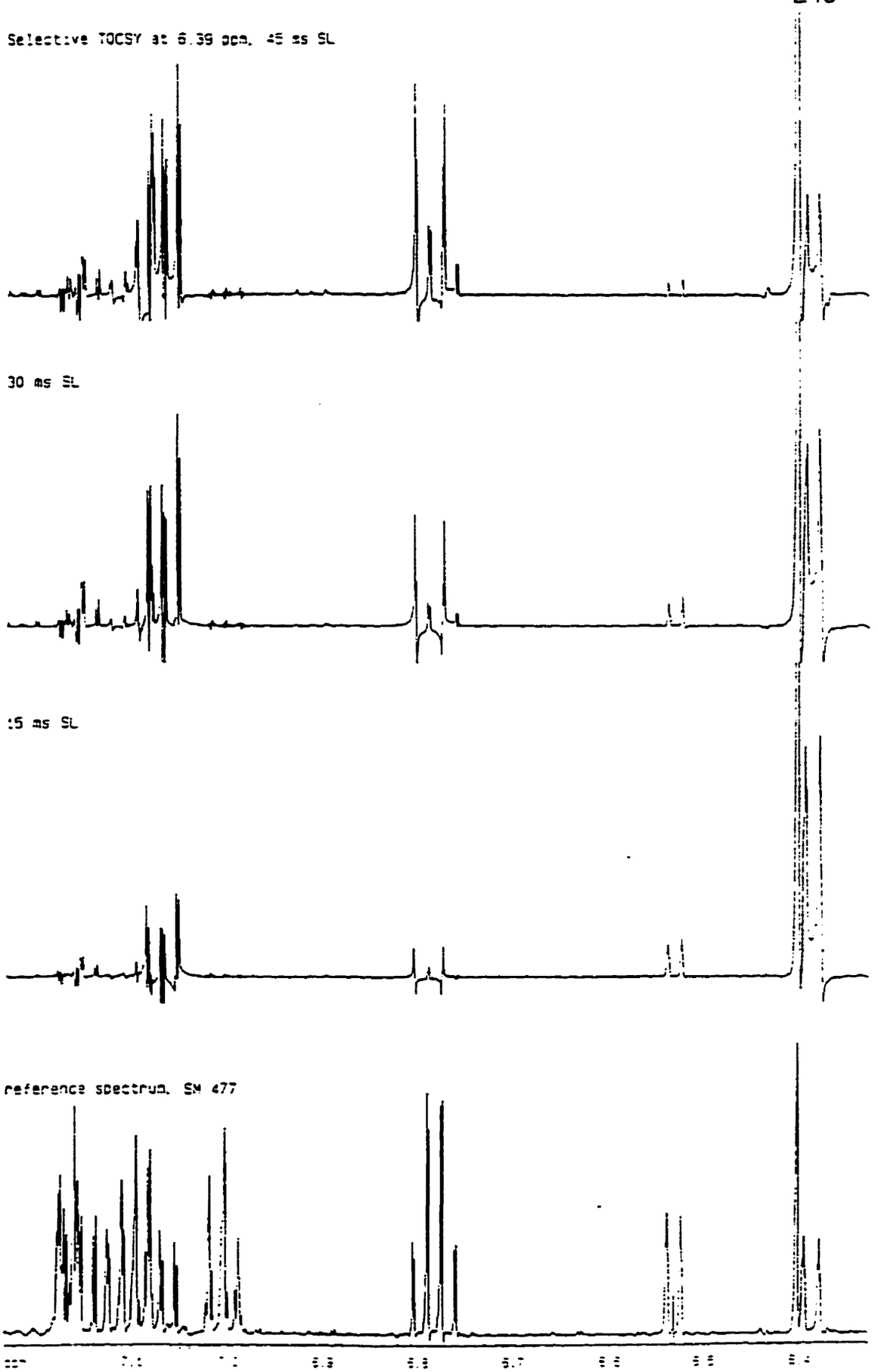


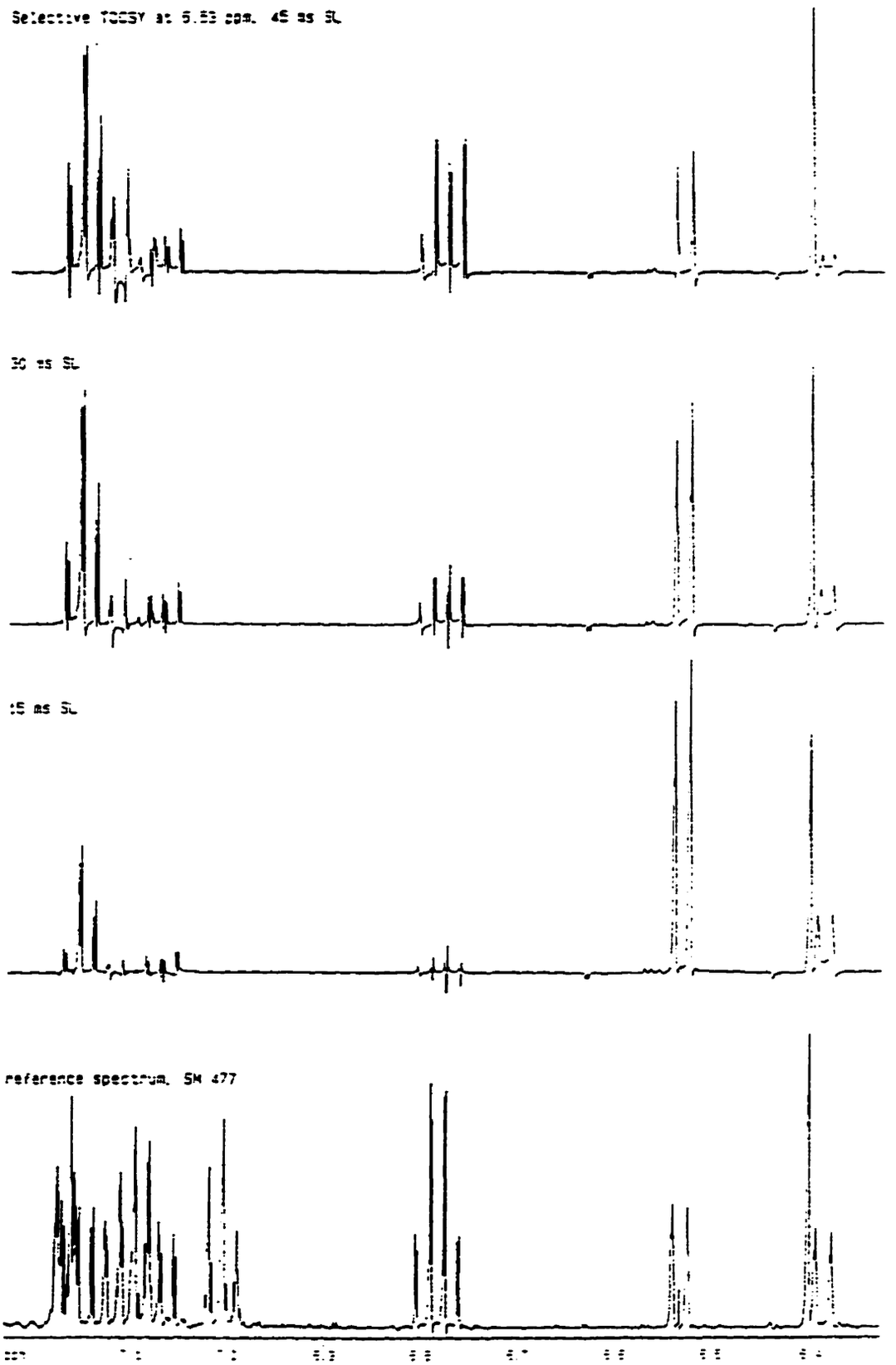
^{1}H NMR spectrum of 138a (AMX-500)
(expansion plot: 6.3 to 8.0 ppm)

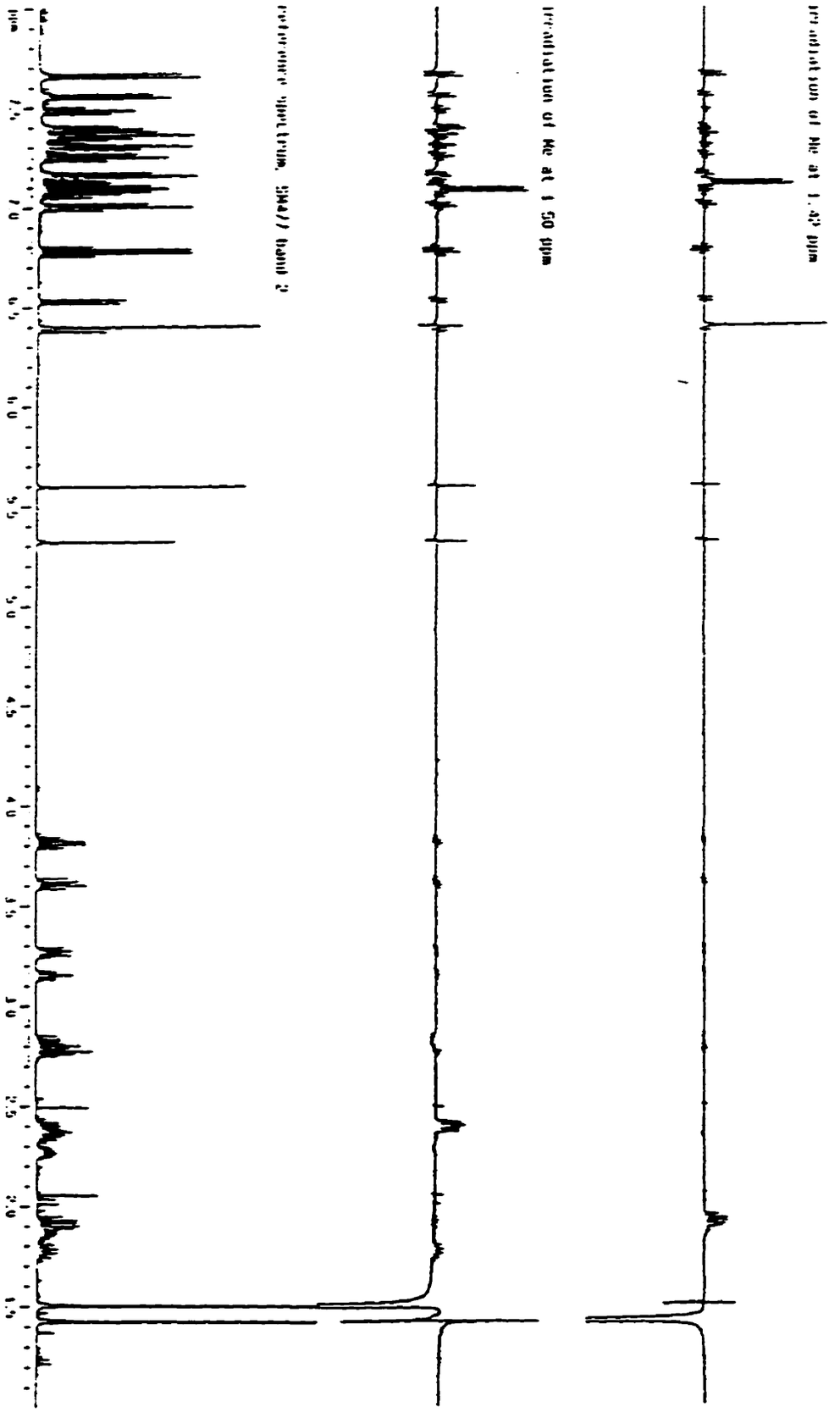


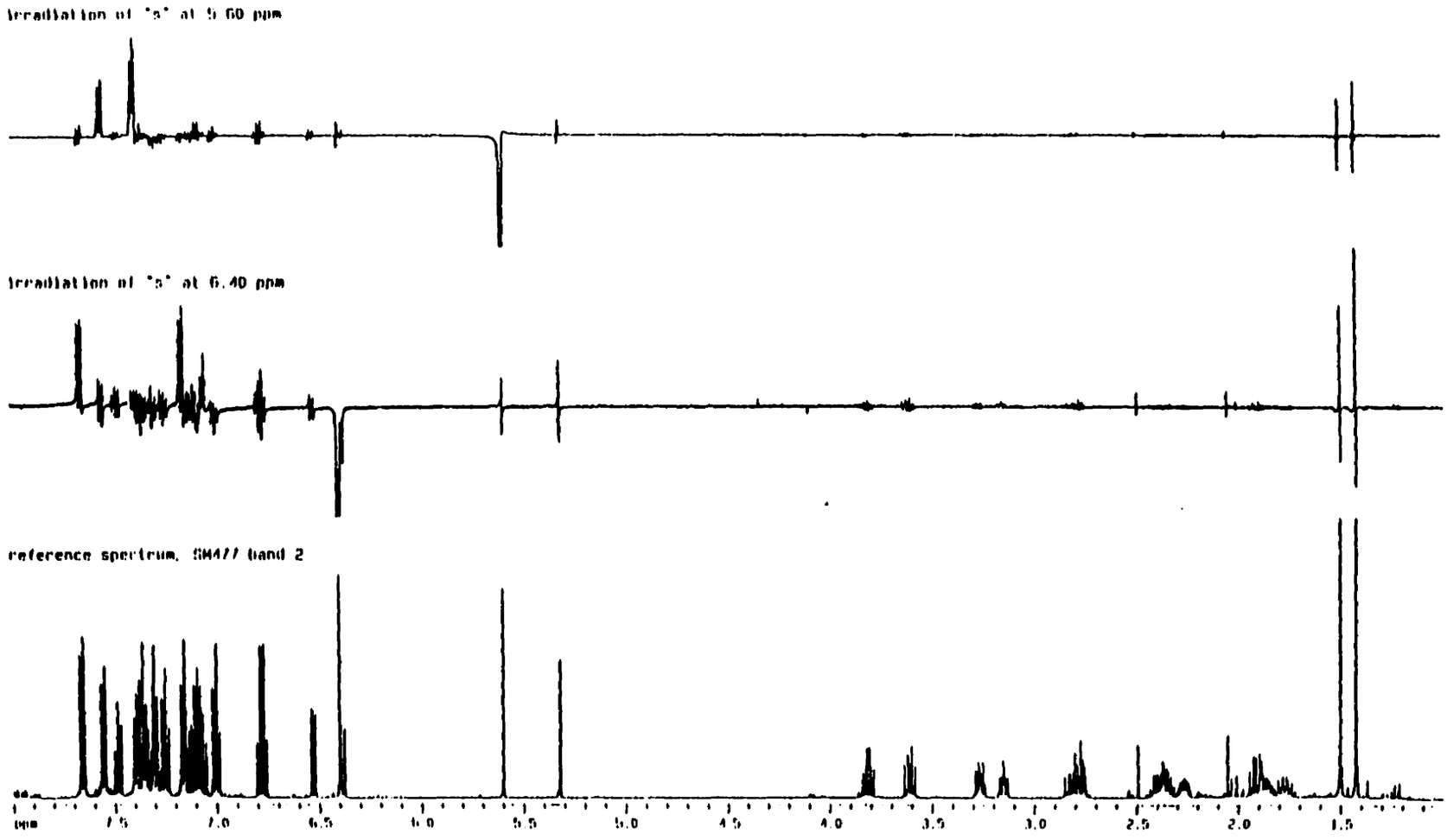

reference spectrum, SN 477

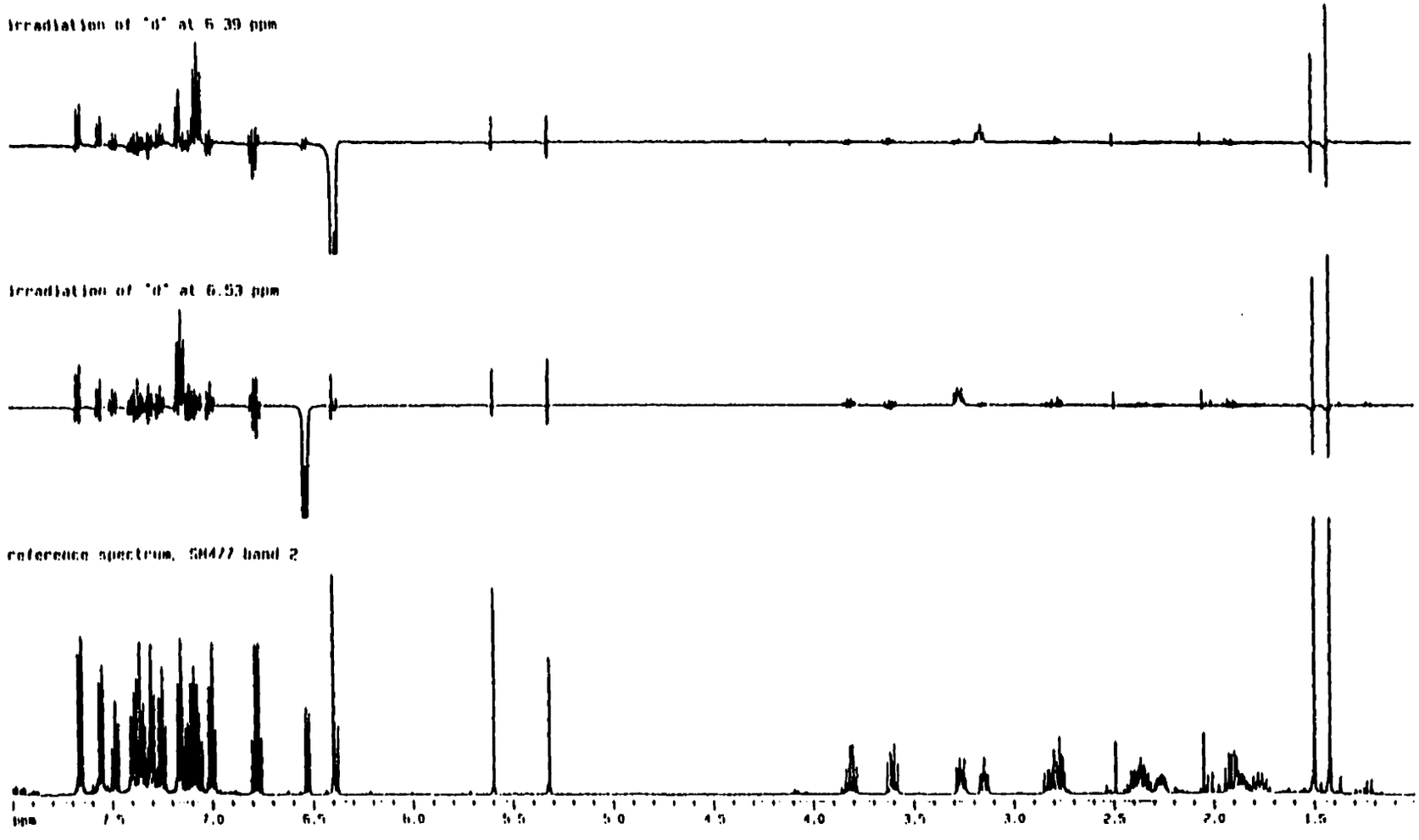

Selective TOCSY at 3.81 ppm, 40 ms SL
29.4 ms SL
15 ms SL
reference spectrum, SM 477


Selective TOCSY at 6.39 ppm, 45 ms SL
30 ms SL
15 ms SL
reference spectrum, SM 477


Selective TOCSY at 5.53 ppm, 45 ms SL
30 ms SL
15 ms SL
reference spectrum, SM 477




Irradiation at "a" at 5.60 ppm
Irradiation at "a" at 6.40 ppm
reference spectrum, SM477 band 2
ppm
7.5
7.0
6.5
6.0
5.5
5.0
4.5
4.0
3.5
3.0
2.5
2.0
1.5


Irradiation of "d" at 6.39 ppm
Irradiation of "d" at 6.53 ppm
reference spectrum, SM477 band 2
ppm
7.5
7.0
6.5
6.0
5.5
5.0
4.5
4.0
3.5
3.0
2.5
2.0
1.5

Appendix B

Appendix B: Table of Contents

X-RAY DATA FOR COMPOUND 141A 252

ORTEP PLOT 252

STRUCTURE DETERMINATION SUMMARY 253

Crystal Data *253*

Data Collection *254*

Solution and Refinement *255*

ATOMIC COORDINATES 256

BOND LENGTHS 257

BOND ANGLES 257

ANISOTROPIC DISPLACEMENT COORDINATES 258

H-ATOM COORDINATES 259

X-RAY DATA FOR COMPOUND 143B 260

ORTEP PLOT 260

STRUCTURE DETERMINATION SUMMARY 261

Crystal Data *261*

Data Collection *262*

Solution and Refinement *263*

ATOMIC COORDINATES 264

BOND LENGTHS 266

BOND ANGLES 267

ANISOTROPIC DISPLACEMENT COORDINATES 269

H-ATOM COORDINATES 271

X-RAY DATA FOR COMPOUND 178 272

ORTEP PLOT 272

STRUCTURE DETERMINATION SUMMARY 273

Crystal Data *273*

Data Collection *274*

Solution and Refinement *275*

ATOMIC COORDINATES 276

BOND LENGTHS 277

BOND ANGLES 278

ANISOTROPIC DISPLACEMENT COORDINATES 279

H-ATOM COORDINATES 280

X-RAY DATA FOR COMPOUND 192 281

ORTEP PLOT 281

STRUCTURE DETERMINATION SUMMARY 282

Crystal Data *282*

Data Collection *283*

Solution and Refinement *284*

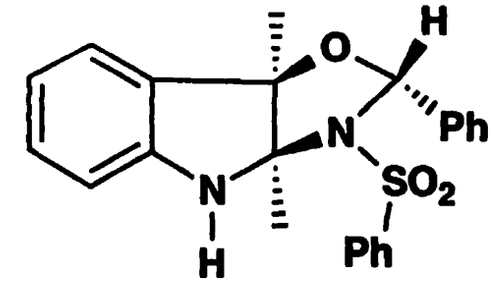
ATOMIC COORDINATES 285

BOND LENGTHS 285

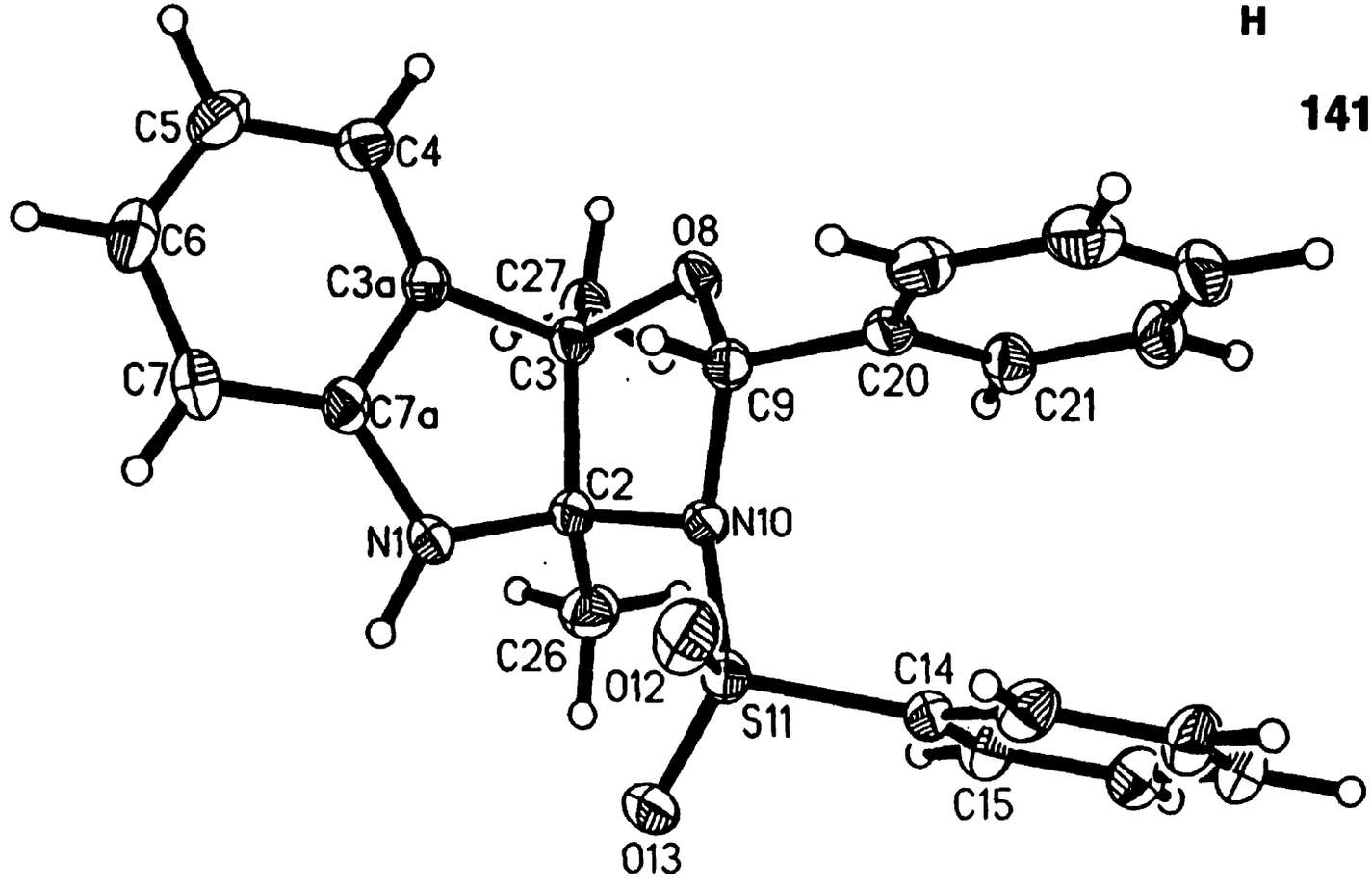
BOND ANGLES 285

ANISOTROPIC DISPLACEMENT COORDINATES 286

H-ATOM COORDINATES 286


H
O
Ph
N
SO2
N
H
Ph

141a


C5
C4
C6
C3a
C27
O8
C7
C7a
C3
C9
C20
C21
C2
N1
N10
C26
O12
S11
C14
C15
O13

STRUCTURE DETERMINATION SUMMARY

Crystal Data

Empirical Formula	$C_{23}H_{22}N_2O_3S$
Color; Habit	Pale yellow needle prism fragment
Crystal Size (mm)	0.48{100}x0.46{110,$\bar{1}\bar{1}$0}
	x0.62{1$\bar{1}$0,$\bar{1}$10}x0.66{001}
Crystal System	Monoclinic
Space Group	$P2_1/c$
Unit Cell Dimensions	$\underline{a}$ = 11.670(2) Å
	$\underline{b}$ = 12.116(2) Å
	$\underline{c}$ = 13.928(2) Å
	β = 91.41(2)°
Volume	1968.8(6) $Å^3$
Z	4
Formula Weight	406.5
Density(calc.)	1.371 g/cm^3
Absorption Coefficient	1.92 cm^{-1}
F(000)	856

Data Collection

Diffractometer Used	Siemens R3m/V
Radiation	MoKα (λ = 0.71073 Å)
Temperature (K)	180
Monochromator	Highly oriented graphite crystal
2θ Range	4.0 to 54.0°
Scan Type	ω
Scan Speed	Variable; 2.93 to 29.30°/min. in ω
Scan Range (ω)	1.40°
Background Measurement	Stationary crystal and stationary counter at beginning and end of scan, each for 25.0% of total scan time
Standard Reflections	2 measured every 100 reflections
Index Ranges	$0 \leq h \leq 14$, $0 \leq k \leq 15$ $-17 \leq l \leq 17$
Reflections Collected	4314
Independent Reflections	4314
Observed Reflections	3558 ($F > 6.0\sigma(F)$)
Absorption Correction	Face-indexed numerical
Min./Max. Transmission	0.8967 / 0.9321

Solution and Refinement

System Used	Siemens SHELXTL PLUS (VMS)
Solution	Direct Methods
Refinement Method	Full-Matrix Least-Squares
Quantity Minimized	$\sum w(F_o - F_c)^2$
Extinction Correction	χ = 0.00104(3), where $F^* = F \left[1 + 0.002\chi F^2/\sin(2\theta) \right]^{-1/4}$
Hydrogen Atoms	Riding model, refined isotropic U
Weighting Scheme	$w^{-1} = \sigma^2(F)$
Number of Parameters Refined	285
Final R Indices (obs. data)	R = 3.47 %, wR = 3.59 %
(R Indices (all data)	R = 4.10 %, wR = 3.62 %)
Goodness-of-Fit	3.30
Largest and Mean Δ/σ	0.055, 0.001
Data-to-Parameter Ratio	12.5:1
Largest Difference Peak	0.34 $eÅ^{-3}$
Largest Difference Hole	-0.39 $eÅ^{-3}$

Table 1. Atomic coordinates ($x10^4$) and equivalent isotropic displacement coefficients ($Å^2 x10^4$)

	x	y	z	U(eq)
N(1)	222(1)	982(1)	3035(1)	259(4)
C(2)	404(1)	1975(1)	2464(1)	210(5)
C(3)	-465(1)	2860(1)	2865(1)	196(4)
C(3A)	-1051(1)	2234(1)	3647(1)	197(4)
C(4)	-1932(1)	2570(2)	4225(1)	270(5)
C(5)	-2430(2)	1809(2)	4827(1)	327(6)
C(6)	-2035(2)	726(2)	4857(1)	306(6)
C(7)	-1138(1)	388(1)	4294(1)	256(5)
C(7A)	-657(1)	1155(1)	3679(1)	206(5)
O(8)	236.7(9)	3759.4(9)	3224.5(8)	223(3)
C(9)	1297(1)	3300(1)	3528(1)	203(4)
N(10)	1528(1)	2531(1)	2722(1)	209(4)
S(11)	2703.4(3)	1780.2(3)	2808.1(3)	241(1)
O(12)	3008(1)	1566(1)	3794.9(9)	333(4)
O(13)	2563(1)	869(1)	2157(1)	340(4)
C(14)	3753(1)	2670(1)	2339(1)	224(5)
C(15)	3637(2)	3022(1)	1396(1)	277(5)
C(16)	4450(2)	3724(2)	1029(1)	321(6)
C(17)	5365(2)	4068(2)	1609(1)	340(6)
C(18)	5480(2)	3707(2)	2541(1)	332(6)
C(19)	4672(1)	2997(2)	2919(1)	279(5)
C(20)	2173(1)	4197(1)	3671(1)	199(4)
C(21)	2463(1)	4871(1)	2907(1)	246(5)
C(22)	3277(2)	5689(1)	3033(2)	343(6)
C(23)	3815(2)	5836(2)	3917(2)	390(7)
C(24)	3531(2)	5175(2)	4681(2)	383(6)
C(25)	2704(1)	4354(2)	4560(1)	275(5)
C(26)	298(2)	1744(2)	1395(1)	314(6)
C(27)	-1306(1)	3349(1)	2141(1)	259(5)

* Equivalent isotropic U defined as one third of the trace of the orthogonalized U_{ij} tensor

Table 2. Bond lengths (Å)

N(1)-C(2)	1.460(2)	N(1)-C(7A)	1.395(2)
C(2)-C(3)	1.587(2)	C(2)-N(10)	1.510(2)
C(2)-C(26)	1.517(2)	C(3)-C(3A)	1.505(2)
C(3)-O(8)	1.445(2)	C(3)-C(27)	1.511(2)
C(3A)-C(4)	1.382(2)	C(3A)-C(7A)	1.386(2)
C(4)-C(5)	1.385(3)	C(5)-C(6)	1.391(3)
C(6)-C(7)	1.385(2)	C(7)-C(7A)	1.391(2)
O(8)-C(9)	1.413(2)	C(9)-N(10)	1.489(2)
C(9)-C(20)	1.501(2)	N(10)-S(11)	1.648(1)
S(11)-O(12)	1.435(1)	S(11)-O(13)	1.435(1)
S(11)-C(14)	1.769(2)	C(14)-C(15)	1.384(2)
C(14)-C(19)	1.385(2)	C(15)-C(16)	1.381(3)
C(16)-C(17)	1.387(3)	C(17)-C(18)	1.373(3)
C(18)-C(19)	1.389(3)	C(20)-C(21)	1.390(2)
C(20)-C(25)	1.384(2)	C(21)-C(22)	1.381(2)
C(22)-C(23)	1.381(3)	C(23)-C(24)	1.379(3)
C(24)-C(25)	1.392(3)		

Table 3. Bond angles (°)

C(2)-N(1)-C(7A)	110.2(1)	N(1)-C(2)-C(3)	105.2(1)
N(1)-C(2)-N(10)	112.1(1)	C(3)-C(2)-N(10)	100.0(1)
N(1)-C(2)-C(26)	111.9(1)	C(3)-C(2)-C(26)	115.6(1)
N(10)-C(2)-C(26)	111.3(1)	C(2)-C(3)-C(3A)	102.7(1)
C(2)-C(3)-O(8)	105.7(1)	C(3A)-C(3)-O(8)	113.1(1)
C(2)-C(3)-C(27)	116.1(1)	C(3A)-C(3)-C(27)	112.4(1)
O(8)-C(3)-C(27)	106.8(1)	C(3)-C(3A)-C(4)	129.1(1)
C(3)-C(3A)-C(7A)	110.0(1)	C(4)-C(3A)-C(7A)	120.7(1)
C(3A)-C(4)-C(5)	119.1(2)	C(4)-C(5)-C(6)	120.2(2)
C(5)-C(6)-C(7)	121.1(2)	C(6)-C(7)-C(7A)	118.2(2)
N(1)-C(7A)-C(3A)	111.7(1)	N(1)-C(7A)-C(7)	127.5(1)
C(3A)-C(7A)-C(7)	120.8(1)	C(3)-O(8)-C(9)	107.0(1)
O(8)-C(9)-N(10)	101.2(1)	O(8)-C(9)-C(20)	110.1(1)
N(10)-C(9)-C(20)	114.7(1)	C(2)-N(10)-C(9)	106.6(1)
C(2)-N(10)-S(11)	119.2(1)	C(9)-N(10)-S(11)	117.1(1)
N(10)-S(11)-O(12)	110.9(1)	N(10)-S(11)-O(13)	107.2(1)
O(12)-S(11)-O(13)	119.2(1)	N(10)-S(11)-C(14)	102.7(1)
O(12)-S(11)-C(14)	107.8(1)	O(13)-S(11)-C(14)	107.8(1)
S(11)-C(14)-C(15)	119.1(1)	S(11)-C(14)-C(19)	119.5(1)
C(15)-C(14)-C(19)	121.4(2)	C(14)-C(15)-C(16)	119.3(2)
C(15)-C(16)-C(17)	119.7(2)	C(16)-C(17)-C(18)	120.7(2)
C(17)-C(18)-C(19)	120.3(2)	C(14)-C(19)-C(18)	118.6(2)
C(9)-C(20)-C(21)	120.1(1)	C(9)-C(20)-C(25)	120.5(1)
C(21)-C(20)-C(25)	119.5(1)	C(20)-C(21)-C(22)	120.3(2)
C(21)-C(22)-C(23)	120.2(2)	C(22)-C(23)-C(24)	120.0(2)
C(23)-C(24)-C(25)	120.1(2)	C(20)-C(25)-C(24)	120.0(2)

Table 4. Anisotropic displacement coefficients ($Å^2 x 10^4$)

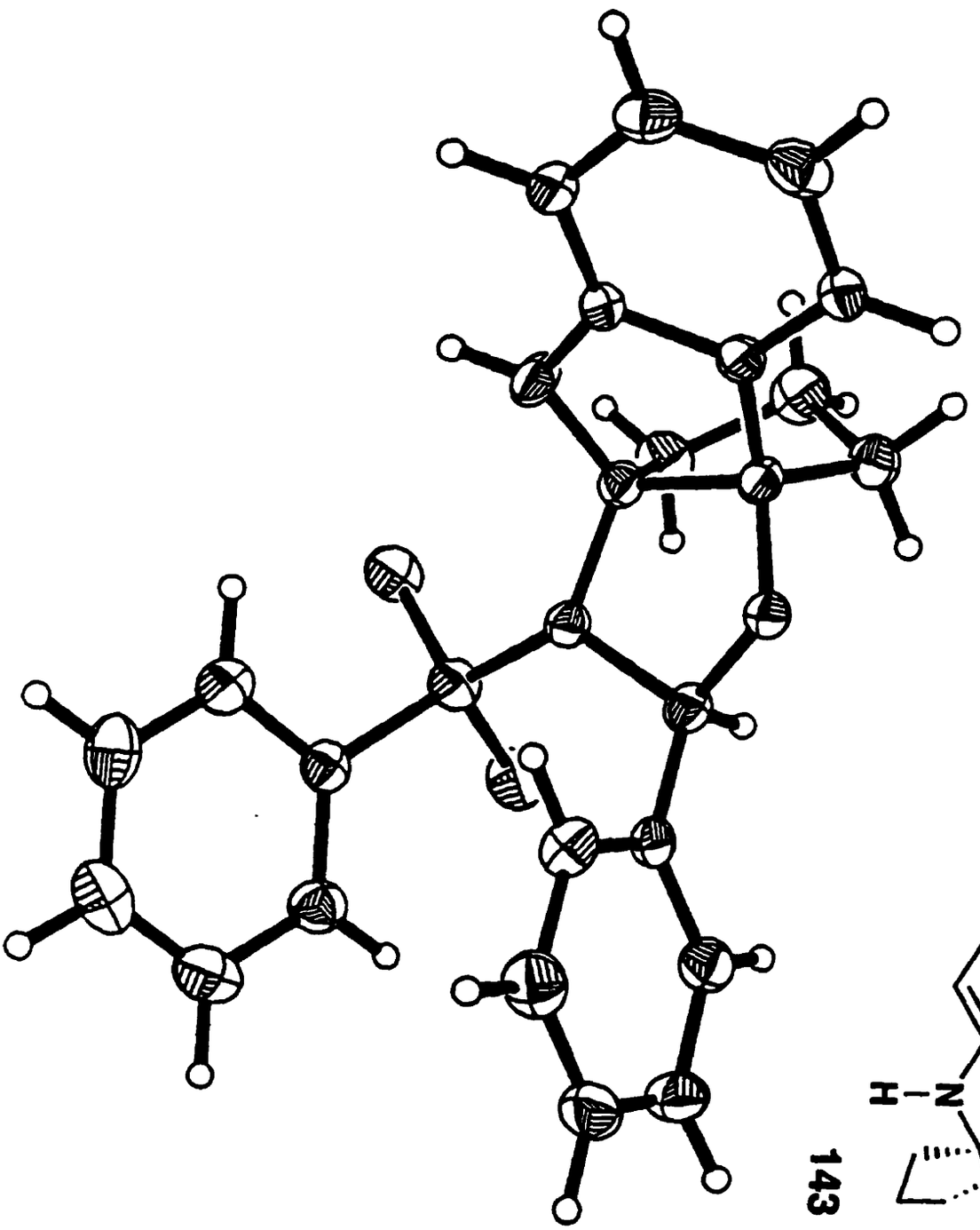
	U_{11}	U_{22}	U_{33}	U_{12}	U_{13}	U_{23}
N(1)	224(7)	154(7)	404(9)	-3(6)	98(6)	4(6)
C(2)	164(7)	174(8)	293(9)	-16(6)	32(6)	-12(7)
C(3)	157(7)	161(7)	272(9)	-21(6)	12(6)	-20(7)
C(3A)	165(7)	204(8)	221(8)	-30(6)	-5(6)	-15(7)
C(4)	238(9)	265(9)	310(9)	12(7)	42(7)	-39(7)
C(5)	289(9)	418(11)	280(9)	-40(8)	90(7)	-43(9)
C(6)	321(10)	357(10)	240(9)	-119(8)	16(7)	36(8)
C(7)	261(9)	227(9)	278(9)	-55(7)	-38(7)	40(7)
C(7A)	160(7)	209(8)	247(9)	-31(6)	-18(6)	-10(7)
O(8)	152(5)	152(6)	366(7)	-5(4)	3(5)	-25(5)
C(9)	175(7)	176(8)	257(8)	17(6)	20(6)	14(7)
N(10)	151(6)	163(6)	315(8)	-1(5)	26(5)	-20(6)
S(11)	179(2)	171(2)	375(2)	21(2)	58(2)	33(2)
O(12)	269(7)	319(7)	411(8)	59(5)	40(6)	148(6)
O(13)	255(7)	182(6)	588(9)	9(5)	105(6)	-64(6)
C(14)	157(8)	173(8)	346(9)	12(6)	57(7)	-8(7)
C(15)	236(9)	276(9)	318(10)	-17(7)	16(7)	-29(8)
C(16)	335(10)	312(10)	319(10)	-19(8)	100(8)	4(8)
C(17)	253(9)	295(10)	480(12)	-66(8)	149(8)	-53(9)
C(18)	185(8)	384(11)	429(11)	-54(8)	33(8)	-86(9)
C(19)	196(8)	313(10)	329(10)	30(7)	19(7)	-11(8)
C(20)	157(7)	170(8)	270(8)	24(6)	14(6)	-21(7)
C(21)	217(8)	195(8)	324(9)	17(6)	-6(7)	28(7)
C(22)	261(9)	201(9)	572(13)	-2(7)	103(9)	47(9)
C(23)	230(9)	280(10)	660(14)	-76(8)	48(9)	-164(10)
C(24)	236(9)	472(12)	438(12)	18(9)	-49(8)	-219(10)
C(25)	238(9)	319(10)	269(9)	30(7)	20(7)	-44(8)
C(26)	292(10)	347(10)	305(10)	-27(8)	43(8)	-85(8)
C(27)	216(8)	224(8)	336(10)	-7(7)	-17(7)	44(7)

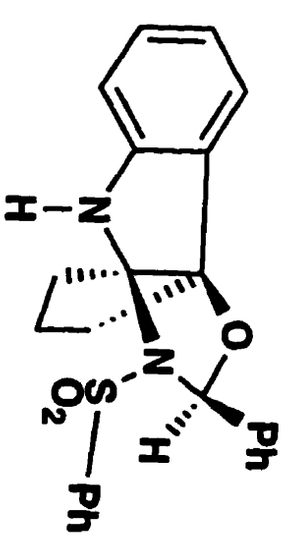
The anisotropic displacement factor exponent takes the form:

$-2\pi^2(h^2a^{*2}U_{11} + \ldots + 2klb^*c^*U_{23})$

Table 5. H-Atom coordinates ($x10^4$) and isotropic displacement coefficients ($Å^2 x10^3$)

	x	y	z	U
H(1)	272	284	2722	51(6)
H(4)	-2198	3320	4204	38(5)
H(5)	-3047	2031	5228	45(6)
H(6)	-2393	204	5273	43(6)
H(7)	-852	-354	4327	31(5)
H(9)	1210	2894	4113	17(4)
H(15)	2998	2779	1004	37(5)
H(16)	4382	3971	375	38(6)
H(17)	5925	4563	1355	39(6)
H(18)	6118	3952	2934	46(6)
H(19)	4750	2732	3567	32(5)
H(21)	2094	4765	2290	25(5)
H(22)	3468	6158	2505	41(6)
H(23)	4393	6395	3999	46(6)
H(24)	3899	5287	5297	49(6)
H(25)	2501	3897	5093	30(5)
H(26X)	471	2401	1042	41(6)
H(26Y)	-467	1503	1236	42(6)
H(26Z)	818	1165	1227	38(6)
H(27X)	-1702	3954	2429	33(5)
H(27Y)	-1850	2798	1937	36(5)
H(27Z)	-911	3607	1587	35(5)





143

STRUCTURE DETERMINATION SUMMARY

Crystal Data

Empirical Formula	$C_{24}H_{22}N_2O_3S$
Color; Habit	Colourless prism
Crystal Size (mm)	$0.76\{10\bar{1}\}x0.48(011,0\bar{1}\bar{1})$
	$x0.38(01\bar{1},0\bar{1}1)$
Crystal System	Monoclinic
Space Group	$P2_1/n$
Unit Cell Dimensions	$\underline{a}$ = 10.397(2) Å
	$\underline{b}$ = 25.958(7) Å
	$\underline{c}$ = 14.912(4) Å
	β = 93.89(2)°
Volume	4016(2) $Å^3$
Z	8
Formula Weight	418.5
Density(calc.)	1.384 g/cm^3
Absorption Coefficient	1.91 cm^{-1}
F(000)	1760

Data Collection

Diffractometer Used	Siemens R3m/V
Radiation	MoKα (λ = 0.71073 Å)
Temperature (K)	200
Monochromator	Highly oriented graphite crystal
2θ Range	4.0 to 50.0°
Scan Type	ω
Scan Speed	Variable; 2.93 to 29.30°/min. in ω
Scan Range (ω)	1.60°
Background Measurement	Stationary crystal and stationary counter at beginning and end of scan, each for 25.0% of total scan time
Standard Reflections	2 measured every 100 reflections
Index Ranges	$0 \leq h \leq 12$, $0 \leq k \leq 30$ $-17 \leq l \leq 17$
Reflections Collected	7111
Independent Reflections	7111
Observed Reflections	5073 ($F > 6.0\sigma(F)$)
Absorption Correction	Face-indexed numerical
Min./Max. Transmission	0.8940 / 0.9389

Solution and Refinement

System Used	Siemens SHELXTL PLUS (VMS)
Solution	Direct Methods
Refinement Method	Full-Matrix Least-Squares
Quantity Minimized	$\sum w(F_o - F_c)^2$
Extinction Correction	χ = 0.00041(2), where $F^* = F \left[1 + 0.002\chi F^2 / \sin(2\theta) \right]^{-1/4}$
Hydrogen Atoms	Riding model, refined isotropic U
Weighting Scheme	$w^{-1} = \sigma^2(F)$
Number of Parameters Refined	586
Final R Indices (obs. data)	R = 3.93 %, wR = 3.57 %
(R Indices (all data)	R = 5.24 %, wR = 3.63 %)
Goodness-of-Fit	2.79
Largest and Mean Δ/σ	0.003, 0.001
Data-to-Parameter Ratio	8.7:1
Largest Difference Peak	0.24 $e\text{Å}^{-3}$
Largest Difference Hole	-0.28 $e\text{Å}^{-3}$

Table 1. Atomic coordinates ($x10^4$) and equivalent isotropic displacement coefficients ($Å^2 x10^3$)

	x	y	z	U(eq)
Molecule 1				
N(1)	-14(2)	991.6(8)	5794(2)	38.1(8)
C(2)	-26(3)	1552(1)	5834(2)	31.5(9)
C(3)	-1479(3)	1710(1)	5822(2)	33.0(9)
C(3A)	-2171(3)	1203(1)	5818(2)	33(1)
C(4)	-3471(3)	1093(1)	5828(2)	47(1)
C(5)	-3858(3)	579(1)	5835(2)	57(1)
C(6)	-2946(4)	194(1)	5847(2)	58(1)
C(7)	-1650(3)	294(1)	5843(2)	46(1)
C(7A)	-1273(3)	809(1)	5822(2)	36(1)
O(8)	-1764(2)	1980.6(7)	4987(1)	34.4(6)
C(9)	-586(2)	2193(1)	4724(2)	30.6(9)
N(10)	342(2)	1780.5(8)	4983(1)	28.0(7)
S(11)	1850.7(6)	1813.5(3)	4742.8(5)	31.0(2)
O(12)	2553(2)	1471.4(7)	5350(1)	42.4(7)
O(13)	2248(2)	2341.9(7)	4701(1)	41.7(7)
C(14)	1833(2)	1556(1)	3653(2)	28(1)
C(15)	2206(2)	1846(1)	2940(2)	36(1)
C(16)	2142(3)	1627(1)	2094(2)	43(1)
C(17)	1720(3)	1129(1)	1970(2)	46(1)
C(18)	1360(3)	842(1)	2685(2)	44(1)
C(19)	1411(3)	1053(1)	3534(2)	36(1)
C(20)	-698(2)	2316(1)	3738(2)	27.7(8)
C(21)	-1005(2)	1939(1)	3106(2)	34.2(9)
C(22)	-1077(3)	2059(1)	2202(2)	42(1)
C(23)	-879(3)	2558(1)	1926(2)	50(1)
C(24)	-592(3)	2935(1)	2556(2)	53(1)
C(25)	-496(3)	2818(1)	3463(2)	38(1)
C(26)	623(3)	1777(1)	6703(2)	46(1)
C(27)	-504(3)	1838(1)	7301(2)	57(1)
C(28)	-1594(3)	2040(1)	6657(2)	52(1)
Molecule 2				
N(1')	7742(2)	1514.8(8)	-242(2)	38.0(8)
C(2')	7288(2)	991.3(9)	-271(2)	27.2(8)
C(3')	8539(2)	652.5(9)	-305(2)	26.2(8)
C(3A')	9593(2)	1042.7(9)	-338(2)	25.4(8)
C(4')	11163(3)	1891(1)	-374(2)	35.0(9)
C(5')	11682(3)	1401(1)	-454(2)	38(1)
C(6')	10892(2)	975(1)	-438(2)	31.3(9)
C(7')	9861(2)	1965(1)	-287(2)	30.5(9)
C(7A')	9073(2)	1535.7(9)	-280(2)	27.0(8)
O(8')	8643(2)	369.8(6)	527(1)	27.9(6)
C(9')	7371(2)	306(1)	800(2)	28.4(8)

N(10')	6803(2)	825.8(8)	606(1)	27.9(7)
S(11')	5300.4(6)	946.3(3)	804.4(5)	31.0(2)
O(12')	4919(2)	1373.6(7)	233(1)	41.4(7)
O(13')	4545(2)	483.4(7)	760(1)	44.0(7)
C(14')	5370(2)	1169(1)	1918(2)	29.4(9)
C(15')	5808(2)	1668(1)	2083(2)	37(1)
C(16')	5848(3)	1856(1)	2950(2)	45(1)
C(17')	5462(3)	1554(1)	3636(2)	48(1)
C(18')	5034(3)	1057(1)	3467(2)	48(1)
C(19')	4977(3)	861(1)	2603(2)	38(1)
C(20')	7419(2)	150.0(9)	1768(2)	27.2(8)
C(21')	8006(3)	458(1)	2431(2)	38(1)
C(22')	8043(3)	305(1)	3319(2)	43(1)
C(23')	7513(3)	-159(1)	3547(2)	46(1)
C(24')	6951(3)	-475(1)	2890(2)	45(1)
C(25')	6898(3)	-319(1)	1999(2)	36(1)
C(26')	6440(3)	841(1)	-1109(2)	40(1)
C(27')	7362(3)	612(1)	-1739(2)	45(1)
C(28')	8318(3)	308(1)	-1133(2)	37(1)

* Equivalent isotropic U defined as one third of the trace of the orthogonalized U_{ij} tensor

Table 2. Bond lengths (Å)

Molecule 1			
N(1)-C(2)	1.457(3)	N(1)-C(7A)	1.395(4)
C(2)-C(3)	1.564(4)	C(2)-N(10)	1.474(3)
C(2)-C(26)	1.536(4)	C(3)-C(3A)	1.499(4)
C(3)-O(8)	1.443(3)	C(3)-C(28)	1.524(4)
C(3A)-C(4)	1.383(4)	C(3A)-C(7A)	1.385(4)
C(4)-C(5)	1.392(5)	C(5)-C(6)	1.377(5)
C(6)-C(7)	1.373(5)	C(7)-C(7A)	1.393(4)
O(8)-C(9)	1.422(3)	C(9)-N(10)	1.476(3)
C(9)-C(20)	1.502(4)	N(10)-S(11)	1.634(2)
S(11)-O(12)	1.432(2)	S(11)-O(13)	1.435(2)
S(11)-C(14)	1.757(3)	C(14)-C(15)	1.379(4)
C(14)-C(19)	1.384(4)	C(15)-C(16)	1.381(4)
C(16)-C(17)	1.375(4)	C(17)-C(18)	1.374(4)
C(18)-C(19)	1.377(4)	C(20)-C(21)	1.382(4)
C(20)-C(25)	1.385(4)	C(21)-C(22)	1.382(4)
C(22)-C(23)	1.378(5)	C(23)-C(24)	1.376(4)
C(24)-C(25)	1.383(4)	C(26)-C(27)	1.527(4)
C(27)-C(28)	1.528(4)		
Molecule 2			
N(1')-C(2')	1.438(3)	N(1')-C(7A')	1.390(3)
C(2')-C(3')	1.574(3)	C(2')-N(10')	1.496(3)
C(2')-C(26')	1.530(4)	C(3')-C(3A')	1.495(3)
C(3')-O(8')	1.439(3)	C(3')-C(28')	1.529(4)
C(3A')-C(6')	1.380(3)	C(3A')-C(7A')	1.394(3)
C(4')-C(5')	1.389(4)	C(4')-C(7')	1.383(4)
C(5')-C(6')	1.379(4)	C(7')-C(7A')	1.383(4)
O(8')-C(9')	1.420(3)	C(9')-N(10')	1.493(3)
C(9')-C(20')	1.497(4)	N(10')-S(11')	1.640(2)
S(11')-O(12')	1.438(2)	S(11')-O(13')	1.434(2)
S(11')-C(14')	1.755(3)	C(14')-C(15')	1.390(4)
C(14')-C(19')	1.380(4)	C(15')-C(16')	1.381(4)
C(16')-C(17')	1.370(5)	C(17')-C(18')	1.383(5)
C(18')-C(19')	1.382(4)	C(20')-C(21')	1.381(4)
C(20')-C(25')	1.386(4)	C(21')-C(22')	1.381(4)
C(22')-C(23')	1.378(4)	C(23')-C(24')	1.376(4)
C(24')-C(25')	1.387(4)	C(26')-C(27')	1.510(4)
C(27')-C(28')	1.518(4)		

Table 3. Bond angles (°)

Molecule 1

C(2)-N(1)-C(7A)	109.1(2)	N(1)-C(2)-C(3)	105.7(2)
N(1)-C(2)-N(10)	111.3(2)	C(3)-C(2)-N(10)	101.1(2)
N(1)-C(2)-C(26)	114.1(2)	C(3)-C(2)-C(26)	106.2(2)
N(10)-C(2)-C(26)	116.7(2)	C(2)-C(3)-C(3A)	103.5(2)
C(2)-C(3)-O(8)	106.2(2)	C(3A)-C(3)-O(8)	110.8(2)
C(2)-C(3)-C(28)	105.5(2)	C(3A)-C(3)-C(28)	115.6(2)
O(8)-C(3)-C(28)	114.1(2)	C(3)-C(3A)-C(4)	130.7(3)
C(3)-C(3A)-C(7A)	108.9(2)	C(4)-C(3A)-C(7A)	120.4(3)
C(3A)-C(4)-C(5)	118.8(3)	C(4)-C(5)-C(6)	119.7(3)
C(5)-C(6)-C(7)	122.5(3)	C(6)-C(7)-C(7A)	117.4(3)
N(1)-C(7A)-C(3A)	112.5(2)	N(1)-C(7A)-C(7)	126.3(3)
C(3A)-C(7A)-C(7)	121.1(3)	C(3)-O(8)-C(9)	107.3(2)
O(8)-C(9)-N(10)	101.9(2)	O(8)-C(9)-C(20)	110.0(2)
N(10)-C(9)-C(20)	114.6(2)	C(2)-N(10)-C(9)	108.3(2)
C(2)-N(10)-S(11)	121.2(2)	C(9)-N(10)-S(11)	121.7(2)
N(10)-S(11)-O(12)	106.5(1)	N(10)-S(11)-O(13)	110.1(1)
O(12)-S(11)-O(13)	118.9(1)	N(10)-S(11)-C(14)	103.4(1)
O(12)-S(11)-C(14)	108.8(1)	O(13)-S(11)-C(14)	108.0(1)
S(11)-C(14)-C(15)	121.2(2)	S(11)-C(14)-C(19)	117.4(2)
C(15)-C(14)-C(19)	121.3(2)	C(14)-C(15)-C(16)	118.7(3)
C(15)-C(16)-C(17)	120.4(3)	C(16)-C(17)-C(18)	120.4(3)
C(17)-C(18)-C(19)	120.2(3)	C(14)-C(19)-C(18)	119.0(3)
C(9)-C(20)-C(21)	121.0(2)	C(9)-C(20)-C(25)	119.1(2)
C(21)-C(20)-C(25)	119.8(2)	C(20)-C(21)-C(22)	120.0(3)
C(21)-C(22)-C(23)	120.3(3)	C(22)-C(23)-C(24)	119.6(3)
C(23)-C(24)-C(25)	120.6(3)	C(20)-C(25)-C(24)	119.6(3)
C(2)-C(26)-C(27)	102.8(2)	C(26)-C(27)-C(28)	103.5(2)
C(3)-C(28)-C(27)	103.0(2)		

Molecule 2

C(2')-N(1')-C(7A')	111.2(2)	N(1')-C(2')-C(3')	105.0(2)
N(1')-C(2')-N(10')	112.0(2)	C(3')-C(2')-N(10')	101.3(2)
N(1')-C(2')-C(26')	115.8(2)	C(3')-C(2')-C(26')	105.3(2)
N(10')-C(2')-C(26')	115.5(2)	C(2')-C(3')-C(3A')	103.4(2)
C(2')-C(3')-O(8')	105.7(2)	C(3A')-C(3')-O(8')	111.2(2)
C(2')-C(3')-C(28')	105.8(2)	C(3A')-C(3')-C(28')	116.1(2)
O(8')-C(3')-C(28')	113.3(2)	C(3')-C(3A')-C(6')	129.9(2)
C(3')-C(3A')-C(7A')	109.4(2)	C(6')-C(3A')-C(7A')	120.7(2)
C(5')-C(4')-C(7')	121.6(2)	C(4')-C(5')-C(6')	119.9(2)
C(3A')-C(6')-C(5')	119.2(2)	C(4')-C(7')-C(7A')	118.2(2)
N(1')-C(7A')-C(3A')	111.0(2)	N(1')-C(7A')-C(7')	128.6(2)
C(3A')-C(7A')-C(7')	120.5(2)	C(3')-O(8')-C(9')	106.8(2)
O(8')-C(9')-N(10')	101.7(2)	O(8')-C(9')-C(20')	109.7(2)
N(10')-C(9')-C(20')	114.8(2)	C(2')-N(10')-C(9')	106.1(2)
C(2')-N(10')-S(11')	119.0(2)	C(9')-N(10')-S(11')	120.4(2)
N(10')-S(11')-O(12')	105.5(1)	N(10')-S(11')-O(13')	110.9(1)
O(12')-S(11')-O(13')	119.4(1)	N(10')-S(11')-C(14')	104.8(1)
O(12')-S(11')-C(14')	107.4(1)	O(13')-S(11')-C(14')	107.8(1)
S(11')-C(14')-C(15')	117.8(2)	S(11')-C(14')-C(19')	121.0(2)
C(15')-C(14')-C(19')	121.2(3)	C(14')-C(15')-C(16')	119.0(3)
C(15')-C(16')-C(17')	120.3(3)	C(16')-C(17')-C(18')	120.4(3)
C(17')-C(18')-C(19')	120.3(3)	C(14')-C(19')-C(18')	118.8(3)
C(9')-C(20')-C(21')	121.2(2)	C(9')-C(20')-C(25')	119.3(2)
C(21')-C(20')-C(25')	119.5(2)	C(20')-C(21')-C(22')	120.2(3)
C(21')-C(22')-C(23')	120.1(3)	C(22')-C(23')-C(24')	120.2(3)
C(23')-C(24')-C(25')	119.8(3)	C(20')-C(25')-C(24')	120.2(3)
C(2')-C(26')-C(27')	104.7(2)	C(26')-C(27')-C(28')	104.6(2)
C(3')-C(28')-C(27')	103.5(2)		

Table 4. Anisotropic displacement coefficients ($Å^2 x 10^3$)

	U_{11}	U_{22}	U_{33}	U_{12}	U_{13}	U_{23}
Molecule 1						
N(1)	42(1)	24(1)	47(2)	-1(1)	1(1)	10(1)
C(2)	42(2)	27(2)	25(1)	-5(1)	1(1)	3(1)
C(3)	44(2)	31(2)	25(1)	4(1)	7(1)	3(1)
C(3A)	42(2)	38(2)	20(1)	-7(1)	6(1)	0(1)
C(4)	45(2)	67(2)	30(2)	-4(2)	8(1)	5(2)
C(5)	53(2)	84(3)	34(2)	-35(2)	4(2)	3(2)
C(6)	85(3)	53(2)	37(2)	-31(2)	12(2)	-4(2)
C(7)	67(2)	34(2)	39(2)	-17(2)	10(2)	0(1)
C(7A)	51(2)	32(2)	25(2)	-9(1)	4(1)	1(1)
O(8)	35(1)	35(1)	34(1)	5.9(9)	8.6(8)	6.9(8)
C(9)	39(2)	23(1)	30(2)	3(1)	3(1)	-1(1)
N(10)	32(1)	27(1)	25(1)	1(1)	3(1)	5(1)
S(11)	29.5(4)	28.0(4)	34.7(4)	-4.3(3)	-3.1(3)	0.3(3)
O(12)	38(1)	47(1)	40(1)	5.3(9)	-9.8(9)	8(1)
O(13)	44(1)	28(1)	53(1)	-14.2(9)	-1(1)	-4.6(9)
C(14)	22(1)	28(2)	35(2)	-1(1)	3(1)	0(1)
C(15)	32(2)	34(2)	43(2)	-6(1)	2(1)	6(1)
C(16)	43(2)	50(2)	38(2)	1(1)	10(1)	8(2)
C(17)	47(2)	55(2)	37(2)	4(2)	6(1)	-11(2)
C(18)	51(2)	33(2)	48(2)	-4(1)	11(2)	-10(1)
C(19)	40(2)	27(2)	42(2)	-5(1)	10(1)	-2(1)
C(20)	27(1)	30(2)	26(1)	3(1)	1(1)	2(1)
C(21)	35(2)	35(2)	32(2)	1(1)	-1(1)	-1(1)
C(22)	36(2)	55(2)	35(2)	6(1)	-5(1)	-8(2)
C(23)	56(2)	66(2)	29(2)	12(2)	1(1)	8(2)
C(24)	76(2)	44(2)	41(2)	7(2)	8(2)	15(2)
C(25)	51(2)	31(2)	32(2)	3(1)	5(1)	2(1)
C(26)	66(2)	45(2)	27(2)	-18(2)	-8(2)	2(1)
C(27)	88(3)	57(2)	27(2)	-27(2)	8(2)	-8(2)
C(28)	74(2)	41(2)	43(2)	-4(2)	24(2)	-9(2)

Molecule 2

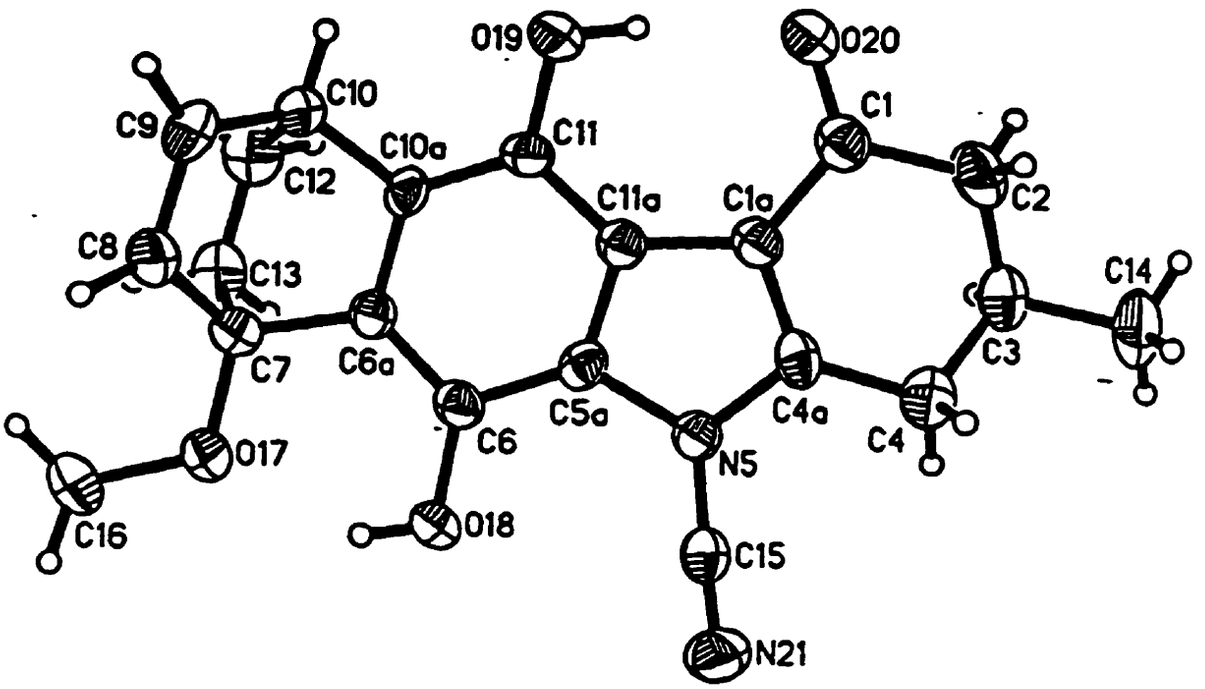
N(1')	27(1)	21(1)	67(2)	4(1)	11(1)	3(1)
C(2')	27(1)	25(1)	30(1)	0(1)	3(1)	-1(1)
C(3')	31(1)	21(1)	26(1)	2(1)	2(1)	1(1)
C(3A')	31(1)	26(1)	20(1)	1(1)	2(1)	-1(1)
C(4')	34(2)	38(2)	33(2)	-10(1)	0(1)	3(1)
C(5')	26(2)	50(2)	39(2)	2(1)	7(1)	6(1)
C(6')	30(1)	31(2)	34(2)	5(1)	8(1)	2(1)
C(7')	35(2)	25(2)	31(2)	0(1)	5(1)	-1(1)
C(7A')	30(1)	26(1)	25(1)	0(1)	4(1)	-2(1)
O(8')	27.1(9)	25(1)	32(1)	4.1(8)	6.3(8)	2.9(8)
C(9')	27(1)	25(1)	34(2)	-1(1)	1(1)	-1(1)
N(10')	26(1)	27(1)	31(1)	4.5(9)	3.6(9)	4(1)
S(11')	23.0(3)	36.3(4)	33.6(4)	0.9(3)	0.5(3)	-0.3(3)
O(12')	33(1)	53(1)	38(1)	16.1(9)	1.0(8)	11(1)
O(13')	32(1)	47(1)	54(1)	-12.4(9)	4.2(9)	-12(1)
C(14')	21(1)	32(2)	36(2)	4(1)	2(1)	0(1)
C(15')	31(2)	35(2)	44(2)	0(1)	2(1)	2(1)
C(16')	40(2)	43(2)	52(2)	3(1)	-5(1)	-14(2)
C(17')	41(2)	65(2)	38(2)	12(2)	0(1)	-9(2)
C(18')	46(2)	61(2)	39(2)	4(2)	8(1)	9(2)
C(19')	35(2)	39(2)	40(2)	-1(1)	5(1)	3(1)
C(20')	24(1)	27(1)	30(2)	4(1)	4(1)	0(1)
C(21')	40(2)	32(2)	41(2)	1(1)	-1(1)	2(1)
C(22')	45(2)	50(2)	34(2)	7(2)	-3(1)	-1(2)
C(23')	52(2)	53(2)	36(2)	14(2)	10(1)	10(2)
C(24')	48(2)	41(2)	49(2)	2(2)	17(2)	14(2)
C(25')	34(2)	34(2)	40(2)	-1(1)	8(1)	-1(1)
C(26')	41(2)	49(2)	31(2)	1(2)	-4(1)	-1(1)
C(27')	58(2)	44(2)	32(2)	-2(2)	-2(2)	-5(2)
C(28')	46(2)	31(2)	35(2)	-6(1)	8(1)	-9(1)

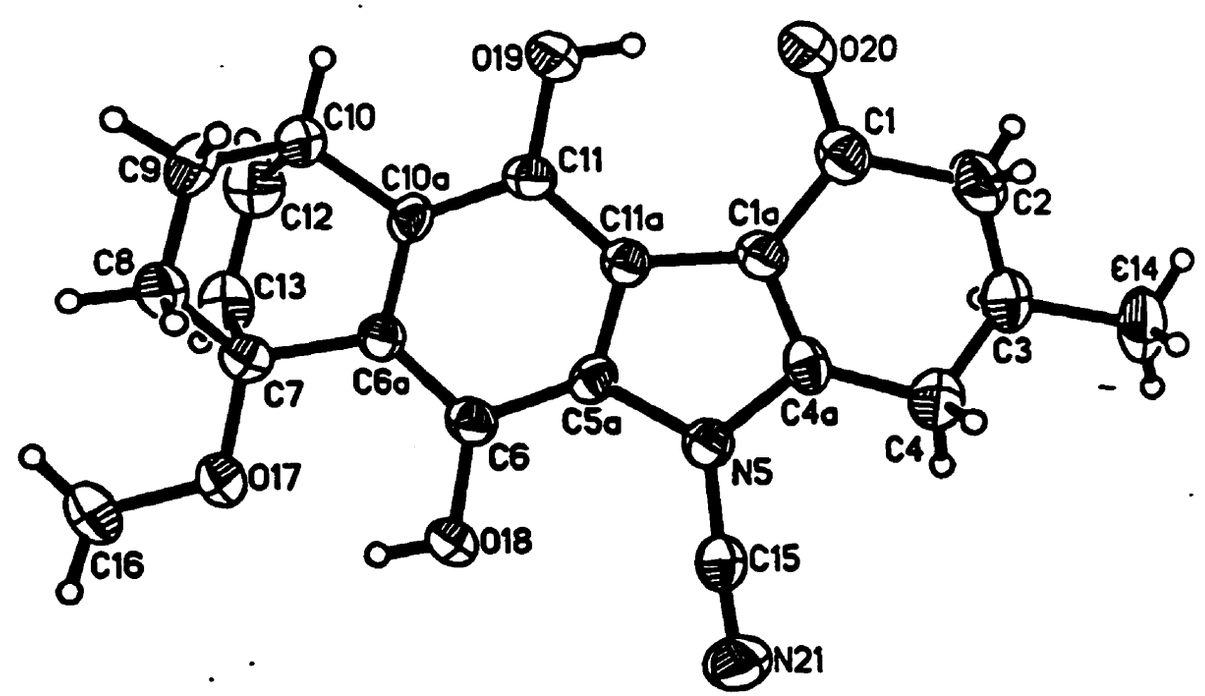
The anisotropic displacement factor exponent takes the form:

$$-2\pi^2(h^2a^{*2}U_{11} + \ldots + 2klb^*c^*U_{23})$$

Table 5. H-Atom coordinates ($x10^4$) and isotropic displacement coefficients ($Å^2 x10^3$)

	x	y	z	U
Molecule 1				
H(1)	689	804	6164	75(11)
H(4)	-4098	1364	5837	34(8)
H(5)	-4754	489	5828	71(11)
H(6)	-3223	-158	5859	69(10)
H(7)	-1023	23	5858	71(11)
H(9)	-379	2500	5063	23(6)
H(15)	2522	2190	3037	31(7)
H(16)	2367	1825	1584	53(9)
H(17)	1686	974	1384	44(8)
H(18)	1074	493	2598	52(9)
H(19)	1160	855	4038	47(8)
H(21)	-1158	1592	3296	33(7)
H(22)	-1282	1794	1766	50(9)
H(23)	-927	2638	1296	59(9)
H(24)	-471	3284	2366	79(12)
H(25)	-278	3080	3902	46(8)
H(26X)	1022	2103	6596	53(9)
H(26Y)	1259	1544	6967	63(10)
H(27X)	-297	2076	7780	74(11)
H(27Y)	-734	1513	7553	59(10)
H(28X)	-2417	1994	6901	45(8)
H(28Y)	-1473	2398	6527	54(9)
Molecule 2				
H(1')	7216	1813	-308	37(7)
H(4')	11724	2185	-375	32(7)
H(5')	12586	1360	-529	32(7)
H(6')	11238	634	-491	37(8)
H(7')	9506	2304	-230	27(7)
H(9')	6925	50	432	23(6)
H(15')	6071	1876	1596	45(8)
H(16')	6148	2201	3071	58(10)
H(17')	5492	1691	4234	54(9)
H(18')	4781	846	3954	63(10)
H(19')	4674	518	2471	32(7)
H(21')	8387	779	2268	53(9)
H(22')	8444	525	3775	51(9)
H(23')	7537	-264	4166	52(9)
H(24')	6605	-803	3046	58(9)
H(25')	6488	-533	1539	53(9)
H(26X')	5999	1136	-1370	52(9)
H(26Y')	5815	588	-960	58(10)
H(27X')	7799	882	-2036	64(10)
H(27Y')	6924	396	-2185	49(9)
H(28X')	7955	-18	-978	40(8)
H(28Y')	9108	250	-1414	43(8)

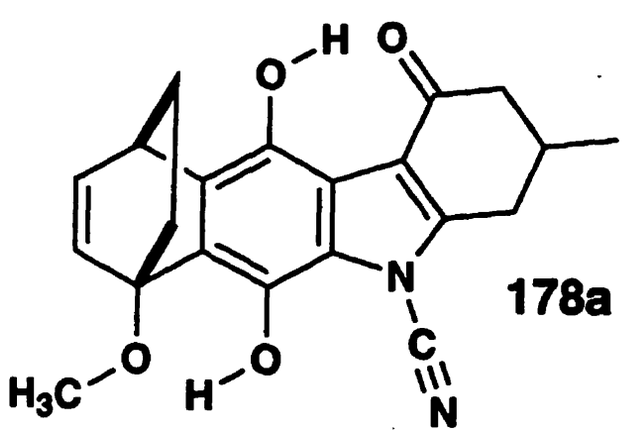

O19
O20
C10
C1
C9
C10a
C11
C12
C11a
C1a
C2
C8
C13
C14
C7
C6a
C3
C6
C5a
C4a
C4
O17
N5
C16
O18
C15
N21


O19
O20
C10
C1
C9
C10a
C11
C12
C11a
C1a
C2
C8
C13
C14
C7
C6a
C3
C6
C5a
C4a
C4
O17
N5
C16
O18
C15
N21

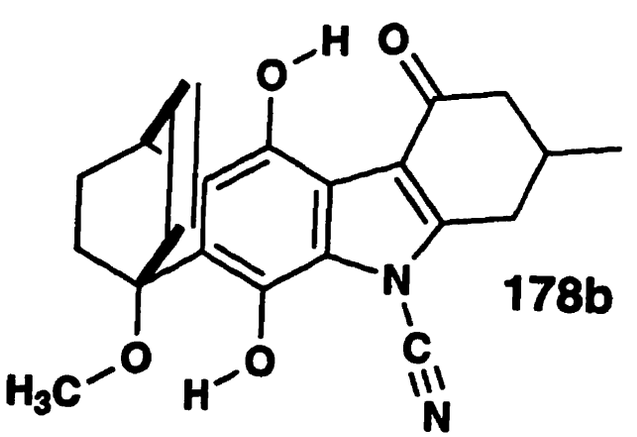
STRUCTURE DETERMINATION SUMMARY

Crystal Data

Empirical Formula	$C_{21}H_{20}N_2O_4$
Color; Habit	Colourless needle prism fragment
Crystal Size (mm)	0.54{10$\bar{1}$}x0.16{011}
Crystal System	Monoclinic
Space Group	$P2_1/n$
Unit Cell Dimensions	$\underline{a}$ = 7.832(3) Å
	$\underline{b}$ = 20.465(7) Å
	$\underline{c}$ = 11.361(4) Å
	β = 105.72(3)°
Volume	1752.8(11) Å^3
Z	4
Formula Weight	364.4
Density(calc.)	1.381 g/cm^3
Absorption Coefficient	0.97 cm^{-1}
F(000)	768



178a



178b

Data Collection

Diffractometer Used	Siemens R3m/V
Radiation	MoKα (λ = 0.71073 Å)
Temperature (K)	200
Monochromator	Highly oriented graphite crystal
2θ Range	4.0 to 50.0°
Scan Type	ω
Scan Speed	Variable; 2.93 to 29.30°/min. in ω
Scan Range (ω)	1.40°
Background Measurement	Stationary crystal and stationary counter at beginning and end of scan, each for 25.0% of total scan time
Standard Reflections	2 measured every 100 reflections
Index Ranges	$0 \leq h \leq 9$, $0 \leq k \leq 24$ $-13 \leq l \leq 13$
Reflections Collected	3342
Independent Reflections	3111 (R_{int} = 2.85%)
Observed Reflections	1826 ($F > 6.0\sigma(F)$)
Absorption Correction	Face-indexed numerical
Min./Max. Transmission	0.9754 / 0.9927

Solution and Refinement

System Used	Siemens SHELXTL PLUS (VMS)
Solution	Direct Methods
Refinement Method	Full-Matrix Least-Squares
Quantity Minimized	$\sum w(F_o-F_c)^2$
Hydrogen Atoms	Riding model, refined isotropic U
Weighting Scheme	$w^{-1} = \sigma^2(F) + 0.0001F^2$
Number of Parameters Refined	262
Final R Indices (obs. data)	R = 6.04 %, wR = 6.18 %
(R Indices (all data)	R = 9.31 %, wR = 6.48 %)
Goodness-of-Fit	2.65
Largest and Mean Δ/σ	0.008, 0.001
Data-to-Parameter Ratio	7.0:1
Largest Difference Peak	0.30 $e\text{Å}^{-3}$
Largest Difference Hole	-0.25 $e\text{Å}^{-3}$

Table 1. Atomic coordinates ($\times 10^4$) and equivalent isotropic displacement coefficients ($Å^2 \times 10^3$)

	x	y	z	U(eq)
C(1)	2564(5)	9551(2)	5643(4)	38(2)
C(1A)	1050(5)	9342(2)	6040(3)	30(1)
C(2)	3729(5)	10061(3)	6430(4)	53(2)
C(3)	3612(6)	10120(3)	7712(5)	59(2)
C(4)	1773(5)	10111(2)	7866(4)	42(2)
C(4A)	697(5)	9609(2)	7052(3)	32(1)
N(5)	-855(4)	9337(2)	7191(3)	30(1)
C(5A)	-1495(4)	8866(2)	6259(3)	27(1)
C(6)	-2943(4)	8450(2)	6090(3)	30(1)
C(6A)	-3172(5)	8004(2)	5136(3)	30(1)
C(7)	-4569(5)	7475(2)	4800(3)	36(2)
C(8)	-5532(5)	7561(2)	3451(3)	37(2)
C(9)	-4363(5)	7541(2)	2692(4)	39(2)
C(10)	-2443(5)	7450(2)	3439(4)	37(1)
C(10A)	-2000(5)	7993(2)	4388(3)	29(1)
C(11)	-588(4)	8419(2)	4550(3)	29(1)
C(11A)	-314(4)	8863(2)	5533(3)	27(1)
C(12)	-2376(5)	6807(2)	4139(4)	44(2)
C(13)	-3568(5)	6827(2)	4921(4)	46(2)
C(14)	4718(6)	10674(2)	8425(5)	58(2)
C(15)	-1493(5)	9456(2)	8168(4)	34(1)
C(16)	-7104(6)	7046(3)	5374(5)	58(2)
O(17)	-5717(4)	7521(2)	5578(3)	53(1)
O(18)	-4008(3)	8499(1)	6868(2)	39(1)
O(19)	484(3)	8390(1)	3781(2)	40(1)
O(20)	2853(4)	9352(2)	4688(3)	51(1)
N(21)	-1954(5)	9569(2)	9020(3)	52(2)

* Equivalent isotropic U defined as one third of the trace of the orthogonalized U_{ij} tensor

Table 2. Bond lengths (Å)

C(1)-C(1A)	1.443(6)	C(1)-C(2)	1.510(6)
C(1)-O(20)	1.236(5)	C(1A)-C(4A)	1.367(6)
C(1A)-C(11A)	1.450(5)	C(2)-C(3)	1.488(7)
C(3)-C(4)	1.498(7)	C(3)-C(14)	1.521(7)
C(4)-C(4A)	1.483(5)	C(4A)-N(5)	1.384(5)
N(5)-C(5A)	1.419(5)	N(5)-C(15)	1.357(6)
C(5A)-C(6)	1.389(5)	C(5A)-C(11A)	1.397(6)
C(6)-C(6A)	1.392(5)	C(6)-O(18)	1.373(5)
C(6A)-C(7)	1.514(5)	C(6A)-C(10A)	1.410(6)
C(7)-C(8)	1.524(5)	C(7)-C(13)	1.526(6)
C(7)-O(17)	1.424(6)	C(8)-C(9)	1.417(6)
C(9)-C(10)	1.525(5)	C(10)-C(10A)	1.521(5)
C(10)-C(12)	1.532(6)	C(10A)-C(11)	1.382(5)
C(11)-C(11A)	1.409(5)	C(11)-O(19)	1.367(5)
C(12)-C(13)	1.453(7)	C(15)-N(21)	1.144(6)
C(16)-O(17)	1.429(6)		

Table 3. Bond angles (°)

C(1A)-C(1)-C(2)	115.8(4)	C(1A)-C(1)-O(20)	122.6(3)
C(2)-C(1)-O(20)	121.6(4)	C(1)-C(1A)-C(4A)	121.1(3)
C(1)-C(1A)-C(11A)	130.9(4)	C(4A)-C(1A)-C(11A)	108.0(3)
C(1)-C(2)-C(3)	116.6(4)	C(2)-C(3)-C(4)	115.4(4)
C(2)-C(3)-C(14)	113.9(5)	C(4)-C(3)-C(14)	111.9(5)
C(3)-C(4)-C(4A)	109.7(4)	C(1A)-C(4A)-C(4)	126.2(4)
C(1A)-C(4A)-N(5)	108.7(3)	C(4)-C(4A)-N(5)	125.1(4)
C(4A)-N(5)-C(5A)	109.3(3)	C(4A)-N(5)-C(15)	123.4(3)
C(5A)-N(5)-C(15)	126.7(3)	N(5)-C(5A)-C(6)	129.0(4)
N(5)-C(5A)-C(11A)	106.7(3)	C(6)-C(5A)-C(11A)	124.2(3)
C(5A)-C(6)-C(6A)	115.9(4)	C(5A)-C(6)-O(18)	118.9(3)
C(6A)-C(6)-O(18)	125.2(3)	C(6)-C(6A)-C(7)	126.7(4)
C(6)-C(6A)-C(10A)	120.9(3)	C(7)-C(6A)-C(10A)	112.4(3)
C(6A)-C(7)-C(8)	107.3(3)	C(6A)-C(7)-C(13)	106.3(3)
C(8)-C(7)-C(13)	107.0(3)	C(6A)-C(7)-O(17)	109.3(3)
C(8)-C(7)-O(17)	113.1(3)	C(13)-C(7)-O(17)	113.4(4)
C(7)-C(8)-C(9)	112.6(3)	C(8)-C(9)-C(10)	111.5(3)
C(9)-C(10)-C(10A)	107.8(3)	C(9)-C(10)-C(12)	106.5(3)
C(10A)-C(10)-C(12)	106.9(3)	C(6A)-C(10A)-C(10)	112.3(3)
C(6A)-C(10A)-C(11)	122.5(3)	C(10)-C(10A)-C(11)	125.2(4)
C(10A)-C(11)-C(11A)	117.2(4)	C(10A)-C(11)-O(19)	119.6(3)
C(11A)-C(11)-O(19)	123.1(3)	C(1A)-C(11A)-C(5A)	107.2(3)
C(1A)-C(11A)-C(11)	133.5(4)	C(5A)-C(11A)-C(11)	119.2(3)
C(10)-C(12)-C(13)	110.8(4)	C(7)-C(13)-C(12)	111.7(4)
N(5)-C(15)-N(21)	176.7(4)	C(7)-O(17)-C(16)	115.7(4)

Table 4. Anisotropic displacement coefficients ($Å^2 x 10^3$)

	U_{11}	U_{22}	U_{33}	U_{12}	U_{13}	U_{23}
C(1)	32(2)	45(3)	34(2)	-4(2)	5(2)	4(2)
C(1A)	25(2)	39(2)	25(2)	-3(2)	4(2)	3(2)
C(2)	32(2)	68(4)	57(3)	-19(2)	11(2)	-5(3)
C(3)	45(3)	72(4)	62(3)	-28(3)	15(2)	-24(3)
C(4)	44(2)	39(3)	40(3)	-5(2)	8(2)	-1(2)
C(4A)	25(2)	34(2)	33(2)	-5(2)	1(2)	3(2)
N(5)	28(2)	33(2)	27(2)	-1(1)	5(1)	0(2)
C(5A)	24(2)	32(2)	20(2)	1(2)	-1(2)	-2(2)
C(6)	22(2)	42(3)	25(2)	0(2)	4(2)	2(2)
C(6A)	25(2)	36(2)	25(2)	-1(2)	4(2)	-1(2)
C(7)	34(2)	44(3)	33(2)	-8(2)	12(2)	-3(2)
C(8)	25(2)	47(3)	35(2)	-4(2)	4(2)	-3(2)
C(9)	41(2)	42(3)	29(2)	-3(2)	-2(2)	-5(2)
C(10)	30(2)	47(3)	33(2)	-5(2)	9(2)	-7(2)
C(10A)	24(2)	35(2)	24(2)	0(2)	0(2)	-4(2)
C(11)	22(2)	41(3)	23(2)	3(2)	5(2)	2(2)
C(11A)	22(2)	33(2)	25(2)	0(2)	3(2)	2(2)
C(12)	38(2)	38(3)	53(3)	8(2)	6(2)	2(2)
C(13)	44(2)	42(3)	48(3)	-6(2)	4(2)	2(2)
C(14)	43(3)	43(3)	82(4)	-12(2)	7(3)	-13(3)
C(15)	29(2)	36(3)	33(2)	-3(2)	4(2)	-2(2)
C(16)	46(3)	66(4)	68(4)	-26(3)	27(3)	-13(3)
O(17)	48(2)	72(2)	48(2)	-32(2)	25(2)	-21(2)
O(18)	30(1)	53(2)	37(1)	-10(1)	16(1)	-8(2)
O(19)	30(1)	54(2)	38(2)	-7(2)	14(1)	-5(2)
O(20)	45(2)	68(2)	45(2)	-19(2)	21(1)	-9(2)
N(21)	47(2)	70(3)	40(2)	-1(2)	14(2)	-13(2)

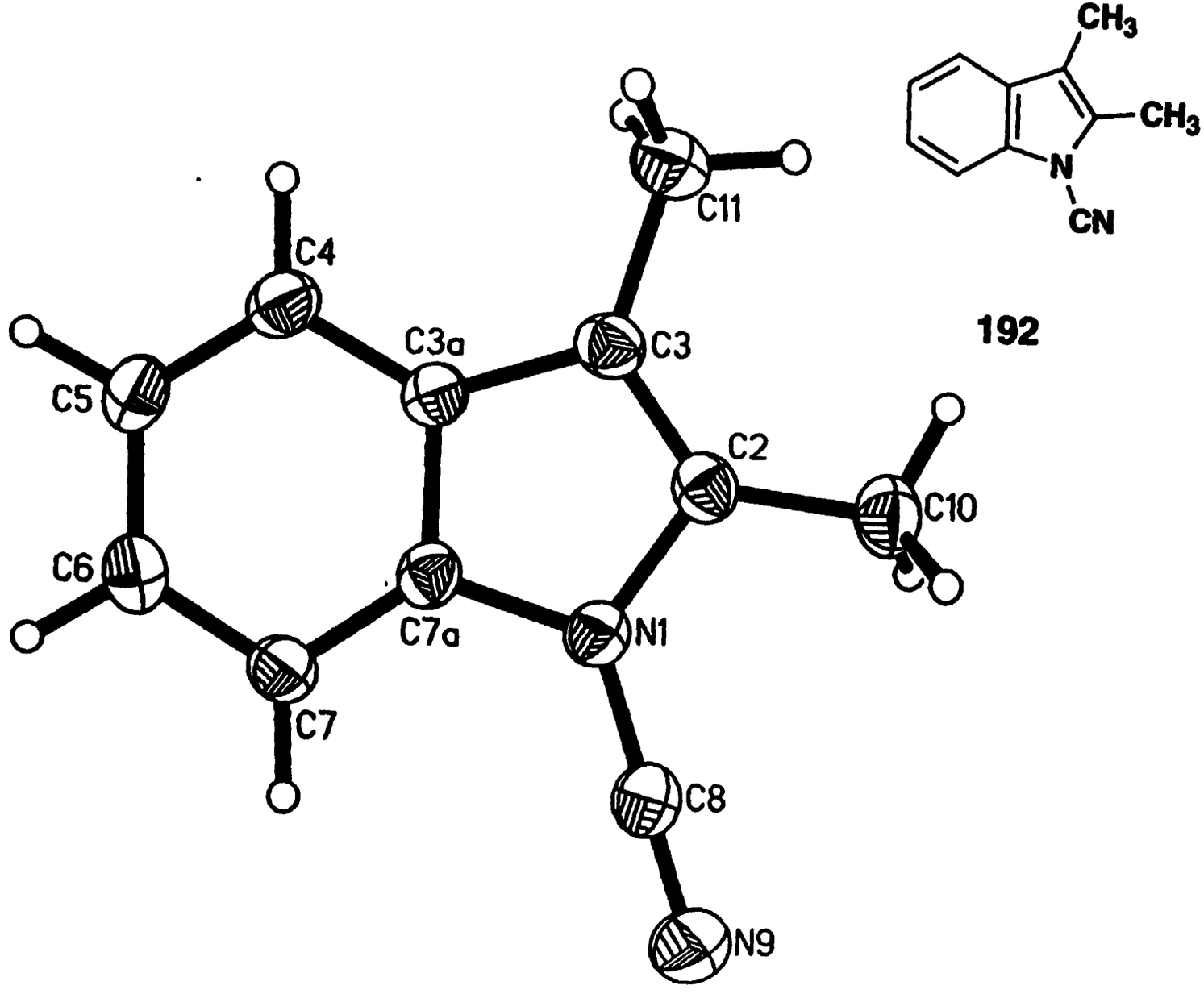
The anisotropic displacement factor exponent takes the form:

$-2\pi^2(h^2a^{*2}U_{11} + \ldots + 2klb^*c^*U_{23})$

Table 5. H-Atom coordinates ($x10^4$) and isotropic displacement coefficients ($Å^2 x10^3$)

	x	y	z	U
H(2X)	3437	10480	6049	152(31)
H(2Y)	4936	9966	6448	56(13)
H(3)	4161	9730	8113	186(38)
H(4X)	1811	10021	8702	72(15)
H(4Y)	1249	10534	7656	37(11)
H(8X)*	-6133	7974	3348	26(12)
H(8Y)**	-6792	7626	3156	26(12)
H(8Z)*	-6409	7224	3206	26(12)
H(9X)*	-4454	7941	2238	26(13)
H(9Y)**	-4723	7581	1818	26(13)
H(9Z)*	-4695	7188	2120	26(13)
H(10)	-1633	7450	2938	33(11)
H(12X)**	-1186	6732	4629	84(19)
H(12Y)*	-1640	6442	4068	84(19)
H(12Z)**	-2703	6454	3566	84(19)
H(13X)**	-4410	6477	4703	58(15)
H(13Y)*	-3719	6478	5448	58(15)
H(13Z)**	-2903	6768	5757	58(15)
H(14X)	4882	10615	9287	147(30)
H(14Y)	4113	11079	8176	86(18)
H(14Z)	5857	10693	8261	85(17)
H(16X)	-6649	6661	5836	115(25)
H(16Y)	-7503	6936	4522	113(23)
H(16Z)	-8096	7209	5631	108(22)
H(18)	-4817	8211	6671	59(15)
H(19)	1289	8678	3997	70(17)

Occupancy * = 0.4, ** = 0.6.



192

STRUCTURE DETERMINATION SUMMARY

Crystal Data

Empirical Formula	$C_{11}H_{10}N_2$
Color; Habit	Colourless needle prism fragment
Crystal Size (mm)	0.33{100}x0.26(011,$0\bar{1}\bar{1}$)
	x0.22{010}x0.22($01\bar{1}$,$0\bar{1}$1)
	Distances from common centre
Crystal System	Monoclinic
Space Group	$P2_1/n$
Unit Cell Dimensions	$\underline{a}$ = 7.238(1) Å
	$\underline{b}$ = 15.113(2) Å
	$\underline{c}$ = 8.779(1) Å
	β = 110.56(1)°
Volume	899.1(2) $Å^3$
Z	4
Formula Weight	170.2
Density(calc.)	1.257 g/cm^3
Absorption Coefficient	0.76 cm^{-1}
F(000)	360

Data Collection

Diffractometer Used	Siemens R3m/V
Radiation	MoKα (λ = 0.71073 Å)
Temperature (K)	180
Monochromator	Highly oriented graphite crystal
2θ Range	4.0 to 65.0°
Scan Type	ω
Scan Speed	Variable; 2.93 to 29.30°/min. in ω
Scan Range (ω)	1.30°
Background Measurement	Stationary crystal and stationary counter at beginning and end of scan, each for 25.0% of total scan time
Standard Reflections	2 measured every 100 reflections
Index Ranges	$0 \leq h \leq 10$, $0 \leq k \leq 22$ $-13 \leq l \leq 12$
Reflections Collected	3258
Independent Reflections	3258
Observed Reflections	2397 ($F > 6.0\sigma(F)$)
Absorption Correction	Face-indexed numerical
Min./Max. Transmission	0.9621 / 0.9707

Solution and Refinement

System Used	Siemens SHELXTL PLUS (VMS)
Solution	Direct Methods
Refinement Method	Full-Matrix Least-Squares
Quantity Minimized	$\sum w(F_o - F_c)^2$
Extinction Correction	χ = 0.0023(2), where $F^* = F \left[1 + 0.002\chi F^2 / \sin(2\theta) \right]^{-1/4}$
Hydrogen Atoms	Refined isotropic U
Weighting Scheme	$w^{-1} = \sigma^2(F) + 0.00001F^2$
Number of Parameters Refined	159
Final R Indices (obs. data)	R = 4.31 %, wR = 4.61 %
(R Indices (all data)	R = 5.40 %, wR = 4.66 %)
Goodness-of-Fit	2.96
Largest and Mean Δ/σ	0.002, 0.000
Data-to-Parameter Ratio	15.1:1
Largest Difference Peak	0.29 $e\text{Å}^{-3}$
Largest Difference Hole	-0.21 $e\text{Å}^{-3}$

Table 1. Atomic coordinates ($x10^5$) and equivalent isotropic displacement coefficients ($Å^2 x10^4$)

	x	y	z	U(eq)
N(1)	16510(13)	45095(6)	-11778(11)	289(3)
C(2)	21031(17)	39700(7)	2336(13)	290(4)
C(3)	30025(17)	44781(8)	15528(13)	300(4)
C(3A)	31595(15)	53678(7)	9952(13)	271(3)
C(4)	39634(18)	61545(8)	17910(14)	331(4)
C(5)	38859(18)	69046(8)	8634(15)	347(4)
C(6)	30210(18)	68863(8)	-8321(15)	340(4)
C(7)	22065(17)	61158(8)	-16573(14)	313(4)
C(7A)	23108(16)	53755(7)	-7063(13)	263(3)
C(8)	7201(19)	42391(8)	-27059(14)	363(4)
N(9)	-787(21)	40020(8)	-40125(14)	573(5)
C(10)	15766(22)	30167(8)	462(17)	372(5)
C(11)	37359(24)	41856(10)	32894(16)	428(5)

• Equivalent isotropic U defined as one third of the trace of the orthogonalized U_{ij} tensor

Table 2. Bond lengths (Å) and librationally corrected values

N(1)-C(2)	1.422(1)	1.426	N(1)-C(7A)	1.405(1)	1.407
N(1)-C(8)	1.336(1)	1.341	C(2)-C(3)	1.351(1)	1.355
C(2)-C(10)	1.485(2)	1.487	C(3)-C(3A)	1.449(2)	1.451
C(3)-C(11)	1.494(2)	1.499	C(3A)-C(4)	1.398(2)	1.401
C(3A)-C(7A)	1.402(1)	1.406	C(4)-C(5)	1.385(2)	1.388
C(5)-C(6)	1.398(2)	1.402	C(6)-C(7)	1.389(2)	1.392
C(7)-C(7A)	1.382(2)	1.385	C(8)-N(9)	1.146(2)	1.149

Table 3. Bond angles (°)

C(2)-N(1)-C(7A)	109.1(1)	C(2)-N(1)-C(8)	125.4(1)
C(7A)-N(1)-C(8)	125.5(1)	N(1)-C(2)-C(3)	108.4(1)
N(1)-C(2)-C(10)	119.2(1)	C(3)-C(2)-C(10)	132.4(1)
C(2)-C(3)-C(3A)	108.0(1)	C(2)-C(3)-C(11)	126.7(1)
C(3A)-C(3)-C(11)	125.3(1)	C(3)-C(3A)-C(4)	133.5(1)
C(3)-C(3A)-C(7A)	108.1(1)	C(4)-C(3A)-C(7A)	118.4(1)
C(3A)-C(4)-C(5)	118.6(1)	C(4)-C(5)-C(6)	121.4(1)
C(5)-C(6)-C(7)	121.4(1)	C(6)-C(7)-C(7A)	116.1(1)
N(1)-C(7A)-C(3A)	106.4(1)	N(1)-C(7A)-C(7)	129.5(1)
C(3A)-C(7A)-C(7)	124.1(1)	N(1)-C(8)-N(9)	179.6(1)

Table 4. Anisotropic displacement coefficients ($Å^2 x 10^4$)

	U_{11}	U_{22}	U_{33}	U_{12}	U_{13}	U_{23}
N(1)	326(5)	259(4)	266(5)	8(4)	86(4)	-24(3)
C(2)	307(6)	264(5)	311(5)	31(4)	121(4)	15(4)
C(3)	317(6)	298(5)	276(5)	40(4)	94(4)	20(4)
C(3A)	263(5)	271(5)	268(5)	28(4)	78(4)	-13(4)
C(4)	330(6)	336(6)	285(5)	7(5)	56(5)	-45(5)
C(5)	332(6)	284(6)	395(6)	-21(5)	93(5)	-58(5)
C(6)	363(6)	277(5)	378(6)	9(5)	129(5)	24(5)
C(7)	349(6)	302(5)	285(5)	33(5)	106(5)	18(4)
C(7A)	263(5)	248(5)	273(5)	20(4)	86(4)	-26(4)
C(8)	463(7)	272(5)	328(6)	21(5)	107(5)	-26(5)
N(9)	875(10)	379(6)	336(6)	-32(6)	51(6)	-58(5)
C(10)	433(7)	276(6)	424(7)	-19(5)	173(6)	-2(5)
C(11)	548(9)	399(7)	296(6)	32(7)	99(6)	49(6)

The anisotropic displacement factor exponent takes the form:

$-2\pi^2(h^2a^{*2}U_{11} + \ldots + 2klb^*c^*U_{23})$

Table 5. H-Atom coordinates ($x10^4$) and isotropic displacement coefficients ($Å^2 x 10^3$)

	x	y	z	U
H(4)	4574(19)	6170(8)	2971(16)	39(4)
H(5)	4467(19)	7478(9)	1408(16)	40(4)
H(6)	2979(18)	7439(9)	-1472(15)	39(4)
H(7)	1602(19)	6094(8)	-2840(15)	36(3)
H(10X)	1969(24)	2719(11)	1105(21)	74(5)
H(10Y)	2254(26)	2694(12)	-578(20)	78(6)
H(10Z)	156(28)	2914(12)	-507(22)	87(6)
H(11X)	3462(25)	3546(12)	3410(20)	76(5)
H(11Y)	5192(25)	4276(11)	3805(19)	71(5)
H(11Z)	3091(25)	4514(11)	3912(20)	73(5)

References

(1) Hata, T.; Sano, Y.; Sugawara, R.; Matsumae, A.; Kanamori, K.; Shima, T.; Hoshi, T. *J. Antibiot., Ser. A.* **1956**, *9*, 141.

(2) Kennedy, K. A.; Teicher, B. A.; Rockwell, S.; Sartorelli, A. C. *Biochem. Pharmacol.* **1980**, *29*, 1.

(3) Kennedy, K. A.; Rockwell, S.; Sartorelli, A. C. *Cancer Res.* **1980**, *40*, 2356.

(4) Rauth, A. M.; Mohindra, J. K.; Tannock, I. F. *Cancer. Res.* **1983**, *43*, 4154.

(5) Sartorelli, A. C. In *New Approaches to the Design of Antineoplastic Agents*; T. J. Bardos and T. I. Kalman, Eds.; Elsevier Science Publishing Co., Inc.: New York, 1982; pp 51.

(6) Sartorelli, A. C. *Biochem. Pharmacol.* **1986**, *35*, 67.

(7) Ito, S.; Matsuya, T.; Omura, S.; Otani, M.; Nakagawa, A.; Takeshima, H.; Iwai, Y.; Ohtani, M.; Hata, T. *J. Antibiot.* **1970**, *23*, 315.

(8) Omura, S.; Nakagawa, A.; Yamada, H.; Furusaki, A.; Watanabe, T. *Chem. Pharm. Bull.* **1971**, *19*, 2428.

(9) Hata, T.; Omura, S.; Iwai, Y.; Nakagawa, A.; Otani, M. *J. Antibiot.* **1971**, *24*, 353.

(10) Moore, H. W. *Science* **1977**, *197*, 527.

(11) Iwami, M.; Kiyoto, S.; Terano, H.; Kohsaka, M.; Aoki, H.; Imanaka, H. *J. Antibiot.* **1987**, *40*, 589.

(12) Kiyoto, S.; Shibata, T.; Yamashita, M.; Komori, T.; Okuhara, M.; Terano, H.; Kohsaka, M.; Aoki, H.; Imanaka, H. *J. Antibiot.* **1987**, *40*, 594.

(13) Woo, J.; Sigurdsson, S. T.; Hopkins, P. B. *J. Am. Chem. Soc.* **1993**, *115*, 1199.

(14) Williams, R. M.; Rajski, S. R. *Tetrahedron Lett.* **1992**, *33*, 2929.

(15) Stinson, S. *Chem. Eng. News* **1986**, *64*, 26.

(16) Teng, S. P.; Woodson, S. A.; Crothers, D. M. *Biochemistry* **1989**, *28*, 3901.

(17) Kirsch, E. J. In *Antibiotics*; D. Gottlieb and P. D. Shaw, Eds.; Springer-Verlag: New York, 1967; Vol. 2; pp 67.

(18) Falling, S. N.; Rapoport, H. *J. Org. Chem.* **1980**, *45*, 1260.

(19) Murphy, W. S.; O'Sullivan, P. J. *Tetrahedron Lett.* **1992**, *33*, 531.

(20) McClure, K. F.; Benbow, J. W.; Danishefsky, S. J. *J. Am. Chem. Soc.* **1991**, *113*, 8185.

(21) McClure, K. F.; Danishefsky, S. J. *J. Org. Chem.* **1991**, *56*, 850.

(22) Casner, M. L.; Remers, W. A.; Bradner, W. T. *J. Med. Chem.* **1985**, *28*, 921.

(23) Fukuyama, T.; Nakatsubo, F.; Cocuzza, A. J.; Kishi, y. *Tetrahedron Lett.* **1977**, *14*, 4295.

(24) Nakatsobu, F.; Fukuyama, T.; Cocuzza, A. J.; Kishi, Y. *J. Am. Chem. Soc.* **1977**, *99*, 8115.

(25) Fukuyama, T.; Yang, L. In *Studies in Natural Products Chemistry. Bioactive Natural Products (Part A)*; Atta-ur-Rahmann and F. Z. Bash, Eds.; Elsevier: New York, 1993; Vol. 13.

(26) Wakaki, S.; Marumo, H.; Tomioka, G.; Shimizu, G.; Kato, E.; Kamada, H.; Kudo, S.; Fujimoto, Y. *Antibiot. Chemother.* **1958**, *8*, 228.

(27) DeBoer, C.; Dietz, A.; Lummis, N. E.; Savage, G. M. *Antimicrobial Agents Ann.* **1960**, 17.

(28) Lefemine, D. V.; Dann, M.; Barbatschi, F.; Zbinovsky, V.; Monnikendam, P.; Adam, J.; Bohonos, N. *J. Am. Chem. Soc.* **1962**, *84*, 3184.

(29) Stock, J. A. *Antitumor Antibiotics*; Academic Press: New York, 1966; Vol. IV, pp 267.

(30) Webb, J. S.; Cosulich, D. B.; Mowat, J. H.; Patrick, J. B.; Broschard, R. W.; Meyer, W. E.; Williams, R. P.; Wolf, C. F.; Fulmor, W.; Pidacks, C. *J. Am. Chem. Soc.* **1962**, *84*, 3185.

(31) Tulinsky, A. *J. Am. Chem. Soc.* **1962**, *84*, 3188.

(32) Hornemann, U.; Heins, M. J. *J. Org. Chem.* **1985**, *50*, 1301.

(33) Kono, M.; Saitoh, Y.; Shirahata, K.; Arai, Y.; Ishii, S. *J. Am. Chem. Soc.* **1987**, *109*, 7224.

(34) Kono, M.; Kasai, M. *J. Syn. Org. Chem., Japan* **1990**, *48*, 824.

(35) Lipsett, M. N.; Weissbach, A. *Biochemistry* **1965**, *4*, 206.

(36) Egbertson, M.; Danishefsky, S. J. *J. Am. Chem. Soc.* **1987**, *109*, 2204.

(37) Peterson, D. M.; Fisher, J. *Biochemistry* **1986**, *25*, 4077.

(38) Danishefsky, S. J.; Egbertson, M. *J. Am. Chem. Soc.* **1986**, *108*, 4648.

(39) Gutteridge, J. M. C.; Quinlan, G. J.; Wilkins, S. *FEBS Lett.* **1984**, *167*, 37.

(40) Kohn, H.; Li, V.-S.; Schlitz, P.; Tang, M.-S. In *Perspectives in Medicinal Chemistry*; B. Testa, E. Kyburz, W. Fuhrer and R. Giger, Eds.; Verlag Helvetica Chimica Acta, Basel: New York, 1993; pp 331.

(41) Tomasz, M.; Chawla, A. K.; Lipman, R. *Biochemistry* **1988**, *27*, 3182.

(42) Tomasz, M.; Lipman, R.; Chowdary, D.; Pawlak, J.; Verdine, G. L.; Nakanishi, K. *Science* **1987**, *235*, 1204.

(43) Tomasz, M.; Chawla, A. K.; Lipman, R. *Biochemistry* **1988**, *27*, 3182.

(44) Kinoshita, S.; Uzu, K.; Nakano, K.; Shimizu, M.; Takahashi, T. *J. Med. Chem.* **1971**, *14*, 103.

(45) Williams, R. M.; Rajski, S. R. *Tetrahedron Lett.* **1993**, *34*, 7023.

(46) Masuda, K.; Nakamura, T.; Shimomura, K. *J. Antibiot.* **1988**, *41*, 1497.

(47) Fukuyama, T.; Goto, S. *Tetrahedron Lett.* **1989**, *30*, 6491.

(48) Yasuda, N.; Williams, R. M. *Tetrahedron Lett.* **1989**, *30*, 3397.

(49) McClure, K. F.; Danishefsky, S. J. *J. Am. Chem. Soc.* **1993**, *115*, 6094.

(50) Jones, R. J.; Rapoport, H. *J. Org. Chem.* **1990**, *55*, 1144.

(51) Fukuyama, T.; Xu, L.; Goto, S. *J. Am. Chem. Soc.* **1992**, *114*, 383.

(52) Schkeryantz, J. M.; Danishefsky, S. J. *J. Am. Chem. Soc.* **1995**, *117*, 4722.

(53) Cabri, W.; Candiani, I. *Acc. Chem. Res.* **1995**, *28*, 2.

(54) Sainsbury, M. *Tetrahedron* **1980**, *36*, 3327.

(55) Furusaki, A.; Matsui, M.; Watanabe, T. *Is. J. Chem.* **1972**, *10*, 173.

(56) Ajisaka, K.; Takeshima, H.; Omura, S. *J. Chem. Soc., Chem. Commun.* **1976**, 571.

(57) Sato, Y.; Geckle, M.; Gould, S. J. *Tetrahedron Lett.* **1985**, *26*, 4019.

(58) Smitka, T. A.; Bonjouklian, R.; Perun, T. J. J.; Hunt, A. H.; Foster, R. S.; Mynderse, J. S.; Yao, R. C. *J. Antibiot.* **1992**, *45*, 581.

(59) Lin, H. C.; Chang, S. C.; Wang, N. L.; Chang, L. R. *J. Antibiot.* **1994**, *47*, 675.

(60) Young, J. J.; Ho, S. N.; Ju, W. M.; Chang, L. R. *J. Antibiot.* **1994**, *47*, 681.

(61) Seaton, P. J.; Gould, S. J. *J. Antibiot.* **1989**, *62*, 189.

(62) Sato, Y.; Gould, S. J. *Tetrahedron Lett.* **1985**, *26*, 4023.

(63) Sato, Y.; Gould, S. J. *J. Am. Chem. Soc.* **1986**, *108*, 4625.

(64) Seaton, P. J.; Gould, S. J. *J. Am. Chem. Soc.* **1987**, *109*, 5282.

(65) Seaton, P. J.; Gould, S. J. *J. Am. Chem. Soc.* **1988**, *110*, 5912.

(66) Gould, S. J.; Cheng, X.; Melville, C. *J. Am. Chem. Soc.* **1994**, *116*, 1800.

(67) Gould, S. J.; Cheng, X. C.; Halley, K. A. *J. Am. Chem. Soc.* **1992**, *114*, 10066.

(68) Gore, M. P.; Gould, S. J.; Weiler, D. *J. Org. Chem.* **1992**, *57*, 2774.

(69) Cone, M. C.; Hassan, A. H.; Gore, M. P.; Gould, S. J.; Borders, D. B.; Alluri, M. R. *J. Org. Chem.* **1994**, *59*, 1923.

(70) Cone, M. C.; Melville, C. R.; Gore, M. P.; Gould, S. J. *J. Org. Chem.* **1993**, *58*, 1058.

(71) Fujita, T.; Takase, S.; Otsuka, T.; Terano, H.; Kohsaka, M. *J. Antibiot.* **1988**, *412*, 392.

(72) Mithani, S. M. Sc. Thesis, University of Waterloo, 1991.

(73) Vice, S. F.; Friesen, R. W.; Dmitrienko, G. I. *Tetrahedron Lett.* **1985**, *26*, 165.

(74) Davis, F. A.; Stringer, O. D. *J. Org. Chem.* **1982**, *47*, 1774.

(75) Davis, F. A.; Abdul-Malik, N. F.; Awad, S. B.; Harakal, M. E. *Tetrahedron Lett.* **1981**, *22*, 917.

(76) Davis, F. A.; Chattopadhyay, S. *Tetrahedron Lett.* **1986**, *27*, 5079.

(77) Zajac, W. W.; Walters, T. R. J.; Darcy, M. G. *J. Org. Chem.* **1988**, *53*, 5856.

(78) Davis, F. A.; Chattopadhyay, S. *J. Org. Chem.* **1988**, *53*, 2087.

(79) Davis, F. A.; Sheppard, A. C. *Tetrahedron* **1989**, *45*, 5703.

(80) Davis, F. A.; Sheppard, A. C. *Tetrahedron Lett.* **1988**, *29*, 4365.

(81) Dmitrienko, G. I.; Denhart, D.; Mithani, S.; Prasad, G. K. B.; Taylor, N. J. *Tetrahedron Lett.* **1992**, *33*, 5705.

(82) Wang, Z.; Jimenez, L. S. *J. Am. Chem. Soc.* **1994**, *116*, 4977.

(83) Braunschweiler, L.; Ernst, R. R. *J. Magn. Reson.* **1983**, *53*, 521.

(84) Marat, K. *Magn. Reson. Chem.* **1995**, *33*, 529.

(85) Kessler, H.; Oschkinat, H.; Griesinger, C. *J. Magn. Reson.* **1986**, *70*, 106.

(86) Davis, F. A.; Wei, J.; Sheppard, A. C.; Gubernick, S. *Tetrahedron Lett.* **1987**, *28*, 5115.

(87) Bach, R. S.; Wolber, G. J. *J. Am. Chem. Soc.* **1984**, *106*, 1410.

(88) Bach, D. B.; Andres, J. L. *J. Org. Chem.* **1992**, *57*, 613.

(89) Bach, R. D.; Coddens, B. A.; McDouall, J. J. W.; Schlegel, H. B. *J. Org. Chem.* **1990**, *55*, 3325.

(90) Dave, V.; Warnhoff, E. W. *Can. J. Chem.* **1971**, *49*, 1911.

(91) Adam, W.; Ahrweiler, M.; Sauter, M.; Schmieddeskamp, B. *Tetrahedron Lett.* **1993**, *34*, 5247.

(92) Zhang, X.; Foote, C. S. *J. Am. Chem. Soc.* **1993**, *115*, 8867.

(93) Gould, S. J.; Melville, C. R. *Bioorg. Med. Chem. Lett.* **1995**, *5*, 51.

(94) Birch, A. J.; Butler, D. N.; Siddall, J. B. *J. Chem. Soc.* **1964**, 2941.

(95) Kelly, T. R.; Ananthasubramanian, L.; Borah, K.; Gillard, J. W.; Goerner, R. N. J.; King, P. F.; Lyding, J. M.; Tsang, W. G.; Vaya, J. *Tetrahedron* **1984**, *40*, 4569.

(96) Kelly, R. T.; Montury, M. *Tetrahedron Lett.* **1978**, 4311.

(97) Boisvert, L.; Brassard, P. *J. Org. Chem.* **1988**, *53*, 4052.

(98) Jakiwczk, O. Organic Chemistry Thesis, University of Waterloo, 1992.

(99) Heck, R. F. *Acc. Chem. Res.* **1979**, *12*, 146.

(100) Clive, D. L.; Angoh, A. G.; Bennet, S. M. *J. Org. Chem.* **1987**, *52*, 1339.

(101) Tomaja, D. L.; Vogt, L. H. J.; Wirth, J. G. *J. Org. Chem.* **1970**, *35*, 2029.

(102) McKillop, A.; Ray, S. J. *Synthesis* **1977**, 847.

(103) Vogt, L. H. J.; Wirth, J. G.; Finkbeiner, H. L. *J. Org. Chem.* **1969**, *34*, 273.

(104) O'Sullivan, P. J.; Moreno, R.; Murphy, W. S. *Tetrahedron Lett.* **1992**, *33*, 535.

(105) Deghenghi, R.; Engel, C. R. *J. Am. Chem. Soc.* **1960**, *82*, 3201.

(106) Stephany, R. W.; de Bie, M. J. A.; Drenth, A. *Org. Magn. Reson.* **1974**, *6*, 45.

(107) Imae, K.; Nihei, Y.; Oka, M.; Yamasaki, T.; Konishi, M.; Oki, T. *J. Antibiot.* **1993**, *46*, 1031.

(108) Regitz, M.; Maas, G. *Diazo Compounds; Properties and Synthesis*; Academic Press, Inc.: New York, 1986.

(109) Levy, G. C.; Lichter, R. L. *Nitrogen-15 Nuclear Magnetic Resonance Spectroscopy*; John Wiley and Sons: New York, 1979, pp 93, 119.

(110) Gould, S. J.; Tamayo, N.; Melville, C. R.; Cone, M. C. *J. Am. Chem. Soc.* **1994**, *116*, 2207.

(111) Mithani, S.; Weeratunga, G.; Taylor, N. J.; Dmitrienko, G. I. *J. Am. Chem. Soc.* **1994**, *116*, 2209.

(112) Echavarren, A. M.; Tamayo, N.; Paredes, M. C. *Tetrahedron Lett.* **1993**, *34*, 4713.

(113) Gould, S. J.; Cheng, X. C.; Halley, K. A. *J. Am. Chem. Soc.* **1992**, *114*, 10066.

(114) Melville, C. R.; Gould, S. J. *J. Nat. Prod. - Lloydia* **1994**, *57*, 597.

(115) Ayer, S. W.; McInnes, A. G.; Thibault, P.; Walter, J. A. *Tetrahedron Lett.* **1991**, *32*, 6301.

(116) Shin-ya, K.; Furihata, K.; Teshima, Y.; Hayakawa, Y.; Seto, H. *Tetrahedron lett.* **1992**, *33*, 7025.

(117) Arya, D. P.; Jebaratnam, D. J. *J. Org. Chem.* **1995**, *60*, 3268.

(118) Pratt, E. F.; Rice, R. G.; Luckenbaugh, R. W. *J. Am. Chem. Soc.* **1957**, *79*, 1212.

(119) Pratt, E. F.; Luckenbaugh, R. W.; Erickson, R. L. *J. Org. Chem.* **1954**, *19*, 176.

(120) Pratt, E. F.; Rice, R. G. *J. Am. Chem. Soc.* **1957**, *79*, 5489.

(121) Pratt, E. F.; Boehme, W. E. *J. Am. Chem. Soc.* **1951**, *73*, 444.

(122) Buggle, K.; Donnelly, J. A.; Maher, L. J. *J. Chem. Soc., Perkin Trans. 1* **1973**, 1006.

(123) Nagata, W.; Yoshioka, M.; Murakami, M. *J. Am. Chem. Soc.* **1972**, *94*, 4644.

(124) House, H. O. *Modern Synthetic Reactions;* 2nd ed.; W. A. Benjamin, Inc.: Menlo Park, 1972, pp 623.

(125) Nagata, W.; Yoshioka, M.; Hirai, S. *J. Am. Chem. Soc.* **1972**, *94*, 4635.

(126) Hill, R. K.; Conely, R. T. *J. Am. Chem. Soc.* **1960**, *82*, 645.

(127) McKillop, A.; Young, D. W. *Synth. Commun.* **1977**, *7*, 467.

(128) Jacob, P.; Callery, P. S.; Shulgin, A. T.; Castagnoli, N. J. *J. Org. Chem.* **1976**, *41*, 3627.

(129) Guilbault, G. G.; Kramer, D. N. *Anal. Chem.* **1965**, *37*, 1395.

(130) Heinzman, S. W.; Grunwell, J. R. *Tetrahedron Lett.* **1980**, *21*, 4305.

(131) Thomson, R. H. *J. Org. Chem.* **1948**, *13*, 377.

(132) Thomson, R. H. *J. Org. Chem.* **1948**, *13*, 371.

(133) Hannan, R. L.; Barber, R. B.; Rapoport, H. *J. Org. Chem.* **1979**, *44*, 2153.

(134) Kobayashi, M.; Terui, Y.; Tori, K.; Tsuji, N. *Tetrahedron Lett.* **1976**, 619.

(135) Jung, M. E.; Hagenah, J. A. *J. Org. Chem.* **1987**, *52*, 1889.

(136) Jacobsen, N.; Torssell, K. *Acta Chem. Scand.* **1973**, *27*, 3211.

(137) Jacobsen, N.; Torrsell, K. *Liebigs Ann. Chem.* **1972**, *763*, 135.

(138) Brown, P. M.; Thomson, R. H. *J. Chem. Soc., Perkin Trans. 1* **1976**, 997.

(139) Colon, I.; Kelsey, D. R. *J. Org. Chem.* **1986**, *51*, 2627.

(140) Fanta, P. E. *Synthesis* **1974**, 9.

(141) Bringmann, G.; Walter, R.; Weirich, R. *Angew. Chem., Int. Ed. Engl.* **1990**, *29*, 977.

(142) Heck, R. F. In *Organic Reactions*1982; Vol. 27; pp 345.

(143) Larock, R. C.; Baker, B. E. *Tetrahedron Lett.* **1988**, *29*, 905.

(144) Nelson, T. D.; Meyers, A. I. *J. Org. Chem.* **1994**, *59*, 2655.

(145) Horner, L.; Baston, D. W. *Liebigs Ann. Chem.* **1973**, 910.

(146) Ramirez, F.; Dershowitz, S. *J. Org. Chem.* **1958**, *23*, 778.

(147) *Zinc Enolates: the Reformatsky and Blaise Reactions*; Rathke, M. W.; Weipert, P., Eds.; Pergamon Press: New York, ; Vol. 2, pp 277.

(148) Regitz, M. *Synthesis* **1972**, 351.

(149) Regitz, M. *Angew. Chem., Int. Ed. Engl.* **1967**, *6*, 733.

(150) McGuiness, M.; Shechter, H. *Tetrahedron Lett.* **1990**, *31*, 4987.

(151) Taber, D. F.; Ruckle, R. E. J.; Hennessy, M. J. *J. Org. Chem.* **1986**, *51*, 4077.

(152) Monteiro, H. J. *Synth. Commun.* **1987**, *17*, 983.

(153) Perrin, D. D.; Armarego, W. L. F. *Purification of Laboratory Chemicals;* 3rd ed.; Pergamon Press: Oxford, 1988.

(154) Bax, A.; Subramanian, S. *J. Magn. Reson.* **1986**, *67*, 565.

(155) Bodenhausen, G.; Ruben, D. J. *Chem. Phys. Lett.* **1980**, *69*, 185.

(156) Bax, A.; Summers, M. F. *J. Magn. Reson.* **1986**, *108*, 2093.

(157) Dave, V.; Warnhoff, E. W. *Can. J. Chem.* **1976**, *54*, 1015.

(158) Murray, R. E.; Zweifel, G. *Synthesis* **1980**, 150.